THE UNIVERSITY *of* EDINBURGH

Antimicrobial Polymers

Meltem HAKTANIYAN

Doctorate of Philosophy

The University of Edinburgh

2024

Lay Summary

The emergence of antibiotic resistance, due to excessive and poor usage, has necessitated the search for alternative solutions. One such weapon in the battle against microbes are antimicrobial polymers. These polymers have the ability to kill or impede the growth of harmful microbes. Among them, cationic polymers can be specifically engineered to target a wide range of pathogens, including Gram-positive and Gram-negative bacteria, viruses, and fungi. These polymers, in particular, have demonstrated significant potential due to their mechanisms of action, which involve interacting with the diverse negatively charged components of bacterial and fungi cell envelopes. This interaction can lead to the disruption of cell membranes, ultimately resulting in death of the microbe.

In the course of my doctoral research, I conducted the synthesis of a cationic polymers directly from monomers or modification of existing polymers. The initial chapter of my dissertation is dedicated to a review of antimicrobial polymers; this is followed by two chapters with a specific emphasis on optimizing polymer synthesis and evaluation of their antimicrobial and antifungal properties in relation to variations in their molecular weight. In the fourth chapter, a new cationic monomer was synthesized and its corresponding polymers were synthesized and an investigation of their antimicrobial properties as well as their biocompatibilities studied. In the final research chapter, the antimicrobial activity of Tröger's Base polymers and their quaternized derivatives as potential surface coatings were investigated. Stable surface coating was obtained *via* spin-coating and their antimicrobial activity and biocompatibility were evaluated.

Abstract

Antimicrobial polymers are becoming increasingly popular as an alternative approach and solution to traditional antibiotics in the fight against pathogens. Polymers can be designed to target a wide range of pathogens, including both Gram-positive and Gram-negative bacteria, viruses, and fungi. Cationic polymers, in particular, have shown huge potential because of their mechanisms of action, notably their interactions with the various negatively charged cell envelope components of bacteria. This can lead to membrane disruption and ultimately bacterial death. These polymers can be synthesized directly from monomers, or existing polymers can be functionalized to give antimicrobial moieties, such as quaternary ammonium groups, to give an antimicrobial effect.

In this thesis, the antimicrobial properties of polymers containing quaternary ammonium groups against a wide range of microorganisms both in solution and on surfaces were investigated. Thus, a small library of homopolymers, comprised of quaternary ammonium monomers, was synthesized through Reversible Addition Fragmentation Chain Transfer polymerization to give polymers with well-defined molecule weights. The polymerization reactions were optimized, and the antimicrobial activity of these polymers assessed against Gram-negative and two Gram-positive bacteria. A key objective was to examine the effect molecular weight had on the antimicrobial activity of the homopolymers. The most effective polymers were subjected to detailed investigation to assess their impact on bacteria, fungi, mammalian cells, and erythrocytes specifically analysing the effect of polymer molecular weights on their activity. The antimicrobial mechanisms of action of the polymers were

examined in detail, and through this process, identified polymers that were non-toxic to mammalian cells, yet highly bactericidal.

In a complementary research endeavor, a novel metharcylamide monomer based on a pyrrolidinium group, inspired by the product of cyclisation of the diallylamine monomer was synthesised. This was achieved by reacting methacrylic anhydride with (*R*)-3-amino-1-N-Boc-pyrrolidine and used to generate polymers *via* Free Radical Polymerization, again with molecular weight variants. Comprehensive analysis of their antimicrobial activity and biocompatibility was undertaken. The higher molecular weight polymer showed toxic effects on mammalian cells, whilst polymers with lower molecular weights demonstrated bactericidal activity against both Gram-negative and Gram-positive bacteria, with a notably enhanced effect on Gram-positive bacteria.

Finally, the antimicrobial activity of a Tröger's Base polymer and the quaternized derivatives were investigated as potential antimicrobial surface coatings. Polymers were synthesized, coated onto surfaces *via* spin coating and evaluated for antimicrobial activity and biocompatibility.

Contents

Acknowledgements

I would like to express my sincere gratitude to Prof Mark Bradley for their exceptional guidance and mentorship throughout the past four years. Your consistent guidance has played a pivotal role in moulding my academic path and fostering my development as a researcher. Your profound insights, extensive knowledge, and steadfast support have been priceless, and I sincerely appreciate the privilege of learning under your mentorship. I am thankful for your dedication and encouragement, which have significantly contributed to both my academic and personal growth.

I want to extend my gratitude to Dr Annamaria Lilienkampf for taking my supervision after Prof Bradley. Your support has made a significant difference, and I am grateful to have you by my side. Thank you for being there for me. I would like to extend my sincere gratitude to Prof. Neil McKeown for their invaluable feedback provided during my annual progress reviews together with Dr Annamaria Lilienkampf. Their constructive insights and suggestions have significantly contributed to enhancing the robustness and quality of my research.

I extend my heartfelt gratitude to my family and my best friends Nesrin Gizem Cakir and Selin Icmen Yuksel. Your steadfast support and camaraderie have been a continual wellspring of comfort and motivation. Without your unconditional love and support, I could not endure many obstacles in my life.

I am deeply grateful to my dear friend and companion, Ceren Erdem, for being a steadfast companion since the inception of my PhD journey. Thank you, my dear friends Hande Balci, Kutlu Balci, Ahmet Burak Ozyurt, Ozan Bahadir, Abdulkadir Ciris and Ozgu Goksu, for forming a bond akin to a family here in Scotland. Your friendship has been a constant source of comfort and motivation, making the journey much more manageable. I truly appreciate the

moments we have shared together, and I am immensely grateful for the enrichment you have brought to my academic journey. Thank you for being a reassuring presence and a blessing in my life.

I would like to extend my thanks to my friends Dilara Gundogdu, Zuhra Cinar, Ceren Soysal, Dilan Aslan ve Nihan Saracogullari. I felt compelled to express my deepest gratitude for the unwavering support and encouragement you have consistently provided, especially during those moments when I, even myself, harbored doubts.

Thank you especially to Fizza Haseeb to being there for me in both my low and high moods. You are an amazing friend from the moment we became friends. Your willingness to listen, share your valuable insights and extend your help has greatly enhanced my experience. Thank you to the Bradley group, both the longstanding members and the new additions to Lilienkampf group. I've shared countless laughs with all of you, and I consider each of you a lifelong friend.

I sincerely thank the Association of Turkish Alumni and Students in Scotland (ATAS), a charitable organisation, for its significant impact on my academic journey. ATAS provided well-organized social and academic events that allowed me to connect with a diverse network, cope with my PhD stress, and facilitated connections with colleagues and researchers. I appreciate ATAS for making Scotland feel like home.

Finally, I express my gratitude to the founder of the Republic of Turkey, Mustafa Kemal Atatürk, may his soul rest in peace. I extend my thanks to the Republic of Turkiye and Turkish Ministry of Education for providing the funding for my PhD studies.

We came as sparks, now returning as fire.

Abbreviations

AgNP	silver nanoparticle
PEI	polyethyleneimine
EDC	1-ethyl-3-(3-dimethylaminopropyl) carbodiimide hydrochloride
RAFT	Reversible Addition Fragmentation Chain Transfer
PDMAEMA	poly(2-dimethylamino)ethyl methacrylate
PMETACl	poly[2-(methacryloyloxy)ethyl]trimethylammonium chloride)
NMP	Nitroxide Mediated Polymerization
ATRP	Atom Transfer Radical Polymerization
CTA	Chain Transfer Agent
CTA1	4-cyano-4-[(dodecylsulfanylthiocarbonyl)sulfanyl]pentanoic acid
CTA2	4-cyano-4-(phenylcarbonothioylthio)pentanoic acid
CTA3	*S*-ethoxythiocarbonyl mercaptoacetic acid
ACVA	4,4-azobis(4-cyanovaleric acid)
AAPH	2,2'-azobis(2-methylpropionamidine)dihydrochloride
DMAEMA	2-(dimethylamino)ethyl methacrylate
METACl	[2-(methacryloyloxy)ethyl]trimethylammonium chloride
3METACl	3-(methacryloylamino)propyl] trimethylammonium chloride

VBMT	vinyl benzyl trimethylammonium chloride
PVMBT	poly(vinyl benzyl trimethylammonium chloride)
DADMAC	diallydimethyl ammonium chloride
PDADMAC	poly(diallydimethyl ammonium chloride)
D_2O	Deuterium oxide
$CDCl_3$	Deuterochloroform
THF	Tetrahydrofuran
MIC	minimum inhibition concentration
SEM	Scanning Electron Microscopy
NPN	1-N-phenyl-naphthylamine
MTT	3-(4,5-dimethylthiazol-2-yl)-2,5-diphenyl-2H-tetrazolium bromide
XTT	2,3-Bis(2-methoxy-4-nitro-5-sulfophenyl)-2H-tetrazolium-5 carboxanilide inner salt
HFIP	Hexafluoroisopropanol
DMSO	Dimethyl sulfoxide
$CHCl_3$	Chloroform

Chapter 1

1. Introduction

Parts of this chapter are published as:

Haktaniyan, M.; R.; Bradley, M. Polymers showing intrinsic antimicrobial activity. *Chem. Soc. Rev*., **2022**, 51, 8584.

The growth of microorganisms such as bacteria, fungi, yeast, and algae must be controlled to ensure the survival of higher species such as plants, and animals and as such microorganisms have developed natural defence mechanisms to contain the spread of microbes. However, these methods often prove inadequate in complex, crowded human society. This inadequacy has led to microbial infections becoming a major cause of death, with infection and contamination by microorganisms always a significant concern for human health in hospitals, food packaging and storage facilities, water supplies, and sanitation [1].

The most common ways of transmitting diseases are through physical contact, consuming contaminated substances, or inhaling particles that are full of microorganism. Antimicrobial agents are often used to treat these if the body cannot control them, albeit not always successfully. One particular issue is that the treatment of microbial infections has become more challenging, as antibiotic-resistant strains proliferate making eradication difficult and

complicating treatment efforts. Despite the approval of 10 new antibiotics in the past 5 years [2], it is evident that there is still a significant amount of work that needs to be done.

A significant field of research is the discovery of polymers with antimicrobial activities which could have attractive benefits in certain areas/applications. Thus, antibacterial polymers typically exhibit long-lasting action, as they are not degraded like many small molecules (*e.g.*, penicillins are readily hydrolysed) and they can be immobilised to provide antimicrobial activity on surfaces [3].

Antimicrobial polymers can be classified based on the mode of action of their antimicrobial activity. This activity can be either inherent, induced through the chemical nature of the polymer chains, or achieved by releasing entrapped organic or inorganic compounds (*e.g.*, silver nanoparticles). With such diverse options available, there are huge opportunities for developing effective antimicrobial polymers that can help in the fight against harmful microbes [4].

1.1. Antimicrobial Polymers

The antimicrobial properties of certain polymers can be either intrinsic or enhanced through their chemical nature. Intrinsic antimicrobial activity refers to the polymer's natural ability to restrict the growth or survival of microorganisms due to its intrinsic properties, including having functional groups such as quaternary ammonium or phosphonium salts that are known for their antimicrobial effects based on interaction with cell membrane of bacteria.

A critical review of the current state-of-the-art of polymers with intrinsic antimicrobial activity was researched and written as part of my PhD and can be found here:

Chem Soc Rev

REVIEW ARTICLE

View Article Online
View Journal | View Issue

Cite this: *Chem. Soc. Rev.*, 2022, **51**, 8584

Polymers showing intrinsic antimicrobial activity

Meltem Haktaniyan and Mark Bradley *

Pathogenic microorganisms are considered to a major threat to human health, impinging on multiple sectors including hospitals, dentistry, food storage and packaging, and water contamination. Due to the increasing levels of antimicrobial resistance shown by pathogens, often caused by long-term abuse or overuse of traditional antimicrobial drugs, new approaches and solutions are necessary. In this area, antimicrobial polymers are a viable solution to combat a variety of pathogens in a number of contexts. Indeed, polymers with intrinsic antimicrobial activities have long been an intriguing research area, in part, due to their widespread natural abundance in materials such as chitin, chitosan, carrageen, pectin, and the fact that they can be tethered to surfaces without losing their antimicrobial activities. In addition, since the discovery of the strong antimicrobial activity of some synthetic polymers, much work has focused on revealing the most effective structural elements that give rise to optimal antimicrobial properties. This has often been synthesis targeted, with the generation of either new polymers or the modification of natural antimicrobial polymers with the addition of antimicrobial enhancing modalities such as quaternary ammonium or guanidinium groups. In this review, the growing number of polymers showing intrinsic antimicrobial properties from the past decade are highlighted in terms of synthesis; often based on post-synthesis modification and their utilization. This includes as surface coatings, for example on medical devices, such as intravascular catheters, orthopaedic implants and contact lenses, or directly as antibacterial agents (specifically as eye drops). Surface functionalisation with inherently antimicrobial polymers is highlighted and has been achieved *via* various techniques, including surface-bound initiators allowing RAFT or ATRP surface-based polymerization, or *via* physical immobilization such as by layer-by-layer techniques. This article also covers the mechanistic modes of action of intrinsic antimicrobial polymers against bacteria, viruses, or fungi.

Received 5th July 2022

DOI: 10.1039/d2cs00558a

rsc.li/chem-soc-rev

EaStCHEM School of Chemistry, University of Edinburgh, David Brewster Road, EH9 3FJ, Edinburgh, UK. E-mail: mark.bradley@ed.ac.uk

Meltem Haktaniyan

Meltem Haktaniyan received her bachelor's degree in Chemistry from the Middle East Technical University in Turkey in 2013, where she remained to undertake an MSc in Chemistry, working on the synthesis and modification of temperature-responsive polymers. She also investigated the drug release profile of multilayer thin films of polyoxazolines produced via the layer-by-layer technique with pH and temperature. In 2018, she was awarded a PhD scholarship (provided by the Turkish Ministry of National Education Study Abroad Programme) and joined the Bradley group in November 2019 working on synthesis of natural and synthetic antimicrobial polymers and their biomedical applications.

Mark Bradley

Mark has led research groups in the UK for more than 30 years and has a strong translational pedigree having been involved in some six spinout companies. He has published over 400 peer reviewed research papers with a focus on the synthesis of molecules and materials and their application in allowing the manipulation, control and understanding of specific biological processes and functions. His research group works extensively in the areas of smart materials/polymers and in vivo chemistry (see ***https://www.combichem.co.uk****).*

Introduction

Contamination by pathogens is a major concern in many areas including, implanted medical devices (from catheters to artificial hips), infection due to surgical tools, dental restoration, food packaging and storage, as well water (probably the biggest global infection risk from pathogens).[1] In addition, over the past few decades multi-drug resistant pathogens have become an increasing threat to global healthcare systems, largely because of overuse/abuse of antibiotics. As such, novel approaches to the elimination/control of these pathogens would have an enormous impact on public health. Towards this goal antimicrobial polymers are of particular interest as new classes of agents to detect, mitigate, combat and/or diminish infections caused by bacteria, fungi, viruses or parasites.[1–4]

Antimicrobial polymers

The first synthetic antimicrobial polymers were synthesized by Cornell in 1965[5] as homo and copolymer derivatives of 2-methacryloxytroponones. The design of these antimicrobial polymers was based on host defence peptides and polymer disinfectants[6] and this was followed in the 1980s by the generation of various salicylic acid functionalized polymers which showed antibacterial activity.[7] The antimicrobial activity of natural polymers such as chitosan[8] and ε-poly-lysine[9] were also discovered/recognised. In 1984, Ikeda[10] synthesized a number of cationic polymers based on poly vinyl benzyl ammonium chloride and this has been recognised as a key breakthrough in the area of cationic antimicrobial polymers. Since this time research related to antimicrobial polymers has gained momentum and several reviews on antimicrobial polymers have been published.[2,11–16]

Over the past few decades, there have been incredible efforts to find ever more effective polymer-based antimicrobial agents, either by synthesizing new polymers with different structures, compositions, or architectures or by attempting to enhance the antimicrobial action of existing antibacterial polymers by functionalization. Thus, some polymers, which have no antimicrobial action, can be functionalized with specific groups such as guanidium or quaternary ammonium groups and/or combined with silver nanoparticles to generate antimicrobial properties. Existing polymers with innate antimicrobial activities such as chitin, chitosan, agarose or carrageen have long been of interest, since their abundance and multiple functional groups makes them good candidates for enhancement of their inherent (although limited) antimicrobial activity by modification.[17–19]

In general, bacteria are classified into two groups, Gram-positive or Gram-negative based on their cell envelope structures. For example, Gram-positive bacteria such as *S. aureus*, *E. faecium*, *S. epidermidis etc.* have an inner cytoplasmic membrane covered by a very thick peptidoglycan layer decorated with teichoic acid and lipoteichoic acid. Contrastingly, Gram-negative bacteria[2] have an additional outer membrane made up mostly liposaccharides and phospholipids as an upper layer on top of a thinner peptidoglycan layer. *M. tuberculosis*[20] is an extremely important bacillus that causes Tuberculosis, a leading cause of worldwide morbidity and mortality (in excess of 1.5 million deaths per annum) – and the major contributor to deaths caused by multiple drug resistant bacteria. *M. tuberculosis* is classified as neither Gram-positive nor Gram-negative due to its unique cell envelope composed of three parts: mycolic acid, arabinogalactan polysaccharides and peptidoglycans. As for their antimicrobial mechanism of action, although many papers have tried to explain the working mechanisms of these polymers against pathogens, this phenomenon remains largely a mystery/obscure and clearly varies across bacterial genus. Thus, depending on polymer composition, different antibacterial actions can be observed. To illustrate this, cationic polymers seem mainly to interact with the cell envelope of bacteria that is formally anionic due to the presence of teichoic acid and lipoteichoic acid in the case of Gram-positive bacteria, and liposaccharides and phospholipids in Gram-negative bacteria *via* electrostatic interactions. This local neutralisation of charge is destabilizing and seems to increase the permeability of the cell membrane leading to bacterial death. The interaction of polymers with *M. tuberculosis* is typically driven by hydrophobic interactions due to its waxy, lipid-rich, membrane as well as cationic interactions. Enveloped viruses such as SARS-CoV-2, SARS coronavirus, Ebola virus, HIV, influenza virus and so on are also protected by a lipid membrane[21] and it is believed that hydrophobic interactions are a key interaction by which antimicrobial polymers can destroy enveloped viruses. Recently polysulfonated polymers have been used to eradicate viral surface contamination, with the coating effective over multiple cycles, with the local "highly acidic" environment believed to be responsible for their mode of action. Thus, the antimicrobial mechanism of polymers differs based on the type of pathogen and the interaction of the polymer with the specific microorganism. Typically, the action of antimicrobial polymers can be categorized as either direct killing (bactericidal/fungicidal or virucidal) by contact and/or inhibition of the growth of the microbes (bacteriostatic) in solution or on surfaces.

This review gives a detailed literature overview (from the last decade) on the current state-of-the-art of polymers which demonstrate an intrinsic antimicrobial mode of action either when immobilised on a surface *via* covalent or physical attachment, or as a solution formulation, with the synthesis and mechanism of antimicrobial action of the polymers given in detail throughout the review.

1. Polymers immobilized on surfaces

1.1. Polymers physically attached to surfaces

Polymers can be attached to surfaces by a number of physical or chemical interactions and coated by a variety of coating processes such as, spin-coating, dip-coating, solution casting, spray coating and many other generic printing techniques[22] that layers polymers onto a substate/surface. Physical attachment of polymers onto a surface is simple and facile and applicable to a variety of surfaces; compared to chemical attachment; with few requirements for complex surface processing.

However, uniformity of coating and the stability of the coating due to leaching from the surface should be considered as limitations. Polymers can be coated onto surfaces as a simple binary composition, as a blend of polymers, or as multilayer films.

1.1.1. Single polymer coatings. Coating single layers of polymer has been shown to be a powerful tool in the functionalization of surfaces to tackle pathogen binding. Antimicrobial polymers are typically chemically robust and active for long durations compared to traditional small molecule antibiotics. Polyethyleneimine (PEI) (Table 1 – P10) for example displays antibacterial activity and Hernandez-Montelongo *et al.*[23] showed that ultrathin films of PEI (around 3.5 nm with an approximate roughness of 1 nm) displayed antibacterial activity against *S. aureus* (95% reduction over 24 h) and *P. aeruginosa* (80% reduction over 8 h). Here the PEI films were generated simply by immersing silicon substrates (oxidized with an oxygen plasma) into a polymer solution (1 mg mL^{-1} in pH 4 0.5 M NaCl). The protonated amines, distributed across the polymer, are believed to be responsible for the bactericidal activity *via* disruption of the bacterial membranes. *P. aeruginosa* showed greater resistance to surface-mediated antibacterial action compared to *S. aureus* due to its "self-defence mechanism" namely the response to envelope-acting stressors.[24] This PEI film was nontoxic to fibroblasts over 7 days while maintaining a stability which makes it a useful coating material for possible biomedical applications.

Access to clean drinking water has huge importance to human health however, almost half a billion people across the globe lack access to clean water with contamination by viruses and bacteria a serious threat.[25] Sinclair *et al.*[26] modified negatively charged commercial flat sheet polyether sulfone microfiltration membranes with PEI, to create a virus-free water purification system. Based on the electrostatic interactions between the membrane and the cationic polymer, the polymer (molecular weight 25 and 750 kDa) was deposited onto membrane in various ratios (0.3–1.3 wt%). Due to the coating by PEI, the pore size of membrane decreased slightly with ~22% loss of membrane permeability, however, this simple modification of commercially available membranes led to substantial viral reductions with flow of 5000 L m^{-2} in approximately 2.5 h.

Nagaraja *et al.*[27] prepared hydrophilic, antimicrobial, thin film surface coatings with maleic anhydride-*N*-vinylpyrrolidone copolymers which were readily functionalised with aminophenol, generating an amide bond and a free carboxylic acid on the polymer with the addition a phenolic group. These polymers were created by dip coating, with thicknesses of 1.63 μm on glass and 1.75 μm on metal. The antimicrobial action of the coated surfaces was tested against the pathogens *S. aureus*, *E. coli*, *M. smegmatis* and *C. albicans* and SEM images showed that the polymeric thin film effectively killed all four microorganisms causing disruption of the bacterial and fungal cell membrane with the authors suggesting this was mediated *via* the phenolic groups of the polymers, presumably mediated *via* ROS generation.

Cationic polymers are effective materials to fabricate contact-active surface coatings, but in addition, hydrophobic modification of the polycationic materials also enables them to interact/penetrate into hydrophobic bacterial cell membranes leading to bacteria lysis. Based on this concept, Westman *et al.*[28] investigated hydrophobically modified polyvinylamines (a highly charged (pH dependent) polyelectrolyte) to prepare coatings active against *E. coli* and *B. subtilis* (Table 1 – P11). Polymers were synthesized by hydrolysis of polyvinylformamide with various degrees of conversion of the amide groups into amines. Some of the amine groups were subsequently derivatised utilizing epoxy-alkanes of various chain lengths (hexyl, octyl, dodecyl), and the polymers were used to prepare antimicrobial coatings on glass slides by physical adsorption. The hexyl-modified polyvinylamines showed the most potent

Table 1 Examples of bactericidal polymers used in LbL films and as antibacterial coatings

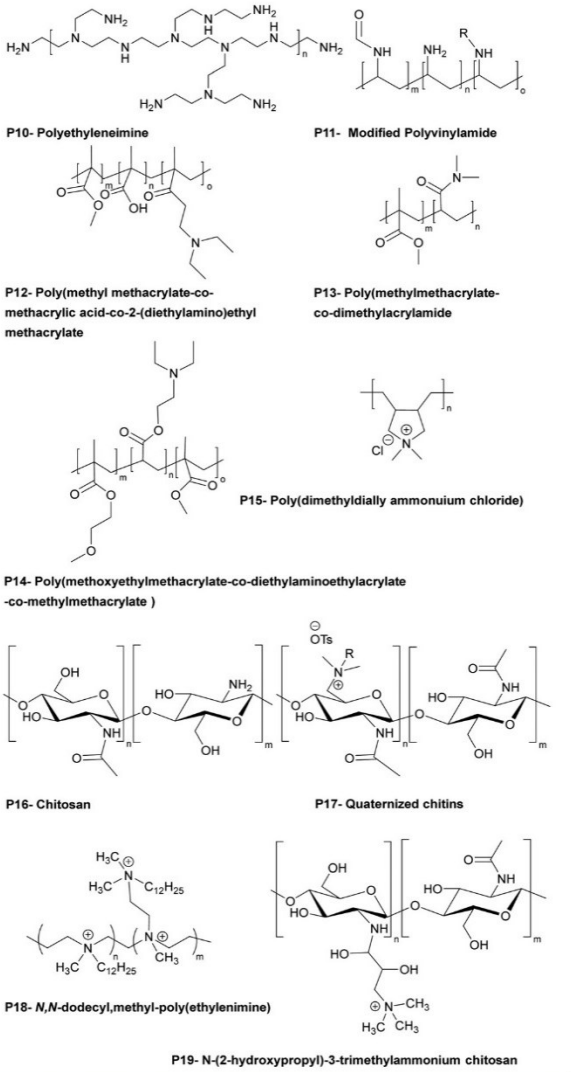

activity against *E. coli* while the octyl derivative displayed greater activity against *B. subtilis*.

The Bradley group developed a number of polymer microarray platforms for the high-throughput screening and identification of biomaterials and examined pathogen attachment and their interaction with polymeric surfaces. One of their studies[29] focused on the identification of novel materials that could rapidly either selectively bind or repel the food-borne pathogens *S. typhimurium* and *E. coli*. In this screen 16 polyacrylates based on methyl methacrylate and glycidyl methacrylate (functionalized with different amines) were also found to inhibit *S. enterica* binding. A polymer composed of methyl methacrylate/methacrylic acid and 2-(diethylamino)ethyl methacrylate, effectively inhibited the adhesion of both *S. typhimurium* and *E. coli* (see Table 1 – P12). Interestingly some polyacrylates showed selective binding of *E. coli*, while not binding *S. typhimurium*. Among the bacteria binding polymers, *S. typhimurium* appeared firmly attached on (poly(hydroxyethyl methacrylate-*co*-dimethyl amino ethyl methacrylate)) coated surfaces. When screening libraries of polyurethanes, polymers synthesised using the diols polybutylene glycol and polypropylene glycol (with a range of diisocyanates) showed selective binding of *S. typhimurium*. In another study[30] interaction of the waterborne protozoan pathogen *G. lamblia* with polymer modified surfaces were investigated. From the 652 screened polymers, 34 hit polymers were identified and investigated in more detail to understand/generate a structure–property relationship. This showed that amide, glycol, and aromatic containing polymers inhibited the adhesion of the pathogen, whereas amine groups containing polymers promoted adhesion. The same group[31] screened a library of polyacrylates/acrylamides, synthesized by free radical polymerisation, to discover anti-adhesive polymeric catheter coatings, looking at the inhibition of binding of mixtures of clinically isolated bacteria (*K. pneumoniae*, *S. saprophyticus* and *S. aureus* or *K. pneumoniae*, *S. mutans*, *S. aureus*, and *E. faecalis*). Due to their flexibility and coating abilities poly(methyl methacrylate-*co*-dimethylacrylamide) and poly(methoxy ethylmethacrylate-*co*-diethylaminoethylacrylate-*co*-methylmethacrylate) (Table 1 – P13, P14) were chosen for coating of polyurethane-based multi-lumen central intravenous catheters and silicone-based double lumen catheters, with 10% w/v acetone coating solutions showing repelling properties against various microorganisms. On both catheters coating by poly(methylmethacrylate-*co*-dimethylacrylamide) displayed the best performance, reducing by $>96\%$ bacterial binding onto the polyurethane catheter and by $>82\%$ onto the silicone catheter.

Hook *et al.*[32] studied polymers using microarray technique showing bacteriostatic (inhibition of growth of bacteria) action using a polymer library produced by mixing 22 acrylate monomers containing ethylene glycol chains of various lengths, fluoro-substituted alkanes, linear and cyclic aliphatic, aromatic and amine moieties. Polymers synthesized by catalytic chain transfer polymerization showed high bacteria adhesion resistance and were coated onto silicone catheters by dip coating after oxygen plasma activation and antimicrobial performance of the coated silicone catheters was compared to commercial silver hydrogel coated latex catheters. Among the hit polymers, a homopolymer of ethylene glycol dicyclopentenyl ether acrylate decreased *P. aeruginosa* attachment by 28-fold and 17-fold compared to bare silicone catheter and silver hydrogel coated latex catheter. For *S. aureus*, copolymers consisting of cyclic monomers [([8-(prop-2-enoyloxymethyl)-3-tricyclo[5.2.1.$0^{2,6}$]decanyl]methyl-prop-2-enoate)] and 4-*tert*-butylcyclohexyl acrylate (7 : 3 ratio) showed a 67-fold reduction and a 30-fold reduction of bacterial binding compared to bare silicone and silver hydrogel coated latex catheters. Analysis of the structure property relationships from the microarray screens allowed the same group[33] to select 116 (meth)acrylate monomers to generate new polymers predicted to resist bacterial attachment. Among the hits, materials were identified that resisted attachment of *P. aeruginosa*, *S. aureus*, and uropathogenic *E. coli*, reducing bacterial coverage up to 81%, 99%, and 99%.

Dundas *et al.*[34] developed a quantitative structure–activity relationship of materials synthesized from (meth)acrylate-based polymers in relation to bacterial biofilm resistance. Among the coatings, catheters coated with a polymer generated using the novel monomer (cyclododecyl methacrylate) reduced by 55-fold binding by six urinary tract pathogens compared with silicone catheters and 14-fold compared to silver hydrogel coated catheters. In this area, Adlington *et al.*[35] used the monomer, (di(ethylene glycol)) methyl ether methacrylate, to provide elasticity, while decreasing the of T_g value of the copolymers. It was also found that a copolymer synthesized from the monomers: ethylene glycol dicyclopentenyl ether acrylate and diethylene glycol methyl ether methacrylate (75 : 25) decreased by 25-fold bacterial attachment of *P. aeruginosa*, *S. aureus*, *E. coli* compared to neat silicone and silver hydrogel coated catheters.

So-called "self-sterilizing surfaces" are a growing area. Bharadwaja *et al.*[36] developed a self-organizing, amphiphilic (anionic) material, made of multiblock polymers (with the mid-block selectively sulfonated) that showed antibacterial and virucidal activity. Two commercially available poly[*tert*-butylstyrene-*b*-(ethylene-*alt*-propylene)-*b*-(styrenesulfonate)-*b*-(ethylene-*alt*-propylene)-*b*-*tert*-butyl styrene] pentablock polymers (with mid-block degrees of sulfonation of either 26 mol% or 52 mol%) spontaneously self-assemble into nanostructures and were evaluated against Gram-negative and Gram-positive bacteria. Polymeric films were prepared and, due to their architecture, permitted water-induced swelling/hydrogel formation. Both polymeric films showed a capability to inactivate *S. aureus* (99.99%) (including methicillin resistant) within 5 min and showed similar levels of inactivation of *E. faecium* and three Gram-negative bacteria (*A. baumannii*, *K. pneumoniae* and *E. coli*). Moreover, these polymers inactivated vesicular stomatitis and influenza A viruses within 5 min with a minimum inactivation level of 67 Plaque forming units mL^{-1}. To explore the role of the mid-block sulfonation, a complementary triblock polymer poly(*tert*-butyl styrene-*b*-styrene-*b*-*tert*-butylstyrene) was synthesized by living anionic polymerization, and mid-block sulfonated (17, 40 and 63 mol%). Testing on *S. aureus*

revealed that between 26% and 40% sulfonated groups were required to eliminate 99.99% of bacteria. Coronavirus 2 (SARS-CoV-2) can be easily transferred *via* different routes including surface contact and airborne droplets.[37,38] After the discovery of the excellent antimicrobial and antiviral activities of the sulfonated polymers, the same group[4] tested sulfonate group bearing polymers (poly[*tert*-butyl styrene-*b*-(ethylene-*alt*-propylene)-*b*-(styrene-*co*-styrenesulfonate)-*b*-(ethylene-*alt*-propylene)-*tert*-butyl styrene]), poly[*tert*-butyl styrene-*b*-(styrene-*co*-styrene sulfonate)-*b*-*tert*-butyl styrene] and (poly[(styrene-*co*-styrene sulfonate)-*b*-(ethylene-*co*-butylene)-*b*-[(styrene-*co*-styrenesulfonate)]]) for inactivation of SARS-CoV-2. The ordered lamellar morphology of the polymer surfaces prepared with >50 mol% of sulfonate groups (*e.g.* poly[*tert*-butylstyrene-*b*-(ethylene-*alt*-propylene)-*b*-(styrene-*co*-styrene sulfonate)-*b*-(ethylene-*alt*-propylene)-*tert*-butyl styrene]) were the most effective in the deactivation of HCoV-229E (<5 min). The mechanism of these polymers is believed to be due to the dramatic pH drop at the polymer/pathogen interface (dependant on the number of sulfonate acid groups on the polymer chain), with rapid pathogen inactivation observed.

Keum *et al.*[39] develop trifunctional antimicrobial, antiviral, and antibiofouling polymers that could be readily coated onto the surface of medical protective clothing. The coating polymers were synthesized by free radical polymerization using various ratios of the monomers (lauryl methacrylate), poly(ethylene glycol) methacrylate and 2-(dimethylamino)ethyl methacrylate quaternized with methyl iodide. Regardless of the monomer ratios explored, all polymers reduced *S. aureus* by >75% and reduced bacterial adhesion by >65%. When sprayed the polymer gave a nano coating layer on hydrophobic surfaces of personal protection equipment, with the spray coated polymer surfaces remaining stable for 24 hours and maintaining their antiadhesion and bactericidal activities. Interestingly, fabric surfaces coated with polymers with lower levels of the quaternary ammonium groups, showed better deactivation activity of porcine epidemic diarrhoea virus (a coronavirus that bears a structural resemblance to the prevailing SARS-CoV-2), reducing virus viability on the surface, compared with the uncoated surface and higher content quaternary ammonium units bearing polymers. The most effective polymers were biocompatible with mammalian cells compared to bacteria and viruses and showed no recognizable local or systemic inflammatory responses in animal experiments.

Mussel inspired dopamine-based materials have gained interest due to their adhesive capabilities and their applicability in biomedical applications as antifouling materials,[40] self-healing materials,[41] their use in separations,[42] and in cell and tissue engineering.[43] Wang *et al.*[44] designed, and synthesized, by RAFT polymerization, a durable, adhesive, antimicrobial coating, based on the diblock poly[(*N*-3,4-dihydroxyphenethyl acrylamide)-*b*-(borneol acrylate)]. Here, the bio-based monomers were synthesized from dopamine that provides the polymers its adhesive properties (as well as phenols for reactive oxygen generation) and borneol which is natural antibiotic found in "medical" herbs such as lavender, valerian, and chamomile. Prior to polymerization dopamine acrylate was protected with triethylsilane groups

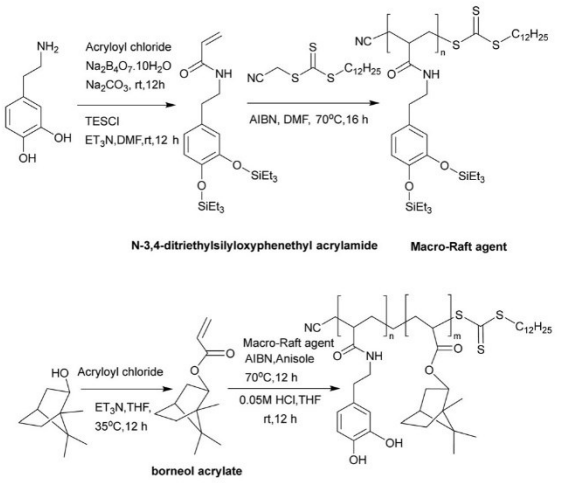

Fig. 1 Synthesis of the monomers: *N*-3,4-dihydroxyphenethyl acrylamide and borneol acrylate and the synthesis of poly[(*N*-3,4-dihydroxyphenethyl acrylamide)-*b*-(borneol acrylate)] *via* RAFT polymerization.[44] Reproduced from ref. 44 with permission from Elsevier.

and then polymerized with the chain transfer agent, 2-cyano-methyl-*s*-dodecyl trithiocarbonate, to generate a macro raft agent (PDA_{10}, M_n: 4.7 kDa, PDI: 1.03). This was used to synthesize copolymers with various block ratios and among the synthesized copolymers, PDA_{10}-*b*-PBA_{55} was selected to perform adhesion and antibacterial tests and was coated onto various substrates. The coated surfaces showed high integrity after rinsing with both water or chloroform and after a peel-off-test due to attachment by the 3,4-dihydroxyphenyl groups. The polymer (PDA_{10}-*b*-PBA_{55}) when coated onto stainless-steel surface inhibited the growth of bacteria (up to 93%) for *E. coli* and 83% for *S. aureus* (Fig. 1 and 2).

The isomers of borneol acrylate were used to prepare a series of borneol-based polymers to understand antibacterial adhesion in relation to monomer/polymer stereochemistry with

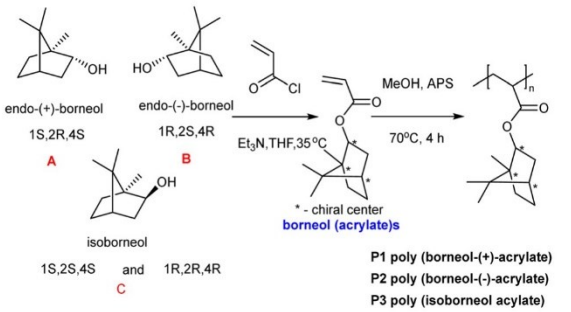

Fig. 2 The synthesis of poly(borneol acrylate)s from borneol (acrylate)s.[45] Reprinted (adapted) with permission from {L. Luo, G. Li, D. Luan, Q. Yuan, Y. Wei and X. Wang, *Appl. Mater.*, 2014, **6**, 19371–19377}. Copyright {2014} American Chemical Society.

polymers coated onto Si-based substrates (approximately 10 μm thickness). Borneol acrylate-based polymer films and the control poly(methyl methacrylate) were cut into circular rings. *E. coli* were placed into the rings and incubated with for 60 h. The poly(borneol acrylate) film rings acted as "perfect prisons", with negligible amounts of *E. coli* observed on the inner and outer surfaces of the ring compared to the control. Among the poly(borneol acrylate) polymers, poly(borneol-(+)-acrylate) and poly(isoborneol acrylate) showed similar activity against *E. coli*, *S. aureus* and *M. racemosus* by inhibiting the bacteria growth on the surface. However, D configurated borneol polymer showed weak antimicrobial action compared to other polymers. Poly(borneol acrylate)s caused the lysis of bacteria (clearly seen in SEM) images in which hydrophobic–hydrophobic interactions between the polymer and bacteria cause the loss of integrity of bacteria after being exposed to poly(borneol acrylate) films. Here, they showed that surface stereochemistry, and especially the bicyclic structure, is crucial for poly(borneol acrylate)s antibacterial adhesion.[45]

The antifungal activity of poly(borneol acrylate)s was explored by Xu *et al.*[46] who developed a non-toxic, antifungal coating to treat fungal biodeterioration in paper production. Poly(borneol acrylate)s were synthesized in methanol with ammonium persulfate as an initiator at 70 °C and coated onto paper after dissolving in DCM and spray coating. The antifungal activity of the "polymer paper" was tested against *A. niger* and *Penicillium* sp., fungi that can easily colonize the surfaces of most materials and rapidly spread *via* fungal spores. Therefore, inhibition to stop the spread of fungal spores is key to creating antifungal coatings. After incubating the polymer coated papers with fungi over eight days, only scattered spores were found on the 10 and 15% poly(borneol acrylate) coated papers. In addition, SEM images found almost no sporangia or hypha and only a few scattered spores could be found on the surface. There is no simple explanation to explain the antifungal mechanism, probably due to hydrophobic nature of the polymer the fungi did not adhere to the surface and prevented the spread of fungal spores on the surface.

Hospital-acquired infections are one of the biggest threats/risks to humans who enter hospitals, due to the long-term use/abuse of antibacterials and other chemicals (such as anticancer agents) within that environment that drive resistance. As such patients are exposed to antibiotic resistant bacteria in routine hospital procedures. *P. aeruginosa* is commonly found to be resistant to antibiotics and can cause serious infections including ventilator-associated pneumonia, catheter associated sepsis and wound-burn infections.[25] To understand which pendant group shows the best activity against *P. aeruginosa*, Chamsaz *et al.*[47] developed a coumarin containing polyester coating containing amine or carboxylic acid pendant chains with coumarin and aliphatic diols, and succinic acid making up the main backbone. The monomers (see Fig. 3) with *t*-butyl protected carboxylate acid groups (giving the anionic pendant groups upon deprotection) or Boc-protected amine group (giving the cationic pendant groups) were polymerized by carbodiimide-mediated polymerization of the diols and diacids

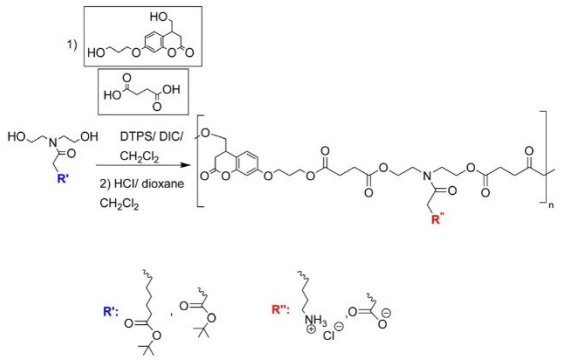

Fig. 3 Synthesis route to coumarin containing polyesters with pendent amine or carboxylic acid groups.[47] Reprinted (adapted) with permission from {E. A. Chamsaz, S. Mankoci, H. A. Barton and A. Joy, *Appl. Mater.*, 2017, **9**, 6704–6711}. Copyright {2017} American Chemical Society.

with the films prepared by spin coating and then deprotected. Only the polymers carrying cationic pendant groups killed bacteria attempting to attach to the surface and prevented biofilm formation. When the polymer film was crosslinked (*via* irradiation, with the coumarin units undergo a [2+2] photocycloaddition reaction to form crosslinked coatings) similar results against *P. aeruginosa* were observed, without any leaching of oligomeric species. As before, the antimicrobial activity is based on the amino groups of the polymers interacting with negatively charged bacterial components. The most active polymer showed no cytotoxicity or hemolytic activity.

1.1.2. Blended polymers on surfaces. Polymers can be mixed/blended and coated onto surfaces to form antimicrobial coatings. Hoque *et al.*[48] synthesized hydrophobically functionalized, water insoluble/organic soluble PEI cationic polymer derivatives as a coating materials active against *S. aureus* and *E. coli* as well as drug resistant and pathogenic fungi *Candida* spp. and *Cryptococcus* spp. Different molecular weight, organic soluble, quaternized linear and branched PEI derivatives were synthesized by Eschweiler–Clarke methylation and quaternized with alkyl bromides before spin coating onto surfaces either alone or with polylactic acid. All polymer derivatisations employed the same quaternization protocol except in the case of the linear PEI derivatives that were obtained by acid-catalysed hydrolysis of poly(2-ethyl-2-oxazoline)s (Fig. 4). Although all polymer coatings showed activity against *S. aureus* and *E. coli*, polymers having C-18 alkyl chains showed optimal antimicrobial activity. Among the synthesized branched and linear PEIs polymers bearing a C-18 alkyl chain (M_w: 750 kDa) (P4c) displayed almost 100% inhibition (5 log reduction) of binding of *S. aureus* and *E. coli* when coated at a density of 0.4 μg dm^{-2} and 12.5 μg dm^{-2}, respectively. In addition, linear C-18 alkyl chain polymers (M_w: 22 kDa) (P9) showed the most potent bactericidal activity with minimum inhibition concentrations of 0.24 μg dm^{-2} for methicillin-resistant *S. aureus* and vancomycin-resistant *Enterococci* and 7.8 μg dm^{-2} for *K. pneumoniae* and *E. coli*. The polymer-coated surfaces were exposed repeatedly to bacteria with the polymeric surfaces

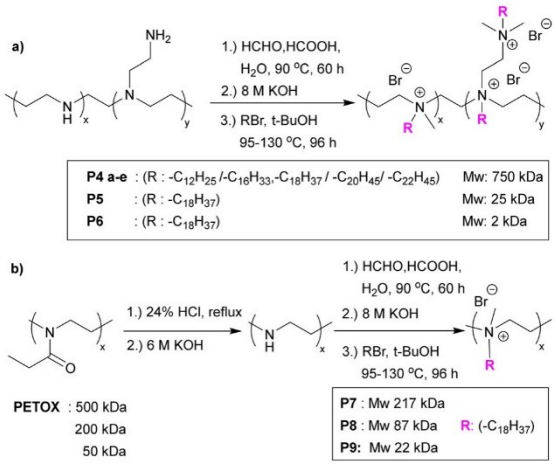

Fig. 4 (a) Functionalization of branched PEI *via* Eschweiler–Clarke methylation and quaternization with various alkyl bromides. (b) Linear PEI polymers synthesised from poly(2-ethyl-2-oxazoline) and modified *via* Eschweiler–Clarke methylation and quaternization with alkyl bromides.[48] Reprinted (adapted) with permission from {J. Hoque, P. Akkapeddi, V. Yadav, G. B. Manjunath, D. S. S. M. Uppu, M. M. Konai, V. Yarlagadda, K. Sanyal and J. Haldar, *ACS Appl. Mater. Interfaces*, 2015, **7**, 1804–1815}. Copyright {2015} American Chemical Society.

remaining fully active after 20 cycles. In addition, P4c and P9 were tested against pathogenic fungi (*C. albicans*, *C. dubliniensis* and *C. tropicalis* and *Cryptococcus* spp. *C. neoformans var. grubii*) (serotype A), *C. gattii* (serotype B) and *C. neoformans var. neoformans* (serotype D). The minimum fungicidal coating activity for the linear C-18 alkyl chain polymer (M_w: 22 kDa) (P9) was found to be 0.63–2.5 μg dm^{-2} for *Candida* spp. and 0.13–0.25 μg dm^{-2} for *Cryptococcus* spp. The same polymer showed the best antifungicidal activity against *C. tropicalis* and *C. neoformans* with minimum fungicidal activities of 0.49 and 0.25 μg dm^{-2} respectively, and in all cases, these hydrophobically modified PEI coatings showed approximately 5-log reductions in fungi viability. Their mechanism of action is again based on their highly cationic nature – enhanced by the presence of the anchoring hydrophobic chains.

The same group[49] reported the antimicrobial activity of biodegradable chitin coatings that were prepared with various degrees of quaternization of chitin (degree of acetylation ~75%). Three different "tosyl-chitins" were prepared by reaction with tosyl chloride in a solvent system consisting of LiCl and *N*,*N*-dimethylacetamide which allowed selective tosylation of only the least sterically hindered C6-hydroxyl groups. The free primary amine groups were then *N*-acetylated before substitution chemistry with *N*,*N*-dimethyl dodecyl amine, *N*,*N*-dimethyl tetradecyl amine, and *N*,*N*-dimethyl hexadecyl amine to give quaternized chitin derivatives. The functionalized chitins were spin-coated onto surfaces either alone or blended with polylactic acid. The polymer coated surfaces showed different antimicrobial activities based on the degree of quaternization and alkyl chain length. Amongst all the polymers, polymers quaternized with a C-16 alkyl chain with degrees of quaternization of 39–48% showed profound antimicrobial activities. The minimum inhibitory amount of the surfaces coated with the two most potent polymers were found to be 0.32 μg mm^{-2} and 0.12 μg mm^{-2} for methicillin resistant *S. aureus*, 0.12 μg mm^{-2} and 0.12 μg mm^{-2} for against *E. faecium*, and 15.6 μg mm^{-2} and 7.8 μg mm^{-2} against *K. pneumoniae*. Dip-coated catheters (48% quaternized with C-16 alkyl chains) gave a reduction in bacteria count dependant on the level of coating, with catheters coated at 7.5 μg mm^{-2} showing a 3.7-log CFU decrease in methicillin-resistant *S. aureus*, with a negligible number of bacteria binding and no biofilm formation on the surface.

Quaternary ammonium salts of chitosan can show antifungal activity, with the cationic groups of chitosan interacting with negatively charged units within the cell wall of fungi, causing the release of intercellular components. Tabriz *et al.*[50] investigated the antifungal properties of a trimethyl quaternized chitosan, blended with polyether sulfones at various concentration (5%, 10% and 15% w/w) to give membrane films for water treatment applications. The antifungal activity of the polymers was tested with the chitosan blend showing better inhibition compared to quaternized chitosan for *F. solani*, whereas the trimethyl chitosan was better for *A. niger*. Additionally, the membrane prepared with the highest concentration of trimethyl chitosan showed a reduction in the number of spores of *A. niger* and *F. solani* by 73% and 63%, respectively.

Polyelectrolyte-surfactant complexes have been explored in applications ranging from medicine[51] to food and cosmetics.[52] Yu *et al.*[53] prepared a water-insoluble catheter coating using electrostatic interactions between poly-L-lysine and the anionic surfactant, 1,4-bis(2-ethylhexyl) sodium sulfosuccinate. The polymer–surfactant complex (in ethanol) adsorbed onto the hydrophobic surface of a polyurethane thermoplastic *via* hydrophobic interactions to generate a stable coating. Contact-killing antibacterial activity was visualized using SEM and showed lesions and distortions on the cell membrane of *S. aureus* and *E. coli* (Fig. 5). In addition, complex coated catheters totally inhibited the adhesion of bacteria under both static and flow conditions, while maintaining antibacterial activity for more than 30 days. An implant-associated bacterial infection experiment showed that poly-L-lysine/1,4-bis(2-ethylhexyl) sodium sulfosuccinate complex coated catheters exhibited excellent inhibition of the inflammatory response, presumably related to the highly acidic succinate surface.[4]

Poly(lactic acid) is one of the most widely used building blocks in the development of 3D printed scaffold/implants due to its ease of printing. However, poly(lactic acid) based substrates lack suitable functional groups which can modified to allow the attachment of polymer brushes directly onto their surface. Thus, Dhingra *et al.*[54] developed a biodegradable 3D-PLA scaffold by blending poly(lactic acid) with tartaric acid based aliphatic polyesters in which the bactericidal polymer, (poly(2-[(methacryloyloxy)ethyl]trimethylammonium chloride) or the antiadhesive polymers ((poly(ethylene glycol) methacrylate)) and poly(2-hydroxyethyl methacrylate)) brushes were tethered. Initially tartaric acid-based biodegradable aliphatic

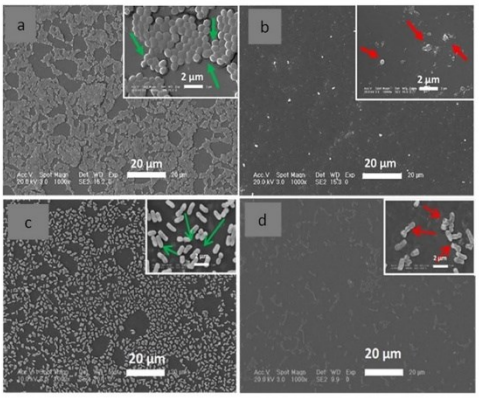

Fig. 5 Catheters (coated with poly-L-lysine/1,4-bis(2-ethylhexyl) sodium sulfosuccinate and uncoated) were incubated with *S. aureus* or *E. coli* (10^6 mL^{-1}) for 24 h. SEM images of: (a). images of *S. aureus* and (c) *E. coli* binding onto the uncoated catheter; (b) images of *S. aureus* and (d) *E. coli* binding onto the complex coated catheters. The green arrows show undamaged bacteria on the uncoated catheter, while the red arrows show the few attached bacteria on the coated catheter with lesions and distortions on the bacterial surface.[53] Modified from ref. 53 with permission from Elsevier.

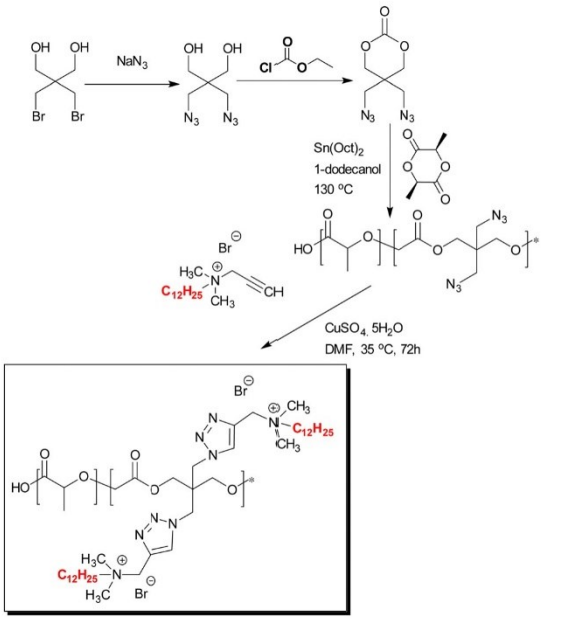

Fig. 6 Synthesis of quaternized ammonium group modified PLA-based copolymers.[55] Modified from ref. 55 with permission from Wiley.

polyesters were synthesized using hexamethylene 2,3-*O*-isopropylidenetartarate with removal of the isopropylidene groups creating free hydroxyl groups on the polyester. After coating of the polyester onto the glass surface, the hydroxyl groups of the polyester were conjugated to an ATRP initiating moiety which enabled graft polymerization of monomers (2-hydroxyethyl methacrylate,2-(methacryloyloxy)ethyl trimethylammonium chloride and poly(ethylene glycol) methacrylate) from the polymer backbone. The polyester modified with cationic bactericidal 2-(methacryloyloxy)ethyl trimethylammonium chloride brushes showed the highest antibacterial activity (>97% and >96% killing efficiency for *E. coli* and *S. aureus*, respectively) and acceptable cytocompatibility. This result showed that the addition of the tartaric acid-based polyesters to PLA could be applicable in the area of biomedical implants.

Poly(ε-caprolactone) is commonly used due to its biocompatibility, non-toxicity, and hydrophobicity; however, poly(ε-caprolactone) has poor mechanical properties and weak cellular affinity. Thus, this polymer was blended with hydrophilic polymers for use in tissue engineering. Aynali *et al.*[55] synthesized biodegradable PLA copolymers by the ring-opening polymerization of L-lactide and cyclic carbonate monomers bearing an azido group (2,2-bis(azidomethyl)trimethylene carbonate) in the presence of 1-dodecanol as an initiator (and tin(II) 2-ethylhexanoate as the catalyst). These polymers were modified with a quaternary ammonium salt (*N*,*N*-dimethyl-*N*-prop-2-yn-1-yldodecane-1-ammonium bromide *via* "click" chemistry) along its backbone (Fig. 6). The best antimicrobial activity being seen with 30% levels of modification. The same author[56] prepared antimicrobial, hydrophilic nanofiber biomaterials *via* electrospinning with poly(ε-caprolactone) and the previously synthesized PLA copolymer (1, 5 and 8%). Fibres mats were collected and their antimicrobial properties evaluated. It was found that increasing the content of the PLA copolymer in the blend enhanced the antimicrobial activity of the fibres (unmodified poly(ε-caprolactone) showed no antimicrobial activity) with the best blend killing 99.5% and 92% of *S. aureus* and *E. coli*, respectively. Clearly, the bactericidal activity of blends is based on the quaternary ammonium groups of the PLA copolymer and functions as a contact active antimicrobial agent (Fig. 7 and 8).

Poly(vinyl alcohol) has been widely used in wound dressing applications due to its hydrophilicity, biocompatibility, and good film-forming abilities. However, it shows poor antimicrobial activity and losses its mechanical properties when wet. Thus, this polymer is typically mixed with others. In this context, Vargoez-Catzim[57] blended various concentrations of poly(2-acrylamido-2-methyl-1-propanesulfonic acid) and cross-linked these with succinic anhydride to develop a new wound dressing. By blending poly(vinyl alcohol) with different ratios (5, 10 and 15%) of poly(2-acrylamido-2-methyl-1-propanesulfonic acid)

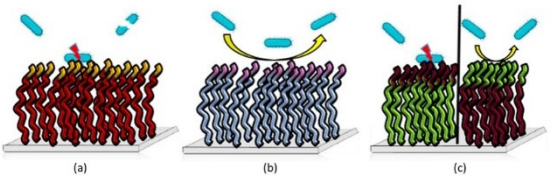

Fig. 7 Representation of polymer brushes and their antimicrobial properties. (a) Polymer brushes showing contact-killing activity. (b) Polymer brushes having antifouling properties. (c) Self-adaptable brushes that change/switch from antimicrobial action to bactericidal to antifouling.

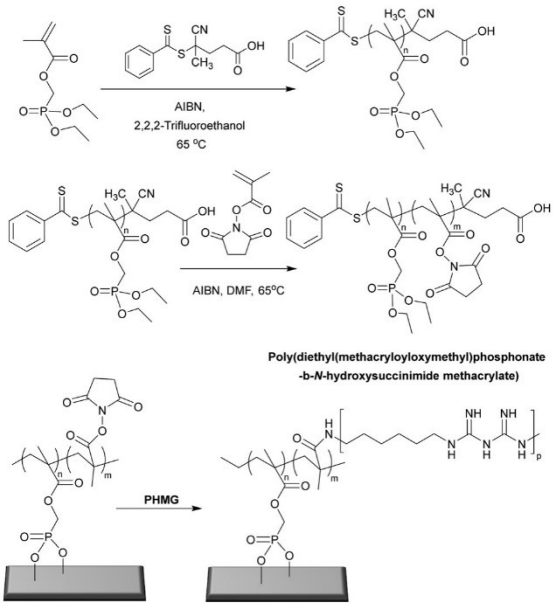

Fig. 8 Synthesis of poly(diethyl(methacryloyloxymethyl)phosphonate-*b*-*N*-hydroxysuccinimide methacrylate) *via* RAFT polymerization and the post-modification of poly((methacryloyloxymethyl)phosphonate-*b*-*N*-hydroxysuccinimide methacrylate) brush surface with poly(hexamethylene biguanide).[97] Reproduced from ref. 97 with permission from Elsevier.

"bilayer membranes" were obtained by the phase inversion method. PVA alone has an MIC value, against *S. aureus* and *E. coli*, of 33 mg mL^{-1} without any bactericidal effect, whereas poly(2-acrylamido-2-methyl-1-propanesulfonic acid)/PVA had significantly lower MIC values (*S. aureus* 1.36 μg mL^{-1} and *E. coli* 39 μg mL^{-1} – some 1000-fold more active). The sulfonic acid pendant groups giving rise to the bactericidal action against both bacteria is due to the creation of a strongly acidic environment that leads to cell membrane destruction. Importantly, the addition of poly(2-acrylamido-2-methyl-1-propanesulfonic) not only provided antimicrobial activity, but the properties of the film were improved, increasing human cell proliferation and cell viability by enhancing surface porosity as well as biocompatibility and improving water uptake.

Poly(vinylidene fluoride) and copolymers of this polymer are of interest due to their biocompatibility, thermal stability, chemical resistance, and mechanical robustness.[58] Han *et al.*[59] prepared poly(vinylidene fluoride-*co*-chlorotrifluoroethylene) to which were grafted quaternary ammonium groups (trimethylamino ethyl methacrylate) or quaternized (4-vinyl pyridines) *via* chlorine-initiated atom transfer radical polymerization. The polymers obtained were blended with poly(vinylidene fluoride-*co*-chlorotrifluoroethylene) and, *via* solvent casting, used to form free standing films. 5 wt% of the polymer bearing the quaternary pyridinium groups showed an antimicrobial effect of greater than 99% against *E. coli*, *S. aureus*, and *C. albicans*, while all blend films displayed excellent biocompatibility. The bactericidal mechanism of the blends was due to the cationic moieties of the polymers interacting with bacteria *via* electrostatic interactions resulting in the disruption of the cell wall/membrane.

Bacterial biofilm formation causes complicated and chronic infections. Biofilms are defined as organized bacteria communities embedded in an extracellular polymeric matrix attached to living or abiotic surfaces. The vast majority of hospital-based chronic infections are due to biofilms which can form life-threatening colonizers on biomedical devices such as catheters (central venous, urinary), prosthetic heart valves, and orthopaedic devices. Biofilm formation starts with colonization onto an either abiotic or biotic surfaces by adhesion of bacteria with the help of flagella and pili in Gram-negative bacteria or surface proteins in the case of Gram-positive bacteria. After attachment, proliferation of biofilms is triggered and results in the production of an extracellular matrix composed of exopolysaccharides, protein, DNA, bacteriolytic products, and compounds from the host. The last stage of biofilm formation is colonization and after the first layer of the surface is covered with bacteria the process evolves to generate macro-colonies on surfaces.[60] Within this formation bacteria are highly resistant to antibiotic therapy, due to the exopolysaccharide matrix that serves as an anchorage/support matrix and makes them less susceptible to the therapeutic agents.[61] In this content, Vishwakarma *et al.*[62] prepared water-soluble synthetic peptidomimetic polyurethanes that were able to disrupt surface established biofilms of *P. aeruginosa*, *S. aureus*, and *E. coli*. The polyurethanes (9–10 kDa) were synthesized by polymerization of hexamethylene diisocyanate and *N*-functionalized diethanolamide as monomers (*via* amidation of methyl esters of lysine, alanine, or phenylalanine with diethanolamine). Polymers were synthesized (ratio of 60/40 co-monomers) to tune charge/hydrophobic ratio to mimic the structural peptides while ensuring polymer solubility. To mimic arginine, the synthesized polymers were guanylated post synthesis. The arginine modified polyurethane showed the best broad-spectrum activity with a minimum inhibition concentration of 2–4 μg mL^{-1} for both Gram-positive and Gram-negative bacteria. On the other hand, all polymer compositions showed broad-spectrum biofilm inhibition at low concentrations (2–16 μg mL^{-1}) for *P. aeruginosa*, *S. aureus* and *E. coli*. The polymers were also tested under flow conditions, with biofilms of *P. aeruginosa* grown for 7 days with or without the polymer. In the presence of the Lys/Phe bearing polymers only surface-attached bacteria were observed (no biofilms). An outer membrane permeability assay showed that these polymers did not exhibit any significant membrane permeabilization and that the polymers inhibit the biofilm formation without direct killing of the bacteria *via* membrane destruction.

1.1.3. Polyelectrolyte multilayer films surfaces. Polyelectrolyte multilayer films (PEMs) can be readily prepared *via* a so-called layer-by-layer technique (LbL) which enables the generation of films onto a wide variety of surfaces[63] by repeated deposition/adsorption of the two interacting polymers.[64] Early PEMs were prepared by repetitive dip-coating (deposition) of layers of polyanionic and polycationic polymers *via* electrostatic

interactions,[65] but multilayer films can also be generated by exploiting a variety of interactions, including hydrogen bonding and hydrophobic interactions. The LbL approach enables coating of a variety of different substrates and incudes metals, glass, and various organic polymers. The layer-by-layer assembly approach offers a simple/easy approach to the preparation of a wide range of new surface coatings.[66] In this section of the review, we explore polyelectrolyte multilayer films and their interactions with pathogens. Polyelectrolyte multilayer film surfaces can be bactericidal *via* contact-killing action and/or provide a non-biofouling surface (bacteriostatic) with inhibition of the growth of microorganisms. In addition, PEMs have been specifically designed to bind pathogens for application in detection/assay systems.

1.1.3.1. Bactericidal PEMs. Some PEMs are bactericidal with contact mediated killing of microorganisms, often driven by the deposition of a cationic polymer top layer which drives the interaction between the surface and the bacteria with disruption of the outer membrane of Gram negative bacteria.[67] Wulandari *et al.*[68] produced a silk porous sponge coated *via* layer-by-layer with the cationic antimicrobial polymer poly-((dimethyl-hexyl ammonium bromide) ethyl methacrylate) that was synthesized by free radical polymerization and used with anionic sodium alginate for LbL generation *via* electrostatic interactions. 5-Bilayer films with an outermost layer of the cationic polymer were sufficient for maximal antimicrobial activity (4-log reduction) against Gram-positive and Gram-negative bacteria. It is worth noting that the coating was non-leachable, and the sponge could be reused up to three times after washing. Furthermore, the same polymers were coated (using the same conditions) onto other substrates, including cotton-based bandages and gauzes and these expressed antimicrobial activities similar to the silk sponge. The antimicrobial action of the coated sponge is based on the top layer coating of the cationic polymer, whose quaternary ammonium centre enables binding with the anionic bacteria, while the hydrophobic *n*-hexyl tail facilitates insertion into the bacteria membrane.

Polyethyleneimine is a synthetic, aliphatic and polycationic polymer (due to the presence of protonated primary, secondary and tertiary amino groups) which also enables interaction with polyanions.[69] The bactericidal action of PEI is driven by the cationic groups which bind to cell membrane phospholipids *via* electrostatic interactions and *en masse* lead to rapture.[70] However additional positive charge density and the addition of hydrophobic alkyl groups improved the bactericidal activity of the modified PEIs (see the section on blended films). Wong *et al.*[71] showed that linear *N*,*N*-dodecyl-methyl-poly(ethylenimine) (Table 1 – P18) and poly(acrylic acid) PEMS exhibited potent bactericidal activity against *S. aureus* and *E. coli* as well as antiviral activity against influenza A/WSN (H1N1). *N*-Alkylated PEIs were synthesized by acid hydrolysis of commercial poly(2-ethyl-2-oxazoline) and alkylated with various bromo alkanes and then quaternerised with iodomethane to produce linear *N*,*N*-dialkyl-*N*-methyl-poly(ethylenimine)s. Polymers were deposited onto silicone substrates alternating with poly(acrylic acid) with the last coating layer of the multilayers being polycationic. The microbicidal action of the films was explained by the initial electrostatic interactions between the cationic surface and the negatively charged bacterial cell wall/membrane and subsequent diffusion of the hydrophobic alkyl chain through the lipid bilayer, leading to disruption of the bacterial membrane. The bactericidal activities of the multilayer films were altered in accordance with the length of the hydrophobic alkyl chain of the cationic polymers and the positive charge density on the film surface which were influenced by the deposition pH of the polyacrylic acid. For example, at low pH (pH 3), poly(acrylic acid) is weakly polyanionic and has a loop conformation in solution. When functionalized PEI polymer chains are adsorbed onto the polyacrylic acid, a thick film results with a ''loopier'', more brush-like architecture which enables greater positively charge on the film surface to interact with the bacterial membrane (Gram-negative). Arguments were made that upon increasing the pH to higher values (pH 7), the poly(acrylic acid) chains undergo a conformational change forming a thin random coil conformation with many more negative charges, and that these polymer chains showed greater electrostatic interactions with the functionalized PEI leading to ''shielding'' of the interaction of positive charges of PEI with the bacterial cell membrane, resulting in the decrease in antibacterial activity of the films. In connection with hydrophobicity, it was observed that the polymer P18 (*N*,*N*-dodecyl-*N*-methyl-poly(ethylenimine), with the longest alkyl side chains) showed the best bactericidal activity against *S. aureus* and *E. coli.* To achieve 100% bactericidal and 60% antiviral performance a LbL films composed of a (PEI/poly(acrylic acid))$_{15}$ bilayer with PEI on top, with poly(acrylic acid) deposition at pH 3 was found to be optimal.

Carrageenans are natural, biocompatible, biodegradable sulfated polysaccharides, with three major classes which vary in the number and position of the sulphate groups on the galactose unit. They are excellent film forming materials. Following on from previously studies, where κ-carrageenan oligosaccharides showed antimicrobial activities against *E. coli*, *S. aureus*, *S. cerevisiae*, *P. citrinum* and *Mucor.* sp.,[72] Briones *et al.*[73] prepared contact-killing surfaces from PEI and κ-carrageenan (kappa), ι-carrageenan (iota), λ-carrageenan (lambda) (Table 2: P20, P21, P22) *via* a layer-by-layer self-assembly driven by the electrostatic interactions between positively charged PEI and the negatively charged sulfate groups of carrageenan (6 layers of coating). The results showed that PEI displayed no inhibition of bacterial growth for *S. aureus* and *E. cloaceae* and 76% inhibition growth for *E. faecalis*. λ-Carrageenan inhibited *S. aureus* by some 25%, while ι-carrageenan inhibited *E. faecalis* by 48% and *E. cloaceae* by 40%. The highest inhibition against *S. aureus* and *E. cloaceae* was obtained by PEI/iota carrageen (67% and 85% reduction), while the greatest inhibition against *E. faecalis* was 78% for PEI/lambda carrageenan. The results revealed that there was a synergetic antibacterial effect when PEI and carrageen were used as multilayer coatings, while again the power of poly-sulfonated materials is highlighted.

Table 2 Examples of polymers used to prepare PEMs with bacteriostatic properties

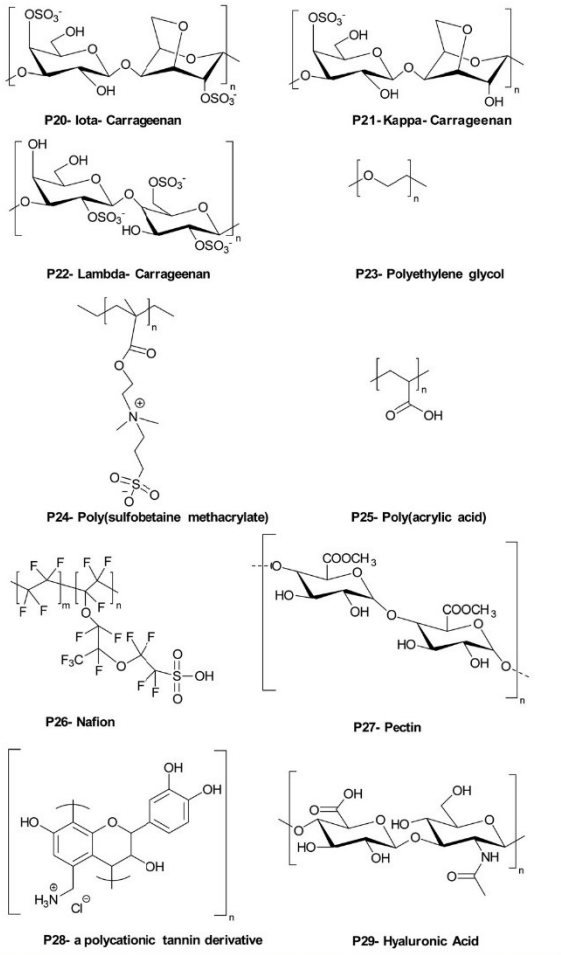

The well-known natural polycation chitosan has inherent antimicrobial activity against many pathogens, with three modes of action: lysis of the pathogens membrane, blocking bacteria from access to nutrients due to its strong metal-chelating properties as well as its DNA-binding ability.[74] Many layer-by-layer assemblies of antibacterial surface coatings based on chitosan have been formed using both synthetic and natural polymers. Kumorek *et al.*[75] constructed films using quaternized (trimethylammonium) functionalized chitosan(*N*-(2-hydroxypropyl)-3-trimethylammonium chitosan chloride) (see Table 1 – P19) and chitosan with tannic acid (TA) to evaluate their antibacterial activities against *E. coli* and *S. aureus*. Multilayers were deposited either on quartz slides with chitosan (see Table 1 – P16), *N*-(2-hydroxypropyl)-3-trimethylammonium chitosan chloride or TA-terminated layers – with 9 or 10 layers deposited. Contact-killing efficiency of the films showed a dependency on the terminal polymer layer coating and chitosan type. Thus, chitosan and *N*-(2-hydroxypropyl)-3-trimethylammonium chitosan chloride terminated LbL films showed better antibacterial activity than the TA-terminated films. Furthermore, *N*-(2-hydroxypropyl)-3-trimethylammonium chitosan chloride terminated multilayers showed improved inhibition of initial bacteria attachment, while the chitosan terminated multilayers were three times more effective at killing bacteria.

Hernández-Montelongo *et al.*[76] prepared LbL films of hyaluronan/chitosan and investigated their physicochemical properties and potential as antimicrobial materials. A 9-mer LbL film was prepared from hyaluronic acid and chitosan with the top layer being chitosan. Films were deposited onto silicon wafers as gel-type films at different pH's (pH 3.0 and pH 4.5) and ionic strengths to see how these changes altered the properties of the multilayer films and affected their antibacterial activity. The addition of salt into the deposition solutions affected the swelling behaviour of the PEM leading to the production of thicker films, while the pH of the deposited film solutions affected the interaction between polymer layers and the antibacterial activity of the films. To illustrate, at pH 4.5, hyaluronic acid (pK_a: 3.0) and chitosan (pK_a: 6.5) were largely in their ionized forms, and the polymer layers electrostatically interacted with each other strongly, thus blocking or shielding of the ammonium group of chitosan by the carboxylic groups of hyaluronic acid. However, at pH 3.0, many of the carboxylic acid groups on hyaluronic acid are non-ionised resulting in reduced interactions with the chitosan and allowing a higher number of ammonium groups to be exposed on the surface to interact with bacterial membranes. Thus, films of chitosan/hyaluronic acid constructed at pH 3.0 showed better bactericidal action against *X. fastidious* a plant pathogenic bacterium (that causes diseases of important crops) than films prepared at pH 4.5.

Another important antimicrobial polymer is ε-poly-L-lysine (ε-PPL), indeed polymers having 25–35 L-lysine residues is widely used in many countries as a food preservative. Zhang *et al.*[77] prepared ε-poly-L-lysine and gum Arabic multilayer films deposited on anodized titanium with the help of polydopamine with the ε-poly-L-lysine immobilized onto the surface in various ways. Thus, titanium surfaces were anodized in the presence of 0.5 wt% hydrofluoric acid to generate titanium dioxide nanotubes, which were immersed into dopamine hydrochloride to coat the surface with polydopamine *via* self-polymerization under slightly alkaline conditions (2 mg mL^{-1} dopamine in 10 mM Tris-HCl, pH = 8.5). Later, the first layer of ε-poly-L-lysine (10 mg mL^{-1}) was covalently grafted onto the polydopamine surface *via* reaction between the amines and the dopamine quinone (under alkaline conditions) and later gum Arabic was deposited onto the ε-PLL *via* electrostatic interactions. LbL films were also deposited onto the titanium dioxide nanotube surface by immersing into ε-PLL and gum Arabic. One-layer of ε-poly-L-lysine grafted onto the surface displayed better bactericidal activity than the dual ε-poly-L-lysine-gum surface, showing rupturing of the cell membranes of *S. aureus* and *E. coli*. The triple-layer film (ε-PPL/GA/ε-PPL) and the penta-layer film (ε-PPL/GA/ε-PPL/GA/ε-PPL) inhibited the attachment of bacteria

onto the surfaces. Furthermore, the layer-by-layer coated surfaces maintained their bacteriostatic action against *S. aureus* and *E. coli* for up to 3 weeks, again the cationic nature of the polymer driving their mode of action.

As mentioned previously, polymers that are cationic and hydrophobically modified show potent contact-killing activity against bacteria. Hydrophobically modified polyvinylamines are an interesting class of polycations which possess a high ratio of cationic groups and alkyl chains that form antibacterial surfaces (see the single polymer coating section). Thus, Illergård *et al.*[78] used hydrophobically modified polyvinylamines to prepare multilayer films with poly(acrylic acid) for an antibacterial surface coating. Multilayers were prepared by immersing, alternatingly, polyvinylamine at pH 7.5 as the cationic polymer and poly(acrylic acid) at pH 3.5 as the anionic polymer. Polymers were coated onto the surface with a number of different layers with the polycationic as the top layer. The 3-layer coated surface prepared with C8-epoxy chain modified polyvinylamine showed growth inhibition of $>99\%$. A live/dead assay proved that the bactericidal activity of the films, damaged the bacterial membrane. Later, they[79] coated anionic cellulosic wood-fibre with C8-epoxy chain modified polyvinylamine (100 mM NaCl, pH 9.5) and poly(acrylic acid) (100 mM NaCl, pH 3.5). Fibres were coated to give one, three and five layered materials (always with a polyvinylamine outmost layer). The films reduced the growth of *E. coli* and *B. subtilis* by 99% after 24 h of contact. The results revealed that even a simple layer coating was sufficient to generate a contact-active surface. To gain insight into the antibacterial mechanisms of physically adsorbed multilayers of polyvinylamine and polyacrylic acid, the surface charge of cellulose fibres was increased *via* radical oxidation (giving higher concentrations of carboxyl groups on the surface) leading to enhanced immobilization levels of polyvinylamine onto the fibre. In this case, the bactericidal action against *E. coli* and *B. subtilis* increased, while SEM images showed that the contact-killing activity of the fibre was due to membrane deformation.[80]

Chen *et al.*[81] investigated cellulose fibre LbL coatings with different polycations – namely poly(diallyl dimethyl ammonium chloride) (Table 1 – P15) and poly(allylamine hydrochloride). Results showed that a triple-layer poly(vinylamine)/poly(acrylic acid)/poly(vinylamine) showed better antibacterial activity compared to poly(diallyl dimethyl ammonium chloride)/poly(acrylic acid) and poly(allylamine hydrochloride)/poly(acrylic acid). The same group[82] changed the middle section (poly(acrylic acid)) to a wood-based cellulose nano-fibril, in order to enhance the antibacterial efficacy of the poly(vinylamine) based films. Bacteria adhesion increased on the fabricated of a triple-layer poly(vinylamine)/cellulose nano-fibril/poly(vinylamine) system but was some 10-fold better compared to the poly(acrylic acid)/poly(vinylamine) film in terms of membrane damage with elongation of the bacteria clearly seen.

1.1.3.2. Bacteriostatic PEMs. An alternative method to tackle pathogen colonisation is the generation of microbe-adhesion resistant surfaces, often by making the surface more hydrophilic. As an example, polyethylene glycol has been widely investigated as an antifouling surface coating. Poly(ethylene glycol) (see Table 2 – P23) grafted poly(acrylic acid) was adsorbed as a terminal layer onto a double layered LbL film of poly(diallyldimethyl ammonium chloride)/poly(acrylic acid) and poly(allylamine hydrochloride)/poly(acrylic acid) and deposited onto poly(dimethylsiloxane) and analysed with *S. cerevisiae.* Although poly(diallyldimethyl ammonium chloride)/poly(acrylic acid) and poly(allylamine hydrochloride)/poly(acrylic acid) showed minor anti-adhesive properties, the PEG grafted poly(acrylic acid)-terminated poly(diallyldimethyl ammonium chloride)/poly(acrylic acid) film was less adhesive by at least 2 orders of magnitude compared to bare poly(dimethyl siloxane).[83]

Antifouling coatings can be generated by zwitterionic polymers which repel microbes due to creation of an interstitial water/hydrogen-bonded network with a water layer adhering to the surface. Phosphobetaines, sulfobetaines and carboxylbetaines are the typically used zwitterionic polymers. Zhu *et al.*[84] fabricated zwitterionic polymers including multilayers *via* the layer-by-layer technique on a poly(vinyl alcohol) thin-film nanofibrous composites with electrostatic interactions between poly(sulfobetaine methacrylate) (Table 2– P24) and tannic acid with coating of a filtration membrane.

Poly(acrylic acid) is one of the mostly widely used counter block polyanions in LbL self-assembled films but shows major changes in forms between pH 3 to pH 6. Tang *et al.*[85] coated polysulfone microfiltration membranes with poly(allylamine hydrochloride) and poly(acrylic acid) (Table 2 – P25) at pH 3 to investigate their bacteriostatic properties. A single bilayer of poly(allylamine hydrochloride) and poly(acrylic acid) coated onto the membrane was used to analyse *E. coli* deposition kinetics to understand the bacteriostatic properties of the polyelectrolyte coted membrane. There was an approximately, 3-fold reduction in the number of *E. coli* found on the surface after coating, with the antiadhesive property of the modified membrane based on the highly swelling and hydrated polyelectrolyte coating preventing bacterial adhesion.

Gîfu *et al.*[86] investigated the antimicrobial activity of a 20-mer LbL film of hydrophobically modified sodium poly(acrylate) ($PAC_{18}Na$) complexes, with various chain lengths of cationic surfactants (decyl, dodecyl, tetradecyl and octadecyl trimethyl ammonium bromide) and poly(diallyldimethyl ammonium chloride) against *S. aureus*, *E. coli*, *P. aeruginosa*, and *C. albicans*. The best activity was found against *S. aureus*, with films of sodium poly(acrylate) complexed with tetradecyl and octadecyl trimethyl ammonium bromide, while poly(diallyldimethyl ammonium chloride) displayed total inhibition of growth after 2 h. *P. aeruginosa* showed greater resistance to the antimicrobial activity of the films, but after 6 h, films of sodium poly(acrylate) complexed with octadecyl trimethyl ammonium bromide and poly(diallyl dimethyl ammonium chloride) inhibited its growth. *C. albicans* was the least sensitive to the antimicrobial activity of the films with octadecyltrimethyl ammonium bromide complexed poly(acrylate) and poly(diallyldimethyl ammonium chloride) being the only film showing moderate inhibition of fungal growth after 24 h of exposure.

Gibbons *et al.*[87] built a new family of layer-by-layer coatings using Nafion (a Teflon-like backbone bearing sulfate groups) (see Table 2 – P26) the enzyme lysozyme and chitosan. (Nafion/Lysozyme)$_6$, (Nafion/Chitosan)$_6$, and (Nafion/Lysozyme/Nafion/Chitosan)$_2$ coatings showed excellent inhibition of *E. coli* and *S. aureus* growth (>99.9% compared to 58% for Nafion alone).

1.1.3.3. Bactericidal and bacteriostatic PEMs. There are examples of PEMs that exhibit both bactericidal and bacteria-adhesion resisting properties. Martins *et al.*[88] prepared chitosan-based multilayer films with plant-derived polyionic polysaccharides Carrageenan (iota-carrageenan) and pectin (Table 2 – P27) and evaluated them against *S. aureus* and *P. aeruginosa* as cytocompatible antibacterial coatings. The protonation of the amino groups on chitosan being a key factor in the antimicrobial activity of the polyelectrolyte films, while the hydrophilicity of the polysaccharides in the PEMs would also reduce microbial adhesion. 15 layers of each polymer (around 16 ± 0.9 nm total thickness) were deposited onto oxidized glass substrates at pH 5.0 (X-ray photoelectron spectroscopy showed that the $-NH_3^+$ peak intensities on the surface of the pectin-chitosan film were higher than on the iota-carrageenan-chitosan film showing binding). The bactericidal action of the film was observed after 6 h for *P. aeruginosa* and 24 h for *S. aureus*. The same group[89] also prepared hydrophilic, bactericidal, and anti-adhesive PEM LbL films using polycationic tannin (see Table 2 – P28) as a replacement for chitosan, and the polysaccharides, Carrageenan (iota-carrageenan) and pectin. Here the cationic NH_3^+ and phenolic moieties were argued as being the main reasons for their potent bactericidal action against *S. aureus* and *P. aeruginosa*, while the anionic hydrophilic components of the polysaccharides, (due to the sulfate groups of iota-carrageenan and the carboxylate group of pectin) gave rise to the bacteriostatic properties of the PEMs.

Hoyo-Gallego *et al.*[90] built chitosan/hyaluronic acid (Table 2 – P29) bactericidal and bacteria repelling LbL films on poly(ethylene terephthalate). Without the PEM coating, the number of viable bacteria on the poly(ethylene terephthalate) surface was 1.3 × 105 CFU cm^{-2} while after coating with 10 layers of chitosan/hyaluronic acid, *E. coli* viability on the coated surface decreased significantly (8 CFU cm^{-2}). In addition, the stability of the film was robust due to the presence of lysozyme and hyaluronidase and was stable in phosphate buffer. The authors suggested that the hydrophilic character of hyaluronic acid and the bactericidal nature of chitosan made this film a suitable candidate for biomedical coatings.

Although electrostatic interactions are favourable to design layer-by-layer deposition of polymers, Xu *et al.*[21] produced a layer-by-layer multilayer deposition showing anti-fouling, antimicrobial, and biocorrosion inhibition from polyethyleneimine-β-cyclodextrin and ferrocene-modified chitosan *via* host–guest interaction chemistry on stainless steel. β-Cyclodextrin is the most popular host that able to guest various molecules due to its hydrophilic internal cavity. Similarly, ferrocene is also a widely used guest molecule for β-cyclodextrin. Thus, PEI and chitosan were functionalized with these host–guest groups. Then, poly(dopamine) anchored stainless steel surfaces were coated by alternately dipping into polyethyleneimine-β-cyclodextrin and ferrocene-modified chitosan solutions at pH 5. This took place 1, 5 and 11 times with alternative deposition of PEI and chitosan solutions. The antimicrobial and antifouling efficacies of the multilayer coatings were tested on bacteria (*Pseudomonas* sp. and *S. aureus*), microalgae (*A. coffeaeformis*), and barnacle cyprids. Tests revealed that as the number of host–guest assembled bilayers were increased, the antimicrobial and anti-biocorrosion performance were improved. Only a small number of viable bacteria adhered on the 11-bilayered surface with their antifouling properties much better than those compared to other assembled surfaces. The multilayer coatings were also found to be stable and durable after 35 days immersed in seawater. These environmentally friendly coatings could be useful for combatting biofouling and biocorrosion in marine and aquatic environments.

1.2. Polymers covalently immobilized onto the surfaces

Antimicrobial surfaces can also be created using covalent bonds between polymers and various surfaces is such a route to polymerize/attach functional polymers onto surfaces.[91] For example Su *et al.*[92] designed a surface by constructing a bottom bactericidal layer (800 nm) consisting of the monomer (*N*-(4-vinylbenzyl)-*N*,*N*-dimethylamine) and a crosslinker (ethylene glycol diacrylate) with a second monomer (vinyl pyrrolidone) introduced to give a hydrophilic layer. Poly(*N*-(4-vinylbenzyl)-*N*,*N*-dimethylamine) coatings exhibited more than 99.9% killing of both *E. coli* and *B. subtilis* regardless of the incorporation of vinyl pyrrolidone on the surface. However, incorporation of vinyl pyrrolidone led to much better antifouling resistance and improved biocompatibility.

Fluorinated polycationic polymers were attached onto textiles by Song *et al.*[93] *via* initiated chemical vapor deposition, forming poly(dimethylaminomethylstyrene-*co*-1*H*,1*H*,2*H*,2*H*-perfluorodecyl acrylate). The cationic fluorinated polymer coated surface reduced by some 3-log units the attachment of methicillin resistant *S. aureus* and *E. coli* (99.9% killing efficiency). The antimicrobial mechanism of the polymer was explained by their similarity with other cationic polymers. In addition, the hydrophobic group of the polymer was attributed to the greater binding efficacy shown to *E. coli* resulting in better penetration of the polycations. The polymer surface was tested on lentivirus (an enveloped virus) and again, due to electrostatic interactions between positively charged groups on the polymer surface and the "negatively charged lentivirus" as well as hydrophobic interactions with the viral "membrane", the cationic fluorinated polymer surface damaged the viral structure.

Among the various covalently bonded surfaces, polymer brushes are of particular interest as non-leachable coatings in biomedical applications due to their mechanical stability and tuneable thicknesses. Such grafted polymer chains can be generated using a variety of polymerisation techniques and also allow subsequent modification with other functional groups.[94]

1.2.1. Polymeric brush surfaces. Covalently attached polymer brushes can be generated using either "grafting to" or

"grafting from" methods. The "grafting to" technique requires a reaction between an end-functionalized polymer and suitable functional groups on the surface/substrate to form a tethered polymer chain. Although this technique has advantages compared to other methods, such as enabling the characterization of polymer chains prior to grafting, low density grafted polymer brushes are typically formed due to reactive site hindrance.[95] "Grafting from" techniques comprises a polymerization which begins with surface bound initiators leading to growth of the polymer chains using monomers from solution. Depending on the levels of surface functionalisation and monomer concentration, this technique can produce high grafting densities and broad dispersities with respect to chain length.[96] In antimicrobial applications, polymer brush coatings have been designed to be biocidal and self-adaptable (switchable), altering the antimicrobial action from biocidal to antifouling.

1.2.2.1 Bactericidal polymeric brush surfaces. Metallic implants and devices used in clinical applications tend to generate bacterial associated infections. To combat bacteria associated infection on titanium alloys, Peng *et al.*[97] designed a surface coating made of a novel phosphonate/active ester block polymer composed of phosphonate units (degree of polymerization of 29) that served as the metal anchoring segment and NHS active ester units (various degree of polymerization: 7, 29, and 64) which were conjugated to poly(hexamethylene biguanide). Although all copolymers of poly(diethyl(methacryloyloxymethyl)phosphonate-*b*-*N*-hydroxysuccinimide methacrylate) showed great antimicrobial activity (following conjugation) the polymer having 64 active ester repeat units, and then functionalized with poly(hexamethylene biguanide) showed the best antimicrobial activity, killing and inhibiting 100% of *E. coli* and *S. aureus*. The ruptured membrane along with intracellular matrix release indicated that the polymer showed bactericidal action due to interaction of the guanidine groups with the various negatively charged components in/of the bacteria with no suppression of mammalian cell viability. *In vivo* data showed that the polymer coating significantly inhibited colonisation of bacteria on implants and consequently decreased levels of bacterial associated infection.

Poly(ethylene terephthalate)[98] is perhaps one of the most widely used synthetic polymers due to its low cost, and mechanical and chemical stability. It is also inert and hence often biocompatible. Thus, PET has seen utilization in heart valves, vascular grafts, surgical meshes, and artificial ligaments. However, PET can be contaminated by microbes as it does not have any inherent antimicrobial properties. Therefore, Cao *et al.*[99] covalently grafted poly(hexamethylene guanidine hydrochloride) – a well-known cationic polymeric bactericide that shows potent killing activity against a range of pathogens with a mechanism of action mediated *via* electrostatic interactions with negatively charged cell surface components. Here, a polymeric brush surface was developed using poly(ethylene terephthalate) that was modified *via* aminolysis with ethylenediamine. This amine was then reacted with ethylene glycol diglycidyl ether that had itself been reacted with poly(hexamethylene guanidine hydrochloride). Uncoated and amine group terminated PET surfaces showed no bactericidal activity whereas the polymer brush coated PET surfaces showed excellent bactericidal activity against *E. coli* and *S. aureus*.

Larikov *et al.*[100] prepared glass surfaces with covalently immobilized poly(allylamine) (*via* 3-glycidoxypropyltrimethoxy silane modification of the glass followed by reaction with free amino groups), which showed bactericidal activity against *S. epidermidis* and *S. aureus* (eliminating ~97%) and *P. aeruginosa* (88%). Comparison with electrostatically bound poly(allylamine) surface *vs.* covalently attached polyallylamine surface showed that the killing efficiency of the covalently attached surfaces were much higher with improved robustness and that surface charge was more important than the chain lengths of the polymer.

It is known that cationic polymers bearing quaternary ammonium salts along the polymer chain display high killing of pathogens. Li *et al.*[101] prepared a stable antimicrobial coating with two natural polymer derivatives, agarose and quaternized chitosan *via* the "grafting-to" method onto polymer films [polyurethane and poly(vinyl fluoride)], and titanium foil. Polymers were covalently grafted *via* a "thiol-ol" reaction (conjugation under UV irradiation in the presence of oxygen with dimercaprol serving as both an anchor and as a crosslinker between the surface and grafted polymer). Due to the antiadhesive nature of agarose and the bactericidal nature of chitosan, the prepared surfaces thus offer two different modes of action. The agarose grafted surfaces inhibited biofilm formation of both *P. aeruginosa* and *S. aureus* (99% compared to the uncoated surfaces). In addition, agarose and chitosan grafted surfaces maintained their antibacterial activities for 30 days after repeated ethanol treatment or autoclaving. When the quaternized chitosan grafted polyurethane or poly(vinyl fluoride) surfaces were "contaminated" with drops of viable *S. aureus* and *P. aeruginosa*, a negligible number of bacteria remained alive after contact (in contrast the surfaces were non-cytotoxic to 3T3 fibroblasts). Again, the quaternized ammonium groups (in this case on the chitosan) mediated contact killing of bacteria.

Correia *et al.*[102] developed chitosan scaffolded surfaces functionalized, with *N*,*N*-dimethyldodecylamine quaternized poly(2-oxazoline)s using 2-methyl-2-oxazoline, 2-ethyl-2-oxazoline or 2-bisoxazoline with the 'grafting-from' method performed, using super critical CO_2 as a solvent. They found that quaternized poly(2-methyl-2-oxazoline) grafted chitosan scaffold was the most effective against *S. aureus* and *E. coli* (killing almost 100% in 3 min), which also prevented of biofilm formation. Moreover, this scaffold was able to purify water samples taken from different sources and performed well over multiple cycles.

Koufakis *et al.*[103] investigated poly(2-(dimethylamino)ethyl methacrylate) (PDMAEMA) brushes quaternized with various alkyl chain lengths as biocidal coatings with surface-initiated atom transfer polymerization used to grow polymer chains on silicon wafers. Three different molecular weight of poly(2-(dimethylamino)ethyl methacrylate) (M_w: 30 kDa, 81 kDa and 110 kDa) were synthesized and the polymers were quaternerised

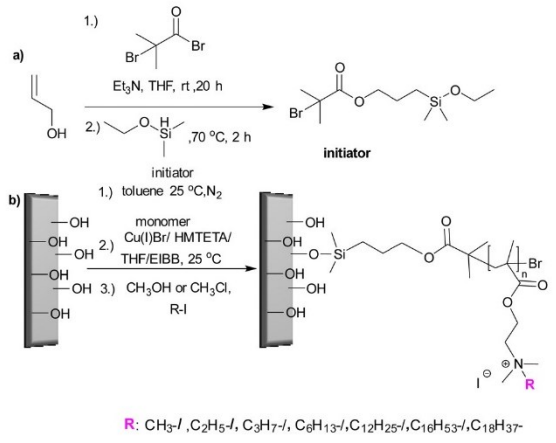

Fig. 9 (a) Silyl-based initiator synthesis; (b) initiator immobilisation and synthesis of PDMAEMA brushes and quaternization with various alkyl chain lengths *via* surface initiated-ATRP.[103] Reproduced with permission from {Koufakis, E.; Manouras, T.; Anastasiadis, S. H.; Vamvakaki, M. Film Properties and Antimicrobial Efficacy of Quaternized PDMAEMA Brushes: Short vs Long Alkyl Chain Length. *Langmuir* 2020, **36**, 3482–3493}. Copyright {2020} American Chemical Society.

with various alkyl halides and tested against *E. coli* and *B. cereus*. (see Fig. 9). Polymers having short alkyl chains (*e.g.*, methyl, ethyl, and propyl) showed a 100–1000-fold decrease in bacterial adhesion, but with 99% killing of adhered bacteria, while non-quaternized and long alkyl chains (more than 6 carbons) showed little reduction in bacteria colonisation. They explained this phenomenon as conformational alteration in the polymer due to formation of a "cumbersome hydrophobic barrier" with the long alkyl chains preventing the interaction of quaternized cationic moieties with the bacteria. On the other hand, polymers with short alkyl chains were able to move more freely, and the positive charges could interact with the negatively charged bacterial cell membrane leading to perforation and lysis. Field emission scanning electron microscopy images (Fig. 10) showed the bactericidal effect of the low molecular weight, methyl quaternized, PDMAEMA brushes with a collapsed bacterial morphology with damaged membranes, while non-quaternized or octadecane quaternized polymers showed intact bacteria adhesion.

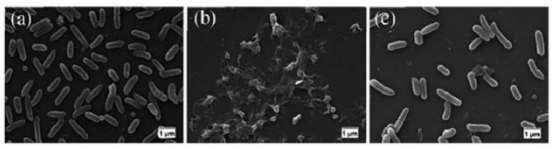

Fig. 10 Field emission scanning electron microscopy images of *E. coli* adhesion onto the surfaces of low molecular weight PDMAEMA brushes: (a) non-quaternized PDMAEMA; (b) methyl quaternized PDMAEMA and (c) octadecyl quaternized PDMAEMA.[103] Reprinted with permission from {Koufakis, E.; Manouras, T.; Anastasiadis, S. H.; Vamvakaki, M. Film Properties and Antimicrobial Efficacy of Quaternized PDMAEMA Brushes: Short vs Long Alkyl Chain Length. *Langmuir* 2020, **36**, 3482–3493}. Copyright {2020} American Chemical Society.

Using similar polymerization techniques Yandi *et al.*[104] prepared poly(2-(dimethylamino)ethyl methacrylate) brushes for use against the marine alga *Ulva linza* and *U. lactuca* in order to understand the anti-algal effects of the brushes, spore adhesion and growth. In this case a self-assembled mono layer surface was formed using α-bromoisobutyrate-11-mercapto-undecane as the initiator for ATRP polymerization. Poly(2-(dimethylamino)ethyl methacrylate) brushes were anti-algal, killing zoospores upon contact as well as inhibiting the growth of spores. This phenomenon was again explained by electrostatic interactions of the negatively charged spores and the cationic groups of the polymer brushes, disrupting the membrane, a similar mechanism to that of poly(2-(dimethylamino)ethyl methacrylate) and its antimicrobial mode of action.

Lu *et al.*[105] prepared poly(diallyldimethyl ammonium chloride) grafted onto cellulose filters whose hydroxyl groups had been reacted with 2-bromisobutyryl bromide (by esterification), thus serving as a macroinitiator in an ATRP reaction to allow the grafting of diallyldimethyl ammonium chloride. Uncoated membranes and different levels of poly(diallyldimethyl ammonium chloride) grafted onto the cellulose membrane were tested for bacterial killing by immersing into bacterial suspensions with a grafting ratio of 13 wt%, reducing bacterial numbers by 98% for *S. aureus* and 92% for *E. coli*.

Undoubtedly, contact lenses are one of the most widely used devices to correct refractive errors and maintain ocular health. However, wearing contact lens use can cause adhesion and colonization of bacteria which can develop conditions such as acute red eye, acute dry eye, microbial keratitis or corneal complications (neovascularization, edema, staining) and so on.[106]

Chan-Park *et al.*[107] developed two silicone contact lens coatings *via* ozone-activation and thermal-polymerization. In the first coating, PEI was grafted with poly(ethylene glycol) methacrylate with the polymer tethered onto the surface *via* thermal polymerization (with the help of peroxide groups after ozone activation of the surface). This surface displayed good *in vitro* antibacterial properties against methicillin resistant *S. aureus* with an average log reduction of 5 (<99.99% killing) and with high mammalian cell viability. Another coating was synthesized starting from the monomers glycidyl methacrylate (for PEI grafting) and *N*-(3-sulfopropyl)-*N*-(methacryloxyethyl)-*N*,*N*-dimethylammonium betaine (as a hydrophilic unit for the coating) with polymerization based on free radical polymerisation followed by macromolecular grafting. The best polymer formulation for antimicrobial activity used 1 wt%, glycidyl methacrylate, 1 wt% of the hydrophilic betaine and 0.5 wt% PEI (M_w: 2 kDa) with a more than 6 log reduction of methicillin resistant *S. aureus* yet with 90% fibroblast cell viability.

Covalent immobilization of antibacterial peptides onto surfaces has gained a great deal of interest due to their fast, effective, and broad-spectrum killing action. Gao *et al.*[108] investigated the antibacterial properties of polymer brush systems coated onto titanium surfaces with primary amines containing copolymers (*e.g.* poly(*N*-(3-aminopropyl))methacrylamide-*co*-(*N*,*N*-dimethylacrylamide)) synthesized by surface initiated

atom transfer radical polymerization. Here, the cysteine functionalized cationic, antimicrobial peptide Tet213 (KRWWKWWRRC), was conjugated onto the copolymer brushes using a maleimide-thiol addition reaction after initial modification of the grafted chains using an *N*-hydroxysuccinimide ester of 3-maleimidopropionic acid. They found that the graft density of the peptide on the surface had a strong effect on the antibacterial activity of *P. aeruginosa*. The same group[109] also tested an antimicrobial peptide tethered brush coating generated from a copolymer of *N*,*N*-dimethylacrylamide-*co*-*N*-(3-aminopropyl)-methacrylamide (5/1 monomer ratio) and the peptide Tet-20 (KRWRIRVRVIRKC) against *P. aeruginosa* and *S. aureus*. Peptide coated titanium wires showed a 5-log decrease in CFU (compared to uncoated), in addition, peptide coated wires, which were implanted into subcutaneous pockets of rats, showed a decrease in *S. aureus* levels by at least 85%. It is likely that the use of the D-amino acid peptide enantiomer would promote the effect, as the L-enantiomer would be degraded by proteases. The antibacterial effect here is mediated by the mixed hydrophobic/cationic peptide and the non-bonding nature of the dimethylacrylamide.

Urinary Tract Infections are the most common type of infection. In hospital settings a major cause is ureteral stents that remain in position for long periods. Unfortunately, *Proteus mirabilis* (*P. mirabilis*), which is the main urease positive pathogen in the ureteral system, starts to form biofilms which induces encrustation (urinary tract stones), hindering the flow of the urine. Later, mucosal injury occurs, and the medical device must be replaced with a surgical operation. Gultekinoglu *et al.*[110] developed an antimicrobial PU stent upon which the cationic polymer PEI was grafted, with the stent showing a significant decrease in bacteria adhesion under static conditions. The same group[111] studied two different molecular weight PEI's (1.8 and 60 kDa) grafted PU stents and also alkylated these with hexyl bromide to enhance their antimicrobial activity within a dynamic biofilm reactor, to observe bacteria adhesion, biofilm formation and encrustation. The grafted PEI affected bacteria adhesion owing to the dynamic motion of the brushes in the liquid environment with the alkylated PEI brushes disrupting the bacteria cell wall upon contact. The high molecular weight PEI grafted stent decreased biofilm formation by up to 2 orders compared to unmodified PU's, in *in vitro* experiments. Free Ca^{2+} and Mg^{2+} ions play a key role in the encrustation process; hence, PEI brush stents were tested in terms of deposition onto the stent surfaces (encrustation). The grafted PEI inhibited Ca^{2+} and Mg^{2+} ions deposition by 81% and 93%, respectively in *in vivo* animal models and showed reduced inflammation in host tissue.

1.2.2.2. Dual-functional polymeric brush surfaces. Hydrophilic polymers and zwitterionic polymers generate a hydration layer that forms a physical-type barrier that gives rise to the anti-adhesive properties of surface. This combination of a robust interfacial hydration layer and steric repulsion generates resistance to protein/bacterial binding.[112–115] Such polymeric brushes can be prepared on various surface such silicone catheters and in this content, Yu *et al.*[116] prepared an antimicrobial polydimethylsiloxane surface coating showing both antifouling and bactericidal activity against *E. coli via* sub-surface-initiated atom transfer radical polymerization. Firstly, a vinyl-terminated initiator was blended with polydimethylsiloxane, then 2-(dimethylamino)ethyl methacrylate was polymerized onto the entrapped initiator *via* atom transfer radical polymerization and then quaternized with 1,3-propanesultone and 1-bromo-undecane to obtain zwitterionic and bactericidal groups on the same polymer brush. Antimicrobial and antifouling activities of the polymer were investigated, and it was found that grafting density, grafting time and degree of quaternization and sulfobetainization of polymer had a great impact on their properties. In terms of antifouling approaches, hydrophilic polymers have been employed to form a hydration layer to prevent attachment of bacteria to surfaces, while exhibiting both microcidial and anti-adhesive actions, again with a focus on reducing catheter related infections. Zhang *et al.*[117] developed a polymeric catheter surface with a foundation zwitterionic polymer layer (poly(3-[dimethyl-[2-(2-methylprop-2-enoyloxy)ethyl]azaniumyl]propane-1-sulfonate)) with an upper layer of poly(methacrylic acid), displaying antifouling, bactericidal and hemocompatible properties. Polyurethane surface functionalization with an initiator allowed a zwitterionic polymer to be grafted from the surface, with poly(methyl methacrylate) grafted onto the zwitterionic brush, and an antibacterial peptide coupled *via* amidation. The hydration layer created by the hydrophilic and negatively charged polymer brushes generated an antifouling surface active against both *E. coli* and *S. aureus* under static and hydrodynamic conditions.

It is a challenge to design a surface that can prevent bacterial infections and show antiadhesive properties while promoting tissue biocompatibility. Hoyos-Nogués *et al.*[118] prepared a titanium surface showing both inhibition of bacterial colonization while promoting osteoblast cell attachment for dentistry applications. Thus, PEG was added by an electrodeposition process, followed by the immobilization of peptides that promoted both cell proliferation (Arg-Gly-Asp (RGD)) and bactericidal action (adding the peptide LF1-consisting of 11 residues from the amino-terminus of lactoferrin). The antibacterial activity was tested against *S. sanguinis* – a primary colonizer in oral biofilms. Due to the low bio-fouling property of the PEG coating on the surface, bacterial attachment was significantly decreased on the PEG and PEG-peptide coated surfaces. In addition, SEM images showed PEGylated surfaces inhibited the formation of filamentous appendages (called fimbria) that lead to bacteria adhesion to solid surfaces and later biofilm formation. Furthermore, the PEG-peptide coated surfaces increased the percentage of dead bacteria, while reducing the adhesion of bacteria compared to a simple PEG coated titanium surface.

Fu *et al.*[119] prepared a novel antimicrobial mix brush surface based on poly(*N*-hydroxyethyl acrylamide) and poly(trimethylamino)ethyl methacrylate chloride on silica surfaces. The mixed polymer brush coating was generated through surface-initiated atom transfer radical polymerization (for the antifouling monomer) and surface-initiated/mediated polymerization

(for the cationic monomer). The 100% poly(*N*-hydroxyethyl acrylamide) surface showed excellent antifouling properties, while the 100% cationic poly(trimethylamino) ethyl methacrylate chloride surface showed bactericidal activity with dead bacteria on the surface. In order to prevent attachment of dead bacteria while maintaining bactericidal activity, an in a ratio of initiators 1 : 1 was used to give a mixed polymer brush having both antifouling and antibacterial activity against Gram-positive and Gram-negative bacteria. The mixed brush surface reduced the attachment of dead bacteria by ~10 fold, while maintaining a high kill level (the killing ability of the cationic brushes based on the interaction of the polymeric cationic groups with the various anionic components of the bacterial membrane/wall causing distortion and leakage of intracellular components, resulting in death of the bacteria).

An antimicrobial surface was created by He *et al.*[120] with the mixing of two types of dopamine-modified polymers (inspired by mussel adhesion chemistry). Thus, butyl, octyl and dodecyl quaternized poly(2-(dimethylamino)ethyl methacrylate) and poly(sulfobetaine methacrylate) was synthesized *via* ATRP with dopamine-modified with a 2-bromoisobuty group as an initiator. The effect of the *N*-alky chain length, of the quaternized ammonium group of poly(2-(dimethylamino)ethyl methacrylate) on antimicrobial activity of a mixed brush surface was noted to decrease with increasing chain length, arguably because of the shielding effect of the *N*-alkyl chains on the hydrophilicity of the polymer. Of note, [poly(sulfobetaine methacrylate)/poly(2-dimethylbutylammonium)ethyl methacrylate] mixed brushes exhibited bactericidal and antifouling properties. When poly(2-dimethylbutylammonium)ethyl methacrylate content was in the range of 10–50% on the surface, the killing efficiency of polymer brushes against *S. aureus* was reached to 74–92%. Longer *N*-alkyl chains polymers (*e.g.* octyl quaternized) displayed a killing level of 69–94% when the quaternized content was in the range of 10–30%. For, poly(sulfobetaine methacrylate)/dodecyl quaternized poly(2-(dimethylamino)ethyl methacrylate) up to 10% was needed for good bactericidal and antifouling activity against *S. aureus*.

1.2.2.3. Self-adapting polymeric brush surfaces. Self-adaptable surfaces that can changes their antimicrobial properties from bactericidal to antifouling by a stimuli-responsive strategy have been an attractive development that has allowed the preparation of new antimicrobial surfaces coatings. Intravenous catheters are the one of the most widely used devices in clinics, unfortunately, catheter-associated infectious are associated with high levels of morbidity and mortality are very common. Thus, innovative catheter coatings are essential. Zhang *et al.*[121] prepared self-adaptive antibacterial surface with switching on of antibacterial action in the presence of bacteria. The first block of the polymer brush coating was a bactericidal poly(2-(dimethyldecylammonium)ethyl methacrylate) using monomer 2-(dimethyldecylammonium) ethyl methacrylate grafted *via* a surface-initiated atom transfer polymerization onto a polyurethane (to had been coupled to initiator). The second block was hydroxyethyl methacrylate, with the hydroxyl group of the polymer oxidized (to aldehydes) to allow conjugation of amine terminated polyethylene glycols (PEG's) *via* Schiff base formation. In the presence of bacteria, the imine bonds hydrolyse due to bacterial metabolism and the creation of a locally acidic microenvironment, thus releasing the upper PEG layer, and thereby revealing the lower bactericidal layer that eliminates the bacteria and inhibits infection. The polymer brush coated surfaces reduced by 97% the level of *S. aureus* binding in the short term (10 h) and killed 82% of bacteria over 24 hours. In addition, the antibacterial activity of this self-adaptive surface was tested under hydrodynamic conditions and showed high antifouling efficiency (88% reduction of bacteria adhesion). By applying a similar strategy, an arginine-based switchable surface coating was generated, turning from bactericidal to antifouling.[122] The key here being the use of L-arginine methyl ester-methacryloylamide polymer brushes grafted by surface-initiated reversible addition–fragmentation chain-transfer. Here, the glass surfaces were modified with polydopamine *via* catechol coordination, and then functionalized with a chain transfer agent to allow RAFT polymerization. Subsequent polymerization was carried out to allow generation of a polymer brush surface. Due to the guanidinium groups on the polymer brushes, the surfaces showed bactericidal activity against *S. aureus* and *E. coli.* Upon hydrolysis of the ester the surface changed from a bactericidal state (due to cationic groups) to an antifouling state due to the zwitterionic groups thus preventing the adhesion of *S. aureus* and *E. coli* and *A. coffeaeformis* (Fig. 11).

pH-responsive tannic acid-scaffold binary polymer brushes have been prepared as coatings. Here azido-modified tannic acid was prepared and coupled as a co-polymer that had been generated using a dibenzocyclooctyne modified chain transfer agent *via* RAFT polymerization as well as cationic dibenzocyclooctyne modified poly-lysine *via* a copper-free azide–alkyne cycloaddition reaction (these were coated onto stainless steel surfaces *via* coordination chelation chemistry). The antimicrobial activity of the surface was tested with *S. epidermidis* and *E. coli* and *A. coffeaeformis*. Since poly(2-diisopropylaminoethyl methacrylate) shows reversible pH switching behaviour, such that when the pH decrease (below the pK_a value of 6.3) the poly(2-diisopropylaminoethyl methacrylate) chains swelland the zwitterionic polymer segment becames dominant, showing

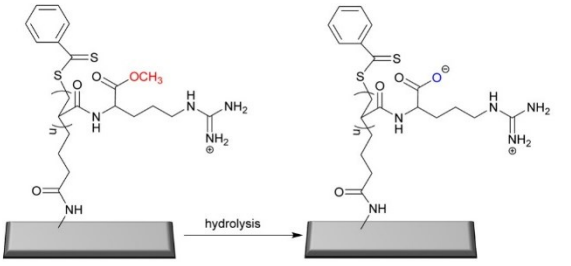

Fig. 11 The hydrolysis of L-arginine methyl ester-methacryloylamide based-brushes used to generate a "switch-on" antifouling surface by ester hydrolysis.[122] Reprinted (adapted) with permission from {G. Xu, X. Liu, P. Liu, D. Pranantyo, K. Neoh and E. Kang, *Langmuir*, 2017, **33**, 6926–6936} Copyright {2017} American Chemical Society.

antifouling properties. However, when the pH increases, the poly(2-diisopropylaminoethyl methacrylate) chains collapse and the poly-lysine chains became "dominant/exposed" showing bactericidal action.[123]

Wu *et al.*[124] developed a polymeric mixed brush surface that altered bacterial attachment in response to pH. Thus, vinyl and alkyl bromine functionalized gold surfaces were prepared and poly(2-(dimethylamino)ethyl methacrylate) was generated *via* thermally initiated free radical polymerization and then visible light photoinitiated polymerization for poly(acrylamide phenylboronic acid) grafting. At low pH's poly(2-(dimethylamino)ethyl methacrylate) have protonated tertiary amino groups and the surface bound *S. aureus*, whereas at higher pH values (pH 9.0) the ammonium groups of the polymer become deprotonated and the boronic acids become boronates making the surface negatively charged and bacteria repellent.

Although cationic groups of polymers typically show high antimicrobial efficacies, they may show toxicity to mammalian cells and promote biofilm formation, due to the non-removal of dead microbes from the surface. For this reason, switchable polymer brush surfaces have the vision of creating an ideal "cleaning" antimicrobial surface. Yan *et al.*[125] designed a hierarchical polymer brush surface having a "zwitterionic" outer most layer with an underlying polycationic bactericidal polymer. Thus [3-(methacryloylamino)propyl]dimethyl(3-sulfopropyl)ammonium hydroxide inner salt and 2-(dimethylamino)ethyl methacrylate were graft polymerized onto silicon wafers bearing photoiniferter moieties. The cationic elements of the polymer brush were further modified with 1-bromoethane to give a stable cationic charge (as quaternary ammonium salt). Since medical devices can be contaminated by airborne bacteria antimicrobial surface should also be effective against microbes in the dry state. Here, the synthesized polymer killed ~76% and ~95% of *S. aureus* and *E. coli*. Here, the mechanism of the polymers is based on the quaternary ammonium groups interacting with the bacteria membrane/cell wall leading to lysis of bacteria with the sulfonated brushes in a collapsed position in the dry state. Under wet conditions such as body fluids containing planktonic bacteria, the sulfonated layer bearing polymer brushes prevent the accumulation of bacteria (reduction of ~98% and ~97% for *S. aureus* and *E. coli*) and showed high killing rates (~80% and ~77% for *S. aureus* and *E. coli*) relative to surfaces prepared with polycationic polymer brushes alone. In addition, the polymer showed that bacteria attachment onto the surface was prevented over longer term. Due to the sulfonated groups of the brushes, the cationic groups stayed physically hindered from mammalian cells, thus the toxicity induced by cationic groups of the polymers was prevented.

Chen *et al.*[126] created a hierarchical polymeric brush surface made up of cationic units [poly(1,3-bis-*N*,*N*-dimethyl-*N*-octylammonium)-2-propylacrylate dibromide] and a zwitterionic poly(sulfobetaine methacrylate) antifouling layer *via* surface-initiated atom transfer radical polymerization. In the design the graft density of the cationic polymer was changed to allow evaluation of the effect on its self-cleaning ability. The optimum graft density of the brush was approximately 61 nm and prevented binding of over 70% of *E. coli* of *S. aureus* compared to the bare surface. The mode of action is believed to be due to high charge density and long alky chains of cationic polymer unit, the brushes could bind bacteria, leading to the breakage of the bacterial cell membrane and lysis of the bacteria.

2. Polymer solutions as antimicrobial agents

Antibiotics provide powerful ammunition for mankind to tackle pathogenic diseases. However, widespread misuse and poor stewardship has led to widespread resistance, specifically, multidrug resistant Gram-negative bacteria whose outer membrane acts as a barrier to many antibiotics. Therefore, new solutions are essential, and polymers have emerged as part of the solution to combat such diseases, with key learnings coming from natural host defence peptides and polymers that typically interact with both the negatively charged (phospholipid) and hydrophobic elements of the bacterial outer membrane (Gram-negative). Thus, if synthetic polymers can be designed and fabricated such that they have facial amphiphilicity effective interactions with the bacterial membranes will occur. Rahman *et al.*[127] synthetized polymers having intrinsic facial amphiphilicity using bile acids (cholesterol-derived amphiphilic steroid acids). Initially monomers were synthesized by esterification with three different bile acids (lithocholic, deoxycholic, and cholic acid) and hydroxyethyl methacrylate and homopolymers synthesized *via* RAFT polymerization. These homopolymers were further modified by esterification (lithocholic, deoxycholic, and cholic acid having one, two and three available alcohol groups) with different lengths of bromoalkanoyl chloride and the alkyl bromide groups on the subsequent polymers substituted with trimethylamine to form quaternary ammonium polymer side chains. Homopolymers of cholic acid showed the best activity against *S. aureus*, *E. coli* and *P. aeruginosa* while the cholic acid derived polymers with a pentyl spacer between the ester and the quaternary ammonium group exhibited the best antimicrobial properties (MIC values 7–15 $\mu g\ mL^{-1}$). The cholic acid polymers bearing five methylene spacers and having a molecular weight around 10 kDa displayed the most effective antibacterial action compared to higher molecular weight polymers. The cationic groups on each cholic acid unit interacted with the outer membrane of the bacteria *via* electrostatic interactions and the hydrophobic cholic acid interlacing into the membrane lead to bacterial death. Recently, the same group[128] used nanostructured polymers with facial amphiphilicity to combat multidrug resistant bacteria. Thus, copolymers of cholic acid methacrylate (2-methacryloyloxy)ethyl cholate, and poly(ethylene glycol)methacrylate were synthesized *via* reversible addition–fragmentation chain transfer polymerization. Copolymers bearing 90 and 70 mol% of cholic acid formed spherical particles, while copolymers at 58 and 47 mol% formed rod like structures in water with an average diameter of 150–400 nm. The spherical particles

inhibited the growth of Gram-negative bacteria (minimum inhibition concentration for the polymer bearing 90% cholic acid was 13 and 10 μg mL^{-1} against *E. coli* and *P. aeruginosa* respectively), while the rod-shaped polymers were effective against *S. aureus*, with the killing mechanism associated with membrane disruption as observed *via* SEM.

Zhou *et al.*[129] designed host-defence peptide mimics *via* glycine-pendent polyoxazolines with four polymers varying in lengths (from 6 to 40-mers) synthesized. The best polymers were found to contain 20 monomers with an MIC value between 3–12 μg mL^{-1} (against *S. aureus*) (including drug resistant strains and *S. epidermidis* and *B. subtilis*). Importantly, *S. aureus* did not show resistance to this polymer and the antibacterial mechanism was explained as the polymer entering the cytoplasm without harming the bacterial membrane and then interacting with bacterial DNA and subsequent triggering of the generation of reactive oxygen species (ROS). Although host defence polycationic antimicrobial peptides are attractive due to their low resistance potential, there are limitations for clinical use due to cost, limited activity, and poor stability. Therefore, synthetic polymers are an attractive alternative. Specifically, cationic polymers have been well explored over the years, playing with composition, architecture, and synthesis. Venkatesh *et al.*[130] investigated the antibacterial actions of commercially available cationic polymers ε-poly-lysine, α-poly-L-lysine, α-poly-L-ornithine, α-poly-D-lysine, α-poly-L-arginine, poly(allylamine), linear polyethyleneimines and branched polyethyleneimines (Fig. 12). All polymers showed antibacterial activity against *P. aeruginosa*, *S. aureus*, and *C. albicans*, yet were not effective as cationic antiseptics. Among all of these, ε-poly-lysine and linear polyethyleneimine showed the best activity, additionally, ε-poly-lysine showed strong antimicrobial activity against ocular fungal pathogens such as *Fusarium* comparable to the ophthalmic antifungal natamycin.

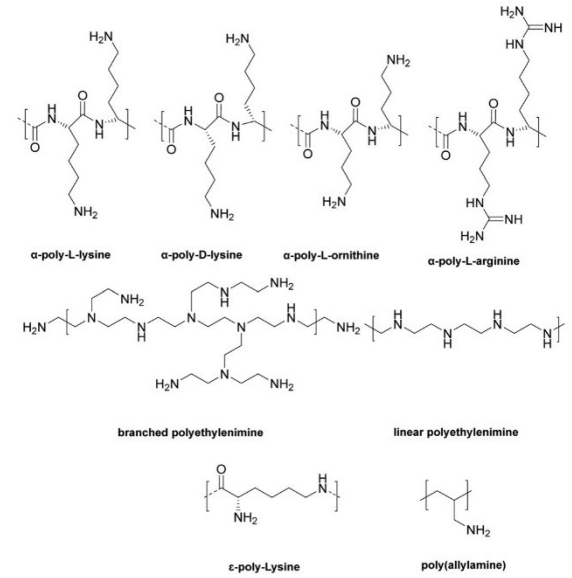

Fig. 12 The structures of a broad family of commercial, cationic, antimicrobial polymers, that are used in applications ranging from food preservation to the pharmaceutical industries.[130] Reproduced from ref. 130 with permission from PMC.

Another natural antimicrobial agent is the cationic peptide, ε-poly-L-lysine (ε-PL). However, its antimicrobial mode of action is uncertain, and, in the literature, there are various inhibition concentration values although the difference is often based on the source of the peptide. Tan *et al.*[131] has helped to clarify the antibacterial action and mechanism of ε-poly-L-lysine towards *S. aureus*. In their study, bacteria were treated with 250, 500 and 750 μg mL^{-1} of polymer, with increasing concentration resulting in greater collapse of the bacteria structure. Using Raman spectroscopy, they showed that ε-poly-L-lysine passed through the membrane and interacted with teichoic acid found in the peptidoglycan layer of the cell wall. The peptidoglycan structure was subsequently destroyed by the polymer, with the polymer also interacting with the plasma membrane leading to an increase in plasma membrane permeability.

Chitosan is extensively used in antimicrobial applications; however, its solubility can be problematic at physiological pH's. The amine group at C-2 and the hydroxyl group at C-6 enable functionalization and Su *et al.*[132] prepared chitosan derivatives *via* modification with arginine at the C-6 position. Due to the amine groups of chitosan and the guanidyl group of the added arginine group the chitosan derivative showed improved solubility as well as antibacterial activity with minimum inhibition concentrations of the polymer being 780 μg mL^{-1} for *S. aureus* and 312 μg mL^{-1} for *E. coli*.

Cyclodextrins are cyclic oligosaccharides of varying sizes (common ones named α, β and γ). β-Cyclodextrin is commonly used due to its hydrophobic interior and hydrophilic exterior, and its availability. β-Cyclodextrin was grafted onto chitosan by Ding *et al.*[133] and tested on *S. xylosus* and *E. coli*. SEM images revealed severely damaged, atrophied, sunken and disrupted cell membranes and cell lysis. The bactericidal mechanism of polymers is based on the quaternized ammonium groups of chitosan under acidic conditions that interact with the negatively charged bacteria membrane/cell wall components. Lower levels of β-cyclodextrin modification showed better bactericidal activity and the β-cyclodextrin modification promoted drug (doxorubicin) uptake by *S. xylosus*, while improving the aqueous solubilities of sulfadiazine, sulfamonomethoxine and sulfamethoxazole.

Phillips *et al.*[134] investigated cationic polymers based on poly(2-(dimethylamino)ethyl methacrylate) (4.5 kDa, 6.1 kDa and 11.2 kDa), poly(2-(dimethylamino)ethyl acrylate) (11 kDa and 3.2 kDa) and poly(2-aminoethylmethacrylate) (11.2 kDa) synthesized *via* reversible addition−fragmentation chain transfer polymerization against *M. tuberculosis* (Fig. 13). Among all the polymers, poly(2-(dimethylamino)ethyl methacrylate) showed the most potent activity (minimum inhibition concentrations as low as 30 μg mL^{-1} against *M. smegmatis*), while the lowest molecular weight poly(2-(dimethylamino)ethyl methacrylate) exhibited antibacterial activity against *E. coli*

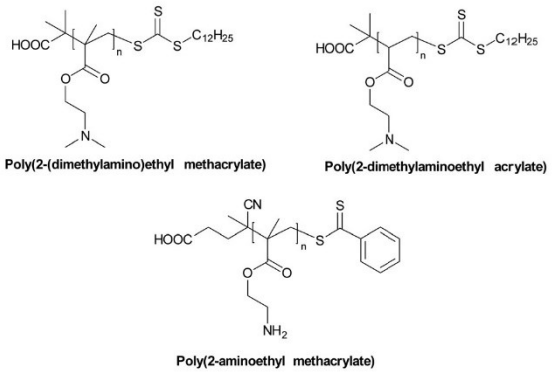

Fig. 13 Structures of the cationic polymers generated *via* RAFT polymerization and screened against *M. smegmatis*. Note: all the polymers will be protonated at physiological pH.[134] Reproduced from ref. 134 with permission from PMC.

and *P. putida*. Poly(2-(dimethylamino)ethyl methacrylate) bound to mycobacteria but did not change the integrity of the cell wall.

Thoma *et al.*[135] investigated the antimicrobial activity of poly(aminoethyl methacrylate)s. Polymers were synthesized *via* RAFT polymerization of the monomer *N*-(*tert*-butyloxycarbonyl)-aminoethyl methacrylate and the RAFT agent 2-cyanoprop-2-yl ethyl dithiocarbonate. Three different molecular weight polymers (2.1, 2.7, 3.2 kDa) were deprotected with TFA to give the primary ammonium group-based polymers and were evaluated on Gram-negative and Gram-positive bacteria including methicillin-resistant *S. aureus*. Polymers showed more of an effect on the inhibition of the growth of Gram-positive bacteria (MIC values lower than 100 μg mL^{-1}) when compared to the Gram-negative bacteria (MIC values around 700 μg mL^{-1}). Importantly the polymers were active in the presence of fetal bovine serum (serum binding can cause a loss of antimicrobial activity) and the polymers showed higher killing rates compared to the antibiotics, norfloxacin and mupirocin. The highest molecular weight polymers caused a 3-log reduction in the number of viable bacteria after 60 min and showed limited cytotoxicity and hemolysis at high concentrations of polymer. *In vivo* using a cotton rat nasal *S. aureus* colonization model, the low molecular weight polymer (used at 2× its MIC) effectively reduced the number of viable bacteria to the same level as mupirocin (when used at 2000× its MIC) (an antibiotic used to eradicate *S. aureus* nasal decolonization).

Fungi have a significant impact/effect on surface colonization *e.g.*, medical devices. Upon starting colonization of a surface, fungi start to build complex, robustly attached films that can often be different colours due to melanisation of the biofilms. Tellez *et al.*[136] synthesized, by RAFT polymerization, a poly(2-(dimethylamino)ethyl methacrylate) library that was screened against various fungi using three different molecular weights of polymer (9.7, 17.8 and 47.4 kDa) with and without quaternization (using various ratios of iodomethane and 1-iodobutane). Among the fungi explored, only one, *C. lunata* did not display complete inhibition when exposed to any of the synthesized polymers. Although all polymers possessed activity against multiple fungi, even when non-quaternized, the lowest molecular weightquaternized polymers showed the best fungicidal activity, presumably the lower molecular weights were able to better diffuse through the fungal cell wall before disruption of the cell membrane.

Mukherjee *et al.*[138] synthetized branched polyethyleneimine derivatives containing alkyl, alkyl ester and alkyl amide groups and evaluated them against drug resistant Gram-positive bacteria and fungi. Branched PEI was initially *N*-methylated and then further alkylated to form amphiphilic cationic polymers (to synthesize the ester and amide alkylating agents; alcohols and amines were reacted with bromoacetyl bromide, and the products subsequently used to alkylate the *N*-methylated PEI). The modified PEIs with short aliphatic ester or alkyl chains did not show antimicrobial activity, whereas the hexyl derivatives showed activity against *S. aureus*, *E. coli* and *C. albians*. Specifically, the hexyl amide functionalized PEI showed the best activity displaying MIC values of 2–4 μg mL^{-1} against methicillin-resistant *S. aureus*, 8 μg mL^{-1} against *E. coli* and 4 μg mL^{-1} against *C. albicans*. Since the hexyl amide functionalized polymers displayed optimal activity, they were further explored. Killing of *S. aureus*, (>5 Log reduction) was found within 4 h at 2× MIC. The hexyl amide functionalized polymers were able to eradicate 80% of biofilms of clinically isolated *S. aureus* at 32 mg mL^{-1}. The polymer also exhibited potent activity against both metabolically inactive stationary phase bacteria and antibiotic-resistant bacteria due to non-specific interactions with the cationic/lipophilic polymer with the bacterial killing. Of note, this polymer maintained its activity upon incubation in complex physiological fluids and did not show any propensity to develop resistance over 15 days (Fig. 14–17).

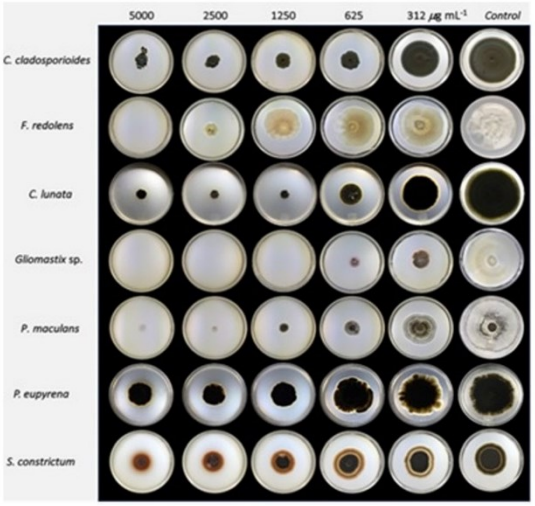

Fig. 14 Inhibition of radial fungal growth observed using poly(2-(dimethylamino)ethyl methacrylate) quaternized with 1-iodobutane.[136] Adapted from ref. 136 with permission from Elsevier.

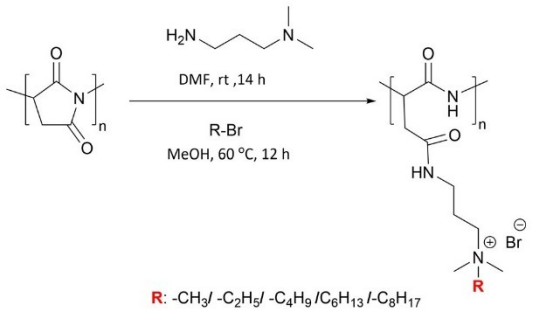

Fig. 15 Synthesis route to the antimicrobial polymers based on a poly(aspartamide) backbone. Poly(succinimide) is ring opened with a primary amine (1-amino-3-dimethylaminopropane) and the tertiary amine subsequently converted to quaternary ammonium groups with different length alkyl chains.[137] Reprinted the permission from {Yavvari, P. S.; Gupta, S.; Arora, D.; Nandicoori, V. K.; Srivastava, A.; Bajaj, A. Clathrin-Independent Killing of Intracellular Mycobacteria and Biofilm Disruptions Using Synthetic Antimicrobial Polymers. *Biomacromolecules* 2017, **18**, 2024–2033} Copyright {2017} American Chemical Society.

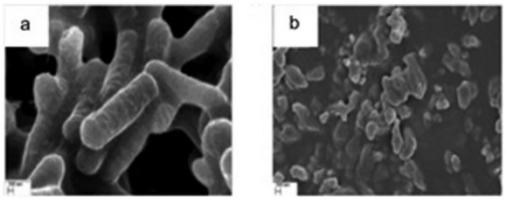

Fig. 16 SEM images of *M. smegmatis* (a) untreated and (b) upon the addition of the derivatised poly(aspartamide) (16 μg mL^{-1}) after 9 hours. In this case, the polymer is quaternerized with methyl iodide. Scale bar = 200 nm.[137] Reprinted the permission from {Yavvari, P. S.; Gupta, S.; Arora, D.; Nandicoori, V. K.; Srivastava, A.; Bajaj, A. Clathrin-Independent Killing of Intracellular Mycobacteria and Biofilm Disruptions Using Synthetic Antimicrobial Polymers. *Biomacromolecules* 2017, **18**, 2024–2033} Copyright {2017} American Chemical Society.

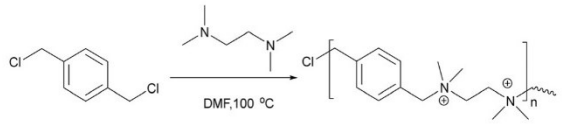

Fig. 17 Synthesis of an antimicrobial "polyionene" *via* the polyaddition reaction of diamines and alkyl dihalides with both monomers readily varied.[143] Reproduced from ref. 143 with permission from Elsevier.

The pH of normal skin is around 5.4–5.9 (which usually prevents the growth of bacteria), while it is known that the pH of infected skin is close to neutral. Hong *et al.*[139] therefore synthesized a pH responsive cationic, amphiphilic random copolymer as a topical antibacterial agent and tested it against drug resistant *S. aureus*. The methacrylate copolymer consisting of aminobutyl methacrylate and ethyl methacrylate (M_w: 2600 Da), synthesized by RAFT polymerization was designed to resemble the antimicrobial peptide magainin (M_w: 2467 Da) and was generated from aminobutyl methacrylate and ethyl methacrylate (2 : 1 ratio). The minimum inhibition concentration (MIC) value was found to be 15–20 μg mL^{-1} against *S. aureus* at pH 7.4. The MIC value was found to increase upon decreasing pH with an MIC value greater than 200 μg mL^{-1} as the pH reached 5.5. This was explained by decreasing pH leading to a diminishing of electrostatic interactions with the polymer (the bacteria become less "charged") which results in reduced antibacterial activity. In addition, this polymer did not show any hemolytic activity or cytotoxicity to human dermal fibroblasts.

Bansal *et al.*[140] investigated *n*-butyl-modified linear polyethyleneimines (M_w: 25 kDa) against skin-based microbes from acne lesions. On five skin-isolated microbes (*B. subtilis*, *S. aureus*, *S. typhimurium*, *K. pneumonia* and *E. coli*) the polymers showed better antimicrobial activity than standard antibiotics (erythromycin, nadifloxacin, azelaic acid, and zinc monomethionine) which are generally used at 400–1200 μg mL^{-1}. The polymers substituted with 20% levels of *n*-butyl groups showed the best action on skin isolated pathogens with MIC values between 130–200 μg mL^{-1} (linear polyethyleneimine had MIC values of 260–290 μg mL^{-1}). Moreover, the 20% *n*-butyl substituted polymer inhibited the growth of *S. epidermidis* over 24 hours.

As an alternative class of antimicrobial polymers, "polyionenes" that contain quaternized ammonium groups along a backbone (in contrast to examples where quaternized ammonium groups are located as pendant groups) display potent antimicrobial properties against pathogens. In general, polyionenes can be synthesized either by step-growth polymerization of suitable monomers *e.g.*, the Menshutkin reaction between alkyl dihalides and nucleophilic di/tertiary amines, self-polyaddition of aminoalkylhalides or cationic functionalization of precursor polymers.[141,142] Liu *et al.*[143] synthesized highly effective, skin compatible, cheap, and water-soluble polyionenes *via* commercially available monomers in a catalyst-free, polyaddition polymerization where the polymer-forming reaction and the installation of the charge occur simultaneously. The best polymer was prepared by reaction of *N*,*N*,*N*′,*N*′-tetramethyl ethylenediamine with di(chloromethyl)-benzene and displayed excellent antimicrobial potency and the highest selectivity over mammalian cells compared to triclosan and chlorhexidine digluconate. The most active polymer inhibited the growth of bacteria between 2–31 mg mL^{-1}, demonstrating strong broad spectrum antimicrobial activity against clinically isolated multidrug-resistant *S. aureus*, *E. coli*, *P. aeruginosa*, *A. baumannii* and *K. pneumoniae*, as well as fungi *C. albicans* and *C. neoformans*. In particular, a killing efficiency of more than 99.9% within 2 min was obtained. Dermal toxicity of the best polymer was evaluated with topical application of the polymer (200 and 500 μg mL^{-1}) showing a better skin compatibility profile in mice compared to the clinically used surgical scrubs betadine and chlorhexidine. In addition, *P. aeruginosa* contaminated skin could be treated with the polymer with the number of bacteria on the skin significantly decreased compared to chlorhexidine handwash.

Alamri *et al.*[144] prepared antimicrobial polymers from polyacrylonitrile that was functionalized with ethylenediamine and

hexamethylenediamine (to give amidines). The amine side chains of the polymers were then functionalized with various benzaldehydes and the polymers were tested against *S. aureus*, *P. aeruginosa*, *E. coli*, *S. typhi*, *A. flavus*, *A. niger*, *C. albicans*, *C. neoformans*. All polymers showed antimicrobial activity with minimum inhibition concentrations as low as 12.5 μg mL^{-1} for polymers bearing long diamine linkers and 4-hydroxybenzaldehyde and 2,4-dihydroxybenzaldehyde side chains. Again, the mode of action relating to the positive charge of the polymers, specifically here the amidine functional group and presumably the free phenolic groups of the decorating benzaldehydes.

Polycarbonates are extensively used polymers due to their optical properties, heat resistance, and strength.[145] Polycarbonates have been modified to allow quaternization and showed antibacterial activity.[146] Thus Qiao *et al.*[147] prepared a library of polycarbonates using a variety of cyclic carbonates (including one with pendent 3-chloropropyl groups) and diols *via* metal-free organocatalytic ring-opening polymerization. Subsequently the 3-chloropropyl groups were displaced with trimethyl amine to give cationic groups along the polymer chains. Although all polymers showed activity against *S. aureus*, the most pronounced activity was found for the polymer having 60% cationic charge (M_w; 16 kDa) with an MIC value of 63 μg mL^{-1}. Field emission scanning electron microscopy images showed cellular lysis of *E. coli* and *S. aureus*.

Nimmagadda *et al.*[148] reported amine containing polycarbonates that showed antibacterial activity synthesised using two cyclic carbonate monomers (one that contained a Boc-protected amine group that becomes hydrophilic upon deprotection and one hydrophobic) with random and diblock copolymers synthesized by ring opening polymerization. The most potent polymer, against three Gram-positive bacterial strains *S. aureus*, *S. epidermidis* and *E. Faecalis*, had MIC values between 1.6–5.0 μg mL^{-1}, and consisted of approximately 20 monomers and formed micelles with a size of 228 nm. The mechanism of the polymer was explained as electrostatic interactions with the surface of bacteria and with free chains penetrating through the cell membrane leading to bacterial death.

Poly(β-hydroxyl amine)s have been produced by polymerization between amines and bis-epoxy functionalities under aqueous conditions. These polymers can then be modified, post-polymerisation, to form quaternary derivatives. Oh *et al.*[149] synthesized a polymer library of poly(β-hydroxyl amine) derivatives and investigated their antimicrobial activities with polymers bearing *n*-butyl quaternary amines showing the best activity against *E. coli* and *S. aureus* (MIC's <10–20 μg mL^{-1}) (the best active polymer with two butyl chains on the quaternary ammonium groups) (see Fig. 18) also inhibited the growth of *M. smegmatis* at (20 μg mL^{-1}). SEM images revealed significant damage to the bacterial membrane after polymer incubation.

Polyhexamethylene guanidine is a bactericidal agent that has been used in many applications such as antiseptics,[150] water treatment,[151] the food industry[152] and personal hygiene applications.[153] Zhuo *et al.*[154] synthesized three oligoguanidine

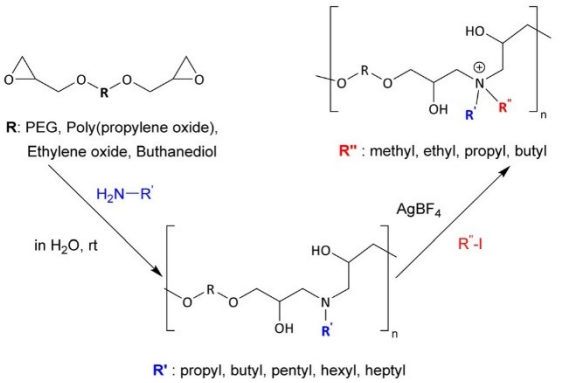

Fig. 18 Synthesis route to a library of poly(β-hydroxyl amine)s by reacting diglycidyl monomers with various primary amines and subsequent quaternization with alkyl iodides.[149] Reproduced from ref. 149 with permission from the Royal Society of Chemistry.

hydrochloride polymers bearing various alkyl chains *e.g.*, butamethylene, hexamethylene and octanethylene and *m*-xylylene guanidine HCl by reacting, at high temperature, equimolar amounts of the appropriate diamine and guanidine hydrochloride. Synthesized oligomers were tested on 370 clinical strains with 96 of them antibiotic resistant. Among all the polymers, poly(octanethylene guanidine) hydrochloride showed the lowest minimum inhibition concentration (0.5–16 μg mL^{-1}) in comparison to poly(hexamethylene guanidine) hydrochloride (1–64 μg mL^{-1}) and the antiseptic and disinfectant, chlorhexidine digluconate (2–64 μg mL^{-1}). Poly(octanethylene guanidine) hydrochloride was highly effective at 1–8 μg mL^{-1} against methicillin resistant *S. aureus*, vancomycin resistant *E. faecium*, multidrug resistant *P. aeruginosa*, ceftazidime resistant *Citrobacter* spp. and *Enterobacter* spp. The antimicrobial mechanism of the polymers was explained as the dual interaction of the hydrophobic alkyl chains of the polymers (anchoring into the membrane) and binding to the negatively charged phospholipids, causing damage to the bacterial membranes, although interactions with teichoic and lipoteichoic acids in the cell wall is also possible.

Studies have shown that the architecture of the polymers have a great impact on their antimicrobial efficiency.[155–158] Thus Namivandi-Zangeneh *et al.*[158] investigated the effect of amphiphilic ternary copolymers composed of oligoethylene glycol, cationic and hydrophobic functional groups with different chain lengths and topologies (*i.e.*, random *vs.* block copolymers, and linear *vs.* hyperbranched polymers) on their antimicrobial activity and hemocompatibility. One of the hyperbranched random copolymers containing 2-ethylhexyl groups was found to have the best antimicrobial activity against *P. aeruginosa* and *E. coli* (MIC of 64 μg mL^{-1}). Interestingly, polymers with different chain lengths (number-average degrees of polymerization of 100, 50 and 20) displayed similar antimicrobial activities but different hemolytic activities. For example, while shorter polymers caused hemolysis, hyperbranched polymers improved hemocompatibility (by >4 times) with only a minor loss

in their antimicrobial activity. Among the hyperbranched polymers, hyperbranched random copolymers that contain 2-ethylhexyl groups were observed to have the best overall biocompatibility and the minimum inhibition concentration of the polymer was found to be 64 μg mL^{-1} against highly pathogenic Gram-negative species and 128 μg mL^{-1} against *V. cholerae.* Moreover, the most potent polymer (at a concentration of 64 μg mL^{-1}) killed 99% of planktonic and 90% of biofilm bacteria, as well as inducing the dispersal of biofilms. Due to the cationic blocks in the polymer structure, antimicrobial modes of bactericidal action were observed for all polymer structures.

Santos *et al.*[159] synthesized a library comprising homopolymers of (3-acrylamidopropyl)trimethylammonium chloride and amphiphilic linear, star-shaped (4 and 6-armed), random and block copolymers of hydrophilic (3-acrylamidopropyl) trimethylammonium chloride and hydrophobic *n*-butyl acrylate (the wide polymer library was generated using a ''supplemental activator and reducing agent atom transfer radical polymerization''). The antimicrobial activity of polymers showed differences and in general amphiphilic polymers were more effective toward *B. subtilis*. Hydrophobicity changes in polymers' composition showed no effect on the antimicrobial activity while the cationic segment of the polymer was necessary to generate antimicrobial activity. The antimicrobial activity of star-shaped polymers and linear polymers with similar molecular weights displayed similar antimicrobial activity, while enhanced antibacterial activities against Gram-positive and Gram-negative antimicrobial activity of polymer was observed with increasing molecular weight. The cationic homopolymer of poly(3-(acrylamidopropyl)trimethylammonium chloride) with the highest molecular weight and the 4-armed star shaped poly(3-(acrylamidopropyl)trimethylammonium chloride) showed the best activity against *S. aureus*, *B. subtilis*, *B. cereus*, *E. coli* and *P. aeruginosa*. Scanning electron microscopy and fluorescence microscopy showed that the cationic homopolymers and amphiphilic copolymers killed *E. coli* by disrupting the bacterial membrane.

It is accepted that polymer hydrophilic and hydrophobic balance is a key parameter in the design of antimicrobial polymers. Barman *et al.*[160] explored the antimicrobial activity of cationic polymers modified with amino acids against drug resistant *A. baumannii* (one of the most notorious pathogens that causes hospital-derived (nosocomial) infections). In this context, cationic polymer precursors, poly(isobutylene-*alt*-*N*-(*N*′,*N*′-dimethylaminopropyl)maleimide) were synthesized by reacting poly(isobutylene-*alt*-maleic anhydride) with *N*,*N*-dimethyl-1,3-propanediamine. The resulting tertiary amine was reacted with esterified amino acids (glycine, L-alanine, D-alanine, L-valine, L-leucine, L-isoleucine, L-phenylalanine, L-tyrosine. L-Aspartic acid, L-glutamic acid) that had been acylated with bromoacetyl bromide to fully quaternerised the polymer (molecular weights were in the range of 17.4–20.8 kDa). The antimicrobial activity of the polymers was determined against both Gram-positive (*S. aureus* and *E. faecium*) and Gram-negative (*E. coli* and *A. baumannii*) bacteria, including methicillin resistant *S. aureus*, ß-lactam-resistant *K. pneumoniae*, and several carbapenem-resistant *A. baumannii*. In general, the antimicrobial activity of the polymers was dependent on hydrophobicity variation originating from the amino acid in the polymer design (see Table 3) (however, with increasing hydrophobicity, the polymers showed toxicity against red blood cells). To illustrate, the glycine modified polymer had a minimum inhibition concentration value of 64 μg mL^{-1} for *S. aureus* and 8–16 μg mL^{-1} for *A. baumannii*, while the valine modified polymer showed minimum inhibition concentration values of 8–16 μg mL^{-1} for *S. aureus*, and 4 μg mL^{-1} against *A. baumannii*. The glycine modified polymer showed total killing (~5 Log CFU mL^{-1} reduction) of the clinically isolated drug resistant *A. baumannii* after 1–2 hours at a concentration of 16 μg mL^{-1}. This polymer not only was rapidly bactericidal against growing planktonic *A. baumannii* but also killed non-dividing stationary-phase bacteria instantaneously (<2 min). It is well-known that *A. baumannii* readily forms biofilms and the biofilm mass of drug-sensitive and drug-resistant *A. baumannii* were reduced by 65–85% at 64–128 μg mL^{-1} for the glycine-modified polymer. Importantly, there was no propensity for resistance development even after 14 passages with low levels of the polymer.

Bactericidal polycationic polymers inactivate bacteria by disrupting the cellular envelope. In some cases, this is to electrostatic interactions with the ''negatively charged bacteria cell membrane'' and replacement of Ca^{2+} and/or Mg^{2+} by the polymeric biocidal cations. Clearly the type of counter anion will play an important role in the antimicrobial activity of quaternary ammonium and phosphonium group bearing antimicrobial polymers with the strength of the ion pair and solvation both important considerations. The Chauhan group studied the influence of counter ion on antimicrobial activity of polycations of poly(4-vinyl-2-hydroxyethyl pyridinium)[161] and poly[1-vinyl-3-(2-sulfoethyl imidazolium betaine)][161] by exchanging

Table 3 Minimum inhibition concentration of the amino acid conjugated polymers (see Fig. 19) against various types of bacteria[160]

Amino acid added	*S. aureus*	*E. faecium*	*E. coli*	*A. baumannii*	Drug resistant *S. aureus*	Drug resistant *K. pneumoniae*	Drug resistant *A. baumannii*
Gly	64	>128	32–64	8–16	>128	128	8–16
L-Ala	64–128	>128	32–64	8–16	>128	128	8–16
L-Val	8–16	16	8	4	64	32	4
L-Leu	8	4–8	8	4	16	16–32	4
L-Ile	8	8	8	4	16	16	4
L-Phe	8	8	16	8	16	32	4–16
L-Tyr	16–32	64–128	32	32	32	64	16
L-Asp	>128	>128	64–128	16–32	>128	>128	16–32
L-Glu	>128	>128	64–128	16–32	>128	>128	16–32

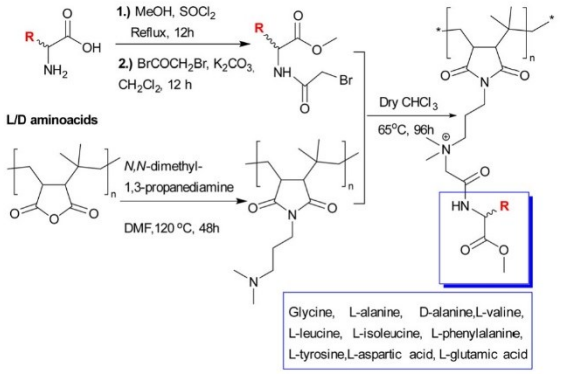

Fig. 19 Synthesis of poly(isobutylene-*alt*-*N*-(*N*′,*N*′-dimethylamino-propyl)maleimide) by reacting poly(isobutylene-*alt*-maleic anhydride) with *N*,*N*-dimethyl-1,3-propanediamine and functionalization with L or D amino acids (reacted with bromoacetyl bromide).[160] Reprinted the permission from {S. Barman, M. M. Konai, S. Samaddar and J. Haldar, Amino Acid Conjugated Polymers: Antibacterial Agents Effective against Drug-Resistant Acinetobacter baumannii with No Detectable Resistance, *Appl. Mater.*, 2019, **11**, 33559–33572} Copyright {2019} American Chemical Society.

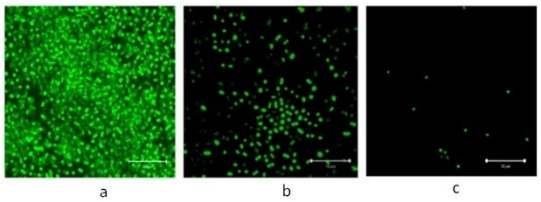

Fig. 20 Confocal images of biofilm disruption of *A. baumannii* stained with crystal-violet after treatment with the glycine-modified polymers: (a) control (no polymer); (b) 64 μg mL^{-1} of the glycine-modified polymer; (c) 128 μg mL^{-1} of the glycine-modified polymer.[160] Reprinted the permission from {S. Barman, M. M. Konai, S. Samaddar and J. Haldar, Amino Acid Conjugated Polymers: Antibacterial Agents Effective against Drug-Resistant Acinetobacter baumannii with No Detectable Resistance, *Appl. Mater.*, 2019, **11**, 33559–33572} Copyright {2019} American Chemical Society.

Cl^- or Br^- with various OH^-, SH^-, NO^{3-}, BF^{4-} and CF_3COO^-. The polymer having hydroxy counter ions exhibited the strongest antifungal and antibacterial activity (minimum inhibition concentrations of 1040 and 520 μg mL^{-1} for *M. circenelliods* and *A. niger* and 650 μg mL^{-1} for *B. coagulans*). This phenomenon was explained by the enhanced the solubility of the polymers (Fig. 19–21).

The counter ion of poly[1-vinyl-3-(2-sulfoethyl imidazolium betaine)] was changed to Cl^-, F^-, OH^-, SH^-, SCN^-, NO^{3-}, BF^{4-} and CH_3COO^-. In terms of Gram-positive bacteria (*B. coagulans*) again the hydroxyl counter ions polymers showed the strongest inhibition of the growth of bacteria. In contrast, for Gram-negative bacteria (*P. aeruginosa*), the F^-, SH^- and NO^{3-} counter ions were the most effective. Regarding the inhibition of the growth of fungi, SH^- displayed maximal activity against *M. circenelliods* while OH^- was found the most effective against

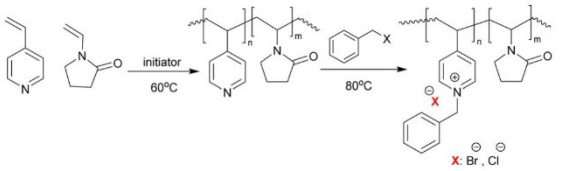

Fig. 21 Synthesis of poly(4-vinylpyridine-*co*-*N*-vinylpyrrolidone) *via* RAFT polymerization and subsequent post-synthesis quaternization with benzyl halides.[163] Reproduced from ref. 163 with permission from MDPI.

B. fulva. It was suggested that the identity of counter anion has an effect on the efficiency and selectivity towards individual microbes due to the discrepancy of polymer morphology and the solubility of polycations in water, resulting in different antimicrobial performance.[162] However, how these anions are related/exchanged with the ions in the buffers and media, and the pH of the applied polymers, are important considerations and are often poorly discussed.

Insoluble pyridinium-containing polymers can capture bacteria intact, while soluble pyridinium polymers can kill bacteria by interacting with, and disrupting, the bacterial cell membrane/wall. Xue *et al.*[163] synthesized water-soluble pyridinium-type copolymers that possessed both antibacterial and antiviral activities. To overcome cytotoxicity and solubility issues *N*-vinyl pyrrolidone was chosen as one of the monomers (along with vinyl pyridine), with the pyridine-based polymers subsequently quaternized with benzyl halides. Various monomer feed ratios were used to optimize the antimicrobial activity. Both homopolymers and copolymers of pyridinium-type polymers (M_w ~ 90–100 kDa) were alkylated and the charge density of the quaternary pyridinium polymers was calculated by colloidal titration. The MIC values of the polymers decreased with an increase in positive charge density, while polymers quaternized with benzyl bromide showing the most potent antimicrobial activity against Gram-negative bacteria (*E. coli*) compared to the ones quaternized with benzyl chloride. This was explained by authors as due to the change in the dissociation ability of the polymers being dependent on the counter ion type. Ito suggested the mode of action of the polymers could be explained as a change in the mechanism related to the displacement of calcium and/or magnesium ions on the cell membrane. If an ammonium ion forms a tight ion-pair with its counter anion it may delay the ionic dissociation of the quaternary ammonium salt, influencing the displacement of those divalent ions. This may explain why benzyl bromide quaternized polymers showed higher antibacterial activity than the ones with benzyl chloride. However, other rational may presumably be due to the reduced levels of alkylation with benzyl chloride *vs.* the bromide. Analysis by AFM showed that the polymers were able to kill *E. coli* within 3 min by disrupting the cellular envelope with leakage of intracellular components. Enveloped virus *e.g.* influenza or herpes are also protected by a lipid membrane[21] and quaternized ammonium cationic polymers can also effectively kill some viruses. In this context, pyridine-based polymers quaternerised with benzyl halides and showed virucidal activity, killing 95% of influenza virus at 50 ppm. The virucidal action of the polymers

was dependant on interactions between the lipid envelope and the polymers, causing disorganization and severe damage to the lipid envelope.

3. Conclusions and future perspective

Microbial-based diseases and contamination are still a major burden on the economies and health care systems of countries around the world. Moreover, microorganisms have gained resistance against existing drugs over the decades due to misuse or overuse – although it should be noted that this is not a recent phenomenon – with resistance against penicillin identified in the 1940's. New alternatives have been sought to solve these life-threatening problems. In the light of successful studies and antimicrobial polymer-based materials are becoming a tool in the arsenal to fight against pathogens, indeed as high-lighted in this review polymeric-based materials were used as surface coatings to destroy SARS-COVID-2. Importantly, since most antibacterial polymers disrupt the cell envelope of bacteria the chance of resistance formation by the pathogens against polymers is unlikely in contrast to conventional antibiotics which are largely specific/single target based. The long-term vision is that antimicrobial polymers with negligible toxicity, could become an additional option to current antibiotics. Clearly as is already happening antimicrobial polymer-based materials are becoming ever more part of our daily lives. Going forwards it is key that multi-drug resistant and clinically isolated pathogens are included much more in studies to enlighten the mechanisms of action of antimicrobial polymers and to broaden their structural scope and application.

Conflicts of interest

There are no conflicts to declare.

Acknowledgements

We would like to thank Dr Daniel Norman and Dr Matthew Owens for their support and ideas during writing this review. This work is funded by an award – a PhD scholarship by Turkish Ministry of National Education Study Abroad Programme.

References

1 A. Muñoz-Bonilla and M. Fernández-García, *Prog. Polym. Sci.*, 2012, **37**, 281–339.
2 K. S. Huang, C. H. Yang, S. L. Huang, C. Y. Chen, Y. Y. Lu and Y. S. Lin, *Int. J. Mol. Sci.*, 2016, **17**, 1578.
3 A. Kyzioł, W. Khan, V. Sebastian and K. Kyzioł, *Chem. Eng. J.*, 2020, **385**, 123888.
4 B. S. T. Peddinti, S. N. Downs, J. Yan, S. D. Smith, R. A. Ghiladi, V. Mhetar, R. Tocchetto, A. Griffiths, F. Scholle and R. J. Spontak, *Adv. Sci.*, 2021, **8**, 1–9.
5 R. J. Cornell and L. G. Donaruma, *J. Med. Chem.*, 1965, **8**, 388–390.
6 E. F. Palermo and K. Kuroda, *Appl. Microbiol. Biotechnol.*, 2010, **87**, 1605–1615.
7 O. Vogl and D. Tirrell, *J. Macromol. Sci., Part A: Pure Appl. Chem.*, 1979, **A13**, 37–41.
8 C. R. Allan and L. A. Hadwiger, *Exp. Mycol.*, 1979, **3**, 285–287.
9 S. Shima, H. Matsuoka, T. Iwamoto and H. Sakai, *J. Antibiot.*, 1984, **37**, 1449–1455.
10 T. S. Ikeda Tomiki, *Makromol. Chem.*, 1984, **185**, 869–876.
11 G. Pasparakis and C. Alexander, *Analyst*, 2007, **132**, 1075–1082.
12 M. Charnley, M. Textor and C. Acikgoz, *React. Funct. Polym.*, 2011, **71**, 329–334.
13 F. Siedenbiedel and J. C. Tiller, *Polymers*, 2012, **4**, 46–71.
14 A. Jain, L. S. Duvvuri, S. Farah, N. Beyth, A. J. Domb and W. Khan, *Adv. Healthcare Mater.*, 2014, **3**, 1969–1985.
15 A. Arora and A. Mishra, *Mater. Today Proc.*, 2018, **5**, 17156–17161.
16 N. F. Kamaruzzaman, L. P. Tan, R. H. Hamdan, S. S. Choong, W. K. Wong, A. J. Gibson, A. Chivu and M. De Fatima Pina, *Int. J. Mol. Sci.*, 2019, **20**, 1–31.
17 M. Liu, J. Li and B. Li, *Langmuir*, 2018, **34**, 1574–1580.
18 P. Teratanatorn, R. Hoskins, T. Swift, C. W. I. Douglas, J. Shepherd and S. Rimmer, *Biomacromolecules*, 2017, **18**, 2887–2899.
19 A. C. Engler, A. Shukla, S. Puranam, H. G. Buss, N. Jreige and P. T. Hammond, *Biomacromolecules*, 2011, **15**, 1666–1674.
20 M. J. Catalão, S. R. Filipe and M. Pimentel, *Front. Microbiol.*, 2019, **10**, 1–11.
21 G. Xu, D. Pranantyo, L. Xu, K. Neoh, E. Kang and S. L. Teo, *Ind. Eng. Chem. Res.*, 2016, **55**, 2–11.
22 A. Kausar, *J. Macromol. Sci., Part A: Pure Appl. Chem.*, 2018, **55**, 440–448.
23 J. Hernandez-Montelongo, E. G. Lucchesi, V. F. Nascimento, C. G. França, I. Gonzalez, W. A. A. Macedo, D. Machado, M. Lancellotti, A. M. Moraes, M. M. Beppu and M. A. Cotta, *Mater. Sci. Eng., C*, 2017, **71**, 718–724.
24 I. A. MacDonald and M. J. Kuehna, *J. Bacteriol.*, 2013, **195**, 2971–2981.
25 WHO/UNICEF Joint Monitoring Programme and S. and H. for Water Supply, *Five years into the SDGs progress on household drinking water, sanitation and hygiene*, 2020.
26 T. R. Sinclair, D. Robles, B. Raza, S. van den Hengel, S. A. Rutjes, A. M. de Roda Husman, J. de Grooth, W. M. de Vos and H. D. W. Roesink, *Colloids Surf., A*, 2018, **551**, 33–41.
27 A. Nagaraja, Y. M. Puttaiahgowda, A. Kulal, A. M. Parambil and T. Varadavenkatesan, *Macromol. Res.*, 2019, **27**, 301–309.
28 E. H. Westman, M. Ek, L. E. Enarsson and L. Wågberg, *Biomacromolecules*, 2009, **10**, 1478–1483.
29 S. Pernagallo, M. Wu, P. Gallagher and M. Bradley, *J. Mater. Chem.*, 2011, **21**, 96–101.
30 H. Pickering, M. Wu, M. Bradley and H. Bridle, *Environ. Sci. Technol.*, 2012, **46**, 2179–2186.

31 S. Venkateswaran, M. Wu, P. J. Gwynne, A. Hardman, A. Lilienkampf, S. Pernagallo, G. Blakely, D. G. Swann, M. P. Gallagher and M. Bradley, *J. Mater. Chem. B*, 2014, **2**, 6723–6729.
32 A. L. Hook, C. Chang, J. Yang, J. Luckett, A. Cockayne, S. Atkinson, Y. Mei, R. Bayston, D. J. Irvine, R. Langer, D. G. Anderson, P. Williams, M. C. Davies and M. R. Alexander, *Nat. Biotechnol.*, 2012, **30**, 868–875.
33 A. L. Hook, C. Y. Chang, J. Yang, S. Atkinson, R. Langer, D. G. Anderson, M. C. Davies, P. Williams and M. R. Alexander, *Adv. Mater.*, 2013, **25**, 2542–2547.
34 A. A. Dundas, O. Sanni, J. Dubern, G. Dimitrakis, A. L. Hook, D. J. Irvine, P. Williams and M. R. Alexander, *Adv. Mater.*, 2019, **31**, 1903513.
35 K. Adlington, N. T. Nguyen, E. Eaves, J. Yang, C. Chang, J. Li, A. L. Gower, A. Stimpson, D. G. Anderson, R. Langer, M. C. Davies, A. L. Hook, P. Williams, M. R. Alexander and D. J. Irvine, *Biomacromolecules*, 2016, **17**, 2830–2838.
36 S. R. J. Peddinti Bharadwaja, S. T. Scholle Frank, G. Vargas Mariana, D. Smith Steven and A. Ghiladi Reza, *Mater. Horiz.*, 2019, **6**, 2056–2062.
37 H. M. Minhas, A. Scheel, P. Garibaldi and B. Liu, *Lancet Infect. Dis.*, 2020, 892–893.
38 M. Jayaweera, H. Perera, B. Gunawardana and J. Manatunge, *Environ. Res.*, 2020, **188**, 1–18.
39 H. Keum, D. Kim, C.-H. Whang, A. Kang, S. Lee, W. Na and S. Jon, *ACS Omega*, 2022, **7**, 10526–10538.
40 L. Q. Xu, D. Pranantyo, K. Neoh, E. Kang, S. L. Teo and G. D. Fu, *Polym. Chem.*, 2015, **7**, 493–501.
41 L. Han, L. Yan, K. Wang, L. Fang, H. Zhang, Y. Tang, Y. Ding, L. Weng, J. Xu, J. Weng, Y. Liu, F. Ren and X. Lu, *Nat. Publ. Gr.*, 2017, e372.
42 F. Gao, H. Qu, Y. Duan, J. Wang, X. Song and T. Ji, *RSC Adv.*, 2014, 6657–6663.
43 S. Kumar, M. Perikamana, J. Lee, Y. Bin Lee, Y. M. Shin, E. J. Lee, A. G. Mikos and H. Shin, *Biomacromolecules*, 2015, **16**, 2541–2555.
44 X. Wang, S. Jing, Y. Liu, S. Liu and Y. Tan, *Polymer*, 2017, **116**, 314–323.
45 L. Luo, G. Li, D. Luan, Q. Yuan, Y. Wei and X. Wang, *Appl. Mater.*, 2014, **6**, 19371–19377.
46 J. Xu, Y. Bai, M. Wan, Y. Liu, L. Tao and X. Wang, *Polymers*, 2018, **10**, 1–12.
47 E. A. Chamsaz, S. Mankoci, H. A. Barton and A. Joy, *Appl. Mater.*, 2017, **9**, 6704–6711.
48 J. Hoque, P. Akkapeddi, V. Yadav, G. B. Manjunath, D. S. S. M. Uppu, M. M. Konai, V. Yarlagadda, K. Sanyal and J. Haldar, *ACS Appl. Mater. Interfaces*, 2015, **7**, 1804–1815.
49 J. Hoque, P. Akkapeddi, C. Ghosh, D. S. S. M. Uppu and J. Haldar, *Appl. Mater.*, 2016, **8**, 29298–29309.
50 A. Tabriz, M. A. Ur Rehman Alvi, M. B. Khan Niazi, M. Batool, M. F. Bhatti, A. L. Khan, A. U. Khan, T. Jamil and N. M. Ahmad, *Carbohydr. Polym.*, 2019, **207**, 17–25.
51 U. Ajdnik, M. Finšgar and L. Fras Zemljič, *Carbohydr. Polym.*, 2020, **232**, 115817.
52 A. A. Sharipova, S. B. Aidarova, D. Grigoriev, B. Mutalieva, G. Madibekova, A. Tleuova and R. Miller, *Colloids Surf., B*, 2016, **137**, 152–157.
53 H. Yu, L. Liu, X. Li, R. Zhou, S. Yan, C. Li and S. Luan, *Chem. Eng. J.*, 2019, **360**, 1030–1041.
54 S. Dhingra, A. Joshi, N. Singh and S. Saha, *Mater. Sci. Eng., C*, 2021, **118**, 111465.
55 F. Aynali, E. Doganci, T. Doruk and H. Sadikoglu, *Polym. Int.*, 2019, **68**, 385–393.
56 F. Aynali, H. Balci, E. Doganci and E. Bulus, *Eur. Polym. J.*, 2021, **149**, 7–8.
57 P. Varguez-Catzim, N. Rodríguez-Fuentes, R. Borges-Argáez, M. Cáceres-Farfán, A. González-Díaz, A. Alonzo-Garcia, S. Duarte, M. Aguilar-Vega and M. O. González-Díaz, *Appl. Surf. Sci.*, 2021, **565**, 150544.
58 J. Lv and Y. Cheng, *Chem. Soc. Rev.*, 2021, **50**, 5435–5467.
59 D. J. Han, S. Kim, H. J. Heo, C. Jin, J. Young Kim, H. Choi, I. J. Park, H. S. Kang, S. G. Lee, J. C. Lee and E. H. Sohn, *Appl. Surf. Sci.*, 2021, **562**, 150181.
60 M. D. Macià, E. Rojo-Molinero and A. Oliver, *Clin. Microbiol. Infect.*, 2014, **20**, 981–990.
61 K. Zhang, X. Li, C. Yu and Y. Wang, *Front. Cell. Infect. Microbiol.*, 2020, **10**, 1–16.
62 A. Vishwakarma, F. Dang, A. Ferrell, H. A. Barton and A. Joy, *JACS*, 2021, **143**, 9440–9449.
63 L. Zhai, *Chem. Soc. Rev.*, 2013, **42**, 7148–7160.
64 I. Erel-unal and S. A. Sukhishvili, *Macromolecules*, 2008, **41**, 3962–3970.
65 C. B. Amphiphiles, *Ber. Bunsetlges. Phys. Chem.*, 1991, **5**, 1430–1434.
66 X. Zhu and X. Jun Loh, *Biomater. Sci.*, 2015, **3**, 1505–1518.
67 J. A. Lichter and M. F. Rubner, *Langmuir*, 2009, **25**, 7686–7694.
68 E. Wulandari, R. Namivandi-zangeneh, P. R. Judzewitsch, R. Budhisatria, A. H. Soeriyadi, C. Boyer and E. H. H. Wong, *ACS Appl. Mater. Interfaces*, 2021, **4**, 692–700.
69 H. Khalil, T. Chen, R. Riffon, R. Wang and Z. Wang, *Antimicrob. Agents Chemother.*, 2008, **52**, 1635–1641.
70 J. Lin, S. Qiu, K. Lewis and A. M. Klibanov, *Biotechnol. Prog.*, 2002, **18**, 1082–1086.
71 S. Y. Wong, Q. Li, J. Veselinovic, B. S. Kim, A. M. Klibanov and P. T. Hammond, *Biomaterials*, 2010, **31**, 4079–4087.
72 F. Wang, Z. Yao, H. Wu, S. Zhang, N. Zhu and X. Gai, *Appl. Mech. Mater.*, 2012, **108**, 194–199.
73 A. V. Briones, T. Sato and U. G. Bigol, *Adv. Chem. Eng. Sci.*, 2014, **04**, 233–241.
74 E. I. Rabea, M. E. T. Badawy, C. V. Stevens, G. Smagghe and W. Steurbaut, *Biomacromolecules*, 2003, **4**, 1457–1465.
75 M. Kumorek, I. M. Minisy, T. Krunclová, M. Voršiláková, K. Venclíková, E. M. Chánová, O. Janoušková and D. Kubies, *Mater. Sci. Eng., C*, 2020, **109**, 111049.
76 J. Hernández-Montelongo, V. F. Nascimento, D. Murillo, T. B. Taketa, P. Sahoo, A. A. De Souza, M. M. Beppu and M. A. Cotta, *Carbohydr. Polym.*, 2016, **136**, 1–11.
77 Y. Zhang, F. Wang, Q. Huang, A. B. Patil, J. Hu, L. Fan, Y. Yang, H. Duan, X. Dong and C. Lin, *Mater. Sci. Eng., C*, 2020, **110**, 110690.

78 J. Illergård, L. Wågberg and M. Ek, *Colloids Surf., B*, 2011, **88**, 115–120.
79 J. Illergård, U. Römling, L. Wågberg and M. Ek, *Cellulose*, 2012, **19**, 1731–1741.
80 M. Illergård, J. Wågberg and L. Ek, *Cellulose*, 2015, **22**, 2023–2034.
81 C. Chen and M. Ek, *Nord. Pulp Pap. Res. J.*, 2018, **33**, 385–396.
82 C. Chen, J. Illergård, L. Wågberg and M. Ek, *Holzforschung*, 2017, **71**, 649–658.
83 H. Schmolke, S. Demming, A. Edlich, V. Magdanz, S. Büttgenbach, E. Franco-Lara, R. Krull and C.-P. Klages, *Biomicrofluidics*, 2010, **4**, 044113.
84 Y. Zhu, X. Yu, T. Zhang and X. Wang, *Appl. Surf. Sci.*, 2019, **483**, 979–990.
85 L. Tang, W. Gu, P. Yi, J. L. Bitter, J. Yeon, D. H. Fairbrother and K. Loon, *J. Membr. Sci.*, 2013, **446**, 201–211.
86 I. C. Gîfu, M. E. Maxim, L. O. Cinteza, M. Popa, L. Aricov, A. R. Leonties, M. Anastasescu, D. F. Anghel, R. Ianchis, C. M. Ninciuleanu, S. G. Burlacu, C. L. Nistor and C. Petcu, *Coatings*, 2019, **9**, 1–13.
87 E. N. Gibbons, C. Winder, E. Barron, D. Fernandes, M. J. Krysmann, A. Kelarakis, A. V. S. Parry and S. G. Yeates, *Nanomaterials*, 2019, **9**, 1563.
88 A. F. Martins, J. Vlcek, T. Wigmosta, M. Hedayati, M. M. Reynolds, K. C. Popat and M. J. Kipper, *Appl. Surf. Sci.*, 2020, **502**, 144282.
89 S. P. Facchi, A. C. de Oliveira, E. O. T. Bezerra, J. Vlcek, M. Hedayati, M. M. Reynolds, M. J. Kipper and A. F. Martins, *Eur. Polym. J.*, 2020, **130**, 109677.
90 S. Del Hoyo-Gallego, L. Pérez-Álvarez, F. Gómez-Galván, E. Lizundia, I. Kuritka, V. Sedlarik, J. M. Laza and J. L. Vila-Vilela, *Carbohydr. Polym.*, 2016, **143**, 35–43.
91 Y. Cho, M. Lee, S. Park, Y. Kim, E. Lee and S. G. Im, *Biotechnol. Bioprocess Eng.*, 2021, **178**, 165–178.
92 C. Su, Y. Hu, Q. Song, Y. Ye, L. Gao, P. Li and T. Ye, *Appl. Biochem. Biotechnol.*, 2020, **12**, 18978–18986.
93 Q. Song, R. Zhao, T. Liu, L. Gao, C. Su, Y. Ye, S. Y. Chan, X. Liu, K. Wang, P. Li and W. Huang, *Chem. Eng. J.*, 2021, **418**, 1–10.
94 N. Hadjesfandiari, K. Yu, Y. Mei and J. N. Kizhakkedathu, *J. Mater. Chem. B*, 2014, **2**, 4968–4978.
95 R. Mohammadi Sejoubsari, A. P. Martinez, Y. Kutes, Z. Wang, A. V. Dobrynin and D. H. Adamson, *Macromolecules*, 2016, **49**, 2477–2483.
96 B. Zdyrko and I. Luzinov, *Macromol. Rapid Commun.*, 2011, **32**, 859–869.
97 J. Peng, P. Liu, W. Peng, J. Sun, X. Dong, Z. Ma, D. Gan, P. Liu and J. Shen, *J. Hazard. Mater.*, 2021, **411**, 125110.
98 T. Çaykara, M. G. Sande, N. Azoia, L. R. Rodrigues, C. Joana and C. J. Silva, *Med. Microbiol. Immunol.*, 2020, **209**, 363–372.
99 W. Cao, D. Wei, Y. Jiang, S. Ye, A. Zheng and Y. Guan, *J. Mater. Sci.*, 2019, **54**, 2699–2711.
100 D. D. Larikov, M. Kargar, A. Sahari, L. Russel, K. T. Gause, B. Behkam and W. A. Ducker, *Biomacromolecules*, 2014, **15**, 169–176.
101 M. Li, D. Mitra, E. T. Kang, T. Lau, E. Chiong and K. G. Neoh, *ACS Appl. Mater. Interfaces*, 2017, **9**, 1847–1857.
102 V. G. Correia, A. M. Ferraria, M. G. Pinho and A. Aguiar-Ricardo, *Biomacromolecules*, 2015, **16**, 3904–3915.
103 E. Koufakis, T. Manouras, S. H. Anastasiadis and M. Vamvakaki, *Langmuir*, 2020, **36**, 3482–3493.
104 W. Yandi, S. Mieszkin, M. E. Callow, J. A. Callow, J. A. Finlay, B. Liedberg and T. Ederth, *Biofouling*, 2017, **33**, 169–183.
105 S. Lu, Z. Tang, W. Li, X. Ouyang, S. Cao, L. Chen, L. Huang, H. Wu and Y. Ni, *Cellulose*, 2018, **25**, 7261–7275.
106 F. Alipour, S. Khaheshi, M. Soleimanzadeh, S. Heidarzadeh and F. E. Hospital, *J. Ophthalmic Vision Res.*, 2017, **2**, 193–204.
107 S. Kumar, R. Pillai, S. Reghu, Y. Vikhe, H. Zheng, C. H. Koh and M. B. Chan-park, *Macromol. Rapid Commun.*, 2020, **41**, 20000175.
108 G. Gao, K. Yu, J. Kindrachuk, D. E. Brooks, R. E. W. Hancock and J. N. Kizhakkedathu, *Biomacromolecules*, 2011, **12**, 3715–3727.
109 G. Gao, D. Lange, K. Hilpert, J. Kindrachuk, Y. Zou, J. T. J. Cheng, M. Kazemzadeh-Narbat, K. Yu, R. Wang, S. K. Straus, D. E. Brooks, B. H. Chew, R. E. W. Hancock and J. N. Kizhakkedathu, *Biomaterials*, 2011, **32**, 3899–3909.
110 M. Gultekinoglu, Y. Tunc, C. Erdogdu, M. Sagiroglu, E. Ayse, Y. Jin, P. Hinterdorfer and K. Ulubayram, *Acta Biomater.*, 2015, **21**, 44–54.
111 M. Gultekinoglu, S. Karahan, D. Kart, M. Sagiroglu, N. Erta, A. H. Ozen and K. Ulubayram, *Mater. Sci. Eng., C*, 2017, **71**, 1166–1174.
112 S. Krishnan, C. J. Weinman and C. K. Ober, *J. Mater. Chem.*, 2008, **18**, 3405–3413.
113 D. Leckband, S. Sheth and A. Halperin, *J. Biomater. Sci., Polym. Ed.*, 1999, **10**, 1125–1147.
114 S. Chen, L. Li, C. Zhao and J. Zheng, *Polymer*, 2010, **51**, 5283–5293.
115 W. L. Chen, R. Cordero, H. Tran and C. K. Ober, *Macromolecules*, 2017, **50**, 4089–4113.
116 X. Yu, Y. Yang, W. Yang, X. Wang, X. Liu, F. Zhou and Y. Zhao, *J. Colloid Interface Sci.*, 2022, **610**, 234–245.
117 X. Y. Zhang, Y. Q. Zhao, Y. Zhang, A. Wang, X. Ding, Y. Li, S. Duan, X. Ding and F. J. Xu, *Biomacromolecules*, 2019, **20**, 4171–4179.
118 M. Hoyos-Nogués, J. Buxadera-Palomero, M. P. Ginebra, J. M. Manero, F. J. Gil and C. Mas-Moruno, *Colloids Surf., B*, 2018, **169**, 30–40.
119 Y. Fu, Y. Yang, S. Xiao, L. Zhang, L. Huang, F. Chen, P. Fan, M. Zhong, J. Tan and J. Yang, *Prog. Org. Coat.*, 2019, **130**, 75–82.
120 Y. He, X. Wan, K. Xiao, W. Lin, J. Li, Z. Li, F. Luo, H. Tan, J. Li and Q. Fu, *Biomater. Sci.*, 2019, **7**, 5369–5382.
121 Y. Zhang, X. Zhang, Y. Q. Zhao, X. Y. Zhang, X. Ding, X. Ding, B. Yu, S. Duan and F. J. Xu, *Biomater. Sci.*, 2020, **8**, 997–1006.
122 G. Xu, X. Liu, P. Liu, D. Pranantyo, K. Neoh and E. Kang, *Langmuir*, 2017, **33**, 6926–6936.

123 G. Xu, K. G. Neoh, E. T. Kang and S. L. M. Teo, *ACS Sustainable Chem. Eng.*, 2020, **8**, 2586–2595.
124 X. Xiong, Z. Wu, Q. Yu, L. Xue, J. Du and H. Chen, *Langmuir*, 2015, **31**, 12054–12060.
125 S. Yan, S. Luan, H. Shi, X. Xu, J. Zhang, S. Yuan, Y. Yang and J. Yin, *Biomacromolecules*, 2016, **17**, 1696–1704.
126 T. Chen, L. Zhao, Z. Wang, J. Zhao, Y. Li, H. Long, D. Yu and X. Wu, *Biomacromolecules*, 2020, **21**, 5213–5221.
127 M. A. Rahman, M. Bam, E. Luat, M. S. Jui, M. S. Ganewatta, T. Shokfai, M. Nagarkatti, A. W. Decho and C. Tang, *Nat. Commun.*, 2018, **9**, 1–10.
128 M. A. Rahman, M. S. Jui, M. Bam, Y. Cha, E. Luat, A. Alabresm, M. Nagarkatti, A. W. Decho and C. Tang, *ACS Appl. Mater. Interfaces*, 2020, **12**, 21221–21230.
129 M. Zhou, Y. Qian, J. Xie, W. Zhang, W. Jiang, X. Xiao, S. Chen, C. Dai, Z. Cong, Z. Ji, N. Shao, L. Liu, Y. Wu and R. Liu, *Angew. Chemie*, 2020, **132**, 6474–6481.
130 V. A. B. Mayandi Venkatesh, E. T. L. Goh, A. J. Y. Raditya Anggara, M. Hussain Urf Turabe Fazil, S. L. Sriram Harini, T. Tun Aung, A. Stephen John Fox, L. Yang, X. J. L. Timothy Mark Sebastian Barkham, R. W. B. Navin Kumar Verma and R. Lakshminarayanana, *Antimicrob. Agents Chemother.*, 2017, **61**, 1–15.
131 Z. Tan, Y. Shi, B. Xing, Y. Hou, J. Cui and S. Jia, *Bioresour. Bioprocess.*, 2019, **6**, 1–10.
132 Z. Su, Q. Han, F. Zhang, X. Meng and B. Liu, *Carbohydr. Polym.*, 2020, **230**, 115635.
133 W. Y. Ding, S. Di Zheng, Y. Qin, F. Yu, J. W. Bai, W. Q. Cui, T. Yu, X. R. Chen, G. Bello-Onaghise and Y. H. Li, *Front. Chem.*, 2019, **7**, 1–14.
134 D. J. Phillips, J. Harrison, S. J. Richards, D. E. Mitchell, E. Tichauer, A. T. M. Hubbard, C. Guy, I. Hands-Portman, E. Fullam and M. I. Gibson, *Biomacromolecules*, 2017, **18**, 1592–1599.
135 L. M. Thoma, B. R. Boles and K. Kuroda, *Biomacromolecules*, 2014, 2933–2943.
136 M. A. De Jesús-Tellez, S. De Rosa-garcía, I. Medrano-galindo, I. Rosales-pe, U. S. Schubert and P. Quintana-owen, *React. Funct. Polym.*, 2021, **163**, 104887.
137 P. S. Yavvari, S. Gupta, D. Arora, V. K. Nandicoori, A. Srivastava and A. Bajaj, *Biomacromolecules*, 2017, **18**, 2024–2033.
138 S. Mukherjee, S. Barman, R. Mukherjee and J. Haldar, *Front. Bioeng. Biotechnol.*, 2020, **8**, 1–19.
139 S. Hong, H. Takahashi, E. T. Nadres, H. Mortazavian, G. A. Caputo, J. G. Younger and K. Kuroda, *PLoS One*, 2017, **12**, 1–17.
140 R. Bansal, R. Pathak, B. Kumar, H. K. Gautam and P. Kumar, *Colloid Polym. Sci.*, 2017, **295**, 1177–1185.
141 Y. Xue, H. Xiao and Y. Zhang, *Int. J. Mol. Sci.*, 2015, **16**, 3626–3655.
142 S. R. Williams and T. E. Long, *Prog. Polym. Sci.*, 2009, **34**, 762–782.
143 S. Liu, R. J. Ono, H. Wu, J. Yng, Z. Chang, K. Xu, M. Zhang, G. Zhong, J. P. K. Tan, M. Ng, C. Yang, J. Chan, Z. Ji, C. Bao, K. Kumar, S. Gao, A. Lee, M. Fevre, H. Dong, J. Y. Ying, L. Li, W. Fan, J. L. Hedrick and Y. Yan, *Biomaterials*, 2017, **127**, 36–48.
144 A. Alamri, M. H. El-Newehy and S. S. Al-Deyab, *Chem. Cent. J.*, 2012, **6**, 1–13.
145 S. P. Rogalsky, O. V. Moshynets, L. G. Lyoshina and O. P. Tarasyuk, *EPMA J.*, 2014, **5**, A133.
146 V. Wee, L. Ng, J. Pang, K. Tan, J. Leong, Z. X. Voo and J. L. Hedrick, *Macromolecules*, 2014, **47**, 1285–1291.
147 Y. Qiao, C. Yang, D. J. Coady, Z. Y. Ong, J. L. Hedrick and Y. Y. Yang, *Biomaterials*, 2012, **33**, 1146–1153.
148 A. Nimmagadda, X. Liu, P. Teng, M. Su, Y. Li, Q. Qiao, N. K. Khadka, X. Sun, J. Pan, H. Xu, Q. Li and J. Cai, *Biomacromolecules*, 2017, **18**, 87–95.
149 J. Oh, S. Kim, M. Oh and A. Khan, *RSC Adv.*, 2020, **10**, 26752–26755.
150 F. G. G. Dias, L. de, F. Pereira, R. L. T. Parreira, R. C. S. Veneziani, T. C. Bianchi, V. F. N. de, P. Fontes, M. de, C. Galvani, D. D. P. Cerce, C. H. G. Martins, F. Rinaldi-Neto, N. H. Ferreira, L. H. D. da Silva, L. T. S. de Oliveira, T. R. Esperandim, F. A. de Sousa, S. R. Ambrósio and D. C. Tavares, *Eur. J. Pharm. Sci.*, 2021, **160**, 105739.
151 I. J. Asiedu-Gyekye, A. S. Mahmood, C. Awortwe and A. K. Nyarko, *Interdiscip. Toxicol.*, 2015, **8**, 193–202.
152 Y. Yuan and H. Chen, *Food Packag. Shelf Life*, 2021, **30**, 100718.
153 M. Rosin, A. Welk, O. Bernhardt, M. Ruhnau, F. A. Pitten, T. Kocher and A. Kramer, *J. Clin. Periodontol.*, 2001, **28**, 1121–1126.
154 Z. Zhou, D. Wei, Y. Guan, A. Zheng and J. J. Zhong, *Mater. Sci. Eng., C*, 2011, **31**, 1836–1843.
155 J. Guo, J. Qin, Y. Ren, B. Wang, H. Cui, Y. Ding, H. Mao and F. Yan, *Polym. Chem.*, 2018, **9**, 4611–4616.
156 M. S. Ganewatta and C. Tang, *Polymer*, 2015, **63**, A1–A29.
157 A. A. Overview, Y. Pan, Q. Xia and H. Xiao, *Polymers*, 2019, **11**, 1238.
158 R. Namivandi-Zangeneh, R. J. Kwan, T.-K. Nguyen, J. Yeow, F. L. Byrne, S. H. Oehlers, E. H. Wong and C. Boyer, *Polym. Chem.*, 2018, **9**, 1735–1744.
159 M. R. E. Santos, P. V. Mendonça, M. C. Almeida, R. Branco, A. C. Serra, P. V. Morais and J. F. J. Coelho, *Biomacromolecules*, 2019, **20**, 1146–1156.
160 S. Barman, M. M. Konai, S. Samaddar and J. Haldar, *Appl. Mater.*, 2019, **11**, 33559–33572.
161 S. K. Sharma and G. S. Chauhan, *J. Mater. Sci.: Mater. Med.*, 2010, 717–724.
162 G. Garg, G. S. Chauhan, R. Gupta and J. Ahn, *J. Colloid Interface Sci.*, 2010, **344**, 90–96.
163 P. Copolymer, Y. Xue and H. Xiao, *Polymers*, 2015, **7**, 2290–2303.

On the other hand, induced antimicrobial activity refers to the process of modifying a polymer's structure or incorporating antimicrobial agents during its synthesis to introduce antimicrobial properties that may not be present in the base polymer. For example, a surface of silicone rubber underwent modification through a radiation grafting process, with gamma irradiation facilitating the grafting of 2-hydroxyethylmethacrylate onto the surface, followed by the subsequent grafting of 4-vinylpyridine to achieve a binary grafting. Then, the pyridine groups were quaternized using butyl or hexyl bromides. These quaternized surfaces exhibited >90% inhibition the growth of *S. aureus* and 45% inhibition the growth of *E. coli* [5].

By incorporating peptides into a polymeric structure, novel materials with inherent antimicrobial characteristics have been developed. The combination of peptides and polymers offers a versatile means of designing advanced antimicrobial materials with possible applications in healthcare, such as coatings for implanted biomedical devices. To illustrate, a 3D printed medical grade polycaprolactone was modified with melimine, and a cationic peptide either covalently attached (EDC coupling) or adsorption (noncovalent interactions). The peptide modified polymer inhibited *S. aureus* growth by >70%, whilst preventing the formation of biofilms for 3 days [6].

The reduction of biofilms and the influence of biofilm formation on abiotic surfaces was studied using a highly-branched poly(*N*-isopropyl acrylamide) modified with Vancomycin. Although the polymers did not totally eliminate all *S. aureus*, significant reduction (10-fold) in bacterial numbers on infected corneas was observed [7].

1.2. Polymers Integrated with Organic Antimicrobial Agents

Organic compounds having antimicrobial properties can be incorporated/attached into polymers *via* non-covalent interactions. The release profile of antimicrobial agent depends on the formulation, the interaction between polymer and the antimicrobial agent and the polymer composition [8]. The compounds are often released from the polymer matrix (often with "burst kinetics"), but some polymers can slowly release antimicrobial agents over time, creating a sustained antimicrobial effect [9] with release of antibiotics from the polymeric system in a controlled manner depending on the linkage (either cleaved *via* hydrolysis or enzymatic degradation) between the drug and the polymer [10].

One of the most common antimicrobial agents, triclosan (2, 4, 4-trichloro-2-hydroxydiphenyl ether) is widely used in personal care products such as soaps, toothpaste, cosmetics. An antimicrobial polymer composite [11] for the coating of sanitary and household furniture was produced by mixing an unsaturated polyester resin (unsaturated polyester of orthophthalic acid), methyl ether ketone peroxide, filler ($CaCO_3$) with triclosan (5 wt.%). The non-porous composite showed antimicrobial activity with most Gram-negative and Gram-positive bacteria eliminated *via* 5-min of contact with the surface, with >90% inhibition of a clinical strain of *C. albicans*. The polymer composite showed similar performance over three cycles of abrasion [11].

Candida species have a tendency to form biofilms on polymeric surfaces which can cause infections in humans where polymer-based medical devices are employed. Thus, a high-density polyethylene was melt-blended with various ratios (*e.g.*, 0 to 0.5 wt.%) of 1-hexadecyl-3-methylimidazolium chloride or 1-hexadecyl-3-methylimidazolium

methanesulfonate (fungicides). The resulting polymer films prevented biofilm formation of fungal species, in addition, polyethylene-based films showed good cytocompatibility [8].

Polymers can also promote the poor stability of drugs in biological systems, reducing the necessary drug loadings needed (*e.g.*, polymyxins are unstable in the bloodstream, and high doses cause toxicity). Thus, polymer-controlled release of polymyxins have been explored [12]. Amphiphilic poly(L-glutamic acid-co-D-phenylalanine) was capable of self-assembly with positively charged polymyxins loaded onto the polymer *via* electrostatic and hydrophobic interactions.

For finer controlled release, a cleavable linker between the polymer and drug can be utilised. As an example, an antimicrobial micelle system was developed for targeted drug delivery that used vancomycin and pH/lipase triggers to control antibiotic release. These micelles had an extended circulation time in the bloodstream and only released antibiotics where needed (pH raised in infection) reducing premature drug release. This was achieved by synthesizing poly(ε-caprolactone) through ring-opening polymerization intiated by acetyl-terminated poly(ethylene glycol) and conjugating vancomycin as a targeting ligand *via* a pH-cleavable hydrazone bond produced micelle carriers (77 nm), that also allowed encapsulation of the antibiotic ciprofloxacin through hydrophobic interactions. Under acidic conditions, the deshielding of vancomycin shells led to a disruption in the balance between hydrophobic and hydrophilic properties. This, in turn, caused micelles to enlarge, facilitating the lipase mediated degradation of the poly(ε-caprolactone) (lipase is overexpressed at the infection site), resulting in the release of encapsulated ciprofloxacin. After single-dose administration

of micelles, the bacterial counts in lung tissues of *P. aeruginosa*-infected mice were decreased 99.9% [13].

The essential oils of peppermint, carvacrol, eugenol, thymol, and linalool are frequently used as antimicrobials [9]. These essential oils primarily damage cell membranes to produce their antibacterial actions, however, they can have poor solubilities and stabilities in aqueous media [9]. Zhu *et al*. [14] investigated the effectiveness of thymol-loaded poly(lactic-co-glycolide microspheres as carriers for thymol which demonstrated enhanced thermal and storage stability. These allowed controlled release of thymol, with the porous structure of the microspheres facilitating the permeation of thymol into the bacterial, leading to disruption of their cytoplasmic membranes. The antibacterial effect was validated by treating naturally contaminated milk with the thymol-loaded microspheres which suppressed the growth of bacteria.

An antibiofilm platform was developed using synthetic antimicrobial polymers as a delivery vehicle for essential oils [15], with two ternary antimicrobial polymers consisting of cationic, low-fouling and hydrophobic groups used to encapsulate carvacrol and eugenol as micelles in oil-in-water emulsions. The emulsions exhibited good inhibition of biofilm formation with synergistic killing activity. A 20-minute treatment biofilm of *P. aeruginosa* with the block copolymer-oil combination resulted in a reduction of bacteria by >99%.

1.3. Polymers Incorporating Inorganic Antimicrobial Agents

Nanoparticle-based strategies are powerful alternatives to conventional therapeutic approaches utilizing traditional antibiotics. Nanoparticles' effectiveness against microbes

depends on their physiochemical attributes, including composition, surface charge, functionalities, size, and shape. Their efficacy varies with the type of bacteria, determined by cell wall composition. Combining nanoparticles with synthetic antimicrobial polymers is an effective strategy against antibiotic resistance, widening the scope of the antimicrobial activity of the polymeric materials [16]. Metallic nanoparticles, especially silver have been used to create various antimicrobial polymeric platforms, such as biomedical textiles, and surfaces for food preparation [17]. It should be noted that silver nanoparticles have been used for over 50 years and the properties of silver as an antimicrobial has long historic prescient – feeding a child from a silver spoon and putting silver coins into milk are two historical examples. In 1891, colloidal silver was employed for the purpose of sterilizing wounds [18].

Various methods are utilized in the production of silver nanoparticles, including physical and chemical techniques. These encompass a broad range of approaches, such as the sol-gel, micelle formation, chemical precipitation, hydrothermal techniques, electrochemical methods, pyrolysis, and chemical vapour deposition, which are utilized in the synthesis of these nanoparticles.

Silver-containing materials exhibit diverse mechanisms of action against bacteria, including physical disruption of the bacterial membrane, generation of reactive oxygen species leading to oxidative stress, and interference with critical cellular processes such as DNA synthesis [19]. Although silver has some toxicity towards mammalian cells [20] its therapeutic window of antimicrobial activity towards a broad spectrum of bacteria, fungi, viruses is high.

In general, the preparation of silver/polymeric nanocomposites involves the *in-situ* reduction of Ag^+ ions, to form metallic nanoparticles within the polymer matrix. Polydopamine has the

ability to convert silver ions into silver nanoparticles (AgNPs) on different materials, without requiring additional reducing agents [21]. The surface modification of polysulfone membranes through the application of polydopamine facilitated the *in-situ* formation of silver nanoparticles on these membranes. This modification resulted in a notable reduction in bacterial adhesion and growth on the polysulfone membranes. Leaching tests showed significantly lower release of Ag^{+} ions, making this technology safe and effective for cleaning drinking water [22].

Synthesized silver nanoparticles can be immobilized onto the surface either by the functionalization of nanoparticles or the membrane surface to promote their binding. A study [23] introduced a novel method for fabricating a membrane through post-modification by grafting nanoparticles onto the surface. In this study, silver nanoparticles were synthesized by reducing silver nitrate in the presence of sodium borohydride and subsequently encapsulating them in positively charged polyethyleneimine (PEI). Plasma-treatment of polysulfone ultrafiltration membrane surface added hydroxyl, and carboxyl groups onto its surface, which subsequently reacted with PEI-AgNP's (both with and without 1-ethyl-3-(3-dimethylaminopropyl) carbodiimide hydrochloride (EDC) coupling. These modified surfaces effectively inactivated *E. coli* (showing more than a 3-log fold reduction), while silver ions were released over the course of 14 days from the surface.

The antiseptic and health benefits of copper were recognized by civilizations as far back as 3000 BC [24]. The first publication about Cu as an antimicrobial coating was in 1962 [25]. The most notable characteristic of metallic or alloyed copper surfaces is their remarkable capability to rapidly and effectively eliminate bacteria or other microorganisms when they come into close

contact. A copper-based polymer composite [26] "Copper Armour™" (copper particles embedded methyl methacrylate resin matrix) were tested over a nine-week period in an adult intensive care unit. At least four type of Cu nanoparticles were seen embedded in the polymeric matrix. In *in vitro* studies, the composite reduced >99.99% of bacteria (*S. aureus*, *P. aeruginosa*, *E. coli* and *L. monocytegenes*) in 1 hour of contact.

Zinc oxide nanoparticles also exhibit notable antimicrobial activity by interacting with the surface of bacteria, followed by penetration through the cell wall, ultimately resulting in the death of the bacteria [27]. A hydrogel composite bandage [28] was developed from a polymer matrix blends of poly vinyl alcohol, starch and chitosan with dispersed zinc oxide nanoparticles used to investigate its wound healing properties. The cell viability of L929 fibroblasts was > 87% after incubation with hydrogels. In *in vivo* wound healing experiments, it was observed that the epidermis had fully fused, and there were no signs of necrosis, granulation, or edema after 14 days.

The prevailing prosthetic choice for individuals who are completely or nearly toothless is still a removable denture composed of polymethylmethacrylate, due to its ease of processing and good mechanical strength. However, dentures are prone to accumulating plaque, which can lead to unfavourable consequences. Thus, a zinc oxide nanoparticle-polymethylmethacrylate nanocomposite [29] was developed for denture to study its effect on fungal biofilm formation. PMMA resin Superarcyl Plus was sprayed with zinc oxide nanoparticles produced *via* either microwave-assisted hydrothermal or solvothermal synthesis. Both composites showed antifungal activity against *C. albicans* solutions, with the best inhibition (4-fold compared to control) observed in composites that contained higher ratios of zinc oxide (activity is *via* the

increased induction of antioxidative stress in microorganisms caused by the release of Zn^{+2} ions).

1.4. Conclusion and Future Work

In conclusion, bacterial infections linked to contamination, specifically, of medical device implants presents a formidable threat, contributing significantly to rising fatality rates due to bacterial infections. This, coupled with the overuse of antibioticshas fueled the emergence of antimicrobial resistance, intensifying the challenge and need at hand. Consequently, antimicrobial polymers emerge as a promising avenue due to their broad-spectrum antimicrobial effectiveness. By leveraging macromolecular antimicrobial polymers, which can disrupt microbial cell membranes in a variety of ways, means that the likelihood of pathogen resistance is diminished compared to conventional antibiotics. Furthermore, recent advancements in polymerization techniques have yielded antimicrobial polymers that possess design versatility and adjustable properties, making them an attractive option for targeting various microorganisms in diverse applications.

Future research on effective antimicrobial polymers should focus on deepening our understanding of the structure-activity relationship that underlies antimicrobial properties, while also facilitating the translation of these technologies from the laboratory to practical applications. Through continued innovation and interdisciplinary collaboration, antimicrobial polymer research should address challenges such as achieving long-term stability, minimizing cytotoxicity, understanding their modes of action, while combating a broad range of microorganisms with a single polymeric material, thereby addressing critical healthcare and environmental challenges associated with microbial infections and contamination.

Chapter 2

Aims of the Thesis

Antimicrobial polymers are a game-changing solution in the fight against pathogens, replacing, in certain applications, traditional antibiotics. These polymers can be customized to effectively combat a broad spectrum of pathogens, including viruses, fungi, and both Gram-positive and Gram-negative bacteria. Among them, cationic polymers have shown exceptional promise, primarily due to their unique mechanisms of action by interacting with the negatively charged cell envelopes of bacteria, resulting in membrane disruption and eventual bacterial death.

The primary objective of my research during my doctoral studies was to synthesize antimicrobial polymers containing quaternary ammonium groups, thereby imparting intrinsic antimicrobial activity without the necessity of additional incorporation of inorganic or organic antimicrobial agents and test them against a wide range of microorganisms, both in solution and on surfaces. The aim of the first project was to utilize Reversible Addition Fragmentation Chain Transfer (RAFT) polymerization to generate homopolymers containing quaternary ammonium groups with size-defined molecular weight polymers. Subsequently, the synthesized polymers underwent testing against both Gram-negative and Gram-positive bacteria. Through this systematic investigation, the influence of polymer molecular weight on antimicrobial effectiveness was sought to be ascertained, thereby contributing to a deeper understanding of the structure-activity relationship governing the antimicrobial properties of

the synthesized homopolymers. Concurrently, the study also involved evaluating the hemolytic and cell toxicity activities of the polymers.

The second project aimed to synthesize a novel monomer and its corresponding polymers, followed by comprehensive analysis and evaluation of their antimicrobial activity and cytocompatibility. This novel monomer could be utilized to create a new range of polymers suitable for diverse antimicrobial applications.

In the third project was aimed to explore the antimicrobial properties of a Tröger's Base polymer and its' quaternized derivatives as a potential new antimicrobial surface coating. The polymers would be applied to surfaces and subjected to further testing for both antimicrobial efficiency and cytocompatibility through the use of bacterial cultures and red blood cells.

Chapter 3

Synthesis of a Homopolymer Library using Ammonium Group Containing Monomers

Parts of this chapter are published as:

Haktaniyan, M.; Sharma, R.; Bradley, M. Size-Controlled Ammonium-Based Homopolymers as Broad-Spectrum Antibacterials. *Antibiotics*, **2023**, *12*, 1320 (22 pages).

3.1. Introduction

The excessive use of conventional antibiotics, that are traditionally generated from natural, often low-molecular-weight compounds, has led to the development of antimicrobial resistance. This has resulted in some current drugs becoming non-functional. As a result, there has been a significant focus on developing antimicrobials that have new modes of action, longer-lasting effects and minimal impact on the environment. One such area is the synthesis of cationic polymers, which are known for their intrinsic antimicrobial properties through their ability to disrupt the cell membrane or envelope of bacteria, ultimately leading to their death. Cationic polymers can be synthesized directly from cationic monomers by either as homopolymers or copolymers combining with other monomers, or modification of existing polymers to give rise to ammonium, phosphonium, sulfonium or guanidinium-based materials. Cationic polymers are a highly versatile collection of compounds, due to their ease of synthesis, ready control of their molecular weights and good water solubility. As a result,

they have found widespread application in areas such as medical and dental implants [30,31] and surface sanitization [32], as well as in drug-delivery formulations [33], water-waste treatment [34], personal-care products [35] , and as disinfectants [36] and bacterial sensors [37].

Quaternary ammonium containing polymers can be synthesized through two common methods: direct polymerization of quaternary ammonium group-bearing monomers (including tertiary amines that can be protonated) or quaternization of amine groups of existing polymers with alkyl halides [38] or by reductive amination [39]. The degree of quaternization can be limited by steric hindrance and the influence of neighbouring (positively charged) groups in the post-quaternization approach – indeed achieving full functionalization through post-quaternization of polymeric secondary and tertiary amines can be challenging. However, since the degree of quaternization is an important factor in the antimicrobial activities of the polymers, variation can be led to irreproducible materials [40].

3.2. Homopolymers as Antimicrobial Agent

Although antibacterial copolymers with quaternary ammonium groups have been reported extensively [41–43], just a few reports have looked at the antimicrobial activity of homopolymers [44–50]. These are described below.

3.2.1. Poly(2-dimethylamino)ethyl methacrylate

Among the cationic polymers, poly(2-dimethylamino)ethyl methacrylate (PDMAEMA) is probably the most commonly used material (the amine becoming an ammonium ion upon protonation) for use in biomedical applications with its incorporation into films, surface coatings, and synthesis *via* various polymerization techniques such as Nitroxide Mediated

Polymerization (NMP), Atom Transfer Radical Polymerization (ATRP) and Reversible Addition Fragmentation Chain Transfer Polymerization (RAFT), has been reported. The efficacy of PDMAEMA as an antimicrobial agent varies on various factors, including its molecular weight, level and type of quarterisation and the microorganism it targets. A study [51] showed that PDMAEMA (12.8 kDa) inhibited the binding and uptake of *Salmonella typhimurium* into the human epithelial intestinal cell line, HT29-MTX-E12. Additionally experiments revealed that PDMAEMA mitigated the inflammatory response triggered by bacterial and its toxins. The same polymer [47] demonstrated efficacy in hindering the growth of clinical isolates of *S. epidermidis*, and mature biofilms of *S. epidermidis* were significantly inactivated.

Polymers [44] have been synthesized through RAFT polymerization, poly(2-(dimethylamino)ethyl methacrylate) (4.5 kDa, 6.1 kDa and 11.2 kDa), poly(2-(dimethylamino)ethyl acrylate) (11 kDa and 3.2 kDa) and poly(2-aminoethylmethacrylate) (11.2 kDa) showed antimicrobial activity against *M. smegmatis* and Gram-negative (*E. coli* and *P. putida*) bacteria. PDMAEMAs demonstrated preferential eradication of mycobacteria in comparison to Gram-negative bacteria, with PDMAEMA (11.2 kDa) exhibiting relatively limited membrane lytic activity.

A quaternary ammonium salt monomer (2-hydroxy-*N*-(2-(methacryloyloxy)ethyl)-*N,N*-dimethyl-ethyl ammonium bromide) [50] was synthesized from 2-(dimethylamino)ethyl methacrylate by alkylation with 2-bromoethanol and polymerized *via* free radical polymerization (estimated molecular weight as 25±6.2 kDa *via* size exclusion chromatography - multi-angle laser light scattering). The minimum inhibition concentration (MIC) values of the polymer for *S. aureus* and *E. coli* were 0.5 mg/mL and 1.0 mg/mL.

3.2.2. Poly[2-(methacryloyloxy)ethyl]trimethyl ammonium chloride

Homopolymers of poly[2-(methacryloyloxy)ethyl]trimethylammonium chloride) (PMETACl) were evaluated [52] for their antibacterial and antifungal activities. Free radical polymerization was employed (Mn 87.4 kDa, Đ 2.38), while polymeric gels were also prepared *via* application of the cross-linker (*N, N'*-methylenebis(acrylamide). The homopolymer inhibited various Gram-positive, Gram-negative bacteria and fungi in the range of 100-1100 μg/mL except for *Sa. Cerevisiae* (>10,000 μg/mL). The polymer gels exhibited the rapid adsorption and "precipitation" of bacteria, leading to the elimination of nearly all bacteria through their adsorption into the gels within 10 minutes.

3.2.3. Poly[(3-methacryloylamino)propyl]trimethylammonium chloride

The biofilm development of *P. aeruginosa* when incubated on surfaces coated with homopolymers of [(3-methacryloylamino)propyl]trimethylammonium chloride (Mn 19.6 kDa, Mw 20.5 kDa, Đ 1.05 and Mn 15.3 kDa, Mw 20.3 kDa, Đ 1.33) - synthesized *via* RAFT polymerization) showed a reduction in bacterial attachment without killing. Although both polymers did not effectively inhibit the growth of planktonic bacteria, the polymer with the higher molecular weight modulated the aggregation behavior of the bacteria on the surface. This modulation occurred through the formation of polymer coverage around the bacterial cells via electrostatic interactions between the "anionic bacteria" and the cationic polymer, resulting in the formation of macroscopic aggregates and a slower adhesion process to the surface to form biofilm [53].

3.3. Controlled Radical Polymerization

With the developments in modern living radical polymerization techniques, often referred to as reversible-deactivation radical polymerization (RDRP) methods such as NMP, ATRP and RAFT, has meant it has become feasible to produce a range of synthetic antimicrobial polymers that are well regulated in their monomer sequence and size, even on large scale [54–56].

The starting point for this was the work of Szwarc (1956) who revolutionized polymer chemistry by introducing the concept of anionic polymerization of styrene using sodium napthalenide. The innovative approach provided a precise control over molecular weight and structure (block polymers could be made) and was a ground-breaking moment in polymer chemistry[57]. Subsequently, the concept of living polymerization *via* radical mechanisms was achieved, which avoids the need to prevent termination by having totally anhydrous reaction environments.

Controlled radical polymerization offers a distinctly different mechanism over conventional free radical polymerization, where chains are continuously formed, propagated, and terminated through radical-radical reactions. To achieve controlled radical polymerization; control agents (specific agents or catalysts) are employed during the polymerization process. These agents temporarily deactivate the growing polymer chains, allowing for precise control over the polymer's growth by establishing an equilibrium between the dormant and active chains (keeping the concentration of reactive species low) [58]. This level of control allows for the synthesis of polymers with controlled molecular weights, narrow molecular weight distributions, and well-defined structures. Moreover, polymers with complex architectures

and site-specific functionality can be synthesized as “blocks of polymer” can be generated *via* the addition of different/new monomers during the polymerisation reaction. As such structures that were previously impossible to achieve *via* free-radical polymerization can be generated [59–61].

3.3.1. Reversible Addition Fragmentation Chain Transfer Polymerization

Since researchers [62] conducted the first RAFT polymerization reaction in 1998, RAFT polymerization has shown that it is a powerful technique for designing complex and versatile polymer architectures. Compared to other controlled polymerization techniques, RAFT polymerization offers wide applicability to various monomers including monomers with functional groups (*e.g.*, OH, NR_2, CO_2H, SO_3H) and tolerates a range of solvents including water. It also works under a variety of experimental conditions, including bulk, emulsion, and suspension polymerization formats. What makes RAFT polymerization particularly advantageous for biomedical applications is that it does not use potentially toxic metal salts. Moreover, the breadth of the chain transfer agents means that the polymers produced through the RAFT process can have a variety of end groups that can be modified or functionalized [63].

In the process of RAFT polymerization, the process starts with an initiation step and the production of radicals (I•) from an initiating radical source (typically using heat or light as in conventional free radical polymerization.) However, in this case when radicals come into contact with monomers, to form the radical species (I-Pn•), they rapidly react with the RAFT “control” agent, also known as the chain transfer agent (CTA) to form a new intermediate radical resulting in a dormant chain which contains the (–S-C(=S)-Z) group. Vitally, this

intermediate exists in equilibrium between active and dormant species. The new radical (R•) reinitiates the process by adding monomers to the growing chains (Pm• - called an active chain) with a reversible-addition-fragmentation equilibrium allowing control over molecular weight and polymer size distribution. Termination might still occur to form dead chains, but this is limited by their very low concentrations [54,62].

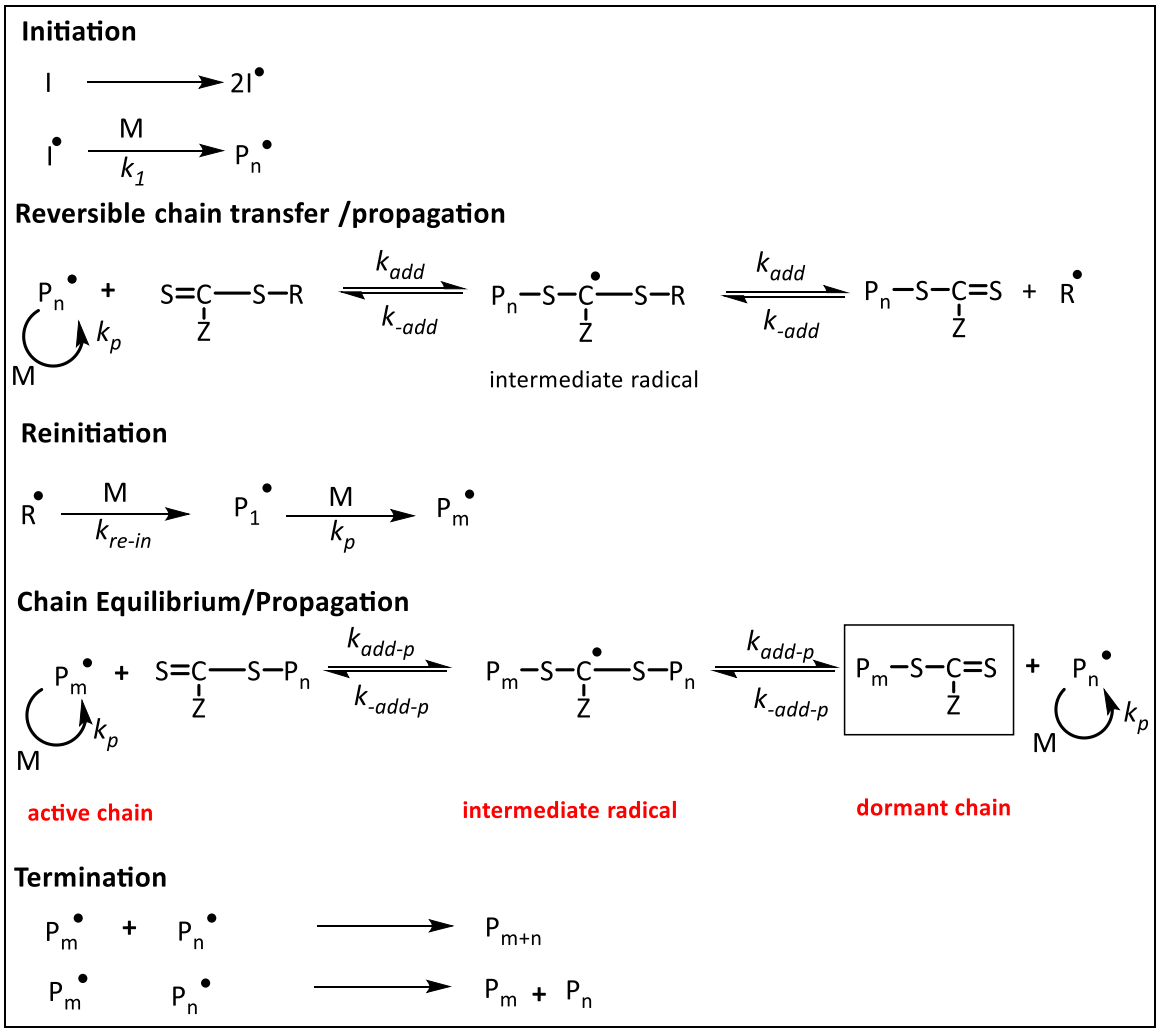

Figure 3.1. Mechanism of Reversible Addition Fragmentation Chain Transfer Polymerization.

3.3.2. Chain Transfer Agent

As mentioned above, the choice of chain transfer agent (CTA) is a key parameter for successful RAFT polymerization. Depending on the monomer type which can be either so-called more activated-monomers *e.g.*, methacrylate derivatives, styrene, butadiene or less activated-monomers *e.g.* diallyl dimethyl ammonium chloride, vinyl acetate, N-vinylpyrrolidone, the CTA needs to be specifically selected [62].

This is because the effectiveness of the chian transfer agent depends on the free-radical leaving group R and the nature of the Z group that can activate or deactivate the C=S double bond thereby controlling and regulating the polymerization process by stabilisation of the intermediate. At the same time, the R- group should be a good leaving group (and returning group) that can reinitiate polymerization rapidly and effectively. There are four main types of chain transfer agents used, trithiocarbonates (1), dithiocarbonates (2), xanthates (3) and dithiocarbomates (4). Trithiocarbonates and dithiocarbonates offer control of polymerizations of more activated monomers, while, xanthates and dithiocarbomates are used for both type of monomers [62]. Due to lone pair(s) of oxygen or nitrogen adjacent to the thiocarbonyl group, the double bond character of the thiocarbonyl decreases due to the zwitterionic canonical forms, destabilizing the radical intermediate, thus less activate monomers can be polymerized by xanthante or dithiocarbamates chain transfer agents [64].

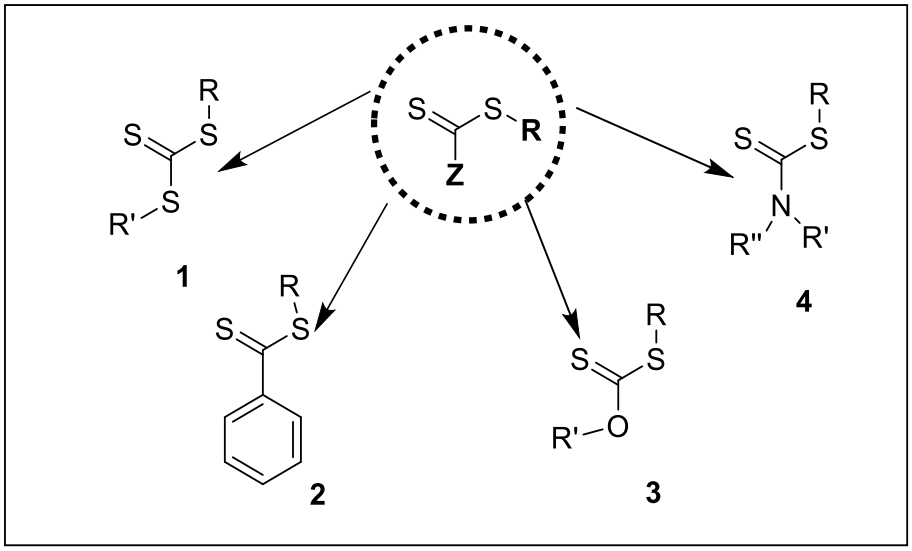

Figure 3.2. General classification of Chain Transfer Agents. Trithiocarbonates (1), dithioesters (2), xanthates (3) and dithiocarbomates (4).

3.4. Aims of the Chapter

In this chapter, a library of homopolymers with quaternary ammonium groups was synthesized using quaternary ammonium group-bearing monomers through RAFT polymerization. The polymerization conditions were carefully optimized to ensure controlled polymer growth (molecular weight around 20 kDa) and well-defined structures for water-soluble homopolymers. Following this, the prepared polymer library was tested against both Gram-negative and Gram-positive bacteria to identify the most effective antimicrobial homopolymers. In addition, the homopolymers were evaluated on mammalian cells (HeLa cells) to evaluate their cytotoxic effects.

3.5. Results and Discussion

Protonated primary, secondary and tertiary amines and quaternary ammonium groups are widely recognized as important moieties in antimicrobial polymers. Among these, quaternary ammonium groups, carry an inherently positive charge that remains unaffected by pH. To ensure control over the molecular weight and size distribution of the polymers, RAFT polymerization was employed in the synthesis of a homopolymer library. This was achieved using either commercially available chain transfer agents (CTA1 & CTA2) or *via* the in-house synthesized chain transfer agent (CTA3). All monomers were initially polymerized through conventional free radical polymerization (AIBN and heat) in order to optimize the conditions for subsequent RAFT polymerization.

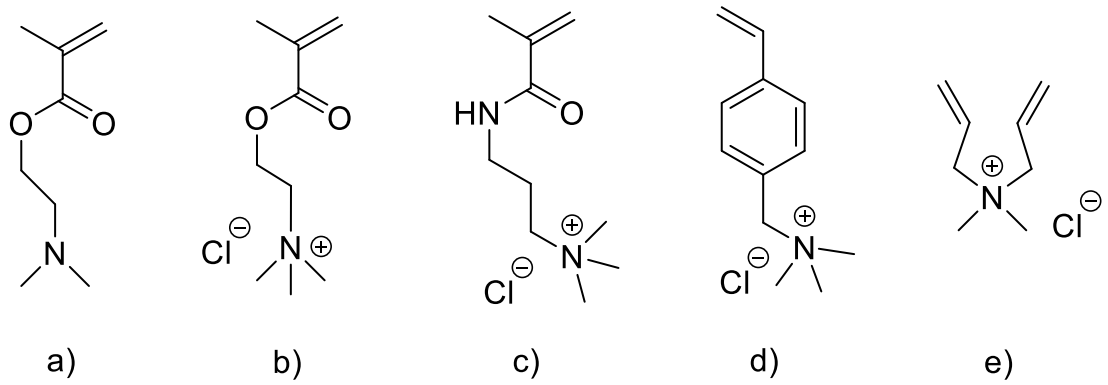

Figure 3.3. Selected monomers for the preparation of the homopolymer library. **a)** (2-(dimethylamino)ethyl methacrylate.); **b)** [2-(methacryloyloxy)ethyl]trimethyl ammonium chloride); **c)** [3-(methacryloylamino)propyl]trimethyl ammonium chloride; **d)** vinyl benzyl trimethylammonium chloride; **e)** diallyldimethyl ammonium chloride.

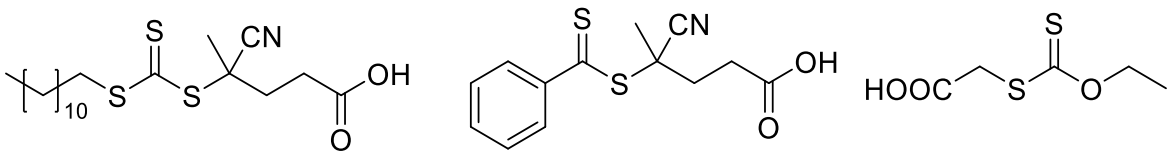

CTA1 CTA2 CTA3

Figure 3.4. Chain transfer agents used for the synthesis of the homopolymer library *via* RAFT polymerization. CTA1: 4-cyano-4-[(dodecylsulfanylthiocarbonyl)sulfanyl]pentanoic acid, CTA2: 4-cyano-4-(phenylcarbonothioylthio) pentanoic acid, CTA3: *S*-Ethoxythiocarbonyl mercaptoacetic acid.

3.5.1. Synthesis of *S*-Ethoxythiocarbonyl Mercaptoacetic Acid (CTA3)

As mentioned above, by selecting the appropriate combination of monomers and a CTA (Chain Transfer Agent), it is possible to control the molecular weight of the polymer with minimal variation in their dispersity (Đ) and yield in the RAFT polymerization. Trithiocarbonate-type (CTA1) or dithioester-type (CTA2) were selected for more activated monomers (monomers a-d), while monomer e (diallyl dimethyl ammonium chloride) was polymerized with the xanthante-type, water soluble, agent (*S*-Ethoxythiocarbonyl mercaptoacetic acid). This was synthesized by reacting potassium ethyl xanthogenate with bromoacetic acid according to the literature [65] in high yield (91%) and high purity >98% (by HPLC analysis at 254 nm, t_R = 4.25 min). ^{1}H NMR spectrum and ^{13}C NMR spectrum agreed with the literature [65].

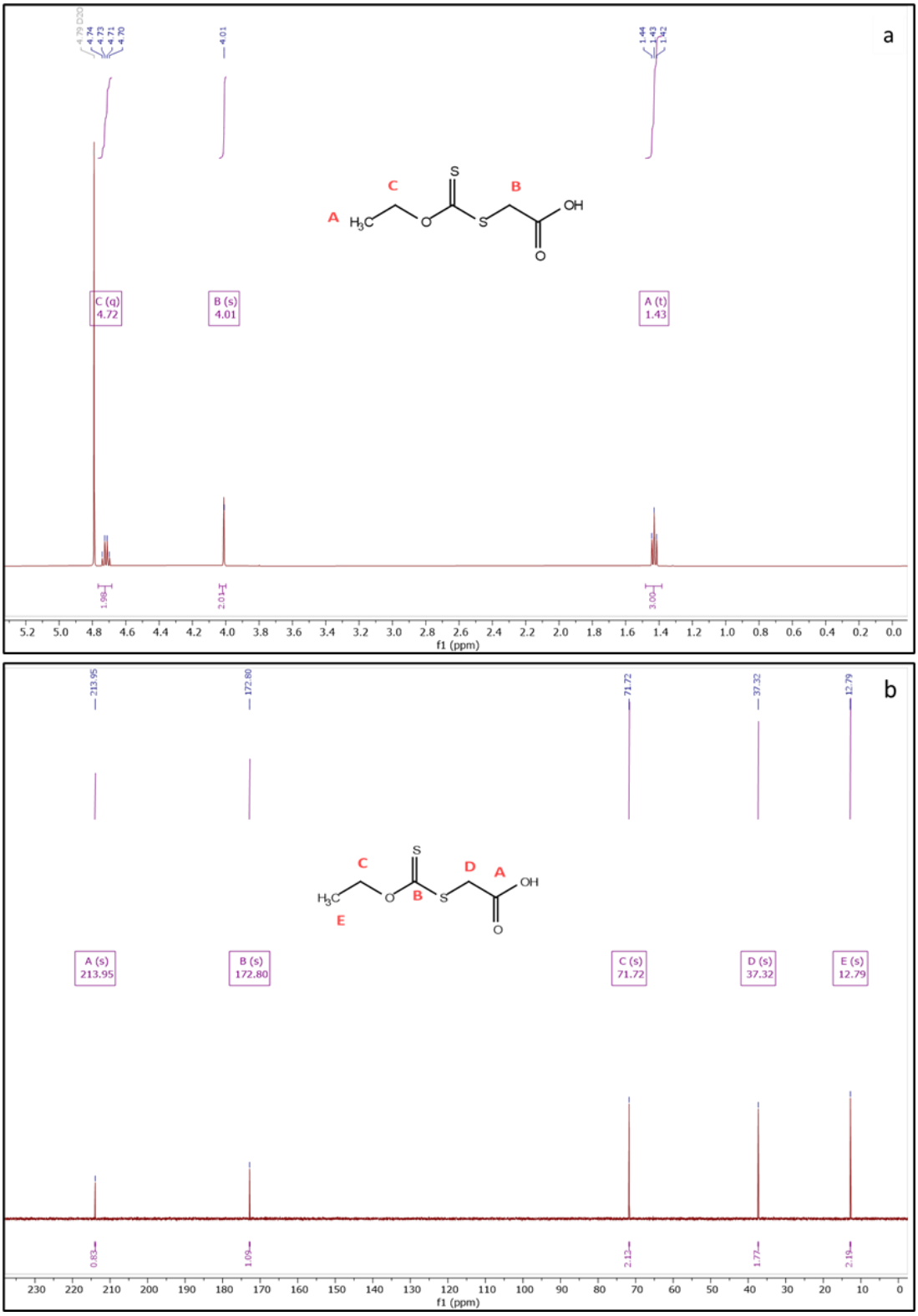

Figure 3.5. a) ^{1}H NMR spectrum of *S*-Ethoxythiocarbonyl mercaptoacetic acid in D_2O, with peak assignments. b) ^{13}C NMR spectrum of the *S*-Ethoxythiocarbonyl mercaptoacetic acid recorded in D_2O, with peak assignments.

3.5.2. Synthesis of the Homopolymer Library

It has been reported that lower-molecular-weight polymers can penetrate into Gram-positive bacteria more efficiently than their higher-molecular-weight counterparts, with cationic polyacrylates (5–10 kDa) optimal for antimicrobial activity against *S. aureus* [66]. However, there is little else known about the effect of their molecular weights on their activity or toxicity in biomedical applications (see Chapter 4). Here, homopolymers were synthesized from five different monomers, initially looking at polymers with a molecular weight of 20 kDa. GPC analysis of the homopolymers typically showed narrow, unimodal peaks with the polymerizations carried out in an aqueous environment, with the exception of 2-(dimethylamino)ethyl methacrylate, which was polymerized in ethanol. Figure 3.6 shows the polymerization conditions used.

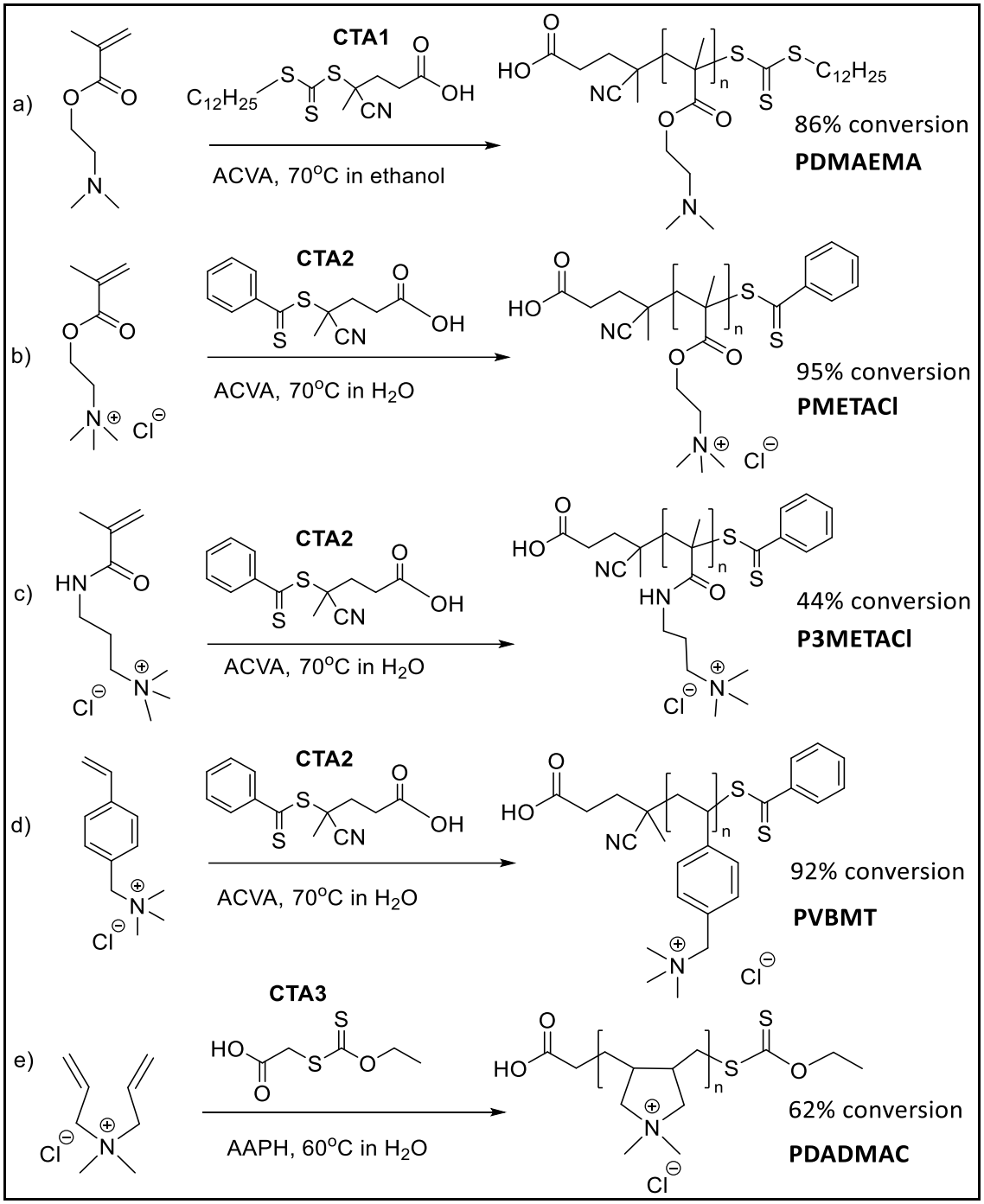

Figure 3.6. RAFT polymerization of quaternary ammonium group bearing monomers with final monomer conversion levels. a) 2-(dimethylamino)ethyl methacrylate); b) [2 (methacryloyloxy)ethyl]trimethylammonium chloride); c) [3 (methacryloylamino)propyl]trimethylammonium chloride; d) vinylbenzyl

trimethylammonium chloride and e) diallyldimethylammonium chloride. Chain transfer agents: CTA1: 4-cyano-4-[(dodecylsulfanylthiocarbonyl)sulfanyl]pentanoic acid), CTA2: 4-cyano-4-(phenylcarbonothioylthio)pentanoic acid, CTA3: S-Ethoxythiocarbonyl mercaptoacetic acid. Initiators: ACVA: 4,4-azobis(4-cyanovaleric acid), AAPH: 2,2'-azobis(2-methylpropionamidine)dihydrochloride.

2-(Dimethylamino)ethyl methacrylate (DMAEMA) is composed of two distinct parts, specifically an ammonium cation (when protonated) that is hydrophilic and a small alkyl chain that is hydrophobic. Due to its amphiphilic nature, PDMAEMA shows bactericidal and/or bacteriostatic activities depending on the tested microorganism (see examples in the section 3.1). Although PDMAEMA is a water-soluble polymer, the RAFT polymerization of DMAEMA in water did not progress with either 4-cyano-4-[(dodecylsulfanylthiocarbonyl)sulfanyl]pentanoic acid (CTA1) perhaps due to its limited solubility in aqueous environments or with 4-cyano-4-(phenylcarbonothioylthio) pentanoic acid (CTA2) due to aminolysis of the dithioester due to the presence of secondary amine groups (the pH >7) [67,68].

The RAFT polymerization of DMAEMA in aqueous environment in the presence of CTA2 has been reported in acidic buffers in the literature [69], and many examples of RAFT polymerization of DMAEMA in solvents such as 1,4-dioxane, acetonitrile or ethanol with various trithioester and dithioester chain transfer agents have been reported [70–73]. Therefore, the RAFT polymerization of DMAEMA was carried out with CTA1 in ethanol at 70°C for 24 hours with using a ratio of $[monomer]_0$/ $[CTA1]_0$ of 167 and a $[CTA1]_0$/$[initiator]_0$ ratio of 6, with monomer conversion during polymerization followed by ^1H NMR analysis. Monomer

conversion was calculated by comparing the integral areas of the vinyl protons of the monomer to the methylene peak of the polymer. The monomer conversion reached 86% after 24 hours with a molecular weight calculated (based on monomer conversion after 24 hours) as Mn = 23 kDa. GPC analysis gave a unimodal, narrow, peak with a molecular weight Mn: 22 kDa, Mw: 28 kDa with a Đ of 1.29. Molecular weight analysis of the polymer via end group integration by NMR was not possible due to the peaks of the chian transfer agent overlapping with those of the methylene group of the polymer backbone.

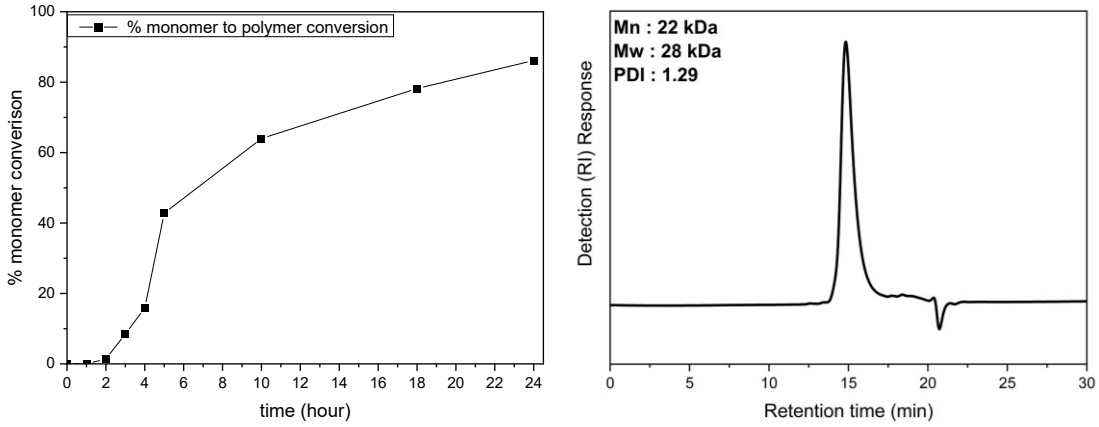

Figure 3.7. % monomer conversion to give PDMAEMA based on ^{1}H NMR spectroscopy ($CDCl_3$) and GPC analysis of PDMAEMA after purification. The eluent was THF with a flow rate 1.0 mL min^{-1} at 35°C. Calibration was achieved using poly(methyl metharcylate) standards.

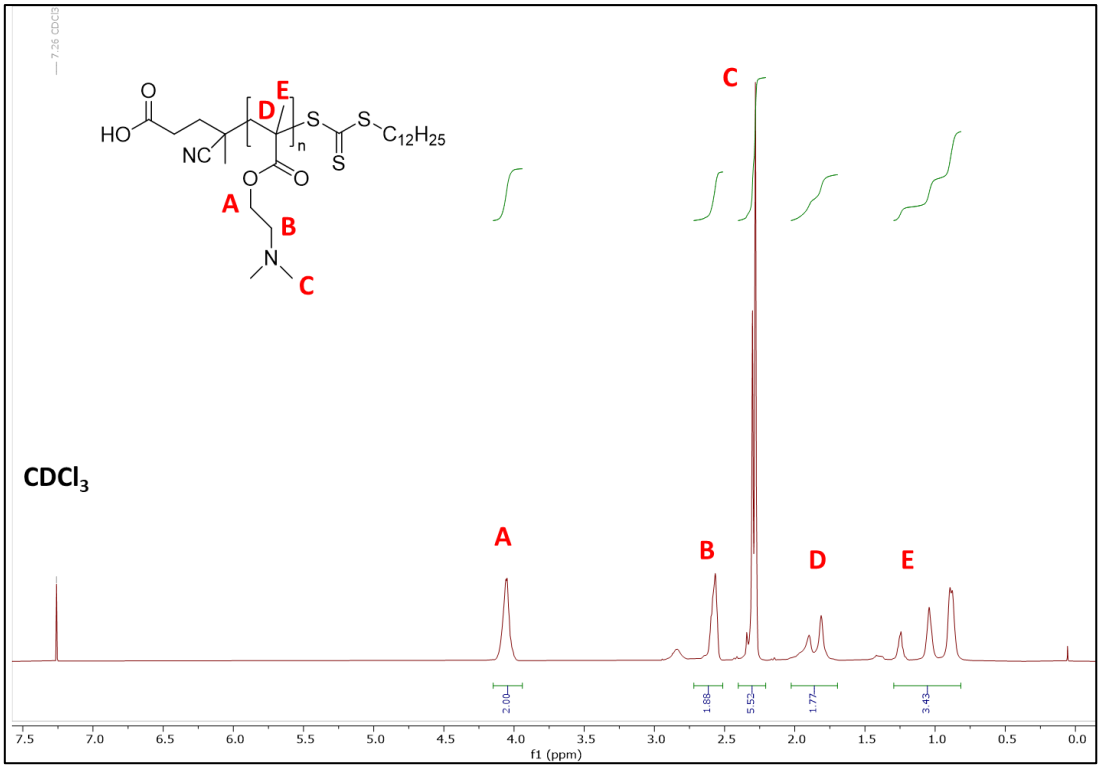

Figure 3.8. ^{1}H NMR spectrum of PDMAEMA recorded in $CDCl_3$, with peak assignments. E and D correspond to the peaks of the polymer main chain; A, C and D represent the peaks of the polymer side chain.

Polymers of the water-soluble, cationic monomer [2-(methacryloyloxy)ethyl]trimethylammonium chloride (METACl) have found use on an industrial scale, and the monomer is typically available as an aqueous solution. This monomer is also soluble in DMF, methanol, ethanol but not in acetone. Prior to RAFT polymerization, the polymer was synthesized *via* free radical polymerization in DMF, water and ethanol. It was found that the reaction in aqueous environment was completed faster with higher molecular weight and lower Đ than the reaction carried out in organic solvents. Thus, RAFT polymerization of METACl was carried out in water using a dithioester-type chain transfer

agent (CTA2) which had greater solubility than the CTA1 used for polymerization of PDMAEMA. In addition, the phenyl group of CTA2 could be clearly observed by ^{1}H NMR spectroscopy. The polymerization of METACl was carried out with CTA2 in water at 70^{o}C (ratio of $[M]_0/[CTA]_0$ = 100 and $[CTA]_0/[I]_0$ = 5. After 5 hours, the polymerization reached around 95% conversion, with the monomer to polymer conversion calculated by integration of the vinyl protons of the monomer to the polymer's methylene peak via ^{1}H NMR spectroscopy. The molecular weight calculated based on monomer conversion (95%) as Mn: 17.1 kDa and GPC showed a narrow unimodal peak with a molecular weight Mn of 17.0 kDa, Mw: 20.3 kDa with a narrow PDI of 1.19.

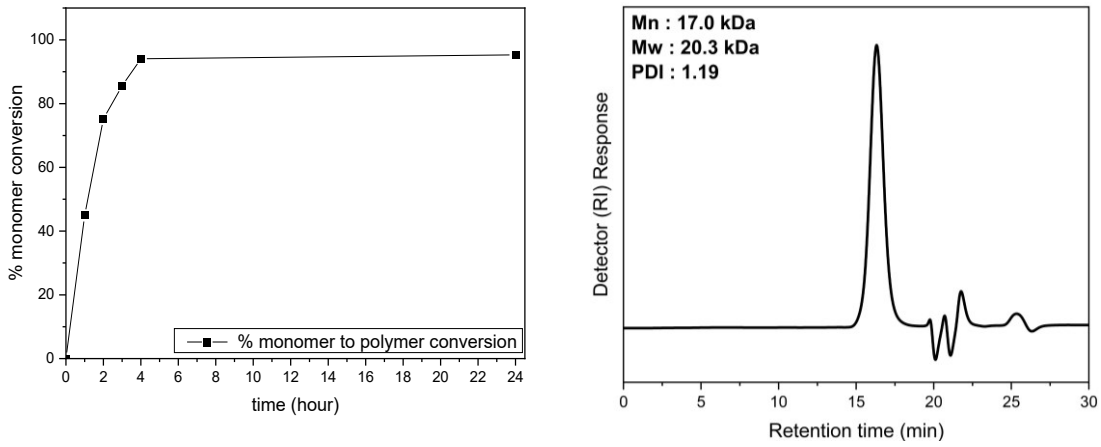

Figure 3.9. % monomer conversion to give PMETACl based on ^{1}H NMR (D_2O) and GPC analysis of PMETACl after purification. The eluent was 0.50 M acetic acid, 0.30 M NaH_2PO_4 at pH 2.5 with a flow rate of 1.0 mL min^{-1} at 25^{o}C. Calibration was achieved using InfinityLab EasiVial poly(ethylene oxide) standards with Mn values ranging from 1.1 to 905 kDa.

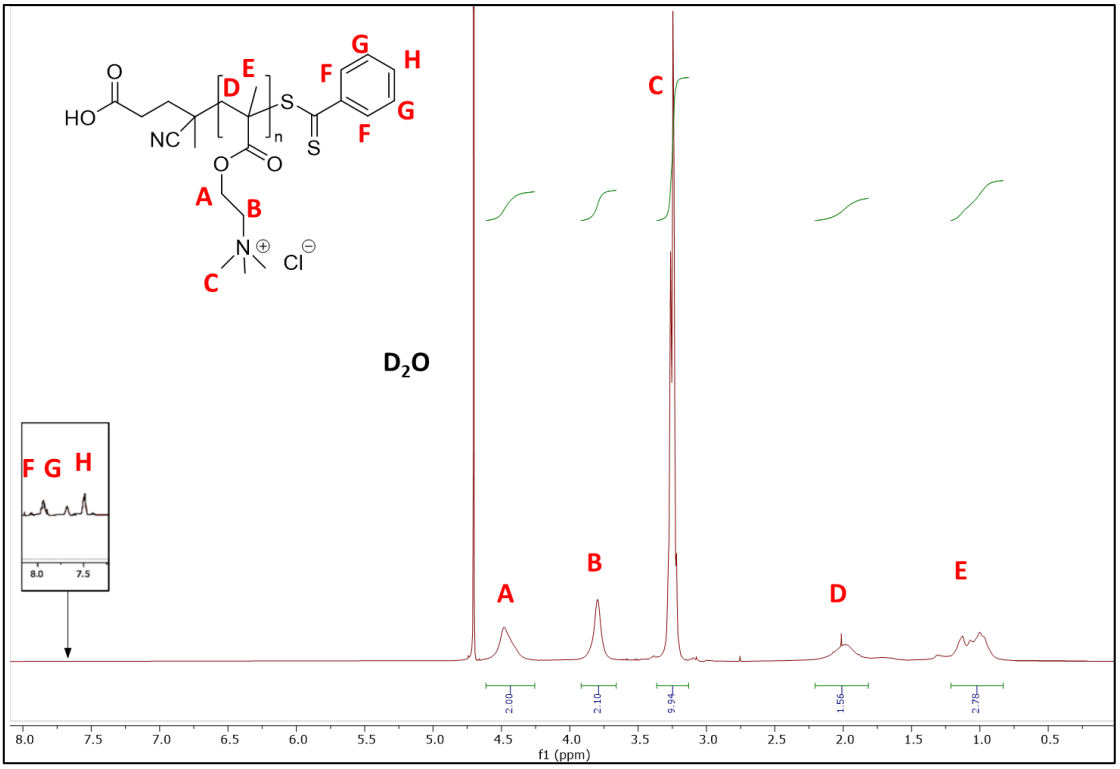

Figure 3.10. ^{1}H NMR spectrum of PMETACl recorded in D_2O, with peak assignments. E and D based on the peaks of the polymer main chain; while A, B and C are the peaks of the polymer side chain. Inset (F, G and H) shows the aromatic region of the chain transfer agent.

The third monomer used for the homopolymer library was 3-(methacryloylamino)propyl] trimethylammonium chloride (3METACl), with polymerization carried out in water (ratio of $[M]_0/[CTA]_0$ = 234 and $[CTA]_0/[I]_0$ = 5). After 5 hours, 44% conversion of monomer was observed (comparing the integrity of the vinyl protons of the monomer to the aliphatic protons of the polymer) (Figure 3.12). This might be related the lower reactivity of meth/acrylamide monomers compared to meth/acrylates. The molecular weights obtained by GPC analysis were Mn = 14 kDa and Mw = 16 kDa (the molecular weight calculated based on monomer conversion after 5 hours (44% conversion) was Mn = 23 kDa).

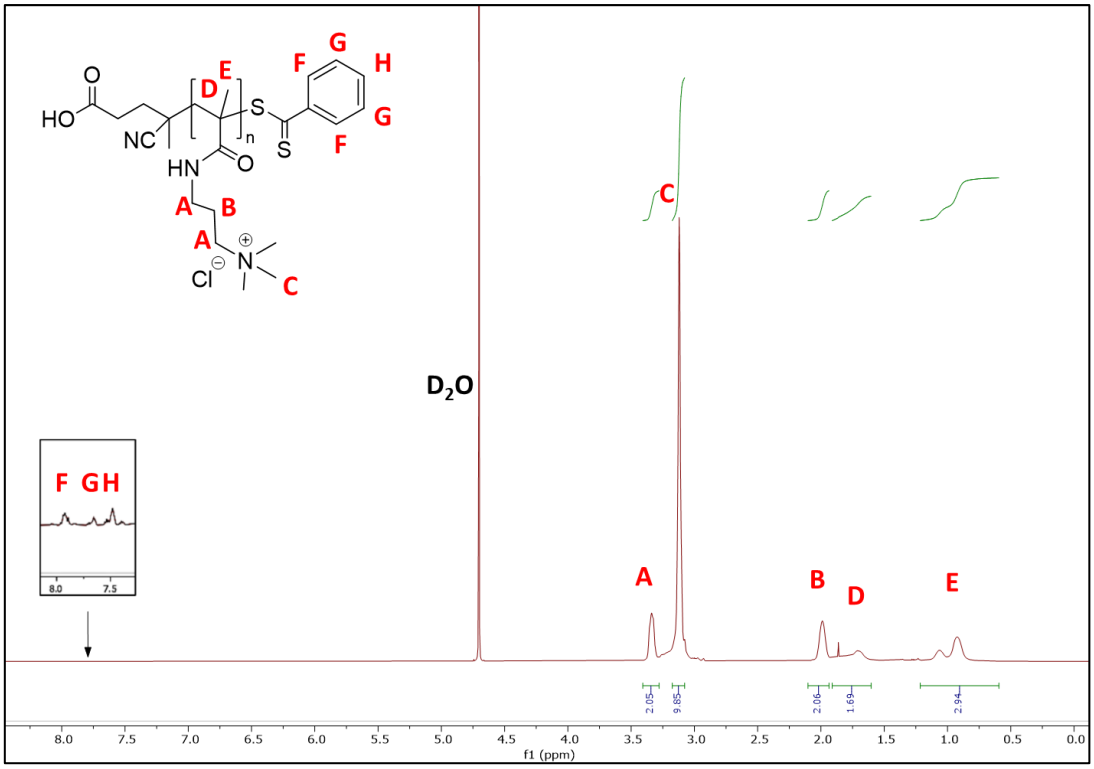

Figure 3.11. ^{1}H NMR spectrum of P3METACl recorded in D_2O, with peak assignments. E and D represent the peaks of the polymer main chain; while A, B and C represent the peaks of the polymer side chain. Inset (F, G and H) shows the aromatic region of the chain transfer agent.

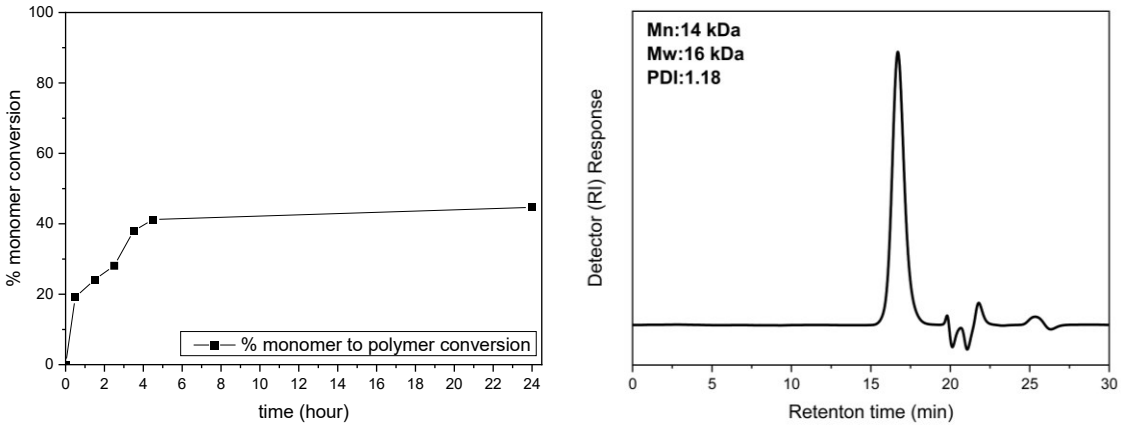

Figure 3.12. % monomer conversion to 3METACl based on ^{1}H NMR spectroscopy (D_2O) and GPC analysis of P3METACl after purification. The eluent was 0.50 M acetic acid, 0.30 M NaH_2PO_4 at pH 2.5 with a flow rate of 1.0 mL min^{-1} at 25°C. Calibration was achieved using

InfinityLab EasiVial poly(ethylene oxide) standards with Mn values ranging from 1.1 to 905 kDa.

The polymerization of vinyl benzyl trimethylammonium chloride (VBMT) was carried out with a ratio of $[M]_0$: $[CTA]_0$ = 190 with a $[CTA]_0$: $[I]_0$ ratio of 7. The monomer conversion to polymer was calculated by the integration of the vinyl protons of the monomer to the methylene peak of the polymer by ^{1}H NMR analysis. Based on ^{1}H NMR spectroscopy, after 5 h, 92% of the monomer was consumed and the molecular weight was calculated as Mn = 20.8 kDa. Molecular weight analysis by polymer *via* end group analysis by NMR was not possible due to overlapping with the side chain of the polymer. GPC analysis gave an Mn = 14 kDa; Mw = 16 kDa with a Đ of 1.11. Again, molecular weights from GPC analysis were lower than expected (calculated *via* NMR analysis) perhaps explained by the structural differences in these homopolymers and the standard polymers used in GPC calibration (polyethylene glycols).

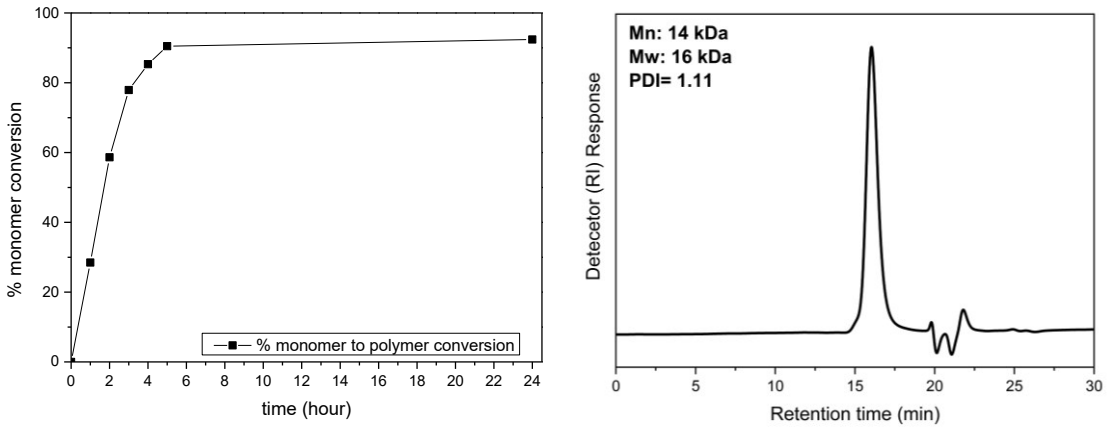

Figure 3.13. % monomer to conversion to VBMT based on ^{1}H NMR (D_2O) and GPC analysis of PVMBT after purification. The eluent was 0.50 M acetic acid, 0.30 M NaH2PO4 at pH 2.5 with

a flow rate of 1.0 mL min−1 at 25°C. Calibration was achieved using InfinityLab EasiVial poly(ethylene oxide) standards with Mn values ranging from 1.1 to 905 kDa.

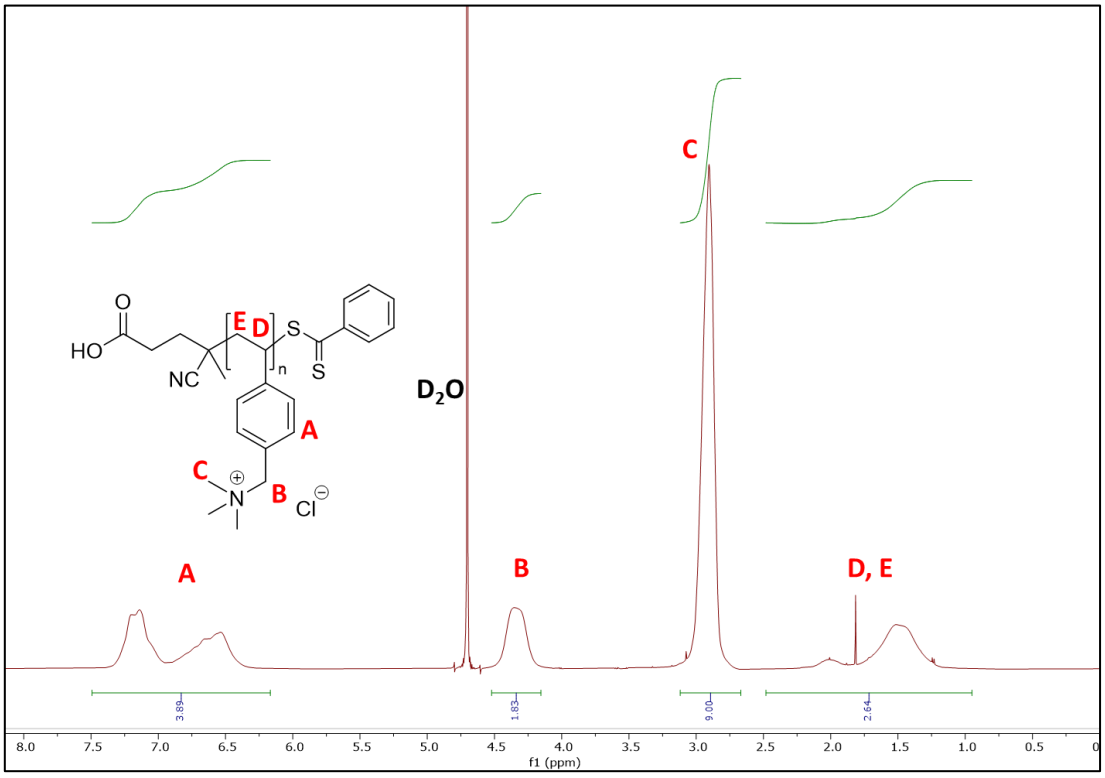

Figure 3.14. ^{1}H NMR spectrum of VBMT recorded in D_2O. E and D represent the peaks of the polymer main chain. A, B and C represent peaks of the polymer side chain.

Diallydimethyl ammonium chloride (DADMAC) has been used for the synthesis of cationic polymers on laboratory and industrial scale due to excellent chemical stability, easy synthesis, abundant availability and cost-effectiveness [74]. Since the first polymerization of DADMAC in 1950s *via* cyclopolymerization [75] , poly (diallydimethyl ammonium chloride) (PDADMAC) has been using in many different applications *e.g.*, in water purification as a coagulant and flocculants [76,77], paper making [78], and biomedical applications such as in sensors [79], for wound

healing [80], and drug delivery [81] due to its higher water solubility and permanent charge density with high stability compared to pendant ammonium polycations. It is worth mentioning that PDADMAC was the first polymer approved by Food and Drug Administration for use in water treatment and is still in use today [82] .

DADMAC polymerization was achieved through conventional free radical polymerization in aqueous media with water-soluble initiators. Commonly ammonium persulfate is employed as an initiator due to interactions with the ammonium groups in the monomer backbone [74]. Previously, optimal conditions for RAFT polymerization of DADMAC was with trithiocarbonate and xanthate-type chain transfer agents. In the presence of xanthate-type chain transfer agent, limited control was achieved. In contrast, trithiocarbonate-type chain transfer agent (3-benzyltrithiocarbonyl propionic acid) allowed a linear molecular weight increases over time. Increasing reaction temperature from 60 to 90^{o}C led to loss control over dispersities while an increase in the concentration of the chain transfer agent resulted in the formation of lower molecular weight chains [83]. Later, the same group showed microwave assisted RAFT polymerization of diallyldimethyl ammonium chloride in the presence of a trithiocarbonate-type chain transfer agent (3-benzyltrithiocarbonyl propionic acid) in aqueous solution at 60^{o}C [84]. However, polymerization was not achieved when carried under the same conditions, despite many attempts, which included changing the reaction time, the concentration of monomer, reaction temperatures and the concentration of chain transfer agent (3-benzyltrithiocarbonyl propionic acid synthesized). Finally, the polymerization of DADMAC was carried out at 60^{o}C for 24 hours within the xanthate-type chain transfer agent (CTA3-*S*-Ethoxythiocarbonyl mercaptoacetic acid) and the water-soluble azo initiator 2,2'-azobis(2-methylpropionamidine)dihydrochloride. Monomer conversion was followed by ^{1}H NMR

analysis and similar reaction kinetics as described in the literature were observed [85]. GPC analysis showed a narrow, unimodal, peak for the polymers. The molecular weight of the polymer was calculated as Mn = 17.5 kDa, similar to those obtained by GPC analysis (Mn = 18 kDa and Mw: 24 kDa with a PDI of 1.36 for 62% conversion) (Figure 3.15). The narrowness of the unimodal peaks obtained via GPC analysis reaction indicated that this was a controlled polymerization.

In RAFT polymerization, molecular weight is calculated based on the equation given below, where $[M]_0$, $[CTA]_0$, and $[I]_0$ are the initial concentrations of monomer, chain transfer agent, and initiator, orderly; p is the monomer conversion, f is the initiator efficiency, 1 − fc/2 represents the number of chains produced in a radical–radical termination, and Mw_M and Mw_{CTA} are the molar masses of the monomer and chain transfer agent, respectively [62].

$$\mathrm{Mn_{th}} = \left(\frac{[\mathrm{M}]_0 . p . \mathrm{Mw_M}}{[\mathrm{CTA}]_0 + 2f[\mathrm{I}]_0(1 - e^{kdt})(1 - \frac{\mathrm{fc}}{2})} \right) + \mathrm{Mw_{CTA}}$$

Initiator-related radicals or radicals derived from initiators can potentially engage in side chain reactions with the chain transfer agent. However, it may be hard to differentiate these reactions due to the high ratios of chain transfer agent to initiator used in carefully planned experiments. When calculating the molecular weight of a polymer using RAFT polymerization, the fraction of dead chains related to the number of chains initiated should be taken into account. However, at a given concentration of the radical source, the number of dead chains remains constant, regardless of other parameters such as targeted degree of polymerization and it is assumed that the fraction of dead chains in RAFT polymerization is significantly lower than that of living polymer chains. Thus, this equation can be simplified to below [62],

$$\mathrm{Mn_{th}} = \left(\frac{[\mathrm{M}]_0 . p . \mathrm{Mw_M}}{[\mathrm{CTA}]_0}\right) + \mathrm{Mw_{CTA}}$$

The molecular weight of the polymer was calculated based on the equation given above, where $[M]_0$, and $[CTA]_0$ are the initial concentrations of the monomer and chain transfer agent; p is the monomer conversion; and Mw_M and Mw_{CTA} are the molar masses of the monomer and chain transfer agent, respectively.

Increasing the concentration of monomer in the reaction should theoretically increase the molecular weight according to the equation given above. However, when the molarity of DADMAC was increased from 3.5 M to 7 M and 11 M while maintaning the same the ratio of chain transfer to initiator, greater conversion with broader molecular weights were observed. This might be related to viscosity increases in the reaction medium leading to the formation of smaller chains due to radical termination. The monomer concentration was kept around 3.5 M and the obtained results were consistent with previous studies about controlled polymerization of DADMAC in which full conversion was not reached 84–86.

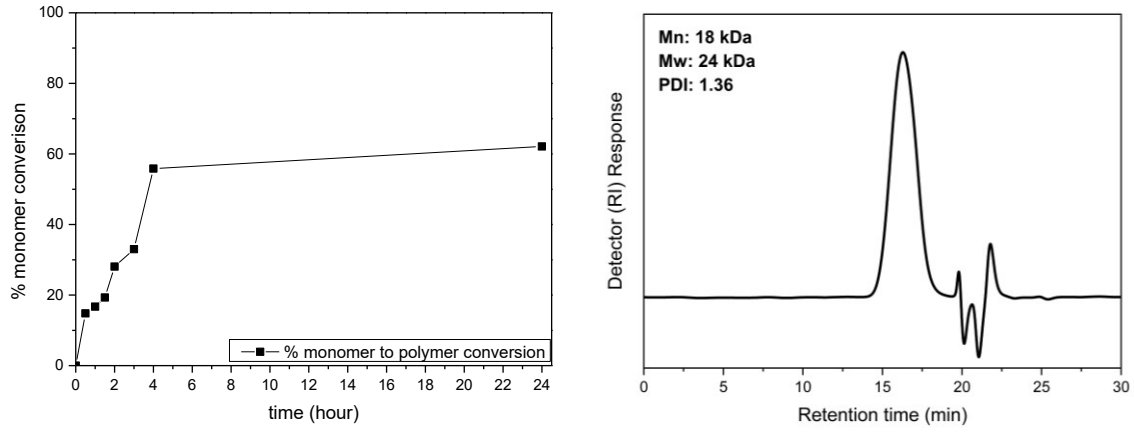

Figure 3.15. % monomer conversion to PDADMAC based on ^{1}H NMR (D_2O) and GPC analysis of PDADMAC after purification. The eluent was 0.50 M acetic acid, 0.30 M NaH_2PO_4 at pH 2.5

with a flow rate of 1.0 mL min^{-1} at 25°C. Calibration was achieved using InfinityLab EasiVial poly(ethylene oxide) standards with Mn values ranging from 1.1 to 905 kDa.

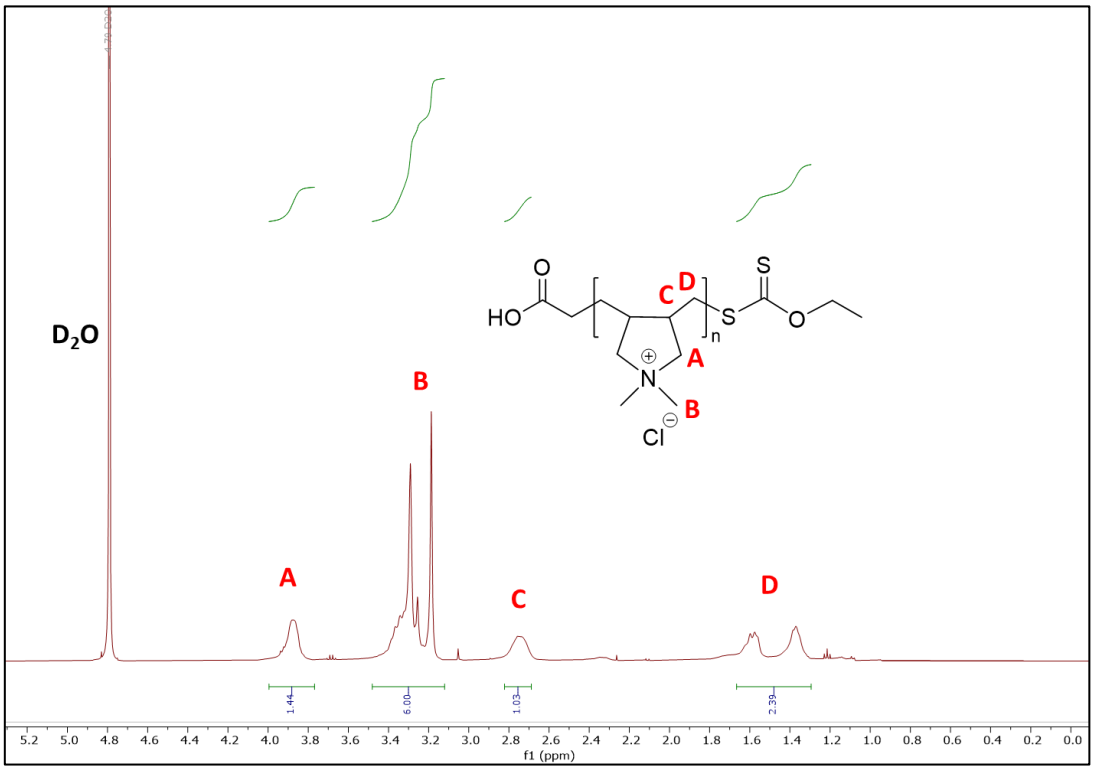

Figure 3.16. ^{1}H NMR spectrum of PDADMAC recorded in D_2O. C and D represent the peaks of the polymer main chain; A and B represent the peaks of the polymer side chain.

Table 3.1. Optimized homopolymers library synthesis via RAFT polymerization

POLYMER	CTA	$[M]_0/[I]_0$	$[CTA]_0/[I]_0$	Mn NMR	Mn-GPC	Mw-GPC	Đ
PDMAEMA	1	167	6	23.0 kDa	22 kDa	28 kDa	**1.29**
PMETACl	2	100	5	17.1 kDa	17 kDa	20 kDa	**1.19**
P3METACl	2	215	5	23.1 kDa	14 kDa	16 kDa	**1.18**
PVMBT	2	190	7	20.8 kDa	14 kDa	16 kDa	**1.11**
PDADMAC	3	175	3.3	17.5 kDa	18 kDa	24 kDa	**1.36**

3.5.3. Antimicrobial Activity of the Quaternary Ammonium Homopolymers

The antimicrobial activities of the homopolymers library were assessed with a resazurin- assay to determine their minimum inhibition concentrations (MIC) - *i.e.,* the lowest concentration polymers able to inhibit visible bacterial growth. Here the blue dye, resazurin (7-hydroxy-3H-phenoxazin-3-one 10-oxide), was reduced to the pink and highly fluorescent resorufin by oxidoreductases within viable bacteria. The antimicrobial activity of the polymers was determined against Gram-negative (*B. subtilis, E. coli)* and Gram-positive (*M. luteus*, *S. typhimurium*) bacteria (see Table 3.2).

Since the molecular weights/chain lengths of the homopolymers vary (Mn 17-23 kDa), expressing the data in molarity displays their comparative strengths in an alternative manner and perhaps enables a fairer comparison with conventional antibiotics, which have low molecular weights (323-477 g/mol). As can be seen Table 2, the inhibition of bacteria by the polymers is affected by the monomers structure, the molecular weight of homopolymer and the bacterial strain. Most polymers showed inhibitory effects (bacteriostatic mode of action) of less than 32 µg/mL for *B. subtilis, E. coli* and *M. luteus*, although *S. typhimurium* proved to be resistant against polymers; P3METACl, PVMBT and PMETACl at this concentration (Table 3.2). PDADMAC, PMETACl and PVBMT had MIC values less than 1 µM (16 µg/mL) for *B. subtilis, E. coli* and *M. luteus*, and an MIC below 2 µM (32 µg/mL) for *S. typhimurium*. All MIC experiments carried out three times and all results were the same.

Table 3.2. MIC values of the homopolymers library against target microorganisms.

Polymer	MICs for Different Target Microorganisms							
	B. subtilis		***E. coli***		***M. luteus***		***S. typhimurium***	
	µg/mL	**µM**	**µg/mL**	**µM**	**µg/mL**	**µM**	**µg/ mL**	**µM**
PDMAEMA	32	1.6	32	1.6	32	1.6	32	1.6
PMETACl	64	1.9	64	1.9	64	1.9	64	1.9
P3METACl	32	1.4	32	1.5	16	0.7	64	2.8
PVBMT	32	0.9	64	1.7	64	1.7	64	1.7
PDADMAC	16	0.9	16	0.9	16	0.9	32	1.8
Standard Antibiotics	**Clindamycin**		**Gentamicin**		**Gentamicin**		**Chloramphenicol**	
	4	9.4	0.5	1.1	0.5	1.1	1	3.1

3.5.4. Cytotoxicity Evaluation of Quaternary Ammonium Homopolymers

Cationic polymers can show cytotoxic effects [86] against mammalian cells due to their interactions with the cell membrane *via* non-specific electrostatic interactions causing holes in the cell membrane, and increased permeabilization which initializes cell death pathways, such as apoptosis [87–89]. 3-(4,5-dimethylthiazol-2-yl)-2,5-diphenyl-2H-tetrazolium bromide (MTT) assay is a common method for evaluating cell proliferation, cytotoxicity, and cellular metabolic activity. The assay is based on the measurement of formazan (a violet-blue/purple water-insoluble molecule) generated by the reduction of the MTT reagent (the water-soluble, yellow coloured, 3-(4,5-dimethylthiazol-2-yl)-2,5-diphenyl-2H-tetrazolium bromide) by metabolically active cells [90]. The cytotoxicity of the homopolymers were evaluated on HeLa cells, incubating the polymers at a range of concentrations (1.25 µM to 10 µM) for 24 h *via* MTT assay. Figure 3.17 showed that PMETACl exhibited negligable toxicity even at the highest

concentration while P3METACl showed toxicity even at the lowest concentration. On the other hand, PDADMAC, PVMBT and PDMAEMA showed increases in toxicity with increases in concentration. The data clearly showed how the structural differences of the polymers affected their toxicity, even though the tested polymers had similar molecular weights.

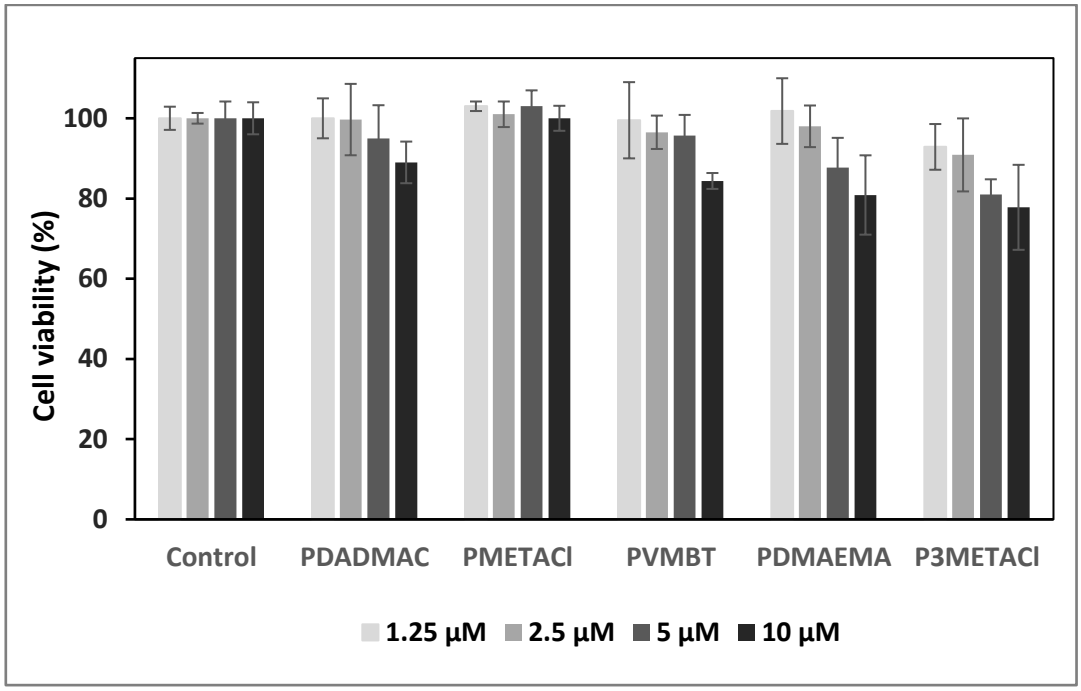

Figure 3.17. Assessment of HeLa cell viability in the presence of the five homopolymers (Mw ~20 kDa) using an MTT assay. Control was HeLa cells without added any polymer.

3.6. Conclusions and Future Work

Five monomers were successfully polymerized with dispersities ranging from 1.11-1.36 which shows successful RAFT polymerization. Water was found to be the best solvent for RAFT polymerization and gave water-soluble quaternary ammonium polymers. Each monomer had

different polymerization kinetics, but the polymers were all synthesized with similar dispersities and obtained molecular weights around 20 kDa.

Among the monomers, polymerization of DADMAC was the most challenging compared to methacrylate/methacrylamide monomers due to its less reactivity. The choice of chain transfer agent was the key point to obtain controlled polymerization. The polymerization of DADMAC was achieved in the presence of the xanthate-type chain transfer agent (*S*-Ethoxythiocarbonyl mercaptoacetic acid) and the water-soluble azo initiator 2,2'-azobis(2-methylpropionamidine)dihydrochloride at 60^{o}C.

The synthesized homopolymer library tested on both Gram-negative and Gram-positive bacteria and MIC values of the polymers were varied in the range of 16-64 mg/mL depending on the tested bacteria strain. Later, cytotoxicity of the homopolymers on HeLa cells was assessed *via* MTT assays. The results revealed varying degrees of toxic effects among the polymers, with a notable observation for being that P3METACl the concentration increased, while PMETACl showed the least toxicity on HeLa cells.

Looking ahead, exploring the cytotoxicity of these homopolymers on different cell lines, including skin cells, could pave the way for potential applications in cosmetics. Such endeavours promise to broaden the scope of practical applications for these antimicrobial polymers.

Chapter 4

The Effect of Molecular Weight on the Antimicrobial Activity and Biocompatibility of the Most Active Homopolymers

Within this chapter, the antimicrobial properties, their mechanisms of action and the biocompatibilities of the lead homopolymers (PDADMAC, PMETACl, and PVMBT) were analysed, specifically looking at the role of molecular weight on these properties.

Parts of this chapter are published as:

Haktaniyan, M.; Sharma, R.; Bradley, M. Size-Controlled Ammonium-Based Homopolymers as Broad-Spectrum Antibacterials. *Antibiotics*, **2023**, *12*, 1320.

The polymers were synthesized and their antibacterial activities were evaluated by the author, while the antifungal analysis/studies were performed by Dr. Om Alkhir Mohamad (Glasgow Dental Hospital).

4.1. Introduction

Throughout their evolutionary journey, microorganisms have showcased an impressive capacity to thrive in a diverse array of environments and circumstances [91]. Throughout history, the spread of disease caused by microorganisms has posed significant global challenges. Illnesses such as tuberculosis, leprosy, syphilis, and various plagues have caused immense loss of life and societal disruptions. Due to misuse of antibiotics, drug-resistant

bacteria infections have become a major threat on public health. According to a systematic analysis of global burden associated with drug resistant infections (excluding tuberculosis), it is estimated that 1.27 million deaths were attributable to resistant bacteria (notably *E. coli*, *S. aureus* and *K. pneumonia* [92]. For tuberculosis, Mycobacterium tuberculosis is still one of the highest ranked lethal infectious agents, causing approximately 1.4 million deaths in 2021 according to World Health Organization [93]. In addition to bacterial infections, the mortality rate associated with fungal infections has also increased due to their ability to colonize host tissues, especially in individuals with compromised immune function. Some fungi (*e.g., Candida*, *Aspergillus* and *Cryptococus*) cause severe and systemic infections leading an emergent public health threat [94]. Yearly, the global incidence of fungal infections has resulted in the loss of approximately 1.7 million lives and over 150 million reported cases [95].

4.2. Cell Walls of Bacteria and Fungi

In 1884, Danish bacteriologist (Gram) found a method to classify bacteria depending on a staining, with hexamethyl-p-phenylenediamine chloride crystal violet retained in the thick peptidoglycan layer of certain bacteria (so-called Gram-positive) while not staining others (named Gram-negative) [96]. Thus, although the inner or cytoplasmic membranes of both bacteria resemble each other, the outer envelopes are highly distinctive with a thick crosslinked peptidoglycan surrounding the cytoplasmic membrane in Gram-negative bacteria. In Gram-negative bacteria a thinner peptidoglycan layer, with an additional outer membrane layer containing phospholipids and lipopolysaccharides, is found [97]. In contrast, Gram-positive bacteria do not have an outer membrane, however it has a much thicker peptidoglycan (around 40-60 nm) layer [98].

Owing to the unique nature of their cell envelope, mycobacteria cannot be classified as either Gram-positive or Gram-negative bacteria. What makes mycobacteria unique is their extremely high lipid content, and the nature of the lipids which can account for up to 60% of the cell envelope by mass. This is significantly higher than the typically 20% found in the lipid-rich cell walls of Gram-negative bacteria. The distinctive cell wall structure of mycobacteria includes mycolic acids which are very long-chain fatty acids covalently attached to the polysaccharide arabinogalactan. In addition, they contain trehalose di-esters and other unique compounds that are characteristic of the mycobacterium genus. These lipids are responsible for many of the unusual properties of mycobacteria, including their remarkable resistance to a wide range of antibiotics (they cannot penetrate- although some, like streptomycin and rifamycin, are effective against them). Another distinctive feature of mycobacteria is their limited permeability to nutrients, which can be up to 1,000 times less than that of the most resistant Gram-negative bacteria, such as *E. coli* and *P. aeruginosa* [99]. This lack of permeability also explains their inability to undergo gene transfer from other bacteria.

The fungal cell wall plays a vital role in maintaining fungal cell integrity and viability, regulating cellular permeability and safeguarding the cell against osmotic and mechanical stresses. In addition, *via* an extensive array of receptors, such as adhesins; it also enables interactions with the external environment [100]. The fungal cell wall has different layers which are made up of glycoproteins, polysaccharides (chitin and glucan) and lipids. Mannoproteins, consisting of protein-linked branched mannose polymers, are predominantly found in the outer layer of the cell wall, linked to β-glucans, which are covalently linked to other components. The middle part of their cell wall is composed of β-glucans (50-60% dry weight) of whole and between

the cell membrane and the β-glucans layers, is a thin layer of rigid chitin, a polymer of N-acetylglucosamine. However, it is typically present in lower quantities compared to the other constituents in the wall structure.

The composition of the cell wall may vary, even within a single fungal specimen, depending on factors such as growth conditions and stage [101–103]. In comparison to mammalian cell membranes, fungi cell membranes are more anionic due to having higher levels of phosphatidylcholine [104].

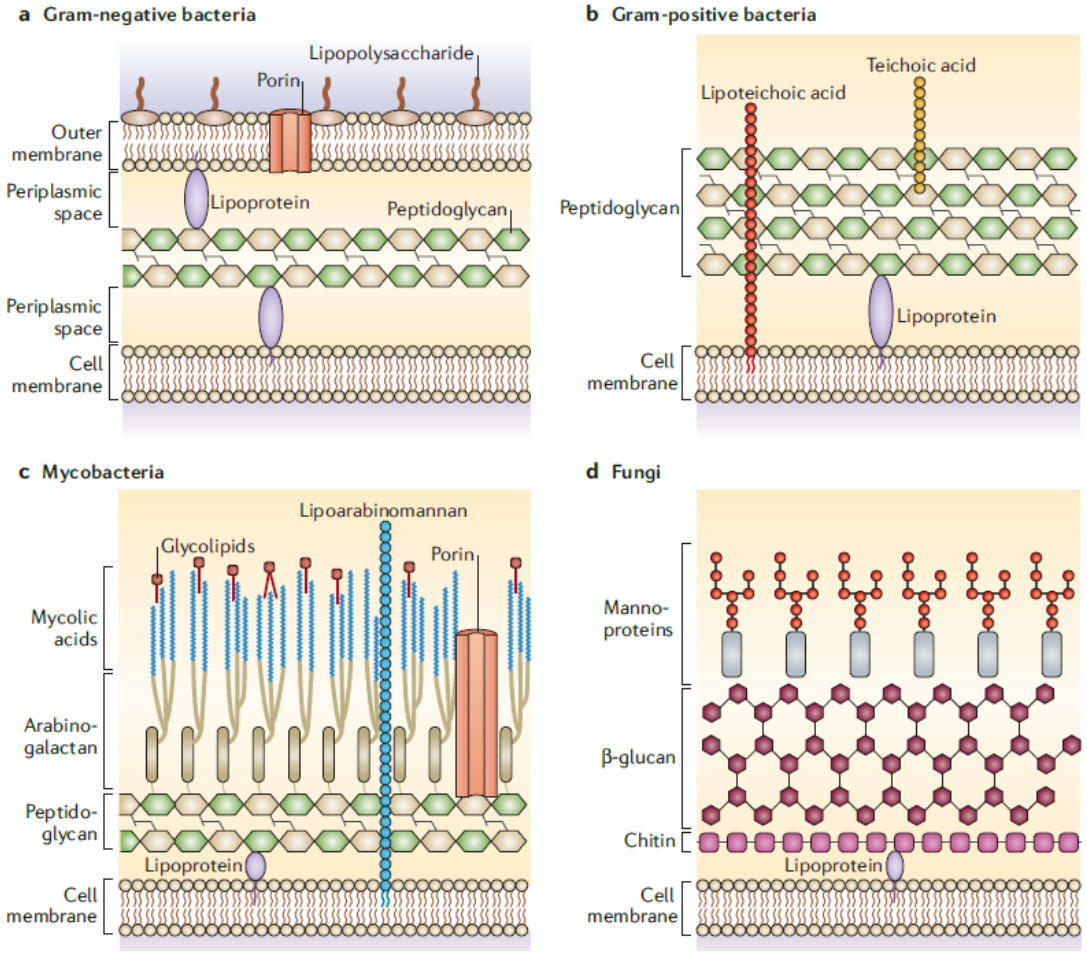

Figure 4.1. Cell wall structure of Gram-negative bacteria, Gram-positive bacteria, mycobacteria and fungi [105].

4.3. Mechanism of Action of Antimicrobial Polymers

Antibiotics are the foremost treatment method for combating out of control infections caused by bacteria. It is well known that cationic materials bind or target specific bacterial components, such as conventional cationic antibiotics including polymyxin that binds Lipid A [106,107], brevibacillin that binds lipoteichoic acid [108] and nisin that binds lipids on the cytoplasmic membrane of Gram-positive bacteria and disturbs peptidoglycan synthesis [109].

Antimicrobial cationic polymers exhibit surface-active properties, with a strong affinity for bacteria, which is further enhanced by their lipophilicities. This affinity is crucial for effectively disrupting the structural organization and integrity of bacterial cell envelopes often leading to cell membrane disruption, resulting in the leakage of cytoplasmic contents and ultimately bacterial lysis [110,111]. As might be imagined the interaction between cationic polymers and bacteria or fungi happens due to a variety of reasons, depending on the bacteria/fungi in question. Thus, the lipopolysaccharides within the outer layer of the cell membrane in Gram-negative bacteria are formally negatively charged at physiological pH [97,111,112] and will interact with positively charged polymers. The cell membrane of Gram-positive bacteria is likewise formally "negatively charged" (often stabilized by divalent cations such as Mg^{2+} and Ca^{2+}), in this case due to high levels of teichoic and lipoteichoic acids [113,114]. As such the rational for cationic polymers (with their enormous diversity) being able to interact with microorganisms is strong. Further penetration into the cytoplasm and interactions with the phospholipid bilayer led to death of bacteria. Cationic polymers can depolarize the membrane of fungi through electrostatic interactions, often disrupting the concentration of essential critical cations such as Na^{+}, K^{+}, Mg^{2+}, and Ca^{2+}. Consequently, the osmotic balance of pathogens is

disrupted, thereby potentiating their antifungal effect [115]. However, the antimicrobial mode of action of ammonium group containing polymers is not fully understood, but is believed to start with the binding of the cationic groups of the polymer onto the various negatively charged bacteria cell envelope components (mentioned above) *via* electrostatic interactions leading to disorganization of its structure and the leakage of low-molecular weight components [96,116].

The efficacy of antimicrobial cationic polymers is dependent upon the type of pathogen and the specific interaction between the polymer and the microorganism. Antimicrobial polymers typically can be considered to exert bactericidal or fungicidal activities or to be bacteriostatic or fungistatic, preventing or slowing down microbial growth either in solution or on surfaces.

4.4 Molecular Weight and the Antimicrobial Activity and Biocompatibility of Polymers

The strength of the antimicrobial activity of the ammonium group containing polymers depends on the molecular weight of the polymers [117,118], the position of the cationic centre (i.e., side chain or main chain) [119], the morphology and architecture of the polymers [120], the polymers hydrophobic/hydrophilic balance [121,122] and perhaps the nature of the counter anion [123]. Among all of these, molecular weight is believed to exerts a significant influence on the antimicrobial activity of polymers. Thus, it has been reported that lower-molecular-weight polymers can penetrate into Gram-positive bacteria more efficiently than their higher-molecular-weight counterparts, with cationic polyacrylates (5–10 kDa) optimal for antimicrobial activity against *S. aureus* [124]. Ikeda *et al.* [117]reported a "bell-shaped curve" between the molecular weight and effectiveness of two types of polymers, namely poly(4-(2-methacryloyloxyethyl)phenyl-4-chlorophenylbiguanide hydrochloride) and poly(vinyl benzyl

ammonium chloride), when tested against *S. aureus*. This study revealed that the polymethacrylates with biguanide pendant groups exhibited highest antibiotic performance in the molecular weight range of 50 kDa to 100 kDa. On the other hand, poly(vinyl benzyl ammonium chloride) displayed a consistent increase in antibiotic activity as molecular weight increased, up to a maximum of 7.7 kDa, which was the highest molecular weight synthesized in the study. The authors concluded that higher molecular weight can enhance the polymers' adsorption, binding, and membrane disruption capabilities, while excessive molecular weight can impede the diffusion capacity of these polymers, a so-called as 'sieving effect' [100]. This phenomenon was first identified by Lienkamp *et al.* [125], whose poly(oxanorbornene)-based synthetic mimics of antimicrobial peptides showed reduced activity with increasing molecular weight. These findings suggest that selecting the optimal molecular weight for a particular polymer is crucial for maximizing its biocidal properties. In addition, variations in the structures of cell membranes/envelopes among different bacterial species should be considered when evaluating the antimicrobial activity of polymers.

Cationic polymers also possess activity against fungi. As a well-known cationic polymer, chitosan has antifungal activity depending on molecular weight, and is either fungistatic or fungicidal depending on the strain tested [126,127]. Despite the valuable research conducted on antifungal activities of chitosan, there is limited research focusing on the antifungal properties of homopolymers containing quaternary ammonium groups. For example, Lin and coworkers [128,129] studied the antifungal action mechanisms of polymeric quaternary ammonium salts. The homopolymer of (2-methacrylamido)propyltetrabenzyldimethylammoniumchloride exhibited antifungal activity against both plant pathogens (*Fusarium oxysporum* f.sp. cubense tropical race 4 *(Foc 4)* and *R. solani*). This activity was associated with the disruption of cellular

components such as the cell wall and plasma membrane, the initiation of lipid peroxidation, impairment of mitochondrial function, and interference with genomic DNA [130,131].

Recently, the influence of hydrophobicity and molecular weight on the antifungal activity against *R. solani* and *Foc4* was evaluated with linear hydrophilic cationic polymers synthesized with varying charge densities and molecular weights (3-8 kDa). It was observed that, in general, the antifungal activity of polymers increased as their molecular weight was raised [132].

The molecular weight of cationic polymers also has crucial importance in biological applications due to their toxicity against mammalian cells. Cationic polymers can show cytotoxic effects [133] against mammalian cells due to their interactions with the cell membrane *via* non-specific electrostatic interactions [134–136]. Fischer *et al.* have shown that polycations possessing a higher molecular weight may exhibit greater toxicity. However, this proposition was founded upon a restricted range of cationic polymers, with only one molecular weight of each within the diverse set of polymers evaluated and contrasted [137].

The cytotoxicity and cellular membrane disruption of HepG2 cells were evaluated when cells incubated with rhodamine end-labelled PDAMAEMAs (11-48 kDa) synthesized *via* ATRP. The shorter polymer (Mw <17 kDa) was observed to be less toxic than the larger polymer (Mw >39 kDa) [134]. It is worth mentioning that the cytotoxic effect of antimicrobial polymers can also vary based on the cell line used.

4.5. Aim of the Chapter

In this chapter, the effect of molecular weight on the antimicrobial activities and cytocompatibilities of the homopolymers poly(diallyldimethyl ammonium chloride), poly[2-(methacryloyloxy)ethyl]trimethylammonium chloride and poly(vinyl benzyl trimethylammonium chloride) were studied in detail. The antimicrobial action mechanism of the polymers and their cytotoxicity were investigated and tested on *M. smegmatis* and three fungi strains to identify the most active and selective broad-spectrum antimicrobial homopolymers.

4.6. Results and Discussion

4.6.1. Synthesis of Different Molecular Weight of the Best Active Polymers

The hypothesis that the cumulative effect of monomer units contributes to the antibacterial properties of the polymer led to an investigation of the effect of different polymer chain lengths on their potency. In this context, three different molecular weights of PDADMAC, PMETACl and PVBMT (see Chapter 3) were selected and synthesized (10 kDa, 20 kDa and 40 kDa) *via* RAFT polymerization by changing the ratio of the chain transfer agent and initiator while keeping the concentration of monomer constant (although giving a slight change in Đ). Molecular weights of the polymers were calculated using the method described in Chapter 3, *via* ^{1}H NMR spectroscopy (samples taken from the reaction mixture and % conversion of monomer was analysed) and GPC analysis (Figure 4.2). Table 4.1 shows that successful RAFT polymerization (PDI < 1.5) of PDADMAC, PMETACl and PVMBT with three different molecular weights.

Table 4.1. Analysis of the molecular weight of PDADMACs, PVMBTs and PMETACls obtained *via* RAFT polymerization.

Polymers	$[M]_0/[CTA]_0$	$[CTA]_0/[I]_0$	Mn NMR	Mn-GPC	Mw-GPC	Đ
PMETACI-10	100	10	10.4 kDa	11 kDa	14 kDa	**1.24**
PMETACI-20	100	5	17.1 kDa	17 kDa	20 kDa	**1.19**
PMETACI-40	100	2.5	39.7 kDa	39 kDa	40 kDa	**1.03**
PDADMAC-10	175	7	11.9 kDa	11 kDa	15 kDa	**1.39**
PDADMAC-20	175	3.3	17.5 kDa	18 kDa	24 kDa	**1.36**
PDADMAC-40	175	1.5	36.8 kDa	35 kDa	48 kDa	**1.37**
PVMBT-10	190	13	13.7 kDa	6 kDa	7 kDa	**1.20**
PVMBT-20	190	7	20.8 kDa	14 kDa	16 kDa	**1.11**
PVMBT-40	190	3.3	37.4 kDa	23 kDa	27 kDa	**1.18**

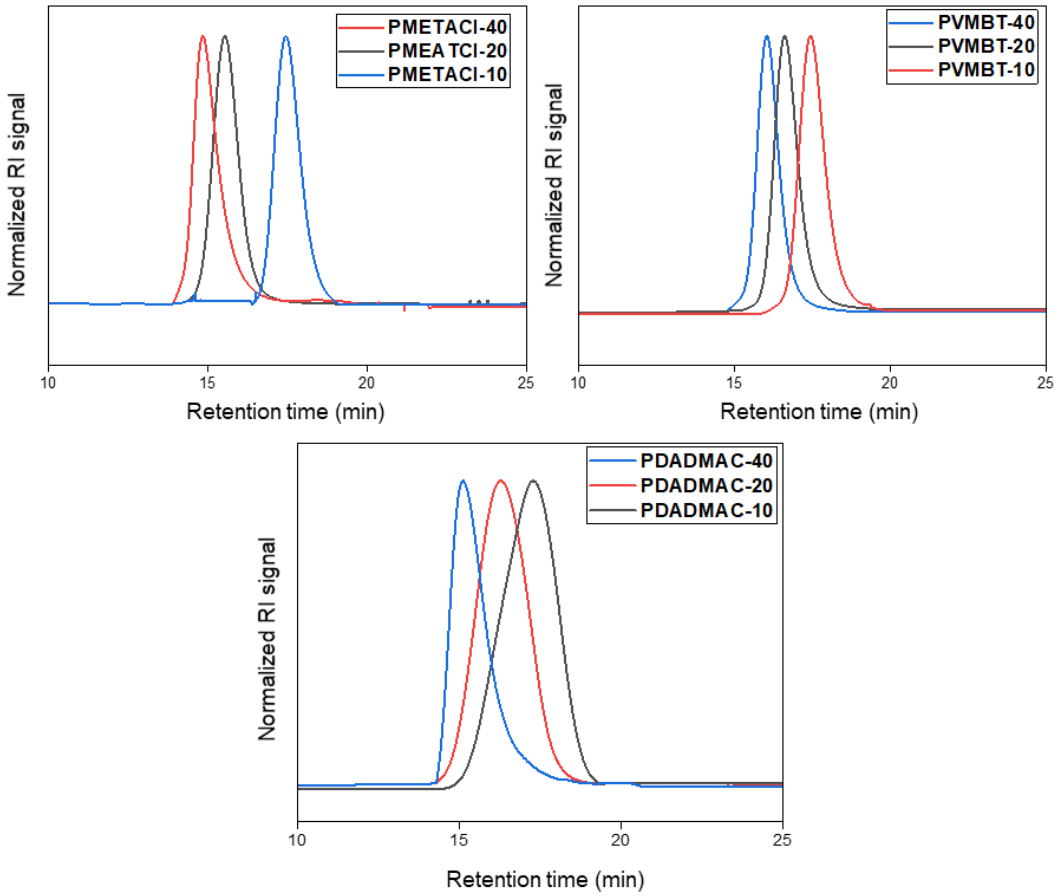

Figure 4.2. GPC analysis of the three different molecular weights of PDADMAC, PMETACl, and PVMBT. The eluent was 0.50 M acetic acid, 0.30 M NaH_2PO_4 at pH 2.5 with a flow rate of 1.0

mL min^{-1} at 25°C. Calibration was achieved using InfinityLab EasiVial poly(ethylene oxide) standards with Mn values ranging from 1.1 to 905 kDa.

4.6.2. Effect of Molecular Weight on the Antimicrobial Activity

By neutralizing the charge at a specific location, the stability of the cell membrane is disrupted, which ultimately enhances its permeability and leads to bacterial death. Thus, by increasing the molecular weight of cationic polymers, multiple interconnected biocidal quaternary ammonium groups found in the polymer chains interact with the cell envelope of the bacteria. This, in turn, enhances the electrostatic interactions with the bacterial cell envelope, potentially making the antimicrobial effect of the polymer with higher polymer chains more pronounced. Here, in Table 4.2 the minimum inhibitory concentration of the different molecular weights of PDADMAC, PMETACl and PVMBT were evaluated with a resazurin assay. The results showed that as hypothesized polymers with higher molecular weights demonstrated greater efficacy in inhibiting bacterial growth within the 16-128 µg/mL range. In general, Gram-negative bacteria present a greater challenge to antimicrobial diffusion due to the presence of an outer membrane in their cell wall compared to Gram-positive bacteria. These polymers were observed to be less effective against *S. typhimurium* than other tested organisms.

Table 4.2. The effect of polymer molecular weight on MIC values as determined by a resazurin assay. The molecular weights corresponding to the nominal low (10 kDa), medium (20 kDa) and high (40 kDa) polymers are given in Table 4.1 (n = 3).

Mn (kDa)	Polymer	MICs for different target microorganisms							
		B. subtilis		***E. coli***		***M. luteus***		***S. typhimurium***	
		µg/mL	**µM**	**µg/mL**	**µM**	**µg/mL**	**µM**	**µg/ mL**	**µM**
10 kDa	**PDADMAC-10**	16	1.35	32	2.69	32	2.69	64	5.37
17 kDa	**PDADMAC-20**	16	0.91	16	0.91	16	0.91	32	1.82
40 kDa	**PDADMAC-40**	16	0.43	16	0.43	16	0.43	32	0.86
12 kDa	**PMETACl-10**	64	6.15	64	6.15	64	6.15	64	6.15
18 kDa	**PMETACl-20**	64	3.74	64	3.74	64	3.74	64	3.74
39 kDa	**PMETACl-40**	32	0.82	32	0.82	32	0.82	64	1.64
14 kDa	**PVMBT- 10**	64	4.67	64	4.67	64	4.67	128	9.34
21 kDa	**PVMBT-20**	32	1.54	32	1.54	64	3.08	64	3.08
38 kDa	**PVMBT-40**	32	0.84	32	0.84	32	0.84	64	1.68

The optimal inhibition of the bacteria growth was observed when employing polymers of higher molecular weight (40 kDa). Inhibition by the highest molecular weight polymers were confirmed by an agar diffusion assay against all four tested bacterial species (Figure 4.3) with the polymers diffusing into the agar and inhibiting the growth of the bacteria strains tested[138]. Zones of inhibition were greatest against *B. subtilis,* but the polymers showed inhibition to all tested organisms compared to the control (H_2O).

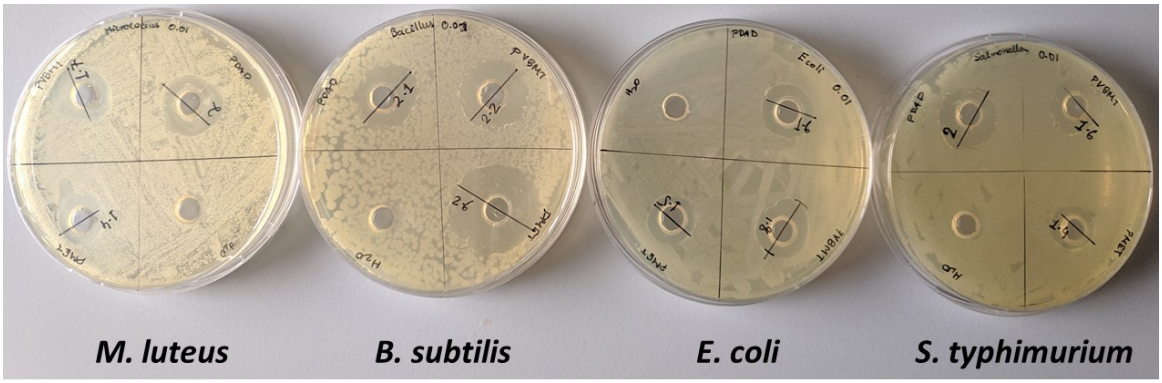

Figure 4.3. Agar plates were inoculated with the target bacterial species and wells of 1 cm diameter were punched into the plates and 100 µL of the polymer solutions (at 2xMIC) were added into the wells and incubated overnight.

Table 4.3. Zone of inhibition (agar well diffusion assays) in cm.

Polymer	*B. subtilis*	*M. luteus*	*E. coli*	*S. typhimurium*
PDADMAC-40	2.1	2	1.6	2.0
PMETACl-40	2.6	1.4	1.5	1.9
PVBMT-40	2.2	1.7	1.8	1.6

Cationic polymers can show cytotoxic effects [133] against mammalian cells due to their interactions with the cell membrane *via* non-specific electrostatic interactions [135]. PDADMAC-40 (40 kDa) was found to be highly toxic to mammalian cells; although it showed excellent inhibition of the growth of bacteria compared to PDADMAC-20 and PDADMAC-10. Therefore, along with PMETACl-40 and PVMBT-40, based on their superior inhibitory performance in comparison to smaller molecular weight polymers, PDADMAC-20 was selected for further experiments to investigate the antimicrobial mechanisms and assess cytocompatibility (instead of PDADMAC-40).

In addition, the selected polymers (PDADMAC-20, PVMBT-40 and PMETACl-40- see Table 4.2.) were tested against the non-pathogenic microorganism *M. smegmatis* as a model organism of pathogenic *M. tuberculosis*. The minimum inhibitory concentrations of the polymers against *M. smegmatis* were again determined using a resazurin assay. The growth of *M. smegmatis* was inhibited in the range of polymer concentrations 4-8 μg/mL, outperforming the antibiotic Rifampicin at 16 μg/mL. The result showed that polymers containing quaternary ammonium salts could offer a solution against mycobacterium on surfaces *e.g.*, leprosy. This enhanced effectiveness may be attributed to their possession of "same-centered" permanently charged entities, along with three methyl groups. These structural characteristics of PDADMAC-20 facilitate increased interaction with the hydrophobic, rigid, and waxy components found in mycobacterial membranes. Indeed, in the literature, enhanced activity against *M. smegmatis* was observed when polymers bearing primary or tertiary amine were replaced by polymers with quaternary ammonium salts [139].

PDADMAC-20 exhibited superior inhibition compared to PMETACl-40, PVMBT-40 and the antibiotic (see Table 4.4). This outcome highlights that the structural characteristics of the polymer have a more significant impact than molecular weight on the observed inhibition of *M. smegmatis,* which has unique cell wall structure compared to Gram-negative and Gram-positive bacteria.

Table 4.4. Summary of the MIC values of the most active homopolymers (n = 3) measured using a resazurin assay.

Polymer	MICs for different target microorganisms									
	B. subtilis		***E. coli***		***M. luteus***		***S. typhimurium***		***M. smegmatis***	
	µg/mL	**µM**	**µg/mL**	**µM**	**µg/mL**	**µM**	**µg/ mL**	**µM**	**µg/ mL**	**µM**
PDADMAC-20	16	0.91	16	0.91	16	0.91	32	1.81	4	0.23
PMETACl-40	32	0.83	32	0.83	32	0.83	>32	>1.86	8	0.21
PVBMT-40	32	0.85	32	0.85	32	0.85	32	0.85	8	0.21
Standard	**Clindamycin**		**Gentamicin**		**Gentamicin**		**Chloramphenicol**		**Rifampicin**	
Antibiotic	4	9.41	0.5	1.05	0.5	1.05	1	3.10	16	19.4

4.6.3. Bactericidal Action Mode of the Best Active Polymers

A Live/Dead assay was used for assessment of bacterial membrane integrity after treatment with the polymers, *via* fluorescent microscopy with double staining with SYTO-9, a membrane-permeable stain (which stains both alive and dead cells due to binding the nucleic acid all cells), and propidium iodide (PI), a membrane-impermeable stain which can only be up-taken by dead bacteria. Bacteria with intact membranes exhibiting green fluorescence are considered alive while those with damaged membranes show red fluorescence signals dead. Figure 4.4 shows the images of bacteria (*E. coli*) after a 4-h incubation period with each of the three polymers (PDADMAC-20, PMETACl-40, and PVMBT-40) at 2xMIC (Figure 4.4). *E. coli* reflected red fluorescence after incubating with all three polymers which confirms the loss of membrane integrity (structural disturbance of the membrane) signifying the bactericidal

action of the compounds, the generally accepted mechanism for ammonium group bearing polymers.

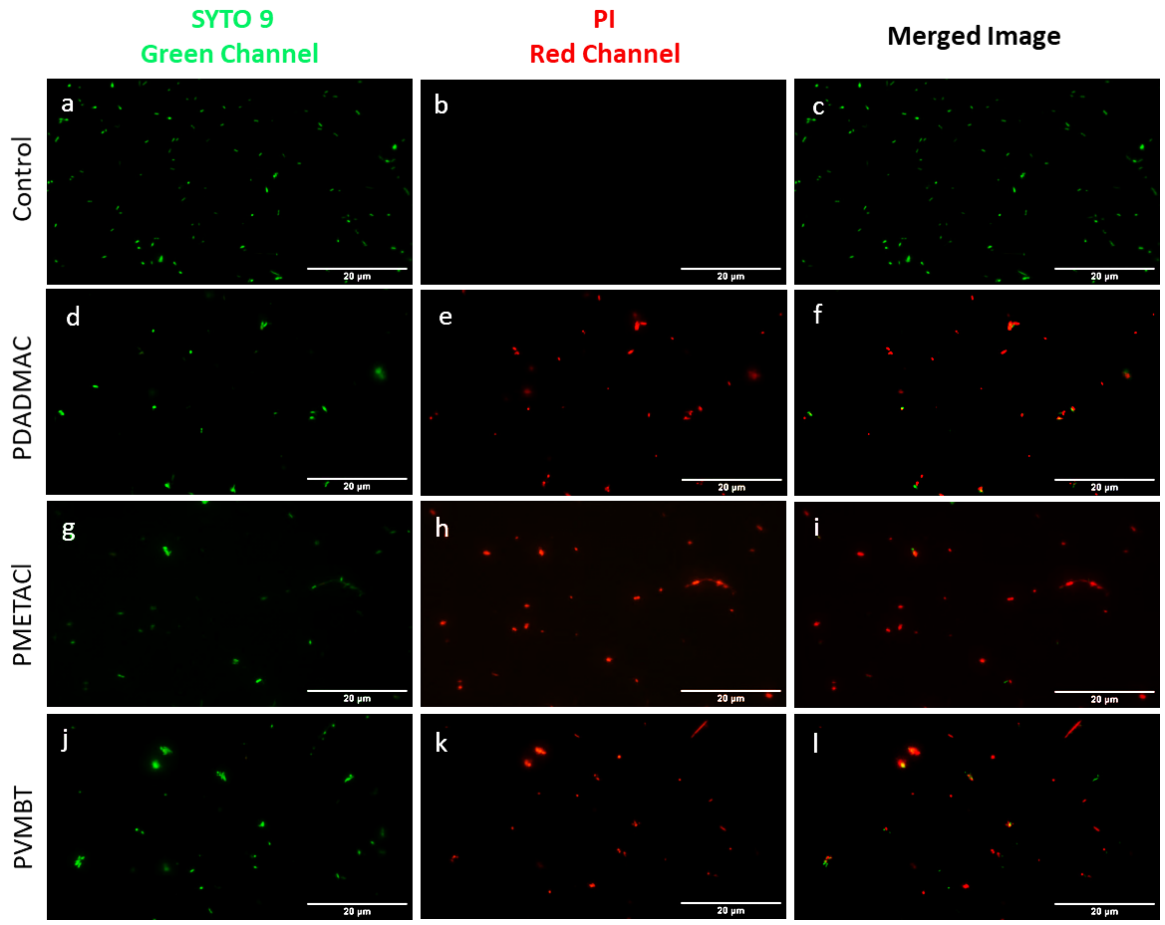

Figure 4.4. Fluorescent microscopy images of *E. coli* stained using a live/dead assay (live are shown in green (SYTO 9) and dead are shown in red (PI)). Control: bacteria were grown in media and treated with PBS (live). Bacteria were imaged on a Zeiss Axiovert 200M, 40× objective, in the FITC channel (λex 488 nm) (a,d,g,j) and the Texas red channel (λex 561 nm) (b, e, h, k). Stacked images of both channels (c, f, i, l). Red fluorescence indicates loss of membrane integrity and signifies the bactericidal action of the compound (scale bar: 20 µm).

Scanning Electron Microscopy (SEM) provides direct visual images of bacteria with changes in morphology of the membrane and cell wall. Quaternary ammonium group bearing polymers

are known to be bactericidal and can demolish the bacterial cell wall. To prove this and to understand the antimicrobial mechanism of the polymers, *E. coli* and *M. luteus* were treated with the best polymers (PDADMAC-20, PVMBT-40 and PMETACl-40) and analysed by SEM to observe the morphological changes. As shown in Figure 4.5, the distortion of the bacteria suggested that the polymers were disrupting/distorting the bacterial envelope of both Gram-negative (*E. coli*) and Gram-positive (*M. luteus*) bacteria with changes in membrane roughness, shrinking and involutions. *E. coli* showed wrinkles and deep hollows, while mis-shaped and raptured cell membrane of *M. luteus* were observed. Moreover, pores were found on the surface of *M. luteus* suggesting permeabilization of the plasma membrane and leakage of the cellular content. These phenomena suggest that these polymers kill both bacteria by destroying their cell walls/membranes.

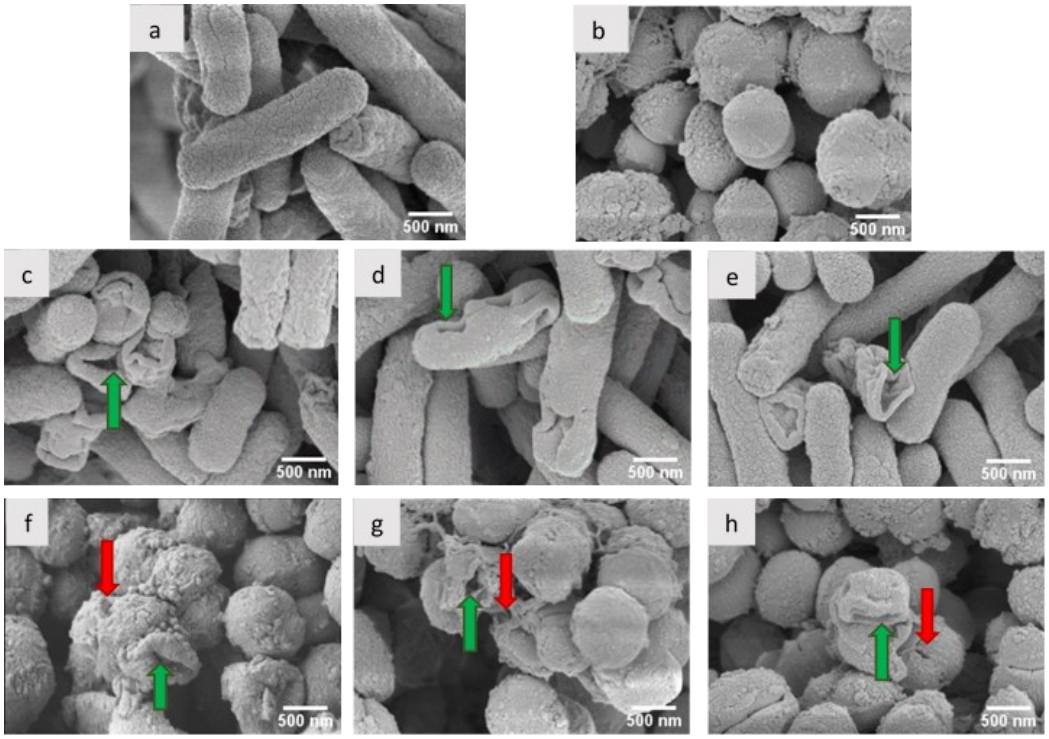

Figure 4.5. SEM images of **(a)** untreated *E. coli*; **(c)** PDADMAC-20-treated *E. coli*; **(d)** PVMBT-40-treated *E. coli*; and **(e)** PMETACl-40-treated *E. coli*. **(b)** Untreated *M. luteus*; **(f)** PDADMAC-

20-treated *M. luteus*; **(g)** PVMBT-40-treated *M. luteus*; and **(h)** PMETACl-40-treated *M. luteus.* Green arrows indicate bacteria with impaired membranes/walls. Red arrows indicate the "pores" on the bacterial surface of *M. luteus*. (Scale bars: 500 nm).

4.6.3.1. Membrane Depolarization Assays

In order to eliminate Gram-negative bacteria, antimicrobial agents should be able to permeabilize or disrupt the outer membrane, which contains lipopolysaccharides stabilized by divalent cations such as Ca^{2+}, Mg^{2+}. In general, cationic polymers interact with negatively charged outer membrane of Gram-negative bacteria *via* electrostatic interactions. Perturbation of the bacterial outer membrane of *E. coli* was assessed using the fluorescent probe, 1-N-phenyl-naphthylamine (NPN) which is a hydrophobic fluorescent probe that emits a very weak fluorescence signal in an aqueous environment. When the outer membrane is disrupted, the NPN dye can penetrate into the cell membrane and accumulate in a hydrophobic environment leading to elevated fluorescence intensity; serving as an indicator of increased permeability [140]. Supported by the SEM images (see Figure 4.5), the outer membrane of *E. coli* was depolarized by the polymers with PVMBT-40 showing a 10-fold increase in fluorescence (Figure 4.6). Presumably, when the quaternary ammonium groups accumulate on membranes *via* electrostatic interactions, the hydrophobic phenyl groups can interact with the lipophilic core of the membrane *via* hydrophobic interactions, promoting the interlacing of the polymer into the membrane leading to enhanced permeability.

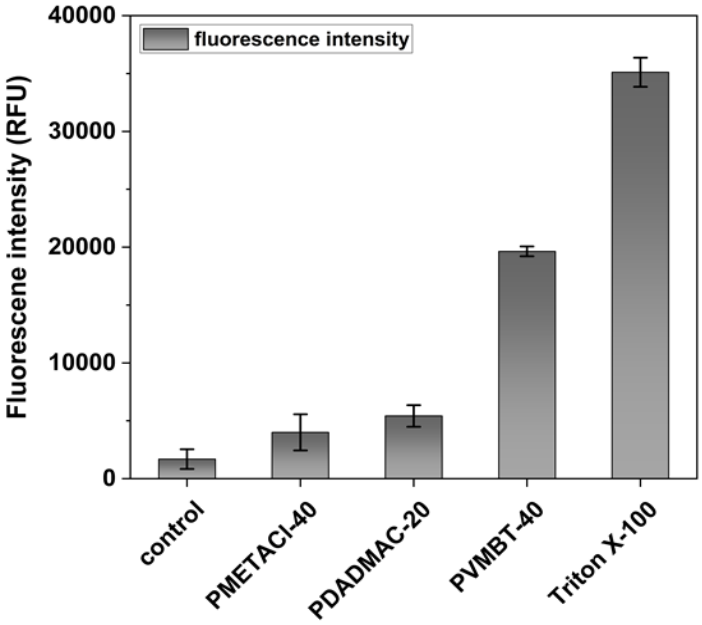

Figure 4.6. Permeabilization of the outer membrane of *E. coli* was measured using a 1-N-phenyl-naphthylamine (NPN) assay in the presence of polymers, PVMBT-40, PDADMAC-20, and PMETACl-40 after 20 min. Bacteria were incubated with NPN for 30 min until stable fluorescence and then the polymers were added at 4xMIC. Bacteria without polymer treatments were used as a negative control (control), while Triton X-100 (1% v/v)-treated bacteria served as the positive control. The error bars are standard deviation of the mean (n = 3).

Gram-positive bacteria have a thick layer of crosslinked peptidoglycan decorated with negatively charged teichoic acid, surrounding their cytoplasmic membrane. Cationic polymers can accumulate onto this *via* electrostatic interactions and penetrate deep into the peptidoglycan layer by virtue of nano-sized pores or defects. The accumulated cationic polymers can then disturb the cytoplasmic membranes integrity, leading to bacterial death. This effect of the polymers on Gram-positive bacteria (*B. subtilis*) was measured by polymer-induced leakage of the fluorescent dye Calcein. The non-fluorescent polar dye, calcein

acetoxymethyl ester penetrates into bacteria by diffusion and accumulates, undergoing hydrolysis to be transformed into fluorescent calcein. Calcein itself is not permeable to the membranes and remains trapped inside. However, when membrane-permeabilizing agents are introduced, it causes the release of calcein, which is detected by an increase in fluorescence [141,142]. Analysis (Figure 4.7) showed that polymers (PDAMAC-20, PMETACl-40 and PVMBT-40) ruptured the cytoplasmic membrane, even in the presence of the thick cell wall. PDADMAC-20 and PMETACl-40 showed as much of a fluorescence increase as Triton X-100 (1% v/v), with PDADMAC-20 acting faster than PMETACl-40, presumably due to its lower molecular weight. The more hydrophilic polymer chains of PMETACl penetrated into the peptidoglycan layer more efficiently than PVMBT-40 presumably interacting with the negatively charged teichoic acids by penetrating through the peptidoglycan layer and reaching the cytoplasmic membrane of *B. subtilis* resulting in bacterial lysis.

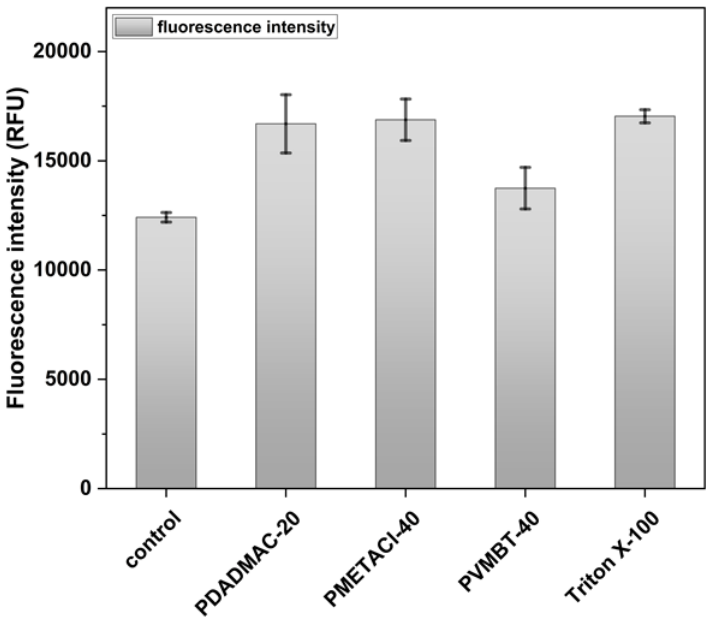

Figure 4.7. Permeabilization of the membrane of *B. subtilis* by polymers PVMBT-40, PDADMAC-20, and PMETACl-40 (at 4xMIC) and the increase in fluorescence of calcein

monitored over 30 min. Calcein-AM-loaded bacteria without polymer treatment were used as a negative control (control), while Triton X-100 (1% v/v)-treated bacteria served as the positive control. The error bars are standard deviation of the mean (n = 3).

4.6.4. Cytotoxicity and Hemolytic Activity of the Active Polymers

As predicted the higher molecular weight of polymers showed better antimicrobial activities. However, the high molecular weight polymers were more toxic than the corresponding low and mid molecular weight materials as determine by an MTT assay [143]. Similar to PDMAEMA (Mw > 39 kDa) [134], PDADMAC-40 was found to be toxic to HeLa cells at 1.25 µM (50 µg/mL) with less than 60% cell viability, while PMETACl-40 and PVMBT-40 displayed toxic effect at higher concentrations. Figure 4.8 shows the HeLa cell viability after incubating with polymers for 24 hours, the three homopolymer of PMETACls were the least toxic (even at 1.28 mM (far beyond MIC of the polymer (16-32µg/mL), with 50% of the cells still viable.

To examine the biocompatibility of the polymers, a hemolysis test was performed to evaluate the toxicity of the three selected polymers, namely PDADMAC-20, PVMBT-40, and PMETACl-40. The amount of leaked hemoglobin (% hemolysis) was measured relative to a positive control (Triton X-100 (1% v/v) defined as giving 100% lysis of red blood cells) and a negative control (PBS treated red blood cells) giving no lysis (see the equation in section 8.4.6). As clearly seen in the Figure 4.9, all of them showed negligible hemolysis, even at the highest concentrations used (1280 µM).

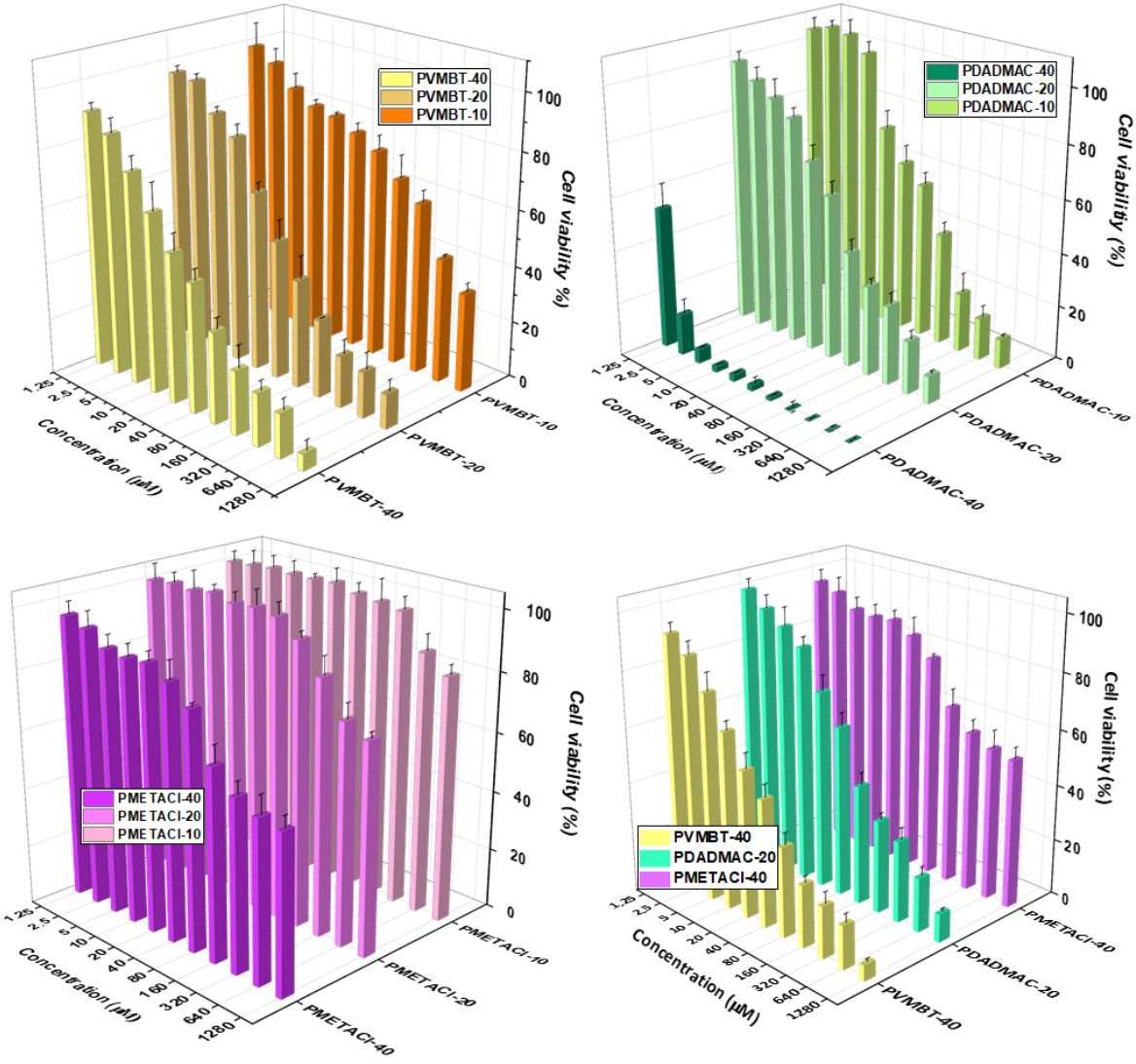

Figure 4.8. MTT cytotoxicity assay of different molecular weights of the polymers PDADMACs, PVMBTs, PMETACls at 1.25-1280 µM on HeLa cells for 24 h. Results are presented as relative cell viabilities compared to that of the untreated negative control (100% cell viability). The error bars are standard deviation of the mean (n = 3).

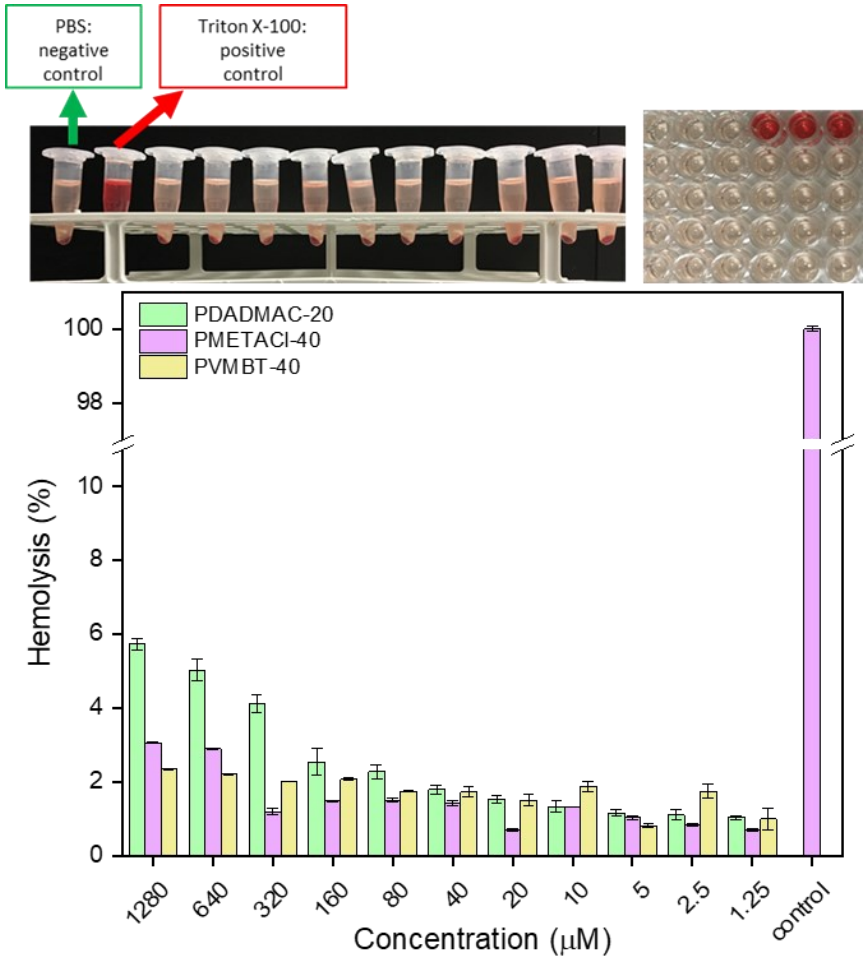

Figure 4.9. The hemolytic activity (sheep erythrocytes) of the polymers PDADMAC-20 and PMETACl-40 and PVMBT-40. The control was Triton X-100. The error bars are standard deviation of the mean (n = 3).

The practical approach to assist selectivity towards bacteria opposed to red blood cells is measured by the HC_{50}/MIC ratio, where HC_{50} is the polymer concentration required to lyse 50% of red blood cells [144]. Thus, PDADMAC-20, PMETACl-40 and PVMBT-40 were quite selective against bacteria over red blood cells in the range of 1.25 µM-1280 µM.

Subsequently, to assess the selectivity of polymers towards bacterial cells and mammalian cells, the therapeutic index was calculated by dividing the value of IC_{50} by the value of MIC.

The IC_{50} (half maximal inhibitory concentration) is commonly utilized in pharmacology and toxicology to assess a compound's effectiveness in inhibiting biological processes or inducing specific effects in cell cultures, while also serving to determine the compound's toxicity by identifying the concentration at which it reduces cellular viability or function by 50%.

However, IC_{50} values obtained through the MTT assay were significantly lower than HC_{50} values based on hemolysis, indicating a narrower range of biocompatible polymers. A potential explanation for the disparity could be attributed to variations in experimental conditions and cell types used in the respective assays [121]. Particularly, the hemocompatible polymers (HC_{50} > 26 mg/mL) such as PDADMAC-20 and PVMBT-40 inhibited the growth of HeLa cells at substantially lower concentrations (IC_{50} of 900 µg/mL (51.818 µM) and 200 µg/mL (5.35 µM), respectively). On the other hand, PMETACl-40 were found highly cytocompatible with an the IC_{50} values 4.4 mg/mL (110 µM). The IC_{50} values were obtained from dose-response curves interpolated using GraphPad Prism version 8.4 for Windows (GraphPad Software).

Table 4.5. Selective toxicity of PDADMAC-20, PMETACl-40 and PVMBT-40 based on MIC and hemolysis and MTT data.

Polymer	**MIC (µg/mL)**				**HC_{50}**	**Selectivity**	**Selectivity**
	E. coli	***B. subtilis***	***M. luteus***	***S. typhimurium***	**mg/mL**	**HC_{50}/MIC**	**IC_{50}/MIC**
PDADMAC-20	**16**	**16**	**16**	**32**	**>26**	**>800**	**>28**
PVMBT-40	**32**	**32**	**32**	**32**	**>51**	**>1600**	**>7**
PMETACL-40	**32**	**32**	**32**	**32**	**>51**	**>1600**	**>138**

4.6.5. Antifungal Activity of the Polymers

Despite the research on the antibacterial activities of polymers with quaternary ammonium groups, these materials have yet to receive significant attention with regard to their potential antifungal properties. Thus, here the antifungal activity of homopolymers; PDADMACs, PVMBTs and PMETACls were evaluated on *C. albicans, C. auris* and *M. furfur*. Minimum inhibitory concentrations, were conducted using the broth dilution method, in accordance with the guidelines outlined by the Clinical and Laboratory Standards Institute [145]. The homopolymers were subjected to serial dilutions, ranging from 500 µM to 1.0 µM and the influence of molecular weight on antifungal activity analysed (see Table 4.6). The findings indicate that the effectiveness of homopolymers was contingent not only upon their molecular weights but also on the specific microorganism under examination. Among the tested polymers, PDADMAC-40 showed the greatest activity on all tested organisms with MIC values 1.0-125 µM while PVMBT-40 showed better activity against *M. furfur* compared to PMETACl-40. This phenomenon may be attributed to the distinctive structure of PDADMAC, which features repeating units containing both hydrophobic and hydrophilic components, along with cationic groups within the main chain resulting in enhanced interactions with the membranes of fungi. Previous studies [146,147] have demonstrated that main chain cationic polymers effectively inhibited the growth of a wide range of pathogenic fungi. The variations observed in the minimum inhibitory concentration (MIC) values among different strains could potentially be attributed to the composition and the extent of negative charge density within their respective outer envelopes. Interestingly all the PVMBTs and PMETACls showed fungistatic activity while PDADMAC-40 and PDADMAC-20 showed fungicidal activity.

Table 4.6. The minimum inhibition and minimum fungicidal concentration of the various homopolymers.

Polymer	*C. albicans*		*C. auris*		*M. furfur*	
	MIC	**MFC**	**MIC**	**MFC**	**MIC**	**MFC**
PDADMAC-40	1	31	125	500	1	4
PDADMAC-20	16	16	250	>500	8	16
PDADMAC-10	62	125	>500	>500	31	31
PMETACl-40	>500	>500	>500	>500	16	500
PMETACl-20	>500	>500	>500	>500	31	>500
PMETACl-10	>500	>500	>500	>500	63	>500
PVMBT-40	>500	>500	>500	>500	8	125
PVMBT-20	>500	>500	>500	>500	31	250
PVMBT-10	>500	>500	>500	>500	125	>500

Fungi are known to exhibit a major virulence factor when in biofilms, which are complex microbial communities that form on both biotic and abiotic surfaces and are typically associated with an extracellular polymer matrix. A tetrazolium salt, 2,3-bis(2-methoxy-4-nitro-5-sulfophenyl)-2H-tetrazolium-5 carboxanilide, (XTT) reduced to water-soluble orange formazan compounds, the intensity of which can then be determined using a microtiter-plate reader, specifically gauges the metabolic activity of the fungi within the biofilm [148,149]. As seen in Figure 4.10, the higher the concentration of polymers applied, the fewer viable cells remained in the biofilms. Among the tested polymers, PDADMAC-40 and PDADMAC-20 again showed the best inhibition activity.

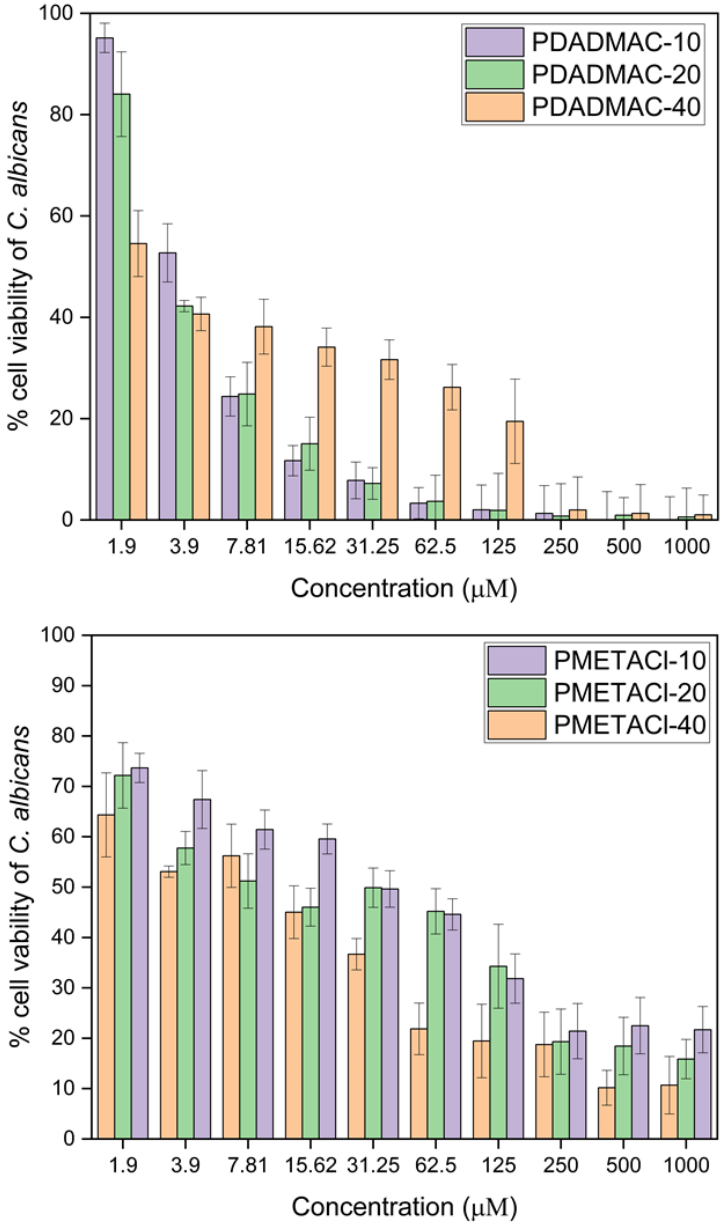

Figure 4.10. The mature biofilms of *C. albicans* were incubated in 96-well plates with various concentrations of PMETACls and PDADMACs with different molecule weights for 24 h and cell viability (percentage of treated biofilms in relation to untreated controls) were assessed by an XTT assay (the control is not shown in the graph). Each bar represents the average data of obtained from triplicates of two independent experiments. The error bars are standard deviation of the mean (n = 3).

Although an XTT assay offers several advantages, including being non-invasive, non-destructive, and requiring minimal processing and proves particularly valuable for evaluating the impact of antimicrobial drugs on biofilms, the optimization can be challenging when dealing with mature biofilms because the relationship between metabolic activity and the number of viable cells may not follow a linear pattern [150]. Thus, PDADMAC-20 and PMETACl-20 (15 µM and 1280 µM) were added to biofilms with qPRC analysis (see Figure 4.11). Polymers were not affective enough to diminish between biofilms of *C. albicans* and *C. auris*, whereas there was an approximately 1.5 log decrease after incubation with *M. furfur.*

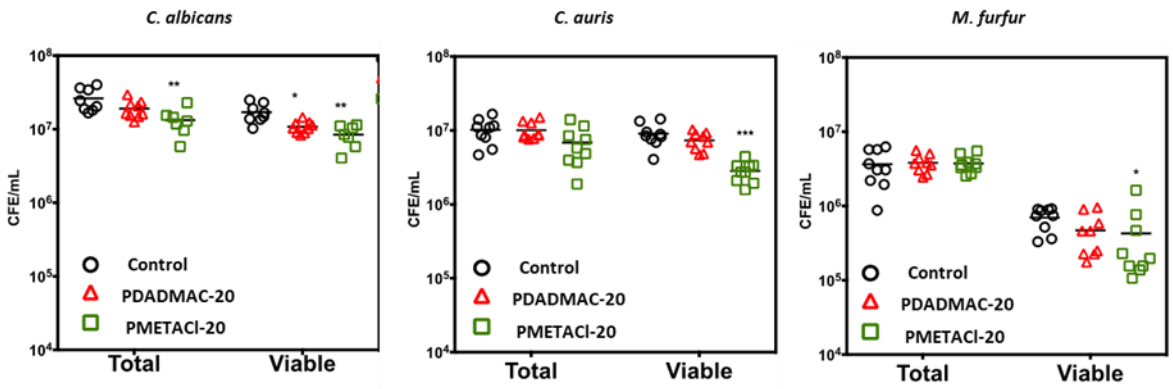

Figure 4.11. The growth of *C. albicans*, *C. auris* and *M. furfur* after incubating with PDADMAC-20 (15 µM) and PMETACl-20 (1280 µM) as assessed using qPCR. Statistical significance was *** $p < 0.005$, ** $p < 0.01$ and * $p < 0.05$, as respectively.

4.7. Conclusions and Future Work

Homopolymers, namely PDADMAC, PVMBT, and PMETACl, were synthesized with three different molecular weights, and their antibacterial activities were evaluated against various

bacterial strains. It was observed that as the molecular weight of the polymers increased, their antimicrobial activity also increased, with evidence of bactericidal effects confirmed through dye-based assays and SEM imaging. However, this increase in molecular weight also led to higher toxicity towards mammalian cells. Among these polymers, PDADMAC-20 exhibited the most potent activity, while PMETACl-40 emerged as the safest option for biomedical applications.

The antifungal activities of these polymers were also assessed against three fungal strains, resulting in some polymers displaying fungistatic effects and others exhibiting fungicidal properties. However, none of them demonstrated strong efficacy in reducing biofilms.

In summary, the antimicrobial activity of the homopolymers explored in this study was found to be dependent on the polymer's structure (including the presence of cationic groups in the main or side chain), molecular weight, and the specific microorganisms being tested. As a future research direction, these polymers could be tested on clinically isolated microorganisms and multi-drug resistant strains to confirm their safety for biological applications. Additionally, investigations into bacteria biofilms may hold promise due to the polymers' potent activity at lower concentrations against bacteria when compared to fungi.

Chapter 5

A Novel Methacrylamide Monomer and Its Antimicrobial Homopolymers

5.1. Introduction

5.1.1. Free Radical Polymerization

It has been over a century since the publication of Staudinger's "Uber Polymerisation" [151] , which marked the beginning of radical polymerization as the most popular technique for synthetic polymer synthesis. This method has been extensively used in industrial-scale production, with approximately 50% of commercial synthetic polymers being prepared through free radical polymerization over the past two decades [152].

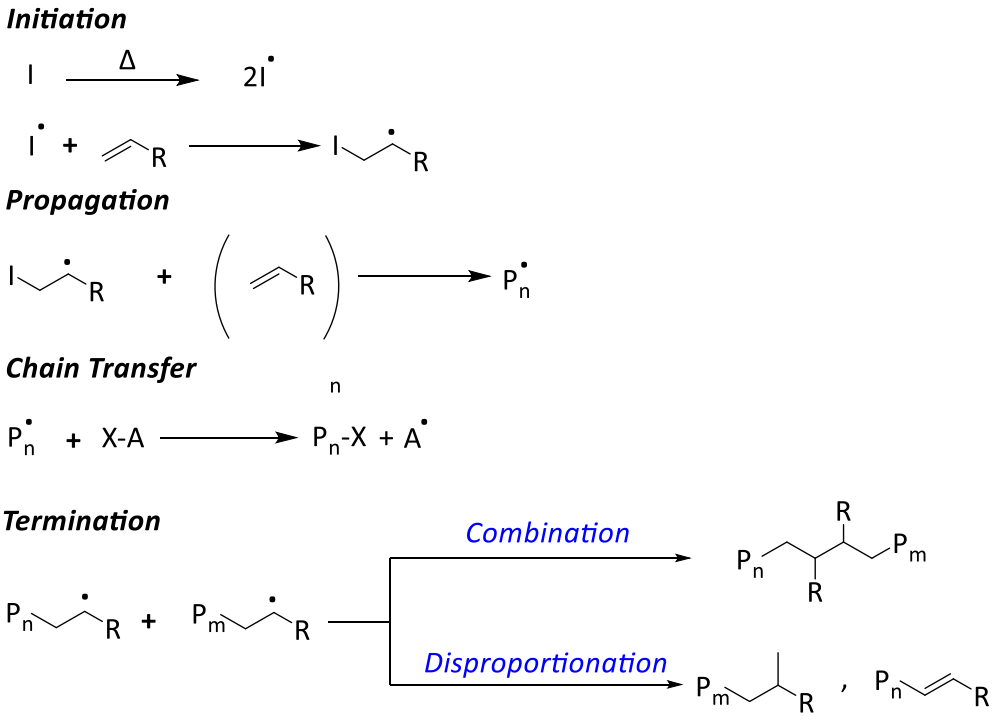

Figure 5.1. The mechanism of conventional free radical polymerization.

Free radical polymerization involves a monomer that contains a reactive double bond; an initiator which generates free radicals and a solvent (if necessary). It is a so-called chain growth polymerization process, with free radical polymerization involving successive addition of monomer units to a "reactive" growing polymer chain occurring through the reaction of the double bond of the monomer unit (formation of an active propagating chain). As shown above, the mechanism of free radical polymerization involves three key steps: initiation, propagation and termination.

The initiation step begins with forming of radicals (I•) from the decomposition of an initiator *via* thermal, electrochemical or photo-activation. The activated initiator (radicals I•) attack a monomer bearing a reactive double bond to give I-M•. This activated chain grows by adding further of monomer units in the so-called propagation step, with the addition of individual monomer units one at a time. In the final step, radicals on the ends of the polymer chains are "quenched" either *via* recombination (in which two chains react to form a single polymer chain) or disproportionation (resulting in the formation of two polymers chains with one saturated and the other unsaturated) or external quenchers stop the chemistry (*e.g.*, oxygen).

In addition to these steps, an additional reaction, called chain transfer, may occur, in which radicals are transferred to another molecule or solvent, terminating the polymer chain but generating another radical species. Indeed, it is a common observation that the actual size of the polymer "molecule" is smaller than what would be predicted based on the experimentally observed rates of termination *via* coupling and disproportionation, attributed to the premature termination of the growing polymer chain. These termination reactions contribute to the dispersity of polymers, with the polymers having varying chain lengths, primarily due to these termination reactions [61,153,154].

Radical polymerization techniques offer numerous benefits, including its versatility in working with a wide range of monomers *e.g.* styrene, meth/acrylates, and vinylic monomers. It can also tolerate various functional groups such as -OH, -NH_2, -COOH and different reaction conditions *e.g.*, bulk, solution, suspension, and emulsion. Furthermore, it is easy to apply without requiring complex technologies to synthesize synthetic polymers on a large scale due to exhibiting a certain level of tolerance to impurities like oxygen and also progresses in water, which makes it easy to execute and hence commonly used [153,154].

5.1.2. Antimicrobial Polymers with Pyrrolidinium Group and Antimicrobial Methacrylamide Polymers

Among the polymers having quaternary ammonium groups, poly (diallydimethyl ammonium chloride) (PDADMAC) stands out on the strength of its exceptional antimicrobial activity (see Chapters 3 and 4). Recently, the antifungal activity of polymeric diallyl quaternary ammonium salts were investigated, with homopolymers synthesized from the monomers, *N,N*-methyl butyl diallyl ammonium chloride, *N,N*-dimethyl benzyl diallyl ammonium, and *N,N*-dimethyl diallyl ammonium *via* free radical polymerization. This revealed that all three homopolymers demonstrated significant, and potent, inhibitory effects against fungi (*Fusarium oxysporum* f. sp. cubense race (Foc4)). Importantly, these substances were found to be virtually non-toxic to silkworms and mice. In comparison to benzalkonium chloride, a typical, commercial, small quaternary ammonium salt, the toxicities of the synthesized materials were considerably lower in zebrafish. Among them, poly(*N,N*-methyl benzyl diallyl ammonium chloride) exhibited the most favourable combination of antifungal activity and low biotoxicity [155].

Timofeeva [156] showed the antimicrobial activity of secondary and tertiary poly(diallylammonium) salts namely poly(diallylammonium trifluoroacetate) and poly(diallylmethylammonium trifluoroacetate). In this case the polymers were synthesized through free radical polymerization from the corresponding monomers in aqueous solution, with the radical initiator APS. Polymers with molecular weights of approximately 25 kDa and 55 kDa were tested against various gram-positive and gram-negative bacterial strains. The minimum inhibitory concentrations (MICs) observed fell within the range of 1.5 to 124 µg/mL, influenced by the polymer's molecular weight and structural characteristics. Subsequently, an investigation into the antimycobacterial activity of these polymers was explored, in combination with poly (diallylethylammonium trifluoroacetate) [157]. All the polymers, with molecular weights around 60 kDa, demonstrated potent bactericidal effects against both *M. smegmatis* and *M. tuberculosis*. Notably, poly(diallylammonium trifluoroacetate) was the most effective (MBC- 7-15 µg/mL). Experiments designed to elucidate the mechanism of action for poly (diallylammonium trifluoroacetate) revealed that it rapidly induced damage and permeability to the inner membrane of *M. smegmatis*.

Here it is important to note that there have been no reports concerning the antimicrobial activities of the polymers consisting of meth/acrylamide or meth/acrylate monomers bearing the pyrrolidinium group.

5.2. Aim of This Chapter

In this chapter, a novel methacrylamide monomer, bearing a pyrrolidinium group, inspired by the polymerisation of diallylammonium chloride was synthesised by reacting methacrylic anhydride with (*R*)-3-amino-1-N-Boc-pyrrolidine. This was used to generate polymers *via* free radical polymerization to give three molecular weight variants. The antimicrobial activities on Gram-positive and Gram-negative bacteria and cytocompatibility on mammalian cells of the polymers were evaluated.

5.3. Results and Discussion

5.3.1. Synthesis of (*R*)-(1-tertbutoxycarbonyl) pyrrolidin-3-yl) methacrylamide

The novel methacrylamide monomer was synthesized by reacting methacrylic anhydride with (*R*)-3-amino-1-N-Boc-pyrrolidine in the presence of triethylamine in a yield 87% (Figure 5.2).

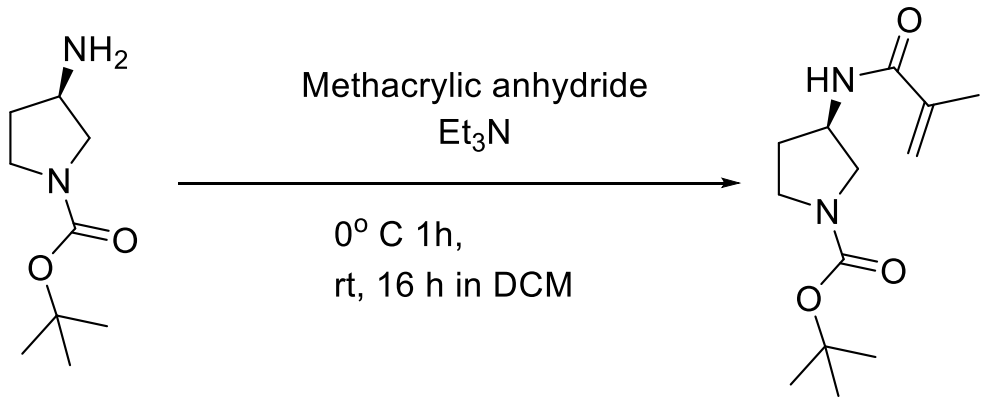

Figure 5.2. Synthesis of (*R*)-(1-tertbutoxycarbonyl) pyrrolidin-3-yl) methacrylamide.

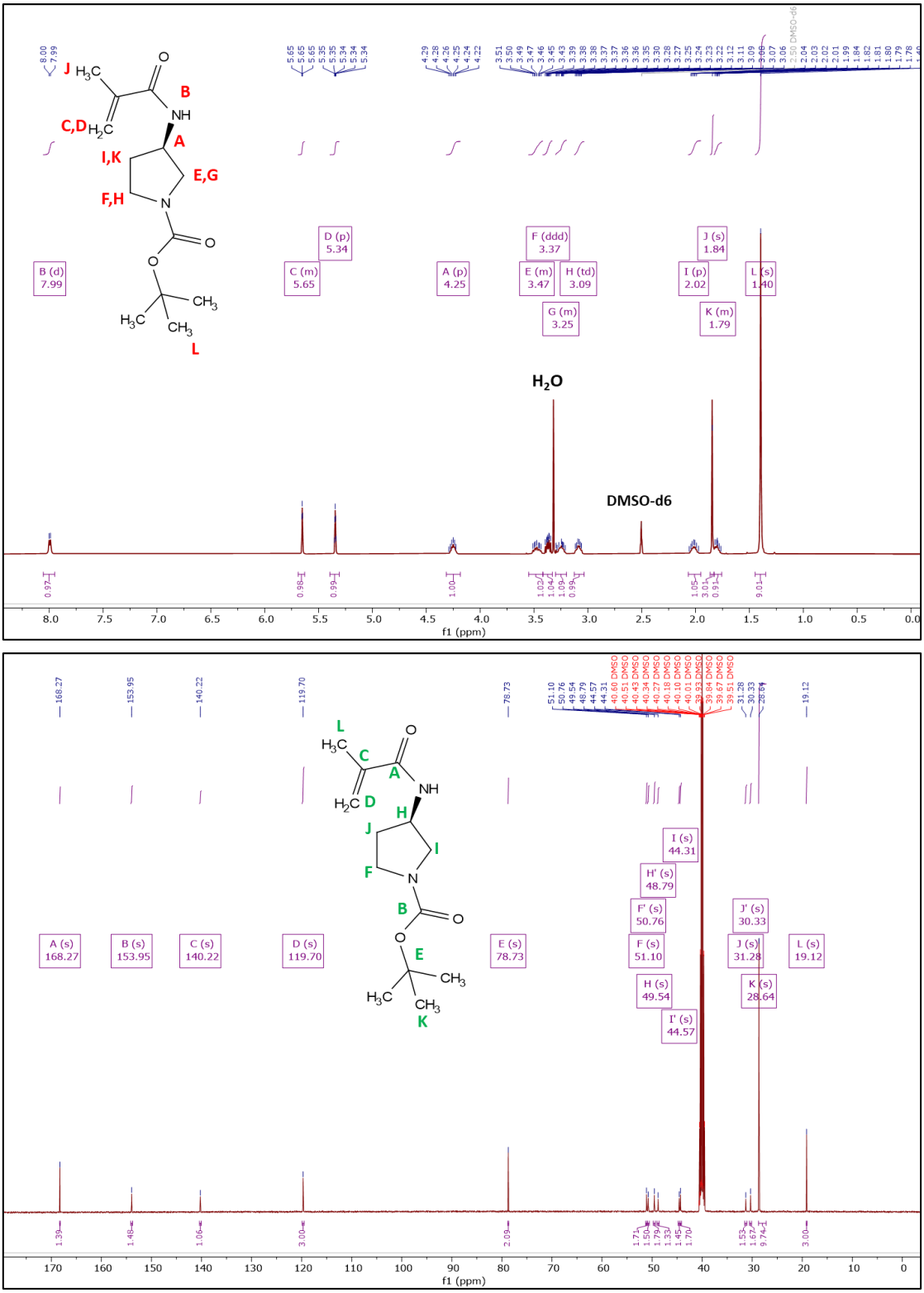

Figure 5.3. ^{1}H spectrum and ^{13}C NMR spectrum of the monomer- (*R*)-(1-tertbutoxycarbonyl) pyrrolidin-3-yl) methacrylamide- recorded in DMSO-d_6.

5.3.2. Polymerization of (*R*)-(1-tertbutoxycarbonyl) pyrrolidin-3-yl) methacrylamide

Prior to polymerization, the solubility of the monomer was investigated and found to be soluble in chlorinated solvents such as chloroform or dichloromethane), alcohols (ethanol, methanol), as well as acetone, dimethyl sulfoxide, tetrahydrofuran, and diethyl ether. However, it was only partially soluble in dioxane (soluble with heating), while insoluble in hexane. To identify the most suitable solvent for the polymerization reaction of the Boc-protected monomer, methanol and tetrahydrofuran were selected as solvents due to the monomer's high solubility, and the initiator azobisisobutyronitrile (AIBN) was employed. However, polymers with the intended molecular weight were not successfully synthesized (Mn 8.9 kDa Mw 30 kDa, PDI 3.30) presumably due to methanol functioning as a transfer agent, resulting in the production of smaller-sized polymers with wide dispersity. In contrast, the polymerization reaction was successful in THF and thus was selected. By changing the monomer to initiator ratio ($[M]_0/[I_0]$), three polymers approx. 10, 20 and 40 kDa, were synthesized. Table 1 shows the conditions of polymerization reactions. All the polymers were deprotected using TFA/DCM to give the pyrrolidinium containing polymers.

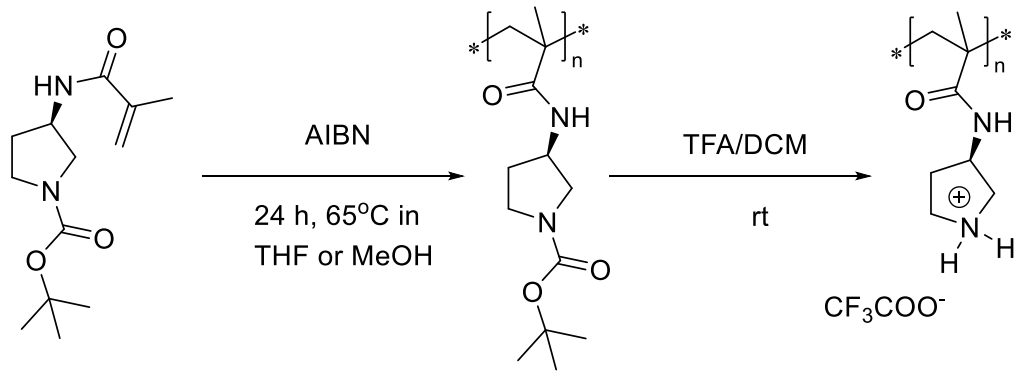

Figure 5.4. Free Radical Polymerization of (*R*)-(1-tertbutoxycarbonyl) pyrrolidin-3-yl) methacrylamide and deprotection with TFA/DCM mixture.

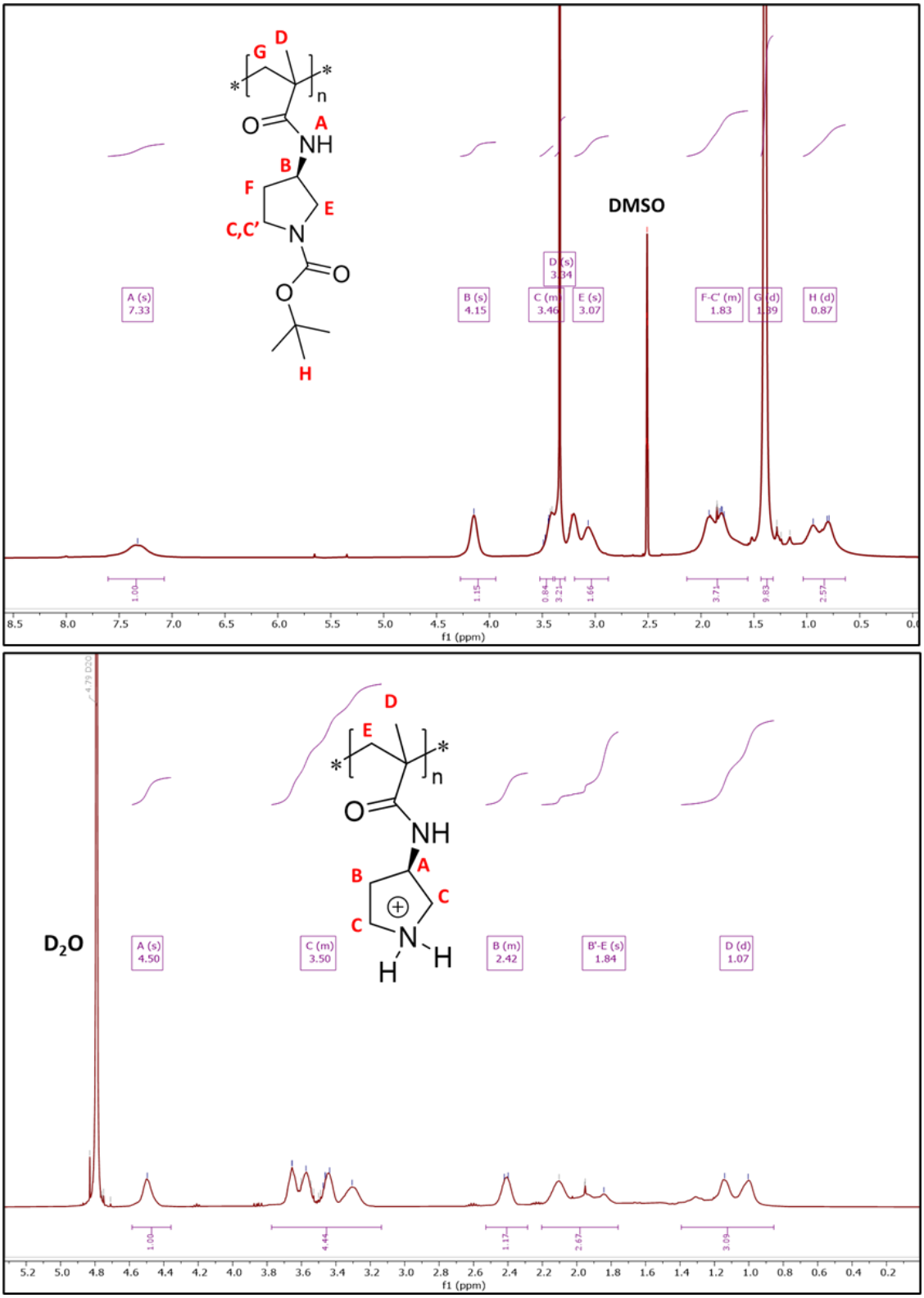

Figure 5.5. ^{1}H spectrum of Poly((*R*)-(1-tertbutoxycarbonyl) pyrrolidin-3-yl) methacrylamide) in DMSO and after boc removal in D_2O.

Table 5.1. The resulting polymers produced by the free radical polymerization of the Boc-protected monomer in THF.

polymer	$[M]_0$	$[I]_0$	$[M]_0/[I]_0$	$Mn_{,GPC}$	$Mw_{,GPC}$	PDI
P-10	0.39	0.0066	58	9.5 kDa	19.9 kDa	2.09
P-20	0.39	0.0036	108	17.1 kDa	34.7 kDa	2.02
P-40	0.39	0.0018	215	40.2 kDa	79.8 kDa	1.98

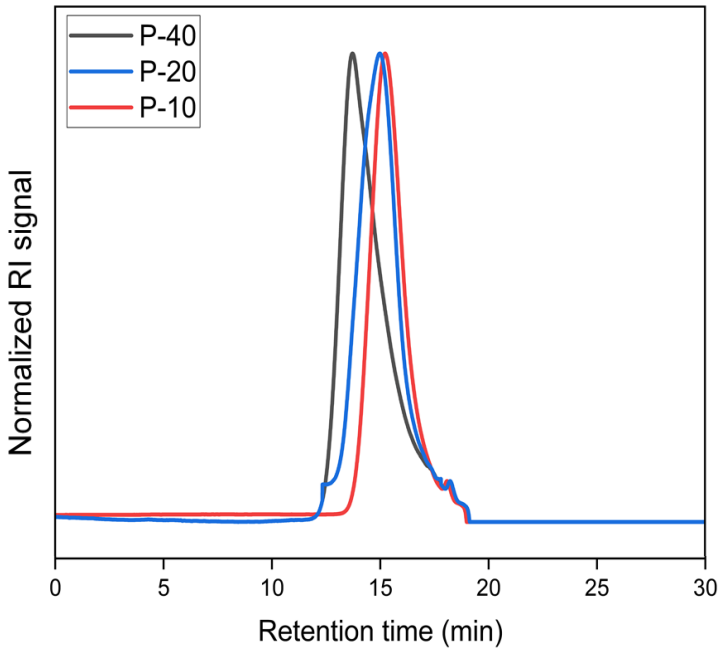

Figure 5.6. GPC analysis of Poly((*R*)-(1-tertbutoxycarbonyl) pyrrolidin-3-yl) methacrylamide) synthesized *via* free radical polymerization. (Eluent: 0.1% (w/v) LiBr in DMF with a flow rate of 1.0 mL min^{-1} at 60°C -PMMA calibration standards).

5.3.3. Evaluation of the Antimicrobial Activity of the Polymers

Minimum inhibition concentration (MIC) of the polymers after Boc group removal were determined *via* a resazurin assay in the range of 1024 µg/mL to 1 µg/mL against *E. coli* and *B. subtilis*, with antibiotics Gentamicin and Clindamycin used as controls. The MICs of all three polymers were found to be 32 µg/mL for *E. coli* and 8 µg/mL for *B. subtilis.* All three polymers showed inhibition of the growth of both bacteria with slightly superior bacteriostatic action against the gram-positive bacteria, *B. subtilis.* Of course, this means that the larger polymer is more active at a molar level.

Table 5.2. MIC values of the polymers against *E. coli* and *B. subtilis* as measured *via* a resazurin assay.

		MICs of tested microorganisms	
Polymer		***E. coli***	***B. subtilis***
P-10		32 µg/mL	8 µg/mL
P-20		32 µg/mL	8 µg/mL
P-40		32 µg/mL	8 µg/mL
Standard Antibiotic	**Gentamicin**	0.5 µg/mL	**-**
	Clindamycin	-	4 µg/mL

A live (green)-dead (red) assay illustrated the bactericidal antimicrobial activity of the polymers (Figure 5.7). Among these polymers, P-40 exhibited the highest bactericidal activity in comparison to the polymers with the lower molecular weights, attributed to the higher charge density in the polymer chain, and interestingly having a lower activity molarity than the other two polymers. This greater chain density presumably results in enhanced

interactions with the bacterial membrane, as indicated by the bacteria appearing red, signifying membrane damage. However, P-40 showed the greatest toxicity against HeLa cells even at its MIC (see subsection 5.3.4).

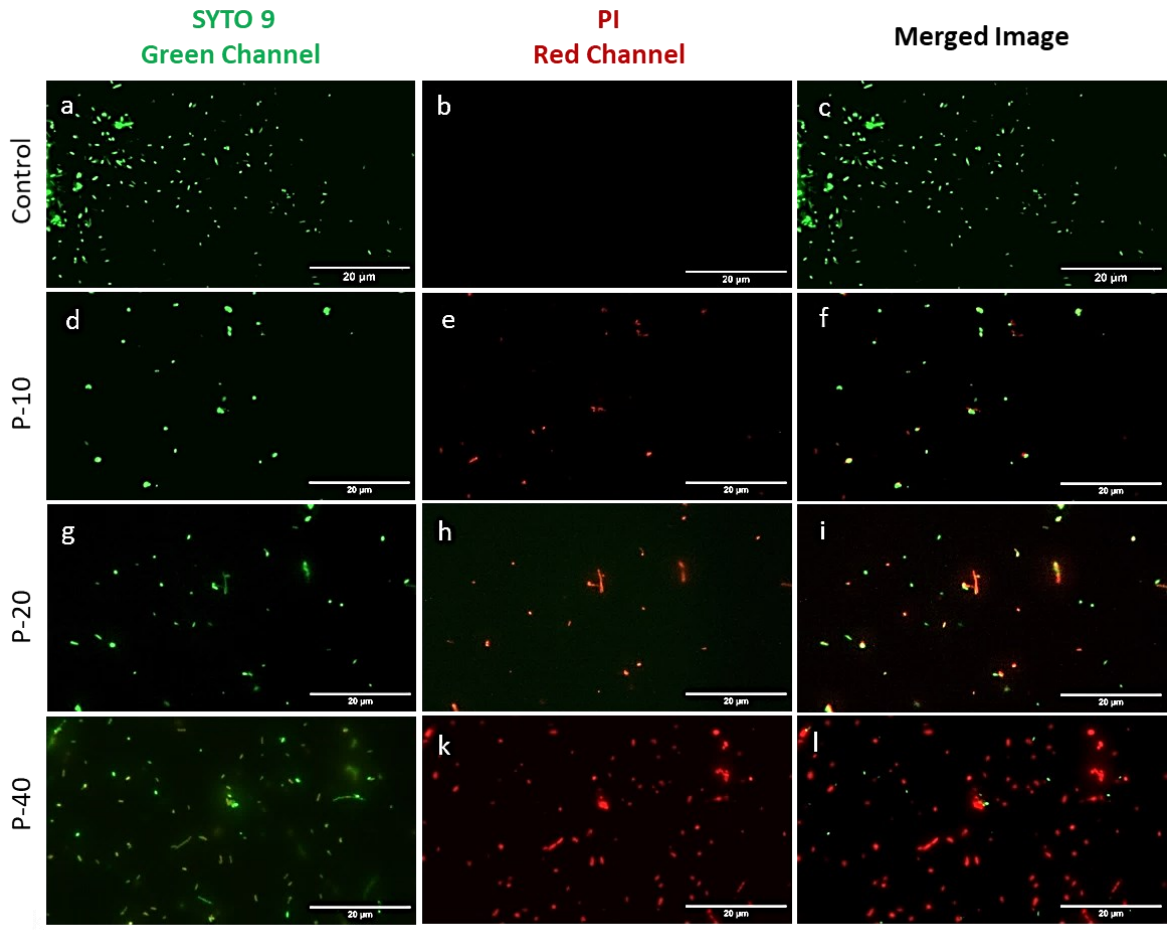

Figure 5.7. Live-Dead assay of *E. coli* incubated with 2xMIC of the polymers (P-10, P-20 and P-40) after 4 hours. Controls cells incubated with PBS. (Scale bar – 20 µm).

To understand the antimicrobial mechanisms of polymers P-10 and P-20, scanning electron microscopy (SEM) was employed to observe the morphological changes in *E. coli* and *B. subtilis* after exposure to these polymers at twice their minimum inhibitory concentrations.

Following a 4-hour incubation with these polymers, the membrane of *E. coli* exhibited pronounced wrinkling and deep recesses, whereas the cell membrane of *B. subtilis* showed rupture and deformation, accompanied by extensive cytoplasmic leakage (Figure 5.8).

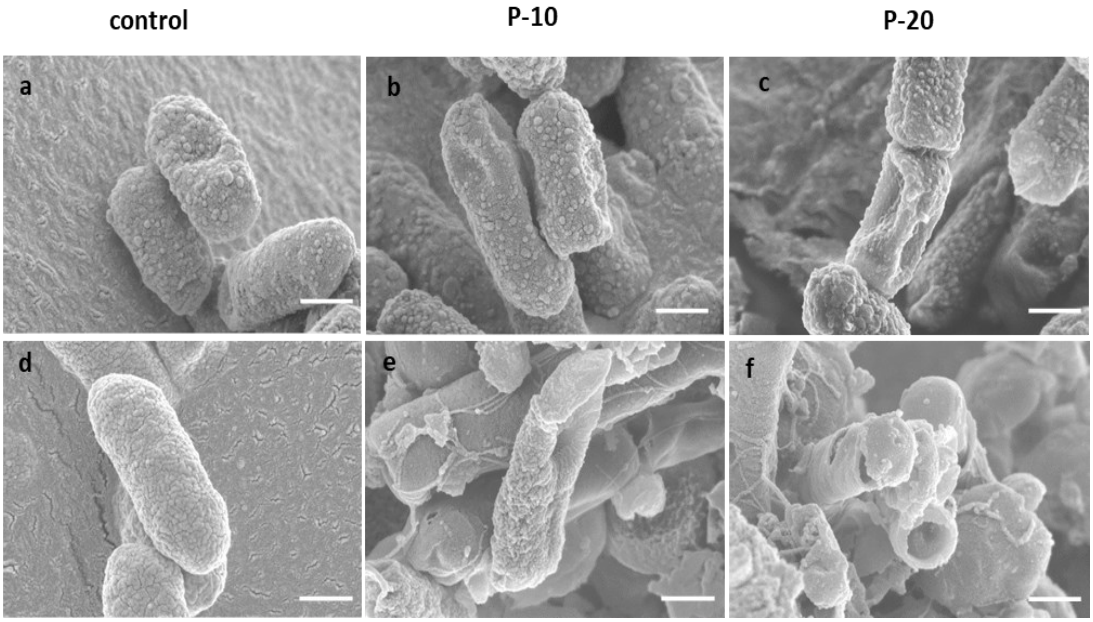

Figure 5.8. SEM images of *E. coli* (a, b, c) and *B. subtilis* (d, e, f) treated with P-10 and P-20 at 2xMICs. (Scale bar- 500 nm).

Dye-based assays provided evidence of the bactericidal action mechanism of the polymers against both gram-positive and gram-negative bacteria. The outer membrane depolarization assay (Figure 5.9-A) revealed an increase in the fluorescence of the NPN dye, which accumulated in the cell membrane before interacting with the polymers over a 30-minute period. Compared to control cells (treated with PBS), a 5-fold increase in fluorescence was observed for P-40 and approximately 4-fold increase was obtained for P-20 and P-10.

A cytoplasmic membrane assay revealed that the polymers were capable of disrupting the cytoplasmic membrane within just 30 minutes of treatment (Figure 5.9-B), a finding

supported by the SEM images. All three polymers showed potent activity, increasing the fluorescence intensity of the Calcein-AM dye as much as the detergent, Triton X-100. This can be attributed to the distinctive structure of the polymer's repeating unit, which bears a pyrrolidinium group as a side chain, providing both cationic and hydrophobic characteristics, a similar trend to that observed for PDADMAC (see Chapter 4.6.4).

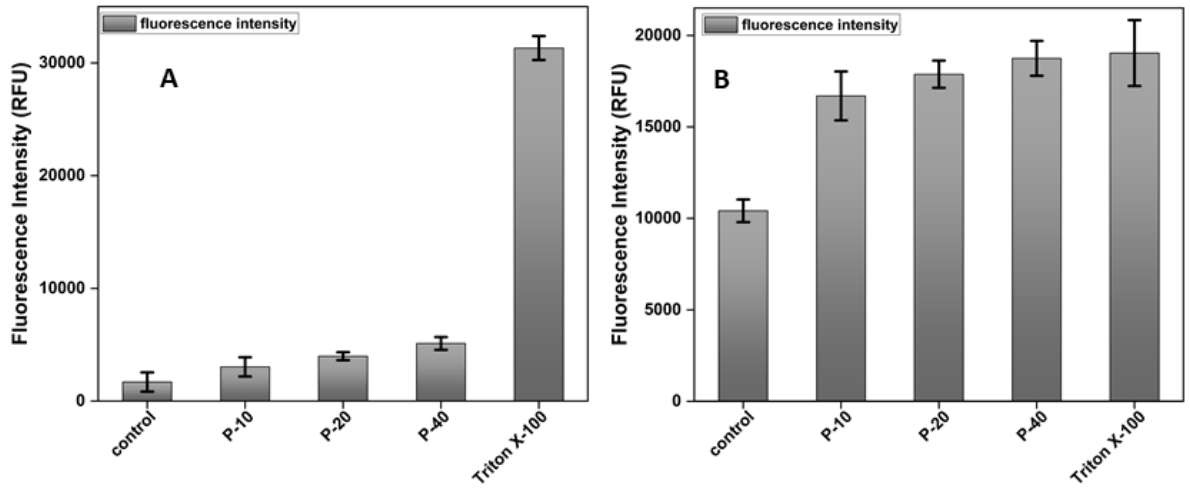

Figure 5.9. Bacteria were incubated with the dyes NPN and Calcein-AM before treating with the polymers at 2xMIC. Outer membrane depolarization assay of *E. coli* in the presence of P-10, P-20 and P-40 (**A**). Cytoplasmic membrane depolarization assay of *B. subtilis* in the presence of P-10, P-20 and P-40 **(B).** Control cells were treated with PBS and 1% (v/v) Triton X-100. The error bars are standard deviation of the mean (n = 3).

5.3.4. Investigation of Cytotoxicity and Hemolytic Activity of the Polymers

The cytotoxicity of the homopolymers were assessed on HeLa-cells by an MTT assay. The higher molecular weight polymer, P-40, showed some limited toxic effects at its MIC (Figure

5.10), although >80% of cells were still viable at this concentration. P-10, P-20 and P-40 all showed increasing toxicity with higher concentrations of the polymers.

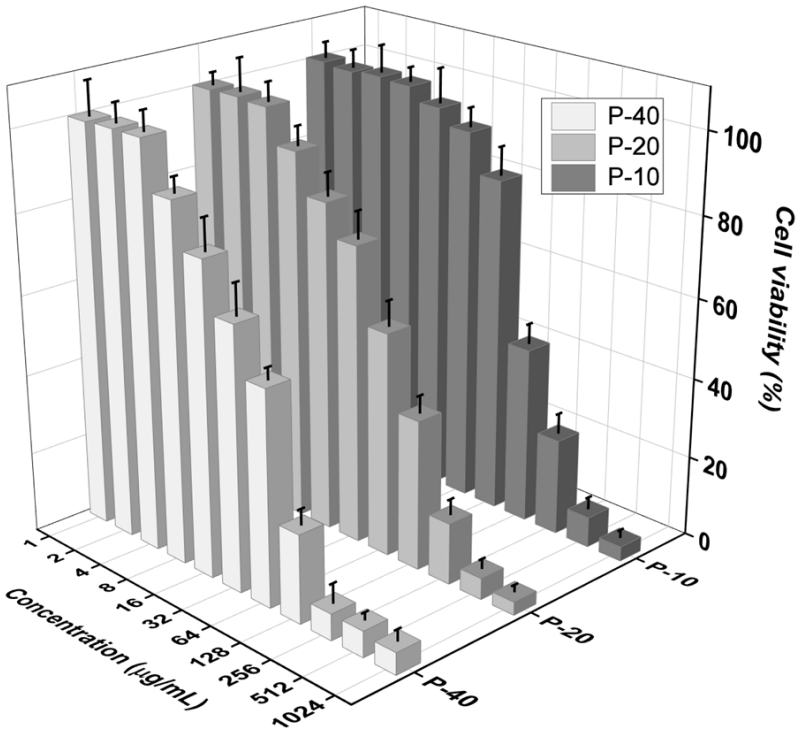

Figure 5.10. MTT cytotoxicity assay of different molecular weights of poly((R)-) pyrrolidin-3-yl) methacrylamide, P-10, P-20 and P-40 at 1-1024 μg/mL on HeLa cells for 24 h. Results are presented as relative cell viabilities compared to that of the untreated negative control (100% cell viability). The error bars are standard deviation of the mean (n = 3).

A hemolysis assay was conducted measuring the extent of hemoglobin release when sheep red blood cells were exposed to varying concentrations of these polymers. As illustrated in Figure 5.11, even at the highest concentrations tested (2048 μg/mL), all three polymers exhibited minimal hemolysis. The percentage of leaked hemoglobin (% hemolysis) was

measured relative to a positive control (Triton X-100 (1% v/v) defined as giving 100% lysis of red blood cells) and a negative control (PBS treated red blood cells) giving no lysis (see experimental section 8.4.6).

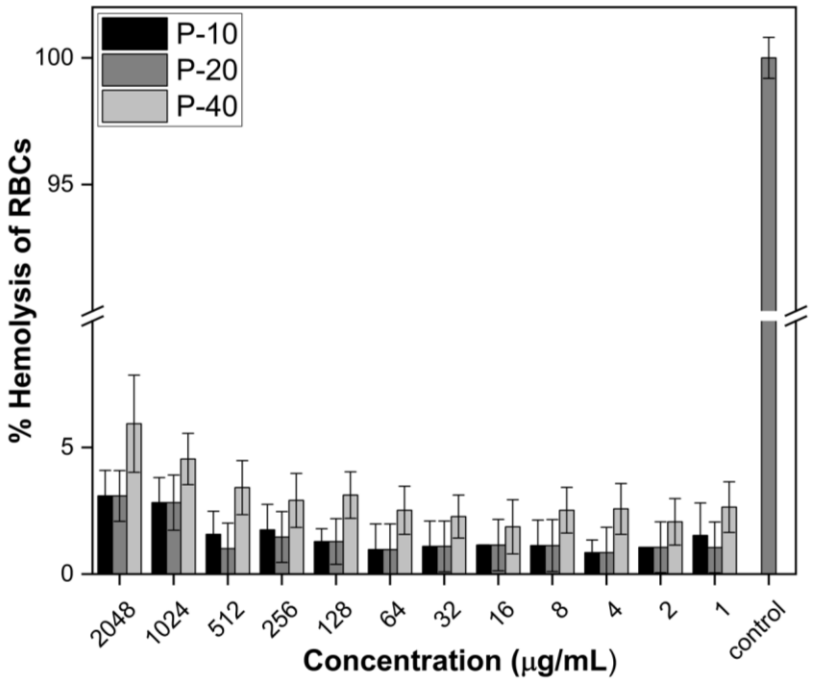

Figure 5.11. The hemolytic activity (sheep erythrocytes) of the polymers with varying concentrations of the polymers was assessed through a hemolysis test. The control was Triton X-100. The error bars are standard deviation of the mean (n = 3).

5.4. Conclusion and Future Work

A new methacrylamide monomer with pyrrolidinium side-groups was synthesized, and the corresponding homopolymers were synthesized *via* free radical polymerization as three different molecular weights. Their antibacterial activities were subsequwntly evaluated on both Gram-negative and Gram-positive bacteria. Increased molecular weights were

associated with enhanced antimicrobial efficacy, as evidenced by bactericidal effects validated through dye-based tests and SEM imaging. These new methacrylamide polymers showed potent activity against Gram-positive bacteria.

In the future, this monomer could be synthesized *via* RAFT polymerization to exert control over molecular weight and subsequently tested on various bacterial and fungi strains, including clinically isolated ones.

In addition, this monomer presents itself as an alternative to diallylammonium chloride, offering a broad spectrum of applications and easier polymerization. Thus, this monomer could be employed for the synthesis of copolymers through its combination with other monomers, perhaps serving as a cationic block within antimicrobial copolymers specifically designed for biomedical applications.

Chapter 6

Investigation of the Antimicrobial Activities of Quaternized Tröger's Base Polymers

6.1 Introduction

In our daily lives, we encounter a multitude of surfaces and objects like doorknobs, railings, buttons, faucets, and even the pages of a journal or a computer keyboard, that are inhabited by microorganisms. While most of these microorganisms are harmless, some can be pathogenic, causing the spread of infectious diseases – a famous historical disease in this context is leprosy. Remarkably, contaminated surfaces are responsible for more than 50% of all microbial infections [158]. Microbial reservoirs are established on contaminated surfaces, which in turn can facilitate the development of biofilm-related infections, indeed such infections may involve medical devices and implants, leading to potential health complications. Many hospital-acquired infections stem from contaminated surfaces and contribute to the spread of bacterial (and viral) diseases, which can cause significant outbreaks. Therefore, it becomes crucial to render such objects, especially in hospital settings, biocidal and effectively eliminate these invading microorganisms to enhance public health and safety [159]. The concept of developing surfaces capable of killing or repelling harmful microorganisms has been under investigation for many years.

It is widely accepted that the adhesion of bacteria to a surface is the primary step in the formation of bacterial biofilms. When bacteria adhere to a surface and subsequently

proliferate, they can form biofilms (often with other bacteria) that significantly enhance bacterial resistance to antibiotics and evade the host's defence systems, potentially leading to serious consequences such as systemic infections or device failures, [160]. Thus, the prevention of bacterial adhesion to surfaces has major importance.

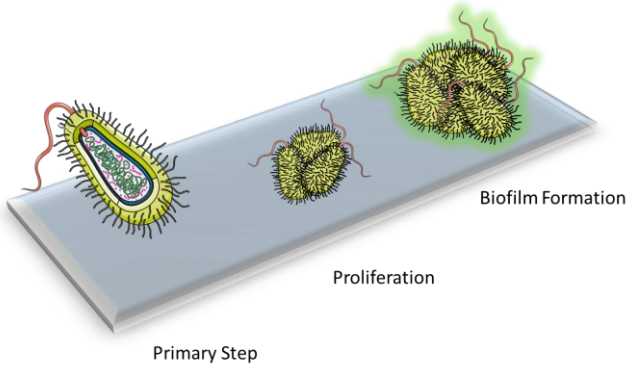

Figure 6.1. Figure of biofilm formation of bacteria on a surface.

Thus, polymers have been significantly investigated as antimicrobial surfaces over the recent decades with three major approaches, namely: (i) non-fouling, (ii) antibiotic release-based, and (iii) contact-killing strategies [158] (Figure 6.2).

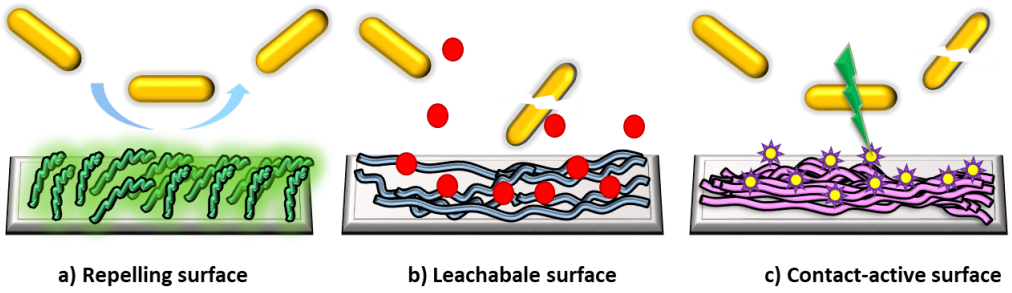

Figure 6.2. Various antibacterial surfaces. a) anti-adhesive surface that resists bacteria adhesion; b) surfaces leaching/releasing antimicrobial agents; c) contact-killing surfaces by bactericidal polymers.

In non-fouling strategies, anti-adhesive surfaces, or antifouling surfaces, have been developed that can either resist or prevent the adhesion of microorganisms. In general, coatings of hydrophilic polymers onto surfaces, either covalently or physically, have been widely applied to fabricate anti-adhesive surfaces. Hydrophilic or zwitterionic polymers form a tightly marshalled hydration layer that forms a physical barrier that results in the anti-adhesive properties of surface, this combination of a robust interfacial hydration layer and steric repulsion generates resistance to protein/bacterial binding [161–164]. One well-known hydrophilic polymer is polyethylene glycol - a gold standard material - that shows excellent antifouling properties and has been extensively used in the formation of anti-adhesive surfaces. Tang *et al.* [165] prepared a highly hydrophilic poly(dimethyl siloxane) silicone surface that had PEG brushes generated *via* surface-initiated reversible addition-fragmentation chain transfer chemistry with polyethylene glycol methacrylate. The anti-adhesive brush coated surfaces were tested with protein (albumin), bacteria (*S. aureus*) and lens epithelial cells and showed significantly decreased levels of protein, cell, and bacteria adhesion. Other hydrophilic polymers include polyacrylamide and 2-hydroxypropylacrylates that have groups that are both hydrogen donors and acceptors. Liu *et al*. [166] prepared polyacrylamide surfaces that showed antifouling properties towards proteins, cells and bacteria binding with old surfaces functionalized *via* surface-initiated atom transfer radical polymerization. If the polymer brush coatings were too thick, the polymer chains self-condensed (due to hydrogen bonding) leading to weakening of the hydration layer (allowing protein adsorption). In contrast less dense polymer brush coatings were not able to form a strong enough hydration layer to prevent protein adsorption. A polymer brush surface tested on two bacteria (*S.*

epidermidis and *P. aeruginosa)* showed a 97% decrease in bacterial attachment compared to the bare gold surfaces.

Besides neutral hydrophilic polymer brushes, zwitterionic polymer brushes have also shown antifouling properties. Zhao *et al.* [167] grafted novel poly(sulfobetaine vinyl imidazole) polymer brushes onto silicon surfaces *via* electrochemical surface-initiated atom transfer radical polymerization. To understand the antifouling effect of the imidazolium group of the polymer, poly(vinyl imidazole) brushes were grafted onto silicon as controls and showed inhibition of *N. maritima* (a marine alga) binding. Compared to poly(vinyl imidazole), poly(sulfobetaine vinyl imidazole) showed excellent inhibition of *E. coli* binding due to the imidazolium and sulfonate functional group of the polymer (forming a hydration layer resulting in decreased protein adsorption and hence bacteria, algae binding). Although these antifouling coatings can significantly diminish the attachment of bacteria to the surface over a specific duration, they lack the capability to eradicate the bacteria and prove ineffective in mitigating bacterial assault and establishment, ultimately resulting in biofouling [168]. On the other hand, antimicrobial agents, such as metallic particles or antibiotics, that are released from the polymeric coating in a concentrated manner within a specific region, are capable of effectively eliminating bacteria. Nevertheless, these coatings frequently encounter significant challenges and will promote bacterial resistance when the released drug doses fall below lethal levels [169].

In the contact-based strategy, bacteria can be eradicated upon contact with a non-leaching surface composed of polymers possessing inherent antimicrobial properties. In general, polymers with cationic groups such as quaternary ammonium or phosphonium groups are employed for designed surfaces in which bacteria can be killed on contact. In 1972, Squith [170]

introduced the concept of contact-active antibacterial surfaces by conducting an experiment to investigate whether an organosilicon-based quaternary ammonium compound would remain effective after being chemically attached to a surface. Cotton and glass surfaces coated with 3-(trimethoxysilyl)-propyldimethyloctadecyl ammonium chloride showed a notable reduction in the number of viable colonies on aerosol coated surfaces in comparison to uncoated surfaces. Endo [171] conducted research on surface-attached poly(phosphonium) salts. The surfaces with the highest phosphonium content were found to be most effective in eradicating *E. coli* and *S. aureus* bacteria due to an increase in charge density. However, since surface charge and coating thickness were not directly measured, this trend might also be attributed to more comprehensive surface coverage resulting from longer reaction times. Scanning electron microscopy images clearly showed the deformation of bacteria by these surfaces, suggesting potential damage to their membranes [171]. In 2002, Tiller *et al.* [172] found that alkyl pyridiniums could effectively kill bacteria *via* contact with covalently immobilized poly(4-vinyl-N-alkylpyridiniumbromide) testing on *S. aureus, S. epidermidis*, *E. coli* and *P. aeruginosa*. *N*-hexylated poly(4-vinylpyridine) showed a 99% reduction in both Gram-negative and Gram-positive bacteria.

Contact-active surfaces of antimicrobial polymers can be prepared using various immobilization techniques, generally categorized into two groups: chemical and physical methods. Chemical methods encompass processes like grafting, resulting in the creation of well-defined polymer structures and grafting densities. Physical methods involve the physical adsorption of water-insoluble and organo-soluble polymers on the surface [173] with methods of application including physical adsorption of the polymer onto the surface via simple

solution and dip coatings, cast-coating, spraying and spin coating techniques. Two oppositely charged polymers can be applied *via* Layer-by-Layer techniques [172].

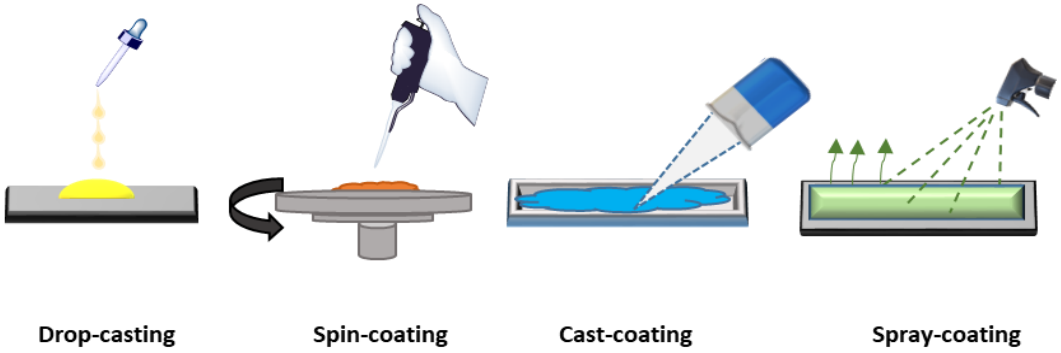

Figure 6.3. Representation of common physical methods to apply coatings of polymers onto surfaces**.**

6.2. Tröger's Base Polymer

2,8-Dimethyl-6H,12H-5,11-methanodibenzo[b,f][1,5]diazocine, known as Tröger's base (TB) , was originally isolated by Tröger in 1887 [174]. However, a comprehensive structural analysis was not carried out until 1935, by Spielman [175]. The structural findings were later confirmed through X-ray diffraction in 1986 [176]. Tröger's base is a well-known substance that possesses a unique property of having two stereogenic nitrogen atoms arranged in a V-shaped configuration. In general, enantiomers that contain stereogenic nitrogen centres are indistinguishable from each other due to their rapid interconversion at room temperature. However, Tröger's base rigid structure is an exception to this rule, owing to the presence of ring strain that prevents rapid inversion and thereby enables their distinguishability. The diastereomer R,S)-TB is not geometrically feasible, thus only the enantiomers R,R or S,S exist [177].

Tröger's base (TB) polymers, also commonly referred to as Tröger's base-containing polymers, represent a class of organic polymers that integrate Tröger's base into their polymer structure. There are two typical synthesis methods for Tröger's base polymers. In the first approach, commonly employed, the functional monomer containing the Tröger's base unit is initially prepared. Subsequently, polymerization takes place through condensation, utilizing activated groups like halogens and carboxylic acids, all the while maintaining the integrity of the Tröger's base structure [178,179]. Alternatively, Tröger's base polymers can be synthesized through a step-growth polymerization process, involving a simple reaction between an aromatic diamine monomer and dimethoxymethane in trifluoroacetic acid [180]. Owing to the unique packing arrangement of the contorted polymer chains, which includes the rigid V-shaped Tröger's base units, intrinsic microporosity is created. Indeed, because of their inherent microporosity and the presence of functionalizable tertiary amino groups, TB polymers have attracted substantial interest for a wide range of potential applications such as gas separation membranes [181], ion exchange membranes [182], supercapacitors [183], organic catalysis [184], sensing [185] etc. Tröger's base polymers also consistently display fascinating physical and chemical properties, thanks to their distinctive structural characteristics, making them versatile materials with diverse potential applications. In particular, there has been a growing interest in the use of TB polymers in the field of membrane technology. Li [186–188] conducted studies on ultrafiltration membranes made from TB polymers (see Figure 6.4) and investigated their antifouling properties. However, there has been no study in the literature that focuses on the antimicrobial properties of TB polymers.

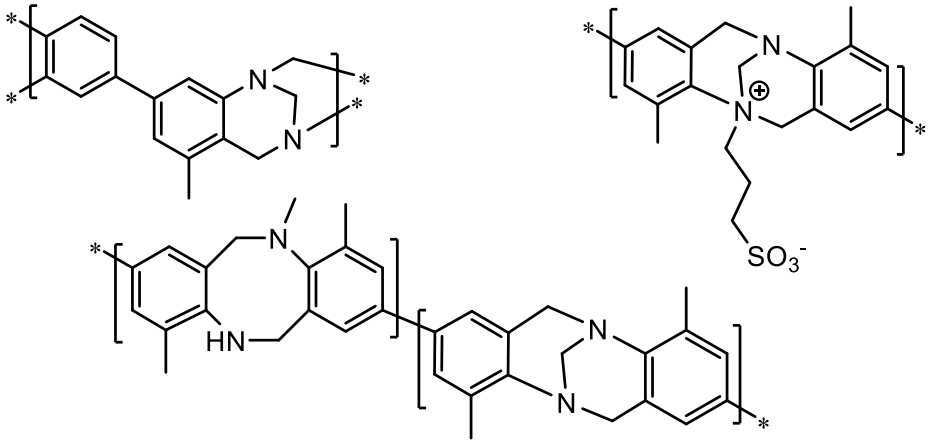

Figure 6.4. Tröger's base polymers that have been used for antifouling membranes[186–188].

6.3. Aim of This Chapter

In this chapter, the antimicrobial activities of a specific polymer (EA-TB) derived from Tröger's Base and ethanoanthracene (EA) and its quaternized derivatives were investigated as potential antimicrobial surface coatings. This polymer was from Prof. Neil McKeown and was synthesized by Dr. Richard Malpass-Evans.

6.4. Results and Discussion

6.4.1. Quaternization of Tröger's base Polymer with Alkyl Bromides/Iodide

Tröger's base polymer (EA-TB) and an excess (6 mol eq. based on the repeating unit) of alkyl bromides/iodides (methyl iodide, 1-bromobutane, 1-bromohexane, 1-bromooctane, 1-bromododecane or benzyl bromide) were stirred for 24 hours at room temperature to from the quaternized EA-TB polymers which were obtained in quantitative yields as dark brown to dark orange solids. Quaternized polymers, depending on the alkylating agents (methyl iodide, 1-bromobutane, 1-bromohexane, 1-bromooctane, 1-bromododecane or benzyl bromide) are coded here as EA-TB-1, EA-TB-4, EA-TB-6, EA-TB-8, EA-TB-12 and EA-TB-Bn.

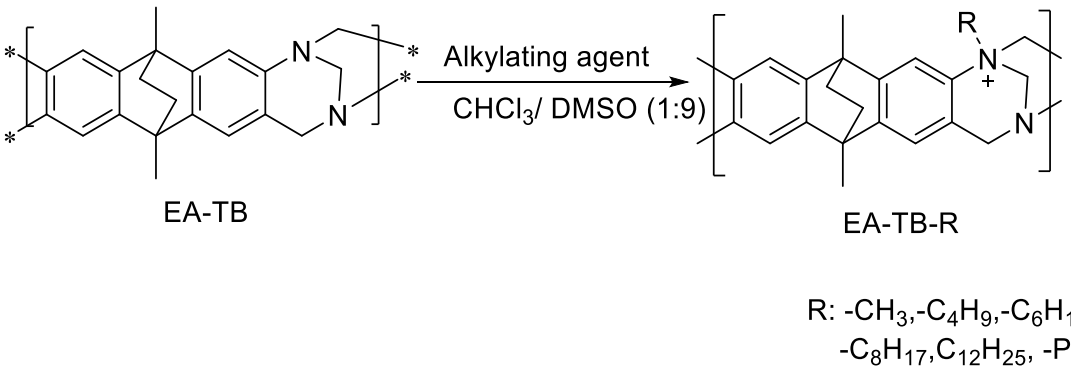

Figure 6.5. Quarterization reaction of EA-TB polymer with alkylating agents (methyl iodide, 1-bromobutane, 1-bromohexane, 1-bromooctane, 1-bromododecane or benzyl bromide) in DMSO/$CHCl_3$ at room temperature**.**

The first challenge was the solubilities of the quaternized EA-TB polymers. These were determined in various solvents, as in order to test their antimicrobial properties the polymer in question should be completely soluble in aqueous solutions (for solution-based assays) or insoluble in aqueous solutions (for polymeric coated surfaces for antimicrobial contact-killing surfaces).

Evaluation showed that the quaternized EA-TB polymers (0.1 mg/mL), were only soluble in dimethyl sulfoxide and hexafluoroisopropanol (HFIP) while dichloromethane and chloroform dissolved the non-quaternized EA-TB polymers. The quaternized EA-TB polymers were insoluble in water, thus their application as surface coatings became an attractive option for evaluating their antimicrobial properties.

Table 6.1. Solubility of Quaternized EA-TB Polymers (0.1 mg/mL) in Various Solvents

POLYMER	HOAc	Acetone	DCM	DMF	THF	H_2O	$CHCl_3$	DMSO	HFIP	Ethanol
EA-TB	+	-	++	-	-	-	++	-	-	-
EA-TB-1	-	-	-	-	-	-	-	++	++	-
EA-TB-4	-	-	-	-	-	-	-	++	++	-
EA-TB-6	-	-	-	-	-	-	-	++	++	-
EA-TB-8	-	-	-	-	-	-	-	++	++	-
EA-TB-12	+	-	-	-	-	-	-	++	++	-
EA-TB-Bn	-	-	-	-	-	-	-	++	++	-

(-) insoluble, (+) partially-soluble, (++) soluble

6.4.2. Optimization of Quaternized Polymers Coating

To coat the polymers onto glass surfaces, drop-casting was initially tried. Quaternized polymers all dissolved in HFIP while non-quaternized polymers dissolved in chloroform. A silicone mask was placed onto the glass surface and polymer solutions (15 µL) were deposited onto the wells and left to evaporate at room temperature. However, due to the high volatility of the solvent, “coffee ring” effects were observed following deposition onto the patterned glass slide surface.

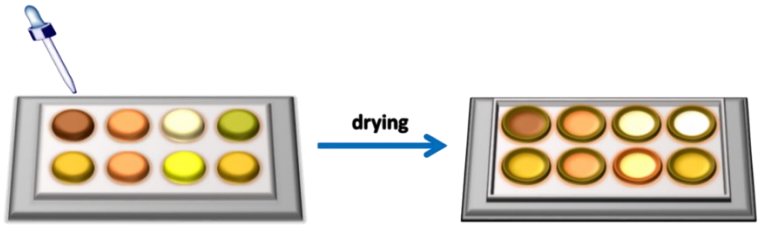

Figure 6.6. Drop-coasting of EA-TB modified polymers (left) and the “coffee ring” effect of polymer coated onto the glass slide after drying (right).

The properties of material surfaces, such as surface charge, morphology, and wetness, are interconnected and have a significant impact on bacterial adhesion. In addition, irregular surfaces promote bacterial adhesion and biofilm formation, while smooth surfaces discourage these processes [189]. For this reason, a uniform surface coating was desired. A method for producing high-quality polymer thin films on a surface is spin coating and this was thus employed. This involves depositing a small amount of coating material onto the center of a substrate, which is spun at a specific speed to evenly distribute the coating material through the action of centrifugal force[190].

Depending on the solubility of the polymers (see Table 6.1) EA-TB-X (X=1, 4, 6, 8, 12 or Bn) and EA-TB polymers (5% w/v) were dissolved in either HFIP or $CHCl_3$ for surface coating. Oxygen plasma cleaned surfaces (glass coverslips) were coated with polymers *via* spin coating However, due to the volatility of the solvent, obtaining uniform coating was challenging. As seen clearly in Figure 6.7, a hole in middle of the film was formed with the first method tried (2000 rpm, 30 sec, 100 µL polymer solution (5% w/v dissolved in HFIP for EA-TB-1 or $CHCl_3$ for EA-TB). Thus, to optimize spin coating uniformity, two solvents, composed of a solvent evaporating rapidly (HFIP) and slowly (1-butanol) were mixed (1:1 ratio) and used to dissolve the polymers. However, the formation of a hole in the coating still remained. A new, two stage method) was applied to remove edge effects and obtain a uniform coating. Thus, the coating process used 2000 rpm (for 4 sec) to allow surface coverage. The slide was then spun at 2000 rpm for 7 sec while drying under nitrogen, then slowly decreasing the coating speed from 2000 rpm to 800 rpm over 30 sec, and then-increasing to 2000 rpm for 3 sec (Figure 6.7). Using this method, sufficient time was provided for the majority of polymer coverage to dry over the substrate in the first step (due to the volatility of HFIP) and then in the second step

decreasing rotational speed allowed drying of the polymer on the substrate, removing the remaining 1-butanol. The final rotation (2000 rpm) prevented formation of the raised edges- This method allowed uniform coating of the quaternized polymers on the glass coverslips. However, the coating of non-quaternized polymers could not be obtained despite the many attempts/approaches, and this might be related to the intrinsic ability of the polymer to form porous films.

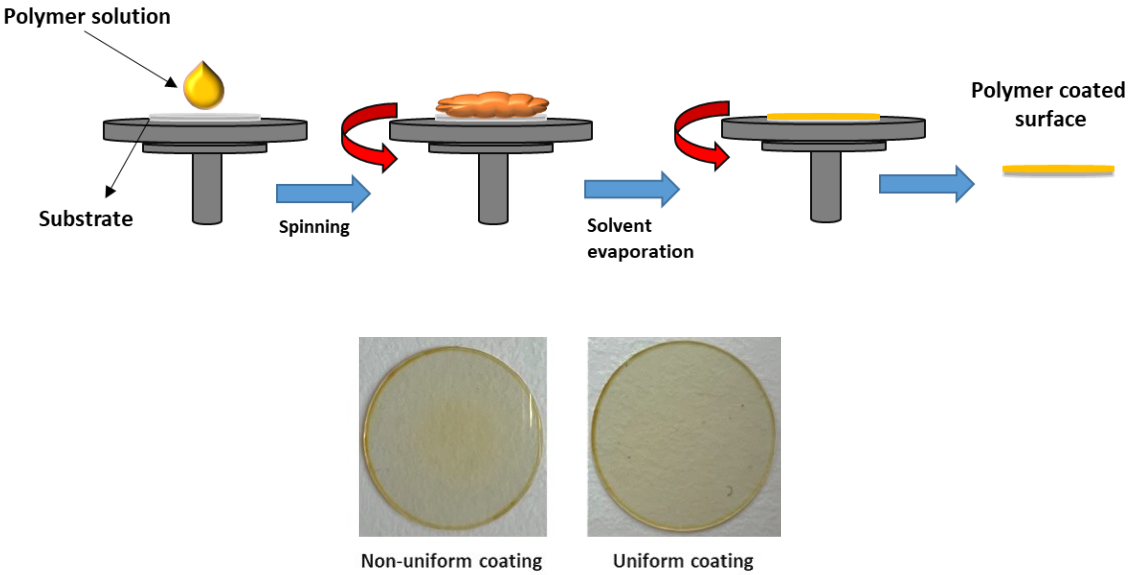

Figure 6.7. Illustration of the spin coating technique. Lower: Non-uniform coating and uniform-coating of EA-TB-1 (5% w/v in HFIP/1-butanol mixture).

After successful coating the quaternized polymers onto the glass coverslips, the stability of the coating was checked by incubating in PBS for 24 hours at 37^{o}C. However, the coatings all lifted up from the surface indeed, some polymers coatings were removed as free-standing films while some coatings fragmented to give small pieces (see Figure 6.8).

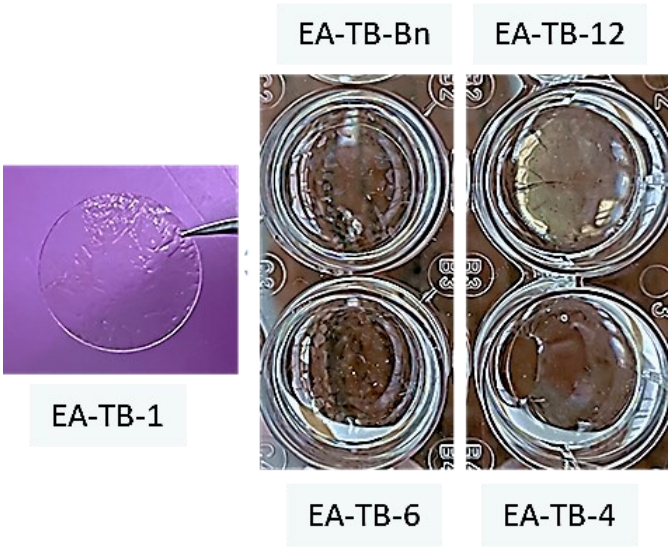

Figure 6.8. Surface coating stability tests of the quaternized polymer coated coverslips immersed in PBS for 24 hours at 37°C. (EA-TB-1, EA-TB-Bn, EA-TB-4 and EA-TB-12 shown as examples).

The unstable polymeric coatings obtained could be related to the nature of the interactions between the deposited polymer chains and the glass surface. The polymers primarily consist of hydrophobic units rather than hydrophilic ones, however, the interactions between the hydroxyl groups on the glass surface formed after oxygen plasma treatment could be electrostatic in nature which can be disturbed by an aqueous environment. Therefore, coverslips made from polyvinyl chloride or coated with polyolefins or tissue growth coverslips- that were polyethylene terephthalate, glycol-modified) were used to improve adhesion of polymers onto surfaces. However, all these coverslips dissolved in HFIP and as a result, all experiments had to be carried out using glass coverslips.

The instability observed in the polymer coatings could be linked to the huge molecular weight distribution of the quaternerized polymers (Mn:2 kDa and Mw:121 kDa). It is possible that the smaller polymeric chains, when alkylated contribute to surface coating instability, by

dissolving in aqueous environment. Thus, a dialysis process was performed in chloroform (cut off 15 kDa) for 3 days to get rid of small molecular weight polymer chains.

In addition, the alkylation ratio of the polymers may be a critical factor contributing to the instability of the polymer coating on the glass surface (see Figure 6.8 unstable surface coating of the polymers quaternized with excess alkylating agents (6 mole eq. based on the repeating unit). Thus, the polymer (EA-TB) was quaternized with two different ratios (1 mole eq. or 3 mole eq. based on the repeating unit) of methyl iodide, benzyl bromide or 1 bromohexane. The synthesized six quaternized polymers (coded as EA-TB-1.1, EA-TB-1.3, EA-TB-Bn.1, EA-TB-Bn.3, EA-TB-6.1 and EA-TB-6.3) were dialysed before coating onto glass coverslips. Coating process was again carried out with the polymer solutions (5% w/v in HFIP/1-butanol mixture) *via* spin coating. Later, the stability of coated surfaces in PBS solution for 24 hours at 37°C was observed. Among the surfaces, methyl iodide quaternized polymers surfaces were stable whereas benzyl bromide and 1-bromohexane quaternized polymers again lifted from the coverslips (Figure 6.9). Thus, methyl iodide quaternized polymers (EA-TB-1.1 and EA-TB-1.3) were used in further experiments.

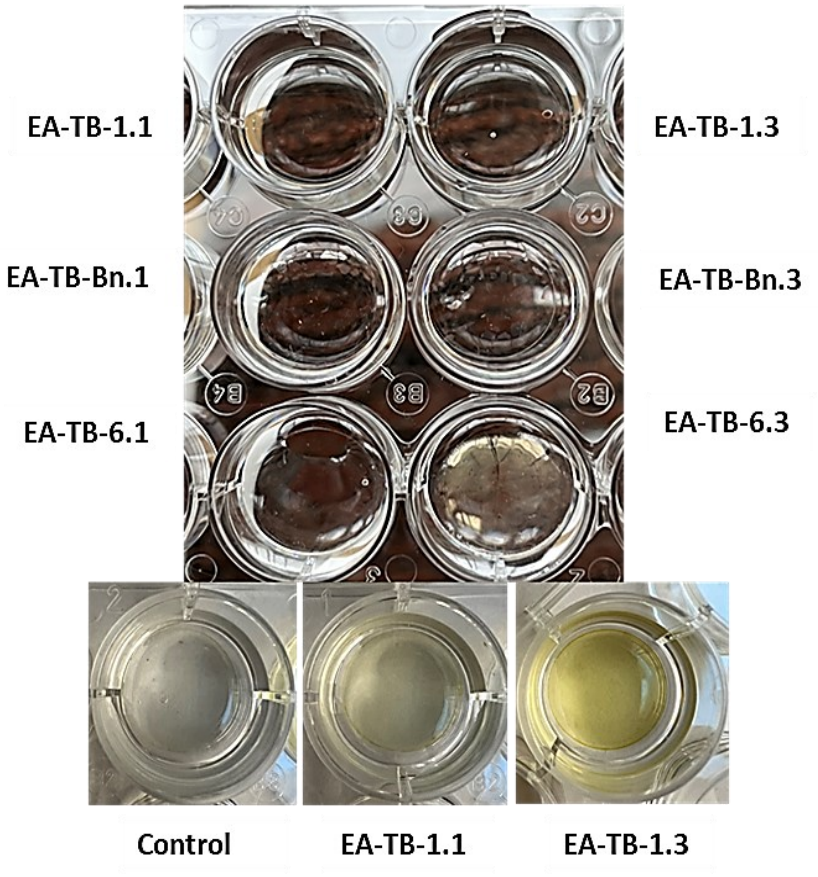

Figure 6.9. Images of glass coverslips (19 mm) coated with EA-TB-1.1, EA-TB-1.3 EA-TB-Bn.1, EA-TB-Bn.3, EA-TB-6.1 and EA-TB-6.3 polymers prepared *via* quaternization of the polymer with alklybromides or methyl iodide when immersed in 2 mL PBS and left for 24 hours in 37°C. Methyl iodide quaternized polymers (EA-TB-1.1 and EA-TB-1.3) remained stable on the surface while benzyl bromide and 1-bromohexane quaternized polymers lifted into solution from the surface.

6.4.3. Characterization of the Surfaces Coated with Methyl Iodide Quaternized EA-TB Polymers

The uniform EA-TB-1.1 and EA-TB-1.3 coating onto glass coverslips were confirmed by SEM. The thickness of the polymer coatings compared to bare glass coverslip were measured as approximately 20 µm by cross-sectional SEM (Figure 6.10).

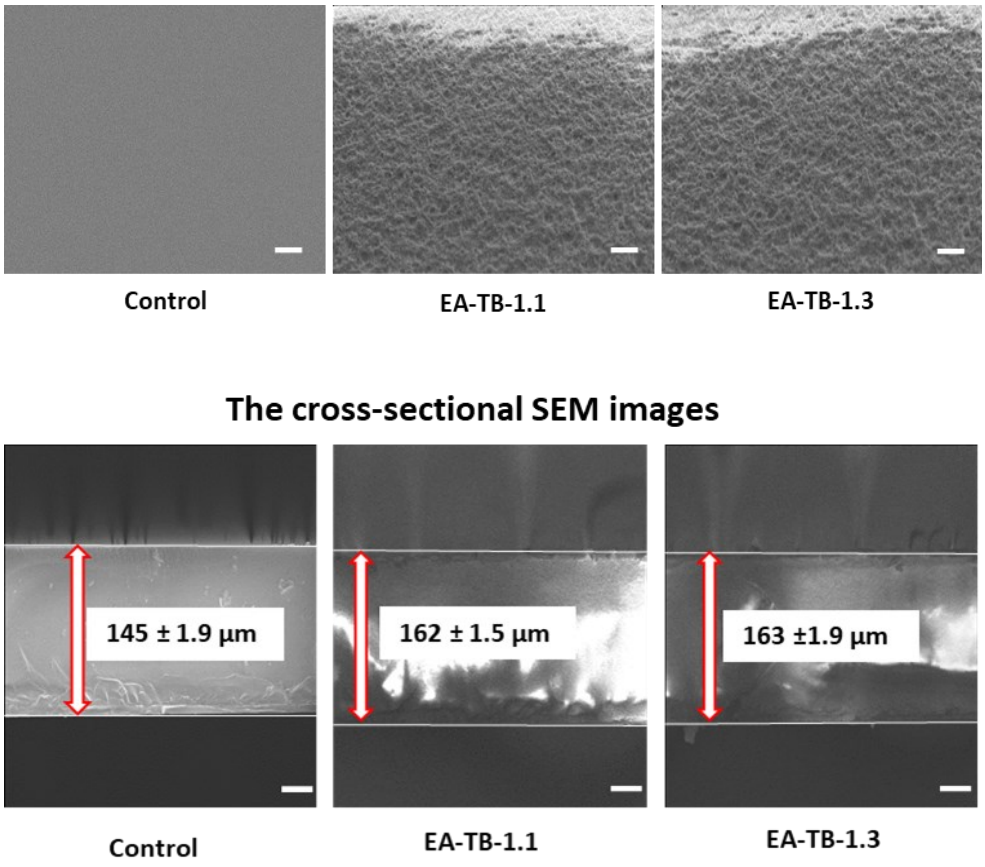

Figure 6.10. The SEM images of EA-TB-1.1 and EA-TB-1.3 coated coverslips and bare glass coverslip (control) (scale bar: 1 µm). The cross-sectional SEM images of EA-TB-1.1 and EA-TB-1.3 coated coverslips (polymer coating and coverslip measured in total) and pristine glass coverslip. The average measurements were calculated based on the measurements of three samples for each.

The wettability of the surface changed significantly after polymer coating with the water contact angle of the pristine substrate (uncoated glass coverslip) and polymer coated substrates shown in Figure 6.11. After polymer coating, the contact angle of uncoated glass (59°) increased to 82° when coated with EA-TB-1.1 and 74° when coated with EA-TB-1.3. The difference in the contact angles of the polymer explained by the different aternization ratios for the polymers, which increases their hydrophilicity as presumably the non-quaternerized amine is protonated.

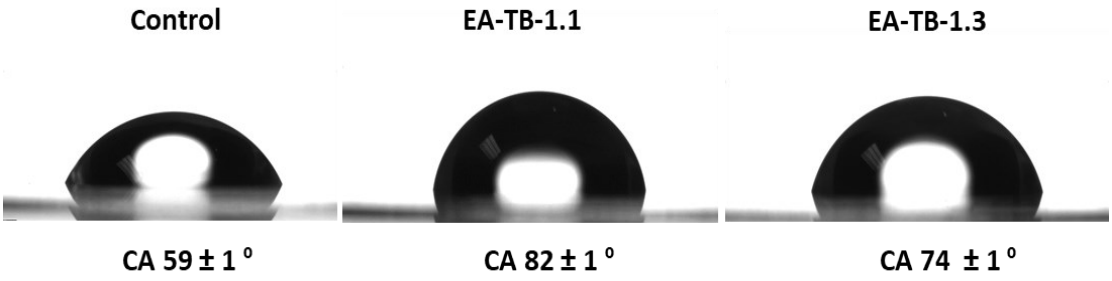

Figure 6.11. The water contact angle measurements performed on the glass coverslips coated with the polymers EA-TB-1.1 and EA-TB-1.3. The control was an oxygen plasma treated glass coverslip.

6.4.4. Antimicrobial Activity of the Methyl Iodide Quaternized EA-TB Polymer Coated Surface

A Live-Dead assay was performed to reveal bacterial viability and population after contacting the polymer coating. The green fluorescent stain (SYTO 9) stains bacteria, whereas the red fluorescent stain (PI) only infiltrates into bacteria that have a compromised membrane. As

clearly seen in Figure 6.12, there were a few dead bacteria seen on the both polymers coated surfaces after incubation for 6 hours, but this was very limited (< 20%).

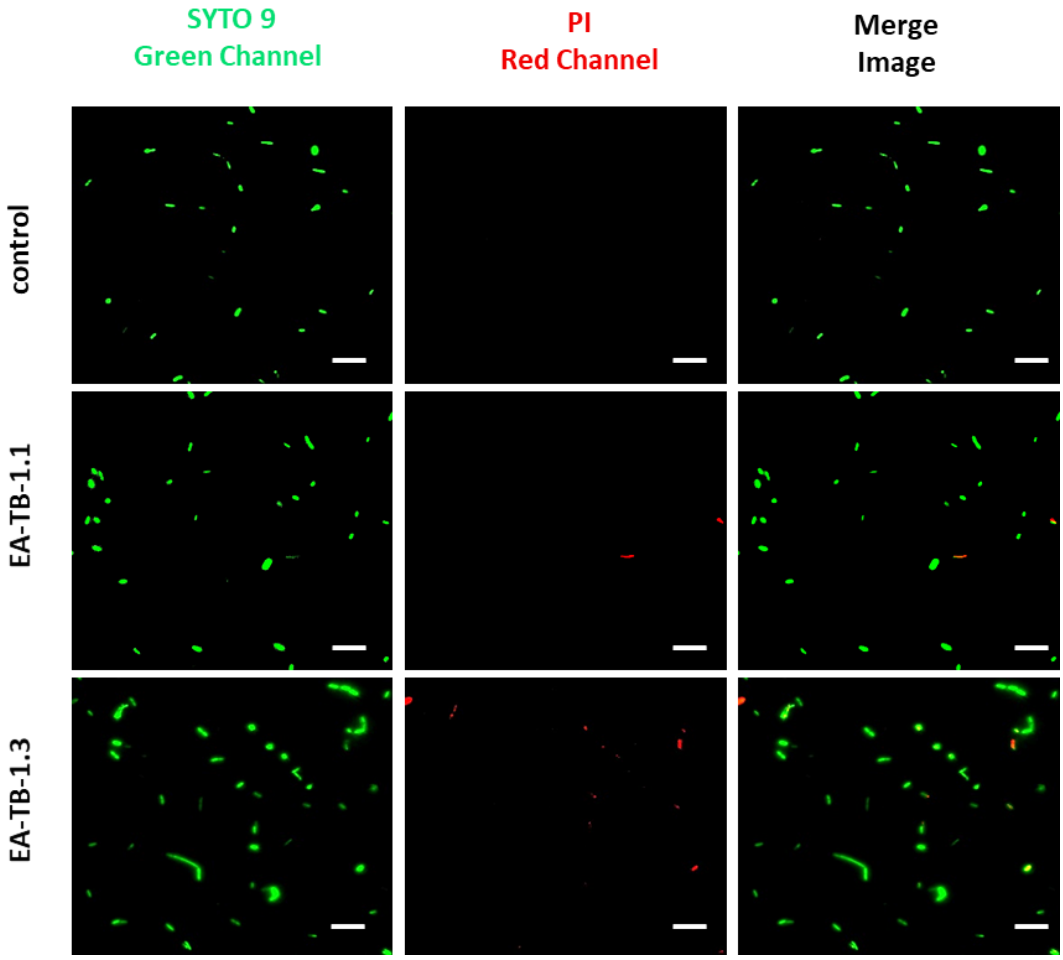

Figure 6.12. Fluorescent microscope images of *E. coli* on the coated surfaces after incubation for 4 h. The control was a glass coverslip. Red indicates dead bacteria and green live bacteria (-Scale: 20 µm).

The antimicrobial activity of the polymer coatings was assessed using the standard plate count method. Thus polymer-coated surfaces were inoculated with *E. coli* for 4 hours, non-adhering bacteria were removed and the adhered bacteria on coverslips were resuspended in growing media and serially diluted and plated for colony counts. However, there was no

decrease in the number of attached bacteria compared to the control (uncoated coverslip) see Figure 6.13). In general, to define a surface as antimicrobial, a 2 or 3-log reduction in the viable bacteria would be expected [191]. Thus, the methyl iodide quaternized EA-TB polymers coated surfaces did not show any antimicrobial activity. The inefficient antimicrobial activity of the polymer coated surfaces may be associated with the positioning of the quaternary ammonium group within the polymer chains on the surface coatings, as the polymer chains exhibit limited degrees of freedoms compared to classic quaternary ammonium groups on polymers (see earlier chapters). Similarly, the polymer proved not to be hemolytic (Figure 6.14).

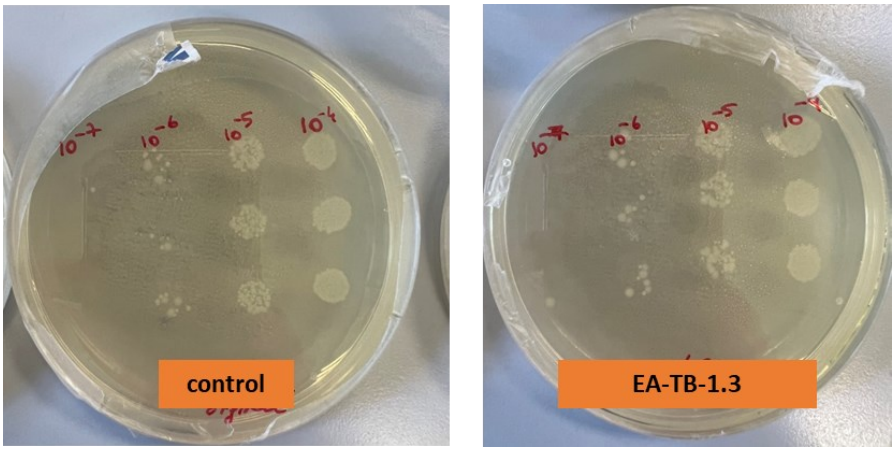

Figure 6.13. Images of bacterial colonies of *E. coli* after incubation on polymer coated glass coverslips. The bacteria that adhered on the coverslips were resuspended and serially diluted and plated on agar plate.

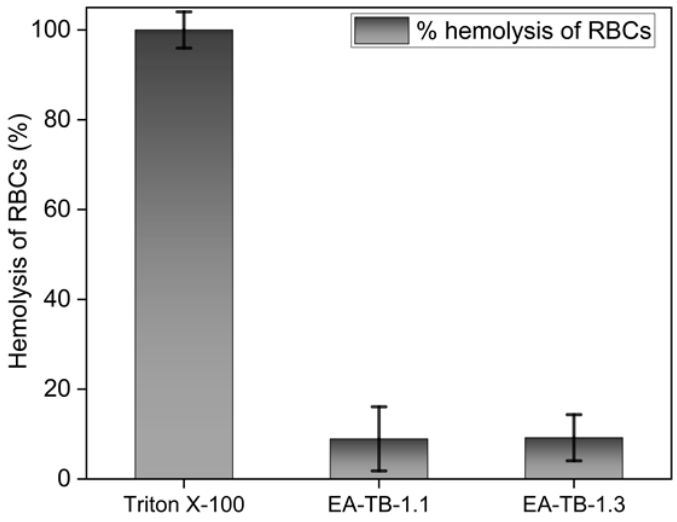

Figure 6.14. Hemolysis activity of the quaternized EA-TB polymer coatings towards defibrinated sheep blood. The percentage of leaked hemoglobin (% hemolysis) was measured relative to a positive control (Triton X-100 (1% v/v) defined as giving 100% lysis of red blood cells). The error bars are standard deviation of the mean (n = 3).

6.5. Conclusion and Future Work

In conclusion, this project aimed to quaternize a specific Tröger's base polymer (EA-TB) with various alkylbromides or methyl iodide for potential use as a novel antimicrobial surface coating. Despite encountering challenges related to solubility and stability of quaternized EA-TB polymers, optimization efforts led to the successful formation of stable coatings on glass surfaces using a limited number of polymers (methyl iodide quaternized EA-TBs). However, these coatings demonstrated no antimicrobial activity against *E. coli* bacteria.

Moving forward, future research should focus on exploring alternative Tröger's base polymers and investigating the feasibility of blending quaternized EA-TB with other polymers to develop more robust coatings capable of adhering to a wider range of surfaces, including plastics commonly found in medical devices like catheters. These endeavors hold promise for advancing the development of effective antimicrobial coatings for various applications.

Chapter 7

Conclusion and Future Outlook

In this thesis, a focused library of homopolymers derived from five distinct monomers having quaternary ammonium groups were successfully synthesized, each approximately around 20 kDa in size, utilizing RAFT polymerization. Subsequent evaluation of the antimicrobial efficacy of these polymers against both Gram-positive and Gram-negative bacteria prompted a focused examination on three selected polymers (PDADMAC, PVMBT, and PMETACl) and unveiled an association between molecular weight and antimicrobial efficacy. The results of antibacterial susceptibility tests and cell viability assays showed a clear correlation between the MIC values and cytotoxicity, and the average molecular weight of the polymer chain. Polymers with higher molecular weights (40 kDa) showed a positive correlation with increased antimicrobial activity against bacterial strains, as confirmed by dye-based assays and SEM imaging. However, this enhancement in molecular weight also corresponded to elevated toxicity towards mammalian cells, underscoring a delicate balance between efficacy and safety. PDADMAC-20 (20 kDa) exhibited the most potent antibacterial activity (MICs 4-32 mg/mL) for *M. smeagmatis*, Gram-postive and Gram-negative bacteria, while PMETACl-40 (40 kDa) (MICs 8-64 mg/mL) emerged as the preferred option for biomedical applications due to its low mammalian cell toxicity. Analysis conducted on fungal strains revealed varying antifungal effects. PDADMACs, PVMBTs and PMETACls showed a fungistatic mechanism of action against *C. albicans*, *C. auris* and *M. furfur*, while PDADMAC-40 and PDADMAC-20 displayed fungicidal activity against *M. furfur* and led to a 1.5-log reduction in fungal containing biofilms.

A new methacrylamide monomer containing a pyrrolidinium side-group ((*R*)-( ) pyrrolidin-3-yl) methacrylamide) was successfully synthesized. The homopolymers of this monomer with three different molecular weights (10 kDa, 20 kDa and 40 kDa) were synthesized through free radical polymerization and the antibacterial properties of them were evaluated against both Gram-negative and Gram-positive bacteria. The results showed that as the molecular weight of the homopolymers increased, their antimicrobial efficacy also increased, which was confirmed by dye-based assays and SEM imaging. It is worth noting that these newly methacrylamide homopolymers were highly effective against Gram-positive bacteria.

In the last project, the development of antimicrobial surface coatings from quaternized Tröger's base polymer (EA-TB) with various alkylbromides or methyl iodide was studied. There were challenges in solubility and stability of polymers of the resulting coatings, but the methyl iodide quaternized EA-TBs, remained stable on the surface, but showed no antimicrobial activity against Gram-negative bacteria (*E. coli)*.

In the future, the scope of antimicrobial effectiveness of the homopolymers could be expanded and tested against clinically isolated microorganisms and multidrug-resistant strains to ascertain their safety for diverse biological applications. Additionally, exploring their potential against bacterial biofilms holds promise. Investigating the potential cytotoxic effects of homopolymers on different cell types, including those of the skin, could lead to their use in cosmetics. These efforts have the potential to broaden the range of practical applications for these antimicrobial polymers.

The synthesized novel monomer presents an appealing alternative to diallylammonium chloride, boasting a wide array of applications and facilitating an easier, more controlable polymerization. Consequently, its utilization in copolymer synthesis, in conjunction with other monomers, holds promise, potentially serving as a cationic block within antimicrobial copolymers tailored specifically for biomedical applications.

To enhance the stability of quaternized Tröger's base polymer on the surface and develop a new antimicrobial coating, blending it with another polymer such as poly(lactic acid) or polystyrene could be explored.

Chapter 8

Experimental

8.1. Materials

All monomers, sodium hydroxide (pellets), and common chemical reagents: 2,2-azobis(2-methylpropionamidine)dihydrochloride (AAPH, 97%), potassium ethyl xanthogenate (96%), bromoacetic acid (97%), 4,4'-azobis(4-cyanopentanoic acid) (ACVA), 4-cyano-4-[(dodecylsulfanylthiocarbonyl)sulfanyl]pentanoic acid (CTA1), 4-cyano-4-(phenylcarbonothioylthio)pentanoic acid (CTA2), anhydrous acetonitrile, ethanol, acetone, hexane, deuterated solvents (D_2O, $CDCl_3$) were purchased from Sigma Aldrich, Fluorochem, Fisher Scientific or Alfa Easer and used as received unless otherwise noted. Except for diallyldimethylammonium chloride (65% wt. in H_2O), all monomers were passed through a basic alumina column to remove inhibitors before polymerization reactions. Chain transfer agent, *S*-Ethoxythiocarbonyl mercaptoacetic acid (CTA3) was synthesized according to the literature [65]. Deionized (DI) water was from a Milli-Q system. Dulbecco's Modified Eagle Medium (DMEM), Opti-MEM (OMEM), 0.25% trypsin−EDTA, fetal bovine serum (FBS), and streptomycin (5000 µg/mL)/penicillin (5000 U/mL) were obtained from ThermoFisher Scientific, UK. 3-[4,5-Dimethylthiazol-2-yl]-2,5 diphenyltetrazolium bromide was purchased from Alfa Easer. Phosphate buffer solution (PBS) were prepared from PBS tablets (Oxoid Ltd, ThermoFisher Scientific, UK). Sheep blood defibrinated (SB054-100 Ml) was provided from TCS Biosciences. Live/Dead™ *Bac*Light™ Bacterial Viability Kit, for microscopy was purchased from Sigma-Aldrich. Calcein-AM was purchased from Sigma-Aldrich. 1-N-phenyl-

naphthylamine (98%) were purchased from Thermo Scientific Acros. *Escherichia coli* (DH5α Competent Cells- catalog number 18265017), *Salmonella typhimurium* SLI344, *Micrococcus luteus* (ATCC 4698) and *Bacillus subtilis* (ATCC 6051) were used as Gram-positive and Gram-negative test strains. Microbial culture broths and agar medium (Invitrogen, UK, Fisher Scientific UK and Merck, UK), buffers and water were sterilized by autoclaving before use. Polymers were filter-sterilized (0.22 µ, Millipore Inc, USA) before use.

8.2. Methods

8.2.1. Synthesis of the Homopolymers *via* Reversible Addition Fragmentation Polymerization

Monomers were subjected to free radical polymerization to determine reaction conditions and understand the compatibility of monomer, initiator, and solvent. Subsequently, all monomers were subjected to RAFT polymerization with a suitable chain transfer agent under the same conditions. During the polymerization reactions, aliquots were taken to follow monomer conversion (by ^{1}H NMR spectroscopy in D_2O or $CDCl_3$). Experimental molecular weights of the polymers were calculated based on the integration of the disappearing of the vinyl protons of the responsible monomer and appearance of the methylene peak of the generated polymer in the ^{1}H NMR, while the theoretical molecular weights were calculated based on the formula below, where $[M]_0$, $[CTA]_0$ are the initial concentrations of monomer, chain transfer agent; *p* is the monomer conversion, and Mw_M and Mw_{CTA} are the molar masses of the monomer and chain transfer agent, respectively.

$$\mathbf{M_{n,th}} = \left(\frac{[\mathbf{M}]_0 \, \boldsymbol{p} \, \mathbf{Mw_M}}{[\mathbf{CTA}]_0}\right) + \mathbf{Mw_{CTA}}$$

The monomer DADMAC was polymerized using the initiator, 2,2'-azobis(2-methylpropionamidine) dihydrochloride (AAPH) and the xanthate-type chain transfer agent, *S*-Ethoxythiocarbonyl mercaptoacetic acid (CTA3) at 60°C. The other monomers were polymerized using the initiator, 4-azobis(4-cyanovaleric acid) (ACVA), and either 4-cyano-4-(phenylcarbonothioylthio) pentanoic acid (CTA2) or 4-cyano-4-[(dodecyl sulfanyl thiocarbonyl)sulfanyl]pentanoic acid) (CTA1) at 70°C as the chain transfer agents. In order to synthesize the desired different molecular weights of the polymers (PDADMAC, PMETACl and PVMBT), the chain transfer and initiator concentrations in the reaction were tuned while monomer concentrations were kept constant.

RAFT Polymerization of Poly(2-(dimethylamino)ethyl methacrylate)

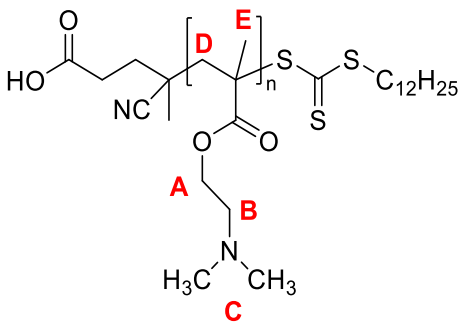

2-(Dimethylamino)ethyl methacrylate (5 mL), radical initiator, 4,4'-azobis(4-cyanopentanoic acid) (ACVA), (0.0084 g), chain transfer agent CTA2 (0.0726 g) and ethanol (10 mL) were mixed in a microwave tube. The solution was degassed by argon bubbling for 30 minutes. The polymerization was carried out at 70°C for 24 hours. The polymer was purified by removal of the ethanol, redissolution in THF, and precipitated using hexane. The polymer was dried under vacuum at 40°C for 2 days to give a yellow-coloured polymer.

^{1}H NMR (500 MHz, $CDCl_3$) δ_H (ppm) 4.06 (s, br, (**A**), -CH_2-O), 2.56 (s, br, (**B**),-CH_2-N), 2.34-2.25 (s, br, (**C**), -N-$(CH_3)_2$, 2.0-1.85 (m, br, (**D**), -CH_2-CH_3), 0.88 (m, br, (**E**) -C-CH_3).

RAFT Polymerization of Poly([2-(methacryloyloxy)ethyl]trimethylammonium chloride)

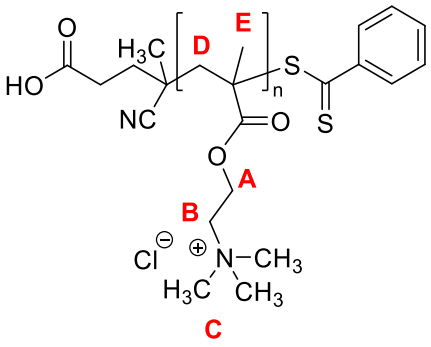

[2-(Methacryloyloxy)ethyl]trimethylammonium chloride) (6 g, 75% wt in H_2O), initiator, 4,4-azobis (4-cyanovaleric acid (8 mg), chain transfer agent CTA1 (40 mg) and water (17.9 mL) were mixed in a 50 mL round bottom flask and the reaction solution was purged with nitrogen for 30 mins. The polymerization reaction was carried out at 70^{o}C for 24 hours. Aliquots were taken at different time intervals to check monomer to polymer conversion by ^{1}H NMR analysis. The resulting polymer was purified by precipitation using acetone, redissolving in methanol and again precipitated using acetone, and dried under vacuum at 40^{o}C to give a salmon-coloured polymer. This polymer was synthesized in three different molecular weights (10 kDa,20 kDa and 40 kDa) by changing the $[CTA1]_0/[I]_0$ ratio.

^{1}H NMR (500 MHz, D_2O) δ_H (ppm) 4.34 (s, br, (**A**), -CH_2-O), 3.86 (s, br, (**B**), -CH_2-N), 2.34-2.25 (s, b, (**C**), -N-$(CH_3)_2$), 2.35-1.98 (m, br, (**D**), -CH_2-CH_3), 0.88 (m, br, (**E**) –C-CH_3).

RAFT Polymerization of Poly[3-(methacryloylamino)propyl]trimethylammonium chloride

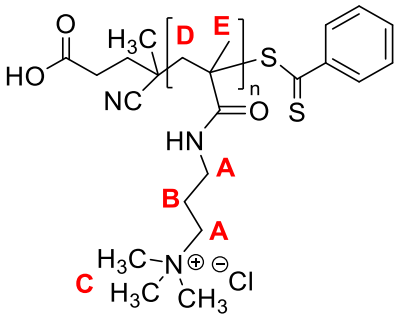

[3-(Methacryloylamino)propyl]trimethylammonium chloride (13 g 50% wt in H_2O), initiator, 4,4-azobis(4-cyanovaleric acid (8 mg), CTA1 (40 mg) and water (17.5 mL) were mixed in a 100 mL round bottom flask and the reaction solution was purged with nitrogen for 30 min. It was then placed into a preheated oil bath at 70°C for 24 hours. The resulting polymer was purified by precipitation with excess acetone, redissolved in methanol and precipitated with acetone, and dried under vacuum at 40°C.

^{1}H NMR (500 MHz, D_2O) δ_H (ppm) 3.37-331 (s, br, (**A**), -CH_2-N), 3.25 (s, br, (**C**), -N^+-$(CH_3)_3$-), 2.25 (s, br, (**B**), -CH_2-), 2.05-1.65 (m, br, (**D**), CH_3), 1.20-0.88 (m, br, (**E**) –C-CH_3).

RAFT Polymerization of Poly(vinylbenzyl trimethylammonium chloride)

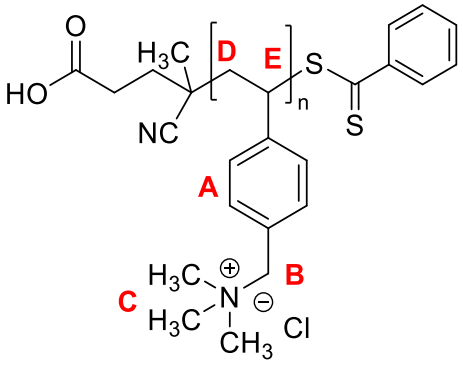

Monomer (4 g), 4,4-azobis(4-cyanovaleric acid) (ACVA) as initiator (7.84 mg), CTA1 (28 mg) and water (25 mL) were mixed in a 50 mL Schlenk flask and purged with nitrogen for 30 min. The polymerization reaction was carried out at 70°C for 24 hours. The resulting polymer was purified by precipitation using THF and dried under vacuum at 40°C. This polymer was synthesized in three different molecular weights (10 kDa,20 kDa and 40 kDa) by changing the $[CTA1]_0/[I]_0$ ratio.

^{1}H NMR (500 MHz, D_2O) δ_H (ppm) 7.5-6.5 (m, br, (**A**), -CH_2-N), 4.35 (s, br, (**B**), -CH_2-N-), 3.0 (s, br, (**C**), -N^+-$(CH_3)_3$-), 2.05-0.88 (br, (**D, E**), -CH_2-CH_2-).

RAFT Polymerization of Poly(diallydimethyl ammonium chloride)

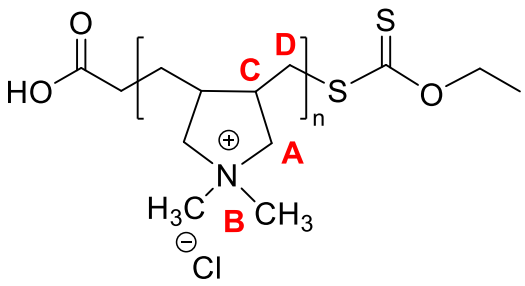

Polymerization of diallyldimethyl ammonium chloride was carried out by the protocol of Demarteau [85]. Diallyldimethyl ammonium chloride (10 mL, 65% wt in H_2O), initiator 2,2'-azobis(2-methylpropionamidine)dihydrochloride (AAPH) (0.019 g), CTA3 (0.041 g), and water (8 mL) were mixed in a 50 mL Schlenk tube. Then, the reaction mixture was degassed by bubbling with argon for 30 min and placed in preheated oil bath at 60°C for 24 hours. The resulting polymer was precipitated in a mixture of acetone/ethanol (1:1) three times and dried under vacuum at 40°C. This polymer was synthesized in three different molecular weights (10 kDa,20 kDa and 40 kDa) by changing the $[CTA1]_0/[I]_0$ ratio.

^{1}H NMR (500 MHz, D_2O) δ_H (ppm) 4.0-3.8(m, b, (**A**), -CH_2-N), 3.4-3.2 (m, b, (**B**), -N^{+}-$(CH_3)_2$-), 2.8 (s, b, (**C**), -N-CH-CH_2-), 1.6-1.2 (b, (**D**), -CH-CH_2-CH_2-).

8.2.2. Synthesis of Chain Transfer Agents

3-benzylsulfanylthiocarbonylsufanyl propionic acid

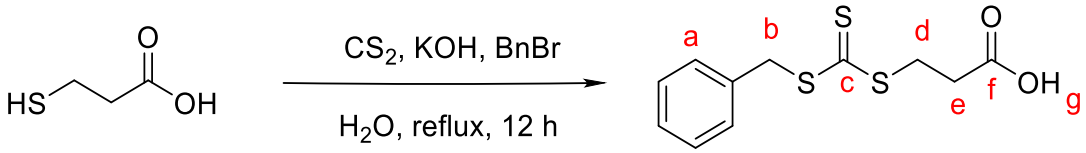

3-benzylsulfanylthiocarbonylsufanyl propionic acid was synthesized by following a published protocol [192]. 3-Mercaptopropionic acid (2 mL, 0.23 mmol) was added dropwise to a solution of KOH (2.6 g, 0.48 mmol dissolved in 25 mL water). Then, CS_2 (3 mL, 0.31 mmol) was added to mixture with stirring for 5 h to form an orange solution. After that, benzyl bromide (3.96g, 0.23 mmol) was added to the mixture and the reaction was stirred for 12 h reflux at 80ºC. After cooling, chloroform was added, and the reaction was acidified with concentrated hydrochloric acid until the organic layer was yellow. The water phase was extracted twice, and the organic layer was washed with saturated sodium chloride solution and with water (2x50 mL). The organic layer was dried over sodium sulphate and purified with column chromatography with 3:1 n-hexane and ethyl acetate.

^{1}H NMR (500 MHz- $CDCl_3$) δ_H (ppm) 10.38 (s, 1H (**g**)-OH), 7.39 – 7.29 (m, 5H, (**a**) Ph), 4.65 (s, 2H, (**b**) CH_2-Ph), 3.65 (t, 2H, (**d**) CH_2-S, J =7.17 Hz), 2.88 (t, 2H, (**e**) CH_2-C=O, J = 7.17 Hz), ^{13}C NMR (125 MHz,) δ_C (ppm) 222.79, 177.72, 134.83, 129.29, 128.77, 127.87, 41.58, 33.00,

30.89. (d).). LC-MS (ESI) for $C_5H_8O_3S_2$: [M-NH_4^+]: calcd.: 290.3; found 290. Data agreed with the literature [192].

_S_-Ethoxythiocarbonyl Mercaptoacetic Acid (CTA3)

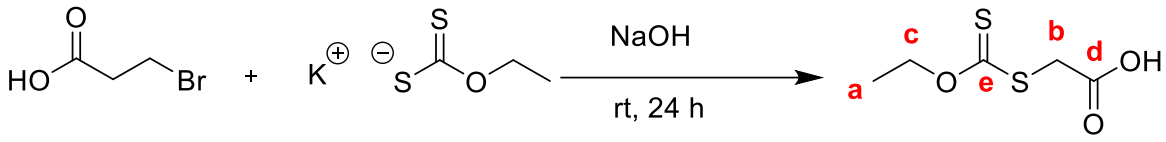

Water-soluble xanthate type chain transfer agent, CTA3 was synthesized according to the protocol of Cao [65]. Sodium hydroxide (1.25 g, 62.4 mmol) was dissolved in chilled water (50 mL) and then bromoacetic acid (1 eq, 4.37 g, 62.4 mmol) was added until a clear solution was obtained. Potassium ethyl xanthogenate (1 eq, 5 g, 62.4 mmol) was added to the mixture over 30 min. The solution was stirred at room temperature for 24 hours, then acidified with 4 M HCl. The resulting mixture was extracted with chloroform (3x50 mL). The organic extracts were dried over anhydrous magnesium sulfate, filtered, and concentrated under vacuum. The solid was washed with hexane and dried under the vacuum to give white crystals.

^{1}H NMR (500 MHz, D_2O) δ_H (ppm) 4.63 (q, J = 7.1 Hz, 2H, (**b**), -CH_2-O), 3.93 (s, 2H, (**c**), -CH_2-), 1.34 (t, J = 7.1 Hz, 3H, (**a**), -CH_3). ^{13}C NMR (126 MHz, D_2O) δ_C (ppm) (**e**), 213.95, (**d**) 172.80, (**c**) 71.72, (**b**) 37.32, (**a**) 12.79.) LC-MS (ESI) for $C_5H_8O_3S_2$: [M-H^+]: calcd.: 179.1.; found: 179.1. Data agreed with the literature [65].

8.2.3. Synthesis of (*R*)-(1-tertbutoxycarbonyl) pyrrolidin-3-yl) methacrylamide

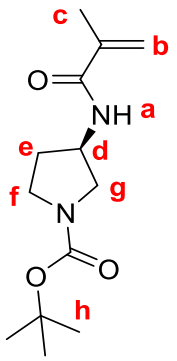

(*R*)-1-N-Boc-3-aminopyrrolidine (5.3 mmol, 1 eq, 0.91 g) and triethylamine (5.85 mmol, 1.2 eq, 0.82 mL) in were dissolved in anhydrous dichloromethane (10 mL). Methacrylic anhydride (1.1 eq. ,5.37 mmol, 0.8 mL) in anhydrous dichloromethane (3.5 mL) was added to the mixture under cooling in an ice bath (0ºC). After the complete addition of the methacrylic anhydride, the ice bath was removed; and the reaction mixture was left overnight at room temperature. The reaction was monitored using TLC (100% ethyl acetate). The sample in the reaction mixture was extracted with three times with citric acid (5% w/v), NaOH (5% w/v) and lastly brine, orderly. The organic phase was dried over sodium sulfate (Na_2SO_4) and filtered and the solvent removed in rotavap to give a residue that was recrystallized using a hexane/dichloromethane (DCM) (9:1).

^{1}H NMR (500 MHz, DMSO) δ_H (ppm) 8.00 (d, J = 6.7 Hz, 1H-**a**), 5.66 (t, J = 1.3 Hz, 1H-**b**), 5.34 (p, J = 1.6 Hz, 1H-**b**'), 4.27 (h, J = 6.6 Hz, 1H-**d**), 3.48 (ddd, J = 18.6, 10.8, 6.8 Hz, 1H-**g**), 3.42 – 3.31 (m, 1H-**g**'), 3.27 – 3.20 (m, 1H-**f**), 3.10 (ddd, J = 13.2, 10.7, 5.4 Hz, 1H-**f**'), 2.02 (dp, J = 13.3, 7.0 Hz, 1H-**e**), 1.85 (t, J = 1.4 Hz, 3H-**c**), 1.80 (dt, J = 14.2, 7.2 Hz, 1H-**e'**), 1.40 (s, 9H-**h**).

^{13}C NMR (125 MHz, DMSO) δ_C (ppm) 168.27 (-NH-**C**=O), 153.95 (-O-**C**=O), 140.23 (-**C**=CH_2), 119.71 (-C=**C**H_2), 78.73 (-O-**C**-$(CH_3)_3$), 51.10, 50.76, 49.54, 48.79, 44.57, 44.31, 31.28, 30.33 (pyrrolidinyl ring), 28.65 (C-(**C**$H_3)_3$), 19.12 (-H_2C=C-**C**H_3).

Due to the rotation of the molecule in DMSO, the peaks of the pyrrolidinyl ring are detected as two peaks for each carbon.

LC-MS (ESI) for $C_{13}H_{22}N_2O_3$: [M-$HCOO^-$]: calcd.:300; found: 299.3.

8.2.4. Polymerization of (*R*)-(1-tertbutoxycarbonyl) pyrrolidin-3-yl) methacrylamide

The monomer, (*R*)-(1-tert-butoxycarbonyl) pyrrolidin-3-yl) methacrylamide (1 g), and the initiator, AIBN (11 mg), were dissolved in THF (10 mL), and the reaction mixture was degassed by bubbling with nitrogen for 20 minutes at 10ºC. The reaction mixture was then placed into an oil bath at 70°C and left for 24 hours. The polymer was precipitated by cold hexane, collected and dried in an oven at 45ºC overnight.

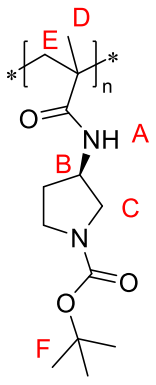

^1H NMR (500 MHz, DMSO) δ_H (ppm) 7.33 (br, 1H, -NH-(**A**), 4.15 (br, 1H, -CH-NH-(**B**), 3.5-2,7 (br, 6H, pyrollidine ring-(**C**), 1.91 (br, 2H, -CH_2-C-(**E**), 1.40 (br, 9H, O-$(CH_3)_3$- (**F**), 0.82 (br, 3H, -C-CH3-(**D**).

^{13}C NMR (125 MHz, DMSO) δ_C (ppm) 176.52, 167.31, 152.94, 139.24, 118.74, 77.63, 48.57, 47.83, 43.97, 27.66, 18.14.

The removal of the protection group from polymers was carried out using trifluoroacetic acid (TFA) in dichloromethane (DCM) (20% v/v TFA in DCM -10 equivalents based on the repeating unit TFA was added). The volatiles were evaporated using a rotary evaporator (with $NaHCO_3$) in the receiver, and the residue was redissolved in methanol and the solvent was removed. This step was repeated 2-3 times. Finally, the polymer was precipitated with diethyl ether after dissolving in methanol and then precipitated again using diethyl ether. The dried polymer was lyophilized.

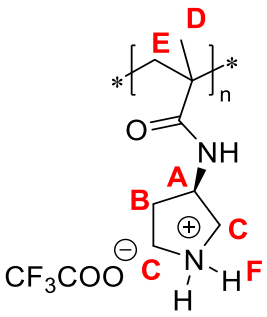

^{1}H NMR (500 MHz, D_2O) δ 4.50 (b, s, 1H-CH-**A**), 3.68 –3.30 (b, m, 4H-**C**), 2.42 (b, s, 2H-**B**), 2.19 -1.84 (b, m, 2H- **E**), 1.14-0.8 (b, t, 3H-**D**).

Although attempts were made to collect ^{13}C NMR data overnight, useful data was not obtained within the investigated timescales due to the extended acquisition times.

8.3 Characterization of Polymers

8.3.1. Nuclear Magnetic Resonance

All monomers, polymers, and chian transfer agents were analysed on a Bruker AVA500 spectrometer in $CDCl_3$ or D_2O at either 500 MHz (H^1 NMR) or 125 MHz (C^{13}).

8.3.2. Molecular Weight Determination of Polymers by GPC analysis

Aqueous-based GPC analysis of the polymers was carried out on an Agilent Technologies 1100 series HPLC system, 8 µm Agilent PL Aquagel-OH 30, and 8 µm Agilent PL Aquagel-OH 40 columns with an RI detector. The eluent was 0.50 M acetic acid, 0.30 M NaH_2PO_4 at pH 2.5 with a flow rate of 1.0 ml min^{-1} at 25°C. Calibration was achieved using InfinityLab EasiVial poly(ethylene oxide) standards with Mn values ranging from 1.1 to 905 kDa.

GPC analysis of poly(2-(dimethylamino)ethyl methacrylate) (PDMAEMA) was carried out on an Agilent 1260 Infinity series HPLC system on two PL-GEL mixed-c columns (5 µm) with both UV and RI detectors. The eluent used was THF at a flow rate of 1.0 ml min^{-1} at 35°C. Molecular weights were obtained relative to poly(methyl methacrylate) standards.

GPC analysis of poly((*R*)-(1-tert-butoxycarbonyl) pyrrolidin-3-yl)methacrylamides were carried out with the same instrument mentioned above (Agilent 1260 Infinity series). The samples were dissolved in a solution of DMF with 0.1% LiBr and then subjected to GPC analysis using the same eluent solvent mixture at a temperature of 60°C. Molecular weights were determined by comparing them to reference poly(methyl methacrylate)s.

8.4. Antimicrobial Activity of the Polymers

8.4.1. Determination of Minimum Inhibitory Concentration

Antibacterial activity was assessed using a resazurin colorimetric assay [193]. Five µL of cryopreserved glycerol stocks of bacterial cultures (*Escherichia coli* DH5α, *Salmonella typhimurium*, *Micrococcus luteus* and *Bacillus subtilis*) were streaked onto Luria Bertani, nutrient agar, tryptic soy agar and nutrient agar plates respectively. A single bacterial colony was transferred to 5 mL of the respective broth media and incubated for 10 h at 37^{o}C and grown until mid-log phase. The culture was diluted, and the concentration adjusted to 0.5 McFarland Standard with sterile Mueller Hinton broth ($2x10^{7}$ CFU/mL). The resazurin solution was prepared in a brown glass vial by dissolving 34 mg of resazurin in sterile distilled water (5 ml) with vortexing for 1h to ensure homogeneity. A single 96-well microtiter plate (Corning, black 96 well flat-bottomed plates) was dedicated to each bacterial species to prevent contamination. The design of the assay was prepared with two rows and two columns from each end filled with sterile water to avoid edge effects. The assay was adapted from previously reported protocols [193]. Two columns of broth sterility controls, 1 column of a growth control, 2 columns of polymer sterility controls (one polymer in each well), 1 column of a positive antibiotic control and lastly, 2 columns of polymer test samples (bacteria with one polymer in each well) were used. All wells were filled with 100 µL Mueller-Hinton broth. The broth sterility and growth control columns contained 100 µL of sterile water, the polymer sterility control and test wells contained 100 µL of polymers (final concentration 128 µg/mL) in the designated wells. Antibiotic wells all at 64 µg/mL contained chloramphenicol (for *S. typhimurium*), gentamicin (for *E. coli* and *M. luteus*) and clindamycin for *B. subtilis*. Five µL of

the diluted bacterial suspension $2x10^7$ CFU/mL was added into all wells (except the broth sterility and polymer sterility control columns) and mixed thoroughly. After an overnight incubation at 37 ^oC, resazurin solution (5 µL, 6.75 mg/mL) was added to all wells and incubated at 37^oC for another 4 h. Changes of colour from blue (resazurin, no bacterial growth) to pink (resorufin, bacterial growth) were recorded at 595 nm on a microplate reader (BioTek Synergy HT). The lowest concentration that did not show colour change was considered as the Minimum Inhibitory Concentration (MIC). Each assay was performed in triplicate, and consistent results were obtained on each occasion. Therefore, it has been noted that the MIC values did not exhibit any standard deviation.

In order to determine the effect of molecular weight on antibacterial activity, three different sized polymers were synthesized for PDADMAC, PMETACl and PVBMT. The concentrations tested were based on the MIC values for these three polymers against the target microbes determined in the previous assay. Each assay was performed in triplicate, and consistent results were obtained on each occasion. Therefore, it has been noted that the MIC values (mg/mL) did not exhibit any standard deviation.

MICs of poly((*R*)-(1-tert-butoxycarbonyl)pyrrolidin-3-yl)metharyclamide)s were determined with the assay mentioned above starting from 2048 µg/mL to the final concentration 1 µg/mL. Consistent results were obtained in each of the three replicates for every assay, and no standard deviation was observed in the MIC values (mg/mL).

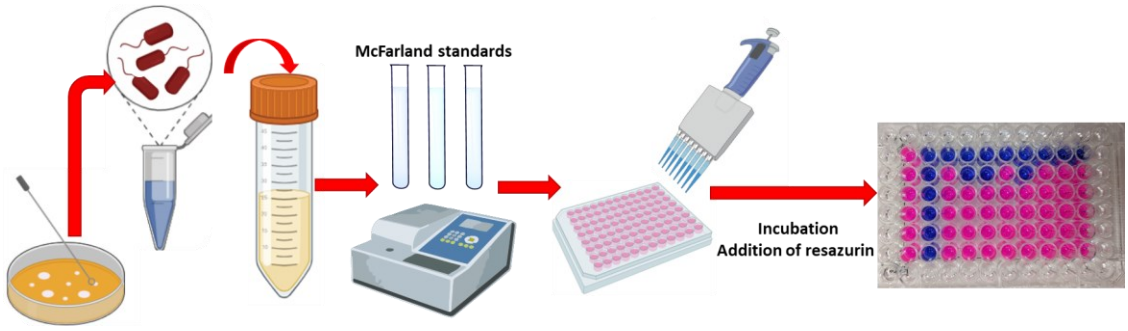

8.4.2. Zone diffusion Assays and Growth Kinetics

Agar plates were coated with bacteria (100 µL at $1x10^6$ CFU/mL), 1 cm diameter wells were punched into the agar and 100 µL of polymer solutions (at 2xMIC) were added into the wells and the zone of inhibition was measured after 8 hours.

8.4.3. Live/Dead Assay

Bacterial cultures (5 mL) grown to late log phase were harvested by centrifugation. The cell pellet was resuspended in 5 mL 0.85% NaCl, aliquoted (each aliquot was 1 mL) and incubated with 4xMIC concentrations of the selected polymers for 4 hours at 37°C. The live cell control consisted of an aliquot incubated with just 0.85% NaCl. After incubation, all samples were washed with 0.85% NaCl twice. A Live/Dead BacLight bacterial viability kit (Invitrogen) was used to check cell viability. The assay was performed according to the instructions in the kit. Component A (1.5 µL of SYTO 9 dye, 200 µL of a 3.34 mM solution in DMSO) was mixed in equal proportions with Component B (1.5 µL of PI dye, 200 µL of a 20 mM solution in DMSO). 3 µL of this dye mixtures were added to 1 mL of all bacterial samples before incubation for 30 min in the dark. Samples were analyzed using an AxioVert 200M inverted fluorescent microscope to analyse for green (λ_{ex} 488 nm λ_{em} 520 nm) and red (λ_{ex} 561 nm, λ_{em} 646 nm) fluorescence.

8.4.4. Bacterial Membrane Integrity Assays

Outer membrane permeabilization assay

The method for determination of outer membrane depolarization assay was adapted from the literature [194]. 1-N-phenyl-1-naphthylamine was dissolved in acetone (3 mM). Gram -ve bacteria *E. coli* were grown to 1.0 OD. Cells were harvested by centrifugation, washed and resuspended at 0.1 OD in 5 mM HEPES buffer with 5 mM glucose at pH 7.2. 10 µL of NPN stock was added to each 1 mL of cells to give a concentration of NPN of 30 µM. 200 µl of bacterial suspension was added to each well of a 96 well plate as five replicates at 37^{o}C and followed by analysis on a fluorescent microplate spectrometer (BioTek Synergy H1) over 30 min (every 1 min) (λ_{ex} 350 nm λ_{em} 429 nm). Then 10 µl of polymers solutions (4xMIC for quaternary homopolymers and 2Xmic for Boc-protected polymers) were added to each well. Triton X-100 (1% v/v) was used as positive control while a bacteria suspension without polymer was used as a negative control. The increase in fluorescence of NPN was monitored and the final fluorescence values after 30 minutes (taken at 5-minute intervals) were plotted. All experiments were repeated three times independently.

Cytoplasmic depolarization assay

The method for determination of inner membrane depolarization assay was adapted from the literature [195]. A stock solution of Calcein-AM was prepared in DMSO (1 mM) and stored in the dark at -20^{o}C. *B. subtilis* was cultured in media overnight and centrifuged (3000 *g*- 5 min) to obtain a pellet. The pellet was washed with PBS and resuspended to a $0D_{600}$ of 1.0 with PBS containing 10% (v/v) broth. The bacteria were incubated at 3 µM Calcein-AM for 1

h at 37 °C. The dye loaded cells were centrifuged (3000 *g* - 5 min) and suspended to 0.1 OD in PBS. 200 µl of bacterial suspension was added into sterile black-wall 96 well plates (three replicates) and monitored for 30 min at (λ_{ex} 485 nm, λ_{em} 515 nm) on a fluorescence plate reader. Bacteria without polymers were used negative control while Triton X-100 (1% v/v) used as positive control. The final fluorescence values after a time of 30 minutes (taken at 5-minute intervals) were plotted as a column graph. All experiments were repeated three times independently.

8.4.5. Scanning Electron Microscopy

Aliquots (10 mL of OD 0.5) of Gram-positive (*M. luteus*) and Gram-negative (*E. coli*) bacteria were incubated with 0.85% NaCl (control) and the polymers (PDAMAC-20, PVMBT-40, PMETACl-40, P-10, P-20 and P-40-all 2xMIC) for two hours. After pelleting, the bacteria were fixed in a solution of 3% glutaraldehyde in 0.1 M sodium cacodylate buffer (pH 7.3) for 2 hours, washed (3x10 minute changes of 0.1 M sodium cacodylate buffer). Samples were then post-fixed in 1% osmium tetroxide (in 0.1 M sodium cacodylate buffer) for 45 minutes, before further 3x10 min washes were performed in 0.1 M sodium cacodylate buffer. Dehydration in graded concentrations of acetone (50%, 70%, 90%, and 3x100% - each for 10 minutes) was followed by critical point drying using liquid carbon dioxide. After mounting on aluminium stubs with carbon tabs attached, the specimens were sputter coated with 20 nm thickness of gold-palladium and viewed using a Hitachi S-4700 scanning electron microscope.

8.4.6. Cytotoxicity and Cytocompatibility of the Antimicrobial Polymers

MTT assay

In vitro cytotoxicity tests were carried out using an MTT assay on HeLa cells based on a previously published protocol with some modification[197]. Cells were grown in complete medium (Dulbecco's Modified Eagle Medium, DMEM, Gibco) supplemented with 2 mM L-glutamine, 10% fetal bovine serum and 1% antibiotics (penicillin 100 U/mL and streptomycin 100 µg/mL) until sub-confluent at 37ºC and 5% CO_2 in a cell incubator (HERAcell ®150, Kendro, Hereaeus Group, Germany). HeLa cells were used at passage numbers below 15 and tested for mycoplasma contamination regularly. For cytotoxicity tests, cells were seeded in a 96-well plate at the density of $1x10^4$ cells per well and cultured in a 100 µL of growth medium. After 24 hours, culture media was replaced with polymer solutions (50 µL) prepared in growth media at increasing concentrations from 1.25 µM to 1.28 mM. The cells were further incubated for 24 hours under the same conditions. After incubation of cells with polymers containing media, all the solutions were carefully removed from the wells and 100 µL MTT solution (5 mg of MTT dissolved in 1 mL PBS and 9 mL serum-free DMEM without phenol-red) was added to each well in a light-protected environment. After 4 h, unreacted dye was removed by aspiration. Cells were carefully washed with PBS twice. 100 µL of solubilizing solution (mixture of 2-propanol and dimethyl sulfoxide in 1:1 volume ratio) was added to each well to dissolve formed formazan crystals. The solution was shaken for at least 30 min to ensure dissolution of all crystals before measuring the absorbance at 570 nm on a BioTek Synergy H1 plate reader. Cells treated with complete medium only were taken as a positive control (100% viability) and cells treated with DMSO (100%) were taken as a negative control.

All tests were repeated three times. The relative cell viability (%) with respect to the control was determined using the formula below:

$$\textbf{Cell viability}\ (\%) = \left(\frac{\mathbf{OD_{sample} - OD_{negative\ control}}}{\mathbf{OD_{positive\ control} - OD_{negative\ control}}}\right)\mathbf{x100}$$

where OD is optical density at 570 nm.

The same protocol was performed for the MTT assay of poly ((*R*)-(1-tertbutoxycarbonyl)pyrrolidin-3-yl)methacrylamides in a concentration range of the polymers from 1024 to 1 µg/mL.

Hemolysis Assays of Antimicrobial Polymers

Hemolysis assay was carried out following a previously published protocol [198]. Sheep red blood cells (RBCs) were diluted 1:20 in PBS (pH 7.4), pelleted by centrifugation (1000 g, 10 min)., and washed three times in PBS (20 mL). The RBCs were then resuspended to 5% (v/v) in PBS. Different concentrations of the PDADMAC-20, PMETACl-40 and PVMBT-40 (150 µL, in the range 1.25 µM-1.28 mM) and were prepared, followed by the addition of the 5% RBC suspension (150 µL). PBS buffer was used as a negative control, and Triton X-100 (1% v/v in PBS) was used as a positive haemolysis control. Samples were incubated at 37°C for 1 h with 300 rpm shaking in an incubator and then centrifuged (2000g, 4 min), 100 µL aliquots of supernatants were transferred into a 96-well microplate where absorbance values were read at 405 nm using a plate reader. Haemolysis percentage was calculated using the absorbance values and the formula below:

$$\textbf{Hemolysis}\ (\%) = \left(\frac{\mathbf{A_{polymer} - A_{negative}}}{\mathbf{A_{positive} - A_{negative}}}\right)\mathbf{x100}$$

where $A_{polymer}$ is the absorbance of the polymer treated cells' supernatant, $A_{positive}$ is the absorbance of the positive control (1% v/v Triton X-100 treated cells' supernatant) and $A_{negative}$ is the absorbance of the negative control (PBS treated cells' supernatant). All experiments were performed as independent triplicates, each consisting of triplicates.

The same protocol was performed for the hemolysis assay of poly((*R*)-(1-tertbutoxycarbonyl)pyrrolidin-3-yl)methacrylamides in a concentration range of the polymers from 2048 to 1 µg/mL.

8.5. Antifungal Assays

8.5.1. Microbial Growth Conditions

All strains were maintained at -80°C in Microbank™ vials (Pro-Lab Diagnostics, Birkenhead, UK) before being cultured on Sabouraud dextrose agar at 30°C for 24-48 hours to achieve colonies with a diameter of approximately 1 mm. Subsequently, the plates were stored at 4°C. A single colony of fungi was selected, inoculated in 10 mL of yeast peptone dextrose (1% w/v yeast extract, 2% w/v peptone, 2% w/v dextrose, 1.5% agar [Sigma-Aldrich, UK]), and incubated for 18 hours at 30°C for *C. albicans* and *C. auris*, and at 37°C for *M. furfur* with shaking at 180 rpm. The cells were then centrifuged at 3000 rpm for 5 minutes, and the collected pellets were resuspended in PBS, washed twice, and diluted 100 times by adding 10 µL of the cell suspension to 990 µL of PBS in a sterile Eppendorf tube. Cell counts were

determined using a Neubauer haemocytometer (cell count × dilution factor × volume of square = colony forming unit [CFU/mL]).

8.5.2. Planktonic Minimum Inhibition Concentration

The determination of Planktonic Minimum Inhibitory Concentration (pMIC) followed the broth microdilution method outlined in the M27-A3 standard for fungi [145] by the Clinical and Laboratory Standards Institute (CLSI). Following overnight fungal growth, cells were adjusted to $2x10^4$ cells/mL in Roswell Park Memorial Institute media from Sigma–Aldrich, Dorset, UK. Polymer concentrations were set at 1 mM. In 96-well round bottom microtiter plates, 100 µL of standardized microorganisms ($2x10^4$ cells/mL) were mixed with 100 µL of serially diluted polymer solutions. The plates were then incubated in 5% CO_2 at 37°C for 24 hours. After this incubation period, pMIC concentrations were identified as the lowest concentration for each treatment that inhibited visible colony formation at the well bottoms. The experiments were conducted in duplicate, with each well being repeated in triplicate for accuracy. The MIC values (mg/mL) were consistent and did not exhibit any standard deviation.

8.5.3. Fungicidal Minimum Inhibition Concentration

10 µL of solution from the wells where no visible growth seen with naked eye was taken and put into agar plates. The plates were incubated for 24 hours to detect any colony formation.

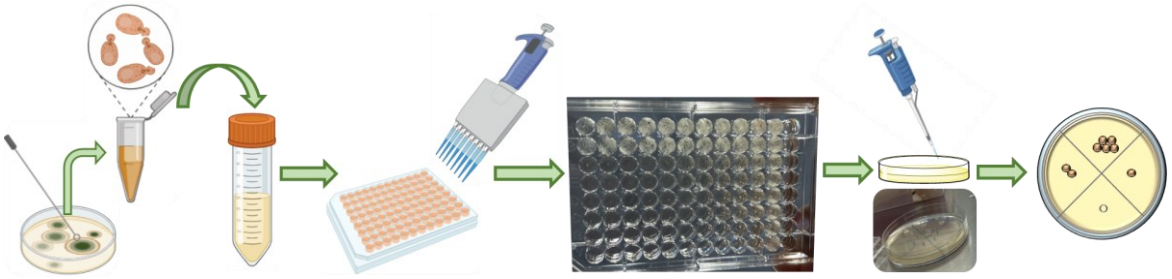

8.5.4. Measurement of metabolic activity of Fungi

XTT assay

The XTT metabolic assay is a widely used technique for assessing the viability of different cell types, including *C. albicans*. This method is known for its speed and cost-effectiveness and is often used to measure the effectiveness of various treatments. *C. albicans* were first diluted to 1×10^6 CFU/mL and 200 µL cell solution was added to 96-well plates as 2 replicates to grow biofilms for 24 hours at 30^{o}C. Next day, media was removed and 200 µL polymer solutions (PDADMACs and PMETACls) starting from 1000 µM to 1.9 µm were added to each well and incubated for another 24 hours. Following incubation, the spent supernatant was discarded and biofilms washed with PBS to remove any non-adhered cells. To assess cell viability, XTT (2,3-bis-[2-methoxy-4-nitro-5-sulfophenyl]-2H-tetrazolium-5-carboxanilide) reduction assay, coupled with the electron-coupling agent menadione, was employed in accordance with the methodology previously outlined [199] . Initially, a solution of 0.25 g/L XTT was prepared by dissolving it in distilled water, followed by filter sterilization using a 0.22-µm-pore size filter unit. This solution was then stored at -80^{o}C. Simultaneously, a stock solution of 10 mM menadione (2-methyl-1,4-naphthoquinone, also recognized as vitamin K3 from Sigma-Aldrich, Dorset, UK) was created in 100% acetone and maintained at -20^{o}C. Before application, the XTT solution underwent thawing, and menadione was introduced to attain a final concentration of 1 µM. Subsequently, a 250 µL portion of the XTT/menadione solution was administered to each pre-washed biofilm and control well, followed by a 2-hour incubation in darkness at 37^{o}C within the LEEC Classic incubator (UK). Following the incubation period, 100 µL of the XTT-derived formazan salt from each well was transferred to

a new 96-well flat-bottom plate (Costar®, Corning Incorporated, NY, USA) for absorbance readings. Absorbance measurements were conducted at a wavelength of 492 nm using a microtiter plate reader (Sunrise, TECAN, Theale, UK).

Biofilm Compositional Analysis Using Quantitative Polymerase Chain Reaction (qPCR)

In order to ascertain the proportional composition of the biofilms, a real-time quantitative PCR was carried out. 500 µL ($1x10^6$ CFU/mL) three fungi species (*C. albicans, C. auris* and *M. furfur)* was grown in 24-well microtiter plates on Nunc™ Thermanox™ Coverslips (24x30 mm) for 24 hours at 37^{o}C (except for *M.furfur* was 72 hours at 30^{o}C). Next day, all media was removed and washed with PBS (500 µL). Then, biofilms were treated with polymers solutions (PDADMAC-20 (15 µM) and PMETACl-20 (1280 µM)) and incubated for another 24 hours. After incubations, supernatants were removed and coverslips were washed with PBS. Coverslips were sonicated in 1 mL of PBS at 35 kHz in an ultrasonic water-bath (Fisher Scientific, Paisley, UK) for 10 min to mechanically disrupt the biomass. Each sonicated sample was equally split when only one sample treated with propidium monoazide (PMA) (5 µL/mL of 50 µM) -a DNA-intercalating dye, to differentiate biofilm viable and dead microorganisms. When exposed to bright light, PMA binds covalently to the DNA of cells with compromised membranes, such as dead cells or cells with damaged membranes. Thus, only alive cells can be detected. Treated samples and control samples were kept in dark 10 min then exposed to UV-light (PMA-Lite device-LET photolysis device) for 5 min to covalently bind DNA to PMA. DNA was then extracted from the obtained samples using the QIAamp DNA mini kit (Qiagen, Crawley, UK) based on manufacturer's instructions. PCR was carried out as previously described protocol [200] with Step-One plus real time PCR machine and StepOne software V2.3

(Life Technologies, Paisley, UK). In brief, fungi (*C. albicans, C. auris* or *M. furfur)* DNA was introduced into a PCR master mix containing Fast SYBR® Green (Thermo Fisher Scientific, Paisley, UK), along with specific forward and reverse primers, all dissolved in irradiated RNase-free water. Simultaneously, serial dilutions of fungal DNA that were extracted from a concentration of 1×10^8 cells/mL were prepared to establish a standard curve for each species. The process of thermal cycling involved an initial step at 50°C for 2 minutes, followed by 95°C for 2 minutes. This was followed by 40 cycles, alternating between 95°C for 3 seconds and 60°C for 30 seconds. The calculation of colony-forming equivalents (CFE) was performed by referring to the standard curve for each respective species.

8.6. Quaternization of Tröger's Base Polymer

The tertiary amino groups of the TB polymer (EA-TB) were quaternized with an excess of alkyl bromides (methyl iodide, 1-bromobutane, 1-bromohexane, 1-bromooctane, 1-bromododecane or benzylbromide). The quaternization reactions were carried out with 1, 3, and 6 equivalents based on the repeating unit. For each reaction, 500 mg polymers (1 eq, 1.66 mmol-repeating units) were added to a microwave vial and dissolved with chloroform/DMSO mixture (1:9 ratio – total 10 mL) overnight and then the relevant alkyl bromide was added dropwise as 6 eq, 3 eq or 1eq compared to repeating units. The reactions were stirred for 24 hours, followed by pouring into a large amount of deionized water and subsequent filtration. The resulting mixture was washed with methanol multiple times to remove any unreacted alkyl bromides, then filtered and dried under vacuum at 45°C.

Yields: EA-TB-1 (83 %), EA-TB-1.3 (99 %), EA-TB-6.1 (45%), EA-TB-6.3 (84 %), EA-TB-Bn.1 (67 %), EA-TB-Bn.3 (99 %).

EA-TB: ^{1}H NMR (500 MHz, $CDCl_3$): δ_H (ppm) 6.94 (m, br, 4H, Ar-H), 4.64 (s, br, 2H, N^+-CH_2-N), 4.05 (s, br, 4H, 2 N-CH_2-Ar), 1.81-0.9 (br, m, 10 H, 2-CH_3, 2-CH_2).

EA-TB-1: ^{1}H NMR (500 MHz, DMSO): δ_H (ppm) 7.82 (s, br, 1H, Ar-H), 7.14 (m, br, 3H, Ar-H), 5.5-4.5 (m, br, 2H, N^+-CH_2-N, 2H, N-CH_2-Ar), 3.86 (m, br, 1H, N-CH_2-Ar), 3.65 (m, br, 3H, N^+-CH_3), 2.1-0.9 (m, br, 2H, CH_2, 6H, 2 Ar-CH_3), 0.86 (s, br, 1H, N^+-CH_2-N).

EA-TB-6: ^{1}H NMR (500 MHz, DMSO): δ_H (ppm) 7.6-6.0 (m, br, 4H, Ar-H), 3.5-3.0 (m, br, 1H, N^+-CH_2-N, 4H, N-CH_2-Ar), 2.01-0.8 (m, br, 24H, 1H, N^+-CH_2-N, 2H N^+-CH_2, 4H, Ar-CH_2, 6H, 2 Ar-CH_3, 11H -N^+-CH_2-C_5H_{11})

EA-TB-Bn: ^{1}H NMR (500 MHz, DMSO): δ_H (ppm) 8.00-6.5 (m, br, 9H), 6.0-4.0 (m, br, 2H, N^+-CH_2-N, 4H, 2 N-CH_2-Ar, 2 N-CH_2-Ar), 2.1-0.9 (m, br,6H, 2 Ar CH_3, 4H, 2 -Ar-CH_2).

The NMR analysis of quaternized Tröger's base polymers was challenging and that overnight data collection was required to collect the ^{1}H NMR spectra. While the collection of ^{13}C NMR data was attempted, due to the long acquisition times useful data was not obtained on the timescales investigated.

8.6.1 Spin Coating of Quaternization of Tröger's Base Polymers

To ensure a uniform and thin film on 19 mm glass coverslips (no. 1 thickness), the following protocol was followed: The circular coverslips underwent a thorough cleaning process, starting with a 15-minute ultrasonic bath in methanol, followed by a15-minute bath in acetone. Subsequently, each coverslip was dried using nitrogen, and a visual inspection was conducted to verify the absence of any debris or imperfections. Immediately before the spin-coating procedure, the coverslips underwent a 10-minute etching in an oxygen plasma

cleaner. The spin coating was carried out using 5% w/v polymer solution in a 1:1 mixture of HIFP/1-butanol.

8.6.2. Stability of Tröger's Base Polymers Coated Coverslips - Contact-Angle Measurements

The polymer-coated coverslips underwent a 2-day incubation at 37°C in phosphate-buffered saline (PBS), pH 7.4. After this incubation period, the surface of each spin-coated sample was visually inspected by naked eye. Only methyl iodide (1 eq and 3 eq) quaternized polymers remained stable on the surface.

Subsequently, the static contact angles of deionized water on both the stable surface coatings (uncoated and methyl iodide-coated coverslips) were measured. This was done using a Drop Shape Analyser model DSA25 from KRUSS and the results were analyzed with DSA1 software. For each measurement, 10 µL of deionized water was deposited on the surface, and the contact angles were immediately measured over a 120-second period at 25°C.

8.6.3. Surface Thickness Measurement of the Polymer Coatings

A Hitachi S-4700 scanning electron microscope was used to measure surface thickness of the polymers and analyse surface morphology of the coatings.

8.7. Antimicrobial Activity of the TB Polymer Coatings

8.7.1 Live/Dead Assay of Polymer Coatings

A live/dead assay [201] was performed to evaluate bacterial viability and population post-interaction with TB polymer coatings. Individual 19 mm circular glass coverslip-coated samples were positioned in a 12-well plate, with each well receiving 500 µL of a bacterial

suspension (*E. coli*-1 x 10^6 CFU/mL) and 500 µL of Mueller-Hinton broth (MHB). Following a 6-hour incubation at 37°C, the coatings were rinsed three rinses with sterile water and were then stained with a 200 µL mixture of propidium iodide (PI) and SYTO 9 for 15 minutes in the dark. Subsequently, the samples were washed with sterile water to eliminate excess dye solution, and the stained samples were sandwiched between a slide and a coverslip. The samples were then observed under a fluorescence microscope (Zeiss Axio Imager2).

8.7.2. Bactericidal Plating Assay

The assay was adapted and modified from previously reported protocols [201] . The bactericidal activities of polymeric coatings were assessed using an overnight broth culture of bacteria (E. coli) adjusted to approximately 1×10^6 CFU/mL. Polymer-coated coverslips were placed in a 12-well plate, and 2 mL of bacterial broth was added to each well. The plate was then kept in the incubator at 37°C for 6 hours. Following incubation, 1 mL of the bacterial solution was collected from each well, serially diluted in sterile LB broth at pH 7.4, and spread onto LB agar plates. These plates were subsequently incubated at 37°C to determine the number of colony-forming units (CFUs). All determinations, including the growth controls, were performed in triplicate to ensure reliability.

8.7.3. Biocompatibility of Polymer Coatings

The hemolysis assay for polymer-coated coverslips was conducted with a slight modification to a previously utilized published protocol [196]. In all experiments, defibrinated sheep blood was employed, and it underwent an extensive washing process involving six rinses with 150 mM NaCl in phosphate-buffered saline (PBS) at a pH of 7.4. The washing was achieved through

centrifugation at 500 g. Following the washing steps, the blood was diluted at a 1:50 ratio in PBS to create the working solution for red blood cells (RBCs). The hemolysis assay was executed by introducing polymer-coated coverslips into 12-well plates and inoculating them with 2 mL of RBC solution at 37^{o}C for 2 hours. To assess cell lysis by measuring the release of hemoglobin, the supernatant RBC solutions were centrifuged at 500g for 10 minutes, and the absorbance was quantified at 405 nm. These results were then compared with controls, which included uncoated glasses as a negative control (0%) and Triton X-100 treated glasses as a positive control (100%). Each determination was repeated in triplicate. Hemolysis percentage was calculated using the absorbance values and the formula given above (see section 7.4.6).

Chapter 9

References

(1) Jain, A.; Duvvuri, L. S.; Farah, S.; Beyth, N.; Domb, A. J.; Khan, W. Antimicrobial Polymers. *Adv Healthc Mater* **2014**, *3*(12), 1969–1985. https://doi.org/10.1002/adhm.201400418.

(2) Cottreau, J. M.; Christensen, A. B. Newly Approved Antimicrobials. *Orthopaedic Nursing* **2020**, *39*(1), 53–58. https://doi.org/10.1097/NOR.0000000000000633.

(3) Liu, J.; Xu, Y.; Lin, X.; Ma, N.; Zhu, Q.; Yang, K.; Li, X.; Liu, C.; Feng, N.; Zhao, Y.; Li, X.; Zhang, W. Immobilization of Poly-L-Lysine Brush via Surface Initiated Polymerization for the Development of Long-Term Antibacterial Coating for Silicone Catheter. *Colloids Surf B Biointerfaces* **2023**, *221*, 113015. https://doi.org/10.1016/j.colsurfb.2022.113015.

(4) Muñoz-Bonilla, A.; Fernández-García, M. Polymeric Materials with Antimicrobial Activity. *Prog Polym Sci* **2012**, *37*(2), 281–339. https://doi.org/https://doi.org/10.1016/j.progpolymsci.2011.08.005.

(5) Gallegos, J.; Cantu-Reyes, M.; Ortega, A.; Magaña, H.; Perez, X.; Garcia-Uriostegui, L.; Hurtado-Ayala, L. A.; Burillo, G. Radiation Grafting of 4-Vinylpyridine and 2-Hydroxyethyl Methacrylate onto Silicone Rubber Films, Quaternization and Antimicrobial Properties. *Radiat Phys Chem* **2023**, *210*, 1–9. https://doi.org/10.1016/j.radphyschem.2023.111002.

(6) Gordon, Y. J.; Romanowski, E. G.; McDermott, A. M. Mini Review: A Review of Antimicrobial Peptides and Their Therapeutic Potential as Anti-Infective Drugs. *Curr Eye Res* **2005**, *30*(7), 505–515. https://doi.org/10.1080/02713680590968637.

(7) Doroshenko, N.; Rimmer, S.; Hoskins, R.; Garg, P.; Swift, T.; Spencer, H. L. M.; Lord, R. M.; Katsikogianni, M.; Pownall, D.; Macneil, S.; Douglas, C. W. I.; Shepherd, J. Antibiotic Functionalised Polymers Reduce Bacterial Biofilm and Bioburden in a Simulated Infection of the Cornea. *Biomater Sci* **2018**, *6*(8), 2101–2109. https://doi.org/10.1039/c8bm00201k.

(8) Martins Leal Schrekker, C.; Sokolovicz, Y. C. A.; Raucci, M. G.; Leal, C. A. M.; Ambrosio, L.; Lettieri Teixeira, M.; Meneghello Fuentefria, A.; Schrekker, H. S. Imidazolium Salts for Candida Spp. Antibiofilm High-Density Polyethylene-Based Biomaterials. *Polymers* **2023**, *15*(5), 1–14. https://doi.org/10.3390/polym15051259.

(9) Namivandi-Zangeneh, R.; Wong, E. H. H.; Boyer, C. Synthetic Antimicrobial Polymers in Combination Therapy: Tackling Antibiotic Resistance. *ACS Infect Dis* **2021**, *7*(2), 215–253. https://doi.org/10.1021/acsinfecdis.0c00635.

(10) Stebbins, N. D.; Ouimet, M. A.; Uhrich, K. E. Antibiotic-Containing Polymers for Localized, Sustained Drug Delivery. *Adv Drug Deliv Rev* **2014**, *78*, 77–87. https://doi.org/10.1016/j.addr.2014.04.006.

(11) Tauanov, Z.; Zakiruly, O.; Baimenova, Z.; Baimenov, A.; Akimbekov, N. S.; Berillo, D. Antimicrobial Properties of the Triclosan-Loaded Polymeric Composite Based on Unsaturated Polyester Resin: Synthesis, Characterization and Activity. *Polymers* **2022**, *14* (4). https://doi.org/10.3390/polym14040676.

(12) Iudin, D.; Zashikhina, N.; Demyanova, E.; Korzhikov-Vlakh, V.; Shcherbakova, E.; Borozn jak, R.; Tarasenko, I.; Zakharova, N.; Lavrentieva, A.; Skorik, Y.; Korzhikova-Vlakh, E. Polypeptide Self-Assembled Nanoparticles as Delivery Systems for Polymyxins

B and E. *Pharmaceutics* **2020**, *12*(9), 1–20. https://doi.org/10.3390/pharmaceutics12090868.

(13) Chen, M.; Xie, S.; Wei, J.; Song, X.; Ding, Z.; Li, X. Antibacterial Micelles with Vancomycin-Mediated Targeting and PH/Lipase-Triggered Release of Antibiotics. *ACS Appl Mater Interfaces* **2018**, *10*(43), 36814–36823. https://doi.org/10.1021/acsami.8b16092.

(14) Zhu, Z.; Min, T.; Zhang, X.; Wen, Y. Microencapsulation of Thymol in Poly(Lactide-Co-Glycolide) (PLGA): Physical and Antibacterial Properties. *Materials* **2019**, *12* (7), 1–11. https://doi.org/10.3390/ma12071133.

(15) Namivandi-Zangeneh, R.; Yang, Y.; Xu, S.; Wong, E. H. H.; Boyer, C. Antibiofilm Platform Based on the Combination of Antimicrobial Polymers and Essential Oils. *Biomacromolecules* **2020**, *21*(1), 262–272. https://doi.org/10.1021/acs.biomac.9b01278.

(16) Gupta, A.; Mumtaz, S.; Li, C. H.; Hussain, I.; Rotello, V. M. Combatting Antibiotic-Resistant Bacteria Using Nanomaterials. *Chem Soc Rev* **2019**, *48*(2), 415–427. https://doi.org/10.1039/c7cs00748e.

(17) Wulandari, E.; Budhisatria, R.; Soeriyadi, A. H.; Willcox, M.; Boyer, C.; Wong, E. H. H. Polymer Chemistry Combating Multidrug-Resistant Bacteria †. *Polym Chem* **2021**, *12*, 7038–7047. https://doi.org/10.1039/d1py01219c.

(18) Alexander, J. W. History of the Medical Use of Silver. *Surg Infect (Larchmt)* **2009**, *10*(3), 289–292. https://doi.org/10.1089/sur.2008.9941.

(19) Huh, A. J.; Kwon, Y. J. “Nanoantibiotics”: A New Paradigm for Treating Infectious Diseases Using Nanomaterials in the Antibiotics Resistant Era. *J. Control. Release* **2011**, *156*(2), 128–145. https://doi.org/10.1016/j.jconrel.2011.07.002.

(20) Jaswal, T.; Gupta, J. A Review on the Toxicity of Silver Nanoparticles on Human Health. *Mater Today Proc* **2023**, *81*, 859–863. https://doi.org/10.1016/j.matpr.2021.04.266.

(21) Tylkowski, B.; Trojanowska, A.; Nowak, M.; Marciniak, L.; Jastrzab, R. Applications of Silver Nanoparticles Stabilized and/or Immobilized by Polymer Matrixes. *Phys. Sci. Rev.* **2019**, *2*(7), 1–16. https://doi.org/10.1515/psr-2017-0024.

(22) Tang, L.; Livi, K. J. T.; Chen, K. L. Polysulfone Membranes Modified with Bioinspired Polydopamine and Silver Nanoparticles Formed in Situ to Mitigate Biofouling. *Environ Sci Technol Lett* **2015**, *2*(3), 59–65. https://doi.org/10.1021/acs.estlett.5b00008.

(23) Mauter, M. S.; Wang, Y.; Okemgbo, K. C.; Osuji, C. O.; Giannelis, E. P.; Elimelech, M. Antifouling Ultrafiltration Membranes via Post-Fabrication Grafting of Biocidal Nanomaterials. *ACS Appl Mater Interfaces* **2011**, *3* (8), 2861–2868. https://doi.org/10.1021/am200522v.

(24) Mitra, D.; Kang, E. T.; Neoh, K. G. Antimicrobial Copper-Based Materials and Coatings: Potential Multifaceted Biomedical Applications. *ACS Appl Mater Interfaces* **2020**, *12*(19), 21159–21182. https://doi.org/10.1021/acsami.9b17815.

(25) Rosenberg, M.; Ilic, K.; Juganson, K.; Ivask, A.; Ahonen, M.; Vrček, I. V.; Kahru, A. Potential Ecotoxicological Effects of Antimicrobial Surface Coatings: A Literature Survey Backed up by Analysis of Market Reports. *PeerJ* **2019**, 2, 1–34. https://doi.org/10.7717/peerj.6315.

(26) Montero, D. A.; Arellano, C.; Pardo, M.; Vera, R.; Gálvez, R.; Cifuentes, M.; Berasain, M. A.; Gómez, M.; Ramírez, C.; Vidal, R. M. Antimicrobial Properties of a Novel Copper-Based Composite Coating with Potential for Use in Healthcare Facilities. *Antimicrob Resist Infect Control* **2019**, *8*(1), 1–10. https://doi.org/10.1186/s13756-018-0456-4.

(27) Sirelkhatim, A.; Mahmud, S.; Seeni, A.; Kaus, N. H. M.; Ann, L. C.; Bakhori, S. K. M.; Hasan, H.; Mohamad, D. Review on Zinc Oxide Nanoparticles: Antibacterial Activity and Toxicity Mechanism. *Nanomicro Lett* **2015**, *7*(3), 219–242. https://doi.org/10.1007/s40820-015-0040-x.

(28) Baghaie, S.; Khorasani, M. T.; Zarrabi, A.; Moshtaghian, J. Wound Healing Properties of PVA/Starch/Chitosan Hydrogel Membranes with Nano Zinc Oxide as Antibacterial Wound Dressing Material. *J Biomater Sci Polym Ed* **2017**, *28*(18), 2220–2241. https://doi.org/10.1080/09205063.2017.1390383.

(29) Cierech, M.; Kolenda, A.; Grudniak, A. M.; Wojnarowicz, J.; Go, M.; Swoboda-kope, E. Significance of Polymethylmethacrylate (PMMA) Modi Fi Cation by Zinc Oxide Nanoparticles for Fungal Bio Film Formation. *Int J Pharm* **2016**, *510*, 323–335.

(30) Gottenbos, B.; Van Der Mei, H. C.; Klatter, F.; Nieuwenhuis, P.; Busscher, H. J. In Vitro and in Vivo Antimicrobial Activity of Covalently Coupled Quaternary Ammonium Silane Coatings on Silicone Rubber. *Biomaterials* **2002**, *23*(6), 1417–1423. https://doi.org/10.1016/S0142-9612(01)00263-0.

(31) Antonucci, J. M.; Zeiger, D. N.; Tang, K.; Lin-Gibson, S.; Fowler, B. O.; Lin, N. J. Synthesis and Characterization of Dimethacrylates Containing Quaternary Ammonium Functionalities for Dental Applications. *Dental Materials* **2012**, *28*(2), 219–228. https://doi.org/10.1016/j.dental.2011.10.004.

(32) Wang, Y.; Yuan, Q.; Li, M.; Tang, Y. Cationic Conjugated Microporous Polymers Coating for Dual-Modal Antimicrobial Inactivation with Self-Sterilization and Reusability Functions. *Adv Funct Mater* **2023**, *33*(19). https://doi.org/10.1002/adfm.202213440.

(33) Murugan, E.; Yogaraj, V. Development of a Quaternary Ammonium Poly (Amidoamine) Dendrimer-Based Drug Carrier for the Solubility Enhancement and Sustained Release of Furosemide. *Front Chem* **2023**, *11*, 1–15. https://doi.org/10.3389/fchem.2023.1123775.

(34) Hennecke, D.; Bauer, A.; Herrchen, M.; Wischerhoff, E.; Gores, F. Cationic Polyacrylamide Copolymers (PAMs): Environmental Half Life Determination in Sludge-Treated Soil. *Environ Sci Eur* **2018**, *30*(16), 1–13. https://doi.org/10.1186/s12302-018-0143-3.

(35) Girase, C. D.; Rajput, Y. N.; Hatkar, V. M.; Kulkarni, R. D. Synthesis and Characterizations of Cationic Poly(DADMAC-Co-AM) Surfactant for Hair Care Applications. *Journal of Polymer Research* **2022**, *29*(8), 1–12. https://doi.org/10.1007/s10965-022-03113-3.

(36) Ali, A.; Ganie, S. A.; Mir, T. A.; Mazumdar, N. Synthesis, Characterization and Disinfection Efficiency Evaluation of Quaternary Ammonium Iodide Derivatives of Gum Arabic. *J Polym Environ* **2023**, No. 0123456789. https://doi.org/10.1007/s10924-023-02874-2.

(37) Sun, X.; Liu, X.; Huang, P.; Wang, Z.; He, Y.; Song, P.; Wang, R. Tri-Cationic Copolymer Hydrogels with Adjustable Adhesion and Antibacterial Properties for Flexible Wearable Sensors. *J Mater Chem C Mater* **2023**, *11*, 6451–6458. https://doi.org/10.1039/d3tc00746d.

(38) Okeke, U. C.; Snyder, C. R. Synthesis, Purification and Characterization of Polymerizable Multifunctional Quaternary Ammonium Compounds. *Molecules* 2019, *24*(1464), 1–11. https://doi.org/10.3390/molecules24081464.

(39) Martins, A. F.; Facchi, S. P.; Follmann, H. D. M.; Pereira, A. G. B.; Rubira, A. F.; Muniz, E. C. Antimicrobial Activity of Chitosan Derivatives Containing N-Quaternized Moieties in Its Backbone: A Review. *Int J Mol Sci* **2014**, *15*(11), 20800–20832. https://doi.org/10.3390/ijms151120800.

(40) Xue, Y.; Xiao, H.; Zhang, Y. Antimicrobial Polymeric Materials with Quaternary Ammonium and Phosphonium Salts. *Int J Mol Sci* **2015**, *16*(2), 3626–3655. https://doi.org/10.3390/ijms16023626.

(41) Pham, P.; Oliver, S.; Wong, E. H. H.; Boyer, C. Effect of Hydrophilic Groups on the Bioactivity of Antimicrobial Polymers. *Polym Chem* **2021**, 12, 5689–5703. https://doi.org/10.1039/d1py01075a.

(42) Phuong, P. T.; Oliver, S.; He, J.; Wong, E. H. H.; Mathers, R. T.; Boyer, C. Effect of Hydrophobic Groups on Antimicrobial and Hemolytic Activity: Developing a Predictive Tool for Ternary Antimicrobial Polymers. *Biomacromolecules* **2020**, *21*(12), 5241–5255. https://doi.org/10.1021/acs.biomac.0c01320.

(43) Asif, I.; Gilani, S. R.; Shahzadi, P. Contrived Approach to Novel Antibacterial Poly(Vinyl Acetate-Co-[2-(Methacryloyloxy)Ethyl]Trimethylammonium Chloride) and Poly(Vinyl Acetate-Co-[Vinylbenzyl]Trimethylammonium Chloride) via RAFT Polymerization with Multi-Characterization. *J. Polym. Res*. **2021**, *28*(11), 444. https://doi.org/10.1007/s10965-021-02812-7.

(44) Phillips, D. J.; Harrison, J.; Richards, S. J.; Mitchell, D. E.; Tichauer, E.; Hubbard, A. T. M.; Guy, C.; Hands-Portman, I.; Fullam, E.; Gibson, M. I. Evaluation of the Antimicrobial Activity of Cationic Polymers against Mycobacteria: Toward Antitubercular Macromolecules. *Biomacromolecules* **2017**, *18*(5), 1592–1599. https://doi.org/10.1021/acs.biomac.7b00210.

(45) De Jesús-Téllez, M. A.; De la Rosa-García, S.; Medrano-Galindo, I.; Rosales-Peñafiel, I.; Gómez-Cornelio, S.; Guerrero-Sanchez, C.; Schubert, U. S.; Quintana-Owen, P. Antifungal Properties of Poly[2-(Dimethylamino)Ethyl Methacrylate] (PDMAEMA) and Quaternized Derivatives. *React Funct Polym* **2021**, *163,* 1-11. https://doi.org/10.1016/j.reactfunctpolym.2021.104887.

(46) Keely, S.; Rawlinson, L. A. B.; Haddleton, D. M.; Brayden, D. J. A Tertiary Amino-Containing Polymethacrylate Polymer Protects Mucus-Covered Intestinal Epithelial Monolayers against Pathogenic Challenge. *Pharm Res* **2008**, *25*(5), 1193–1201. https://doi.org/10.1007/s11095-007-9501-3.

(47) Rawlinson, L. A. B.; O'Gara, J. P.; Jones, D. S.; Brayden, D. J. Resistance of Staphylococcus Aureus to the Cationic Antimicrobial Agent Poly(2-(Dimethylamino Ethyl)Methacrylate) (PDMAEMA) Is Influenced by Cell-Surface Charge and Hydrophobicity. *J Med Microbiol* **2011**, *60*(7), 968–976. https://doi.org/10.1099/jmm.0.025619-0.

(48) Vitro, I.; Skóra, M. Studies on Antifungal Properties of Methacrylamido Propyl Trimethyl Ammonium Chloride Polycations and Their Toxicity. *Microbiol Spectr* **2023**, *11* (3), 1-16. https://doi.org/10.1128/spectrum.00844-23.

(49) Grace, J. L.; Huang, J. X.; Cheah, S. E.; Truong, N. P.; Cooper, M. A.; Li, J.; Davis, T. P.; Quinn, J. F.; Velkov, T.; Whittaker, M. R. Antibacterial Low Molecular Weight Cationic Polymers: Dissecting the Contribution of Hydrophobicity, Chain Length and Charge to Activity. *RSC Adv* **2016**, *6*(19), 15469–15477. https://doi.org/10.1039/c5ra24361k.

(50) Lin, S.; Wu, J. H.; Jia, H. Q.; Hao, L. M.; Wang, R. Z.; Qi, J. C. Facile Preparation and Antibacterial Properties of Cationic Polymers Derived from 2-(Dimethylamino)Ethyl Methacrylate. *RSC Adv* **2013**, *3*(43), 20758–20764. https://doi.org/10.1039/c3ra43525c.

(51) Keely, S.; Rawlinson, L. A. B.; Haddleton, D. M.; Brayden, D. J. A Tertiary Amino-Containing Polymethacrylate Polymer Protects Mucus-Covered Intestinal Epithelial Monolayers against Pathogenic Challenge. *Pharm Res* **2008**, *25*(5), 1193–1201. https://doi.org/10.1007/s11095-007-9501-3.

(52) Shiga, T.; Mori, H.; Uemura, K.; Moriuchi, R.; Dohra, H.; Yamawaki-Ogata, A.; Narita, Y.; Saito, A.; Kotsuchibashi, Y. Evaluation of the Bactericidal and Fungicidal Activities of Poly([2-(Methacryloyloxy)Ethyl]Trimethyl Ammonium Chloride)(Poly (METAC))-Based Materials. *Polymers* **2018**, *10*(9), 1–9. https://doi.org/10.3390/polym10090947.

(53) Foster, L. L.; Yusa, S. I.; Kuroda, K. Solution-Mediated Modulation of Pseudomonas Aeruginosa Biofilm Formation by a Cationic Synthetic Polymer. *Antibiotics* **2019**, *8*(2), 61. https://doi.org/10.3390/antibiotics8020061.

(54) Tian, X.; Ding, J.; Zhang, B.; Qiu, F.; Zhuang, X.; Chen, Y. Recent Advances in RAFT Polymerization: Novel Initiation Mechanisms and Optoelectronic Applications. *Polymers* **2018**, *10*(3), 318. https://doi.org/10.3390/polym10030318.

(55) Semsarilar, M.; Perrier, S. “Green” Reversible Addition-Fragmentation Chain-Transfer (RAFT) Polymerization. *Nat Chem* **2010**, *2*(10), 811–820. https://doi.org/10.1038/nchem.853.

(56) Corrigan, N.; Jung, K.; Moad, G.; Hawker, C. J.; Matyjaszewski, K.; Boyer, C. Reversible-Deactivation Radical Polymerization (Controlled/Living Radical Polymerization): From Discovery to Materials Design and Applications. *Prog Polym Sci* **2020**, *111*, 101311. https://doi.org/10.1016/j.progpolymsci.2020.101311.

(57) Michael, S. “Living” Polymers. *Nature* **1956**, *178*, 1168–1169. https://doi.org/10.1007/1-56898-643-2_1.

(58) Moad Graeme, Rizzardo Ezio, H. T. S. Living Radical Polymerization by the RAFT Process. *Aust. J. Chem.* **2005**, *58*, 379–410. https://doi.org/10.1007/s10118-020-2367-0.

(59) Corrigan, N.; Jung, K.; Moad, G.; Hawker, C. J.; Matyjaszewski, K.; Boyer, C. Reversible-Deactivation Radical Polymerization (Controlled/Living Radical Polymerization): From Discovery to Materials Design and Applications. *Prog Polym Sci* **2020**, *111*, 101311. https://doi.org/10.1016/j.progpolymsci.2020.101311.

(60) Bagheri, A.; Boniface, S.; Fellows, C. M. Reversible-Deactivation Radical Polymerisation: Chain Polymerisation Made Simple. *Chemistry Teacher International* **2021**, *3*(2), 29–32. https://doi.org/10.1515/cti-2020-0025.

(61) Moad, C. L.; Moad, G. Fundamentals of Reversible Addition-Fragmentation Chain Transfer (RAFT). *Chemistry Teacher International* **2021**, *3*(2), 3–17. https://doi.org/10.1515/cti-2020-0026.

(62) Perrier, S. 50th Anniversary Perspective: RAFT Polymerization-A User Guide. *Macromolecules* **2017**, *50*(19), 7433–7447. https://doi.org/10.1021/acs.macromol.7b00767.

(63) Deng, F.; Luo, X. B.; Ding, L.; Luo, S. L. *Application of Nanomaterials and Nanotechnology in the Reutilization of Metal Ion from Wastewater*. Elsevier 2019, 149-178. https://doi.org/10.1016/B978-0-12-814837-2.00005-6.

(64) Keddie, D. J.; Moad, G.; Rizzardo, E.; Thang, S. H. RAFT Agent Design and Synthesis. *Macromolecules* **2012**, *45*(13), 5321–5342. https://doi.org/10.1021/ma300410v.

(65) Cao, J.; Siefker, D.; Chan, B. A.; Yu, T.; Lu, L.; Saputra, M. A.; Fronczek, F. R.; Xie, W.; Zhang, D. Interfacial Ring-Opening Polymerization of Amino-Acid-Derived N-Thiocarboxyanhydrides toward Well-Defined Polypeptides. *ACS Macro Lett* **2017**, *6*(8), 836–840. https://doi.org/10.1021/acsmacrolett.7b00411.

(66) Ikeda, T.; Yamaguchi, H.; Tazuke, S. New Polymeric Biocides: Synthesis and Antibacterial Activities of Polycations with Pendant Biguanide Groups. *Antimicrob Agents Chemother* **1984**, *26*(2), 139–144. https://doi.org/10.1128/AAC.26.2.139.

(67) Thomas, D. B.; Convertine, A. J.; Hester, R. D.; Lowe, A. B.; McCormick, C. L. Hydrolytic Susceptibility of Dithioester Chain Transfer Agents and Implications in Aqueous RAFT Polymerizations. *Macromolecules* **2004**, *37*(5), 1735–1741. https://doi.org/10.1021/ma035572t.

(68) Tran, J. D.; Mikulec, S. N.; Calzada, O. M.; Prossnitz, A. N.; Ennis, A. F.; Sherwin, W. J.; Magsumbol, A. S.; Jameson, A.; Schellinger, J. G. Microwave-Assisted Reversible Addition–Fragmentation Chain Transfer Polymerization of Cationic Monomers in

Mixed Aqueous Solvents. *Macromol Chem Phys* **2020**, *221*(3), 1–7. https://doi.org/10.1002/macp.201900397.

(69) Samsonova, O.; Pfeiffer, C.; Hellmund, M.; Merkel, O. M.; Kissel, T. Low Molecular Weight PDMAEMA-Block-PHEMA Block-Copolymers Synthesized via RAFT-Polymerization: Potential Non-Viral Gene Delivery Agents. *Polymers* **2011**, *3*(2), 693–718. https://doi.org/10.3390/polym3020693.

(70) Richards, S. J.; Isufi, K.; Wilkins, L. E.; Lipecki, J.; Fullam, E.; Gibson, M. I. Multivalent Antimicrobial Polymer Nanoparticles Target Mycobacteria and Gram-Negative Bacteria by Distinct Mechanisms. *Biomacromolecules* **2018**, *19*(1), 256–264. https://doi.org/10.1021/acs.biomac.7b01561.

(71) Pei, Y.; Lowe, A. B. Polymerization-Induced Self-Assembly: Ethanolic RAFT Dispersion Polymerization of 2-Phenylethyl Methacrylate. *Polym Chem* **2014**, *5* (7), 2342–2351. https://doi.org/10.1039/c3py01719b.

(72) Zhu, C.; Jung, S.; Si, G.; Cheng, R.; Meng, F.; Zhu, X.; Park, T. G.; Zhong, Z. Cationic Methacrylate Copolymers Containing Primary and Tertiary Amino Side Groups: Controlled Synthesis via RAFT Polymerization, DNA Condensation, and in Vitro Gene Transfection. *J Polym Sci A Polym Chem* **2010**, *48*(13), 2869–2877. https://doi.org/10.1002/pola.24064.

(73) Arredondo, J.; Champagne, P.; Cunningham, M. F. RAFT-Mediated Polymerisation of Dialkylaminoethyl Methacrylates in: Tert -Butanol. *Polym Chem* **2019**, *10*(15), 1938–1946. https://doi.org/10.1039/c8py01803k.

(74) Biery, A. R.; Knauss, D. M. Recent Advances in the Synthesis of Diallylammonium Polymers. *Mater Today Chem* **2022**, *26*, 101251. https://doi.org/10.1016/j.mtchem.2022.101251.

(75) Butler, G. B.; Angelo, R. J.; Proposed, V. A.; Chain, A. I.; Butler, B. G. B.; Angelo, R. J. Alternating Intramolecular-Intermolecular. *J. Am. Chem. Soc.* **1957**, *79*, 3128–3131.

(76) Zhao, X.; Zhang, Y. Bacteria-Removing and Bactericidal Efficiencies of Pdadmac Composite Coagulants in Enhanced Coagulation Treatment. *Clean (Wiley)* **2013**, *41*(1), 37–42. https://doi.org/10.1002/clen.201100324.

(77) Kochameshki, M. G.; Marjani, A.; Mahmoudian, M.; Farhadi, K. Grafting of Diallyldimethylammonium Chloride on Graphene Oxide by RAFT Polymerization for Modification of Nanocomposite Polysulfone Membranes Using in Water Treatment. *Chemical Engineering Journal* **2017**, *309*, 206–221. https://doi.org/10.1016/j.cej.2016.10.008.

(78) dos Santos, R.; Sarra, G.; Lincopan, N.; Petri, D.; Aliaga, J.; Marques, M.; Dias, R.; Coto, N.; Sugaya, N.; Paula, C. Preparation, Antimicrobial Properties, and Cytotoxicity of Acrylic Resins Containing Poly(Diallyldimethylammonium Chloride). *Int J Prosthodont* **2021**, *34*(5), 635–641. https://doi.org/10.11607/ijp.6506.

(79) Wu, J.; Ren, N.; Lu, Y.; Jia, M.; Wang, R.; Zhang, J. A Poly(Diallyldimethylammonium Chloride)-Mediated R-Phycoerythrin/DNA Hybrid System as a Fluorescent Biosensor for DNA Detection. *Microchem J* **2020**, *152*, 104314. https://doi.org/10.1016/j.microc.2019.104314.

(80) Tran, P. L.; Hamood, A. N.; De Souza, A.; Schultz, G.; Liesenfeld, B.; Mehta, D.; Reid, T. W. A Study on the Ability of Quaternary Ammonium Groups Attached to a Polyurethane

Foam Wound Dressing to Inhibit Bacterial Attachment and Biofilm Formation. *Wound Repair Regen.* **2015**, *23*(1), 74–81. https://doi.org/10.1111/wrr.12244.

(81) Bhalerao, U. M.; Acharya, J.; Halve, A. K.; Kaushik, M. P. Controlled Drug Delivery of Antileishmanial Chalcones from Layer-by-Layer (LbL) Self Assembled PSS/PDADMAC Thin Films. *RSC Adv* **2014**, *4*(10), 4970–4977. https://doi.org/10.1039/c3ra44611e.

(82) Ramamoorthy, A.; Helmy, H. M.; Rajbhandari, R.; Hauser, P.; El-Shafei, A. Plasma Induced Graft Polymerization of Cationic and Fluorocarbon Monomers into Cotton: Enhanced Dyeability and Photostability. *Ind Eng Chem Res* **2016**, *55*(31), 8501–8508. https://doi.org/10.1021/acs.iecr.6b01069.

(83) Assem, Y.; Chaffey-Millar, H.; Barner-Kowollik, C.; Wegner, G.; Agarwal, S. Controlled/Living Ring-Closing Cyclopolymerization of Diallyldimethylammonium Chloride via the Reversible Addition Fragmentation Chain Transfer Process. *Macromolecules* **2007**, *40*(11), 3907–3913. https://doi.org/10.1021/ma0629079.

(84) Assem, Y.; Greiner, A.; Agarwal, S. Microwave-Assisted Controlled Ring-Closing Cyclopolymerization of Diallyldimethylammonium Chloride via the RAFT Process. *Macromol Rapid Commun* **2007**, *28*, 1923–1928. https://doi.org/10.1002/marc.200700377.

(85) Demarteau, J.; Añastro, F. De; Shaplov, A. S. Polymer Chemistry. *Polym Chem* **2020**, *11*, 1481–1488. https://doi.org/10.1039/c9py01552c.

(86) Lv, H.; Zhang, S.; Wang, B.; Cui, S.; Yan, J. Toxicity of Cationic Lipids and Cationic Polymers in Gene Delivery. *Journal of Controlled Release* **2006**, *114*, 100–109. https://doi.org/10.1016/j.jconrel.2006.04.014.

(87) Cai, J.; Yue, Y.; Rui, D.; Zhang, Y.; Liu, S.; Wu, C. Effect of Chain Length on Cytotoxicity and Endocytosis of Cationic Polymers. *Macromol Res* **2011**, *44*, 2050–2057. https://doi.org/10.1021/ma102498g.

(88) Correia, J. S.; Mirón-barroso, S.; Hutchings, C.; Ottaviani, S.; Castellano, L. How Does the Polymer Architecture and Position of Cationic Charges Affect Cell Viability? †. *Polym Chem* **2022**, *14*, 303–317. https://doi.org/10.1039/d2py01012g.

(89) Online, V. A. A Polyion Complex Micelle with Heparin for Growth Factorfactor Delivery and Uptake into Cells. *J Mater Chem B* **2013**, *1*, 1635–1643. https://doi.org/10.1039/c3tb00360d.

(90) Ghasemi, M.; Turnbull, T.; Sebastian, S.; Kempson, I. The MTT Assay: Utility, Limitations, Pitfalls, and Interpretation in Bulk and Single-Cell Analysis. *Int J Mol Sci* **2021**, *22*, 12827.

(91) Knoll, A. H. Paleobiological Perspectives on Early Microbial Evolution. *Cold Spring Harb Perspect Biol* **2015**, *7*(7), 1–17. https://doi.org/10.1101/cshperspect.a018093.

(92) Murray, C. J. L.; Ikuta, K. S.; Sharara, F.; Swetschinski, L.; Robles Aguilar, G.; Gray, A.; Han, C.; Bisignano, C.; Rao, P.; Wool, E.; Johnson, S. C.; Browne, A. J.; Chipeta, M. G.; Fell, F.; Hackett, S.; Haines-Woodhouse, G.; Kashef Hamadani, B. H.; Kumaran, E. A. P.; McManigal, B.; Achalapong, S.; Agarwal, R.; Akech, S.; Albertson, S.; Amuasi, J.; Andrews, J.; Aravkin, A.; Ashley, E.; Babin, F.-X.; Bailey, F.; Baker, S.; Basnyat, B.; Bekker, A.; Bender, R.; Berkley, J. A.; Bethou, A.; Bielicki, J.; Boonkasidecha, S.; Bukosia, J.; Carvalheiro, C.; Castañeda-Orjuela, C.; Chansamouth, V.; Chaurasia, S.; Chiurchiù, S.; Chowdhury, F.; Clotaire Donatien, R.; Cook, A. J.; Cooper, B.; Cressey, T. R.; Criollo-Mora, E.; Cunningham, M.; Darboe, S.; Day, N. P. J.; De Luca, M.; Dokova, K.; Dramowski, A.; Dunachie, S. J.; Duong Bich, T.; Eckmanns, T.; Eibach, D.; Emami, A.;

Feasey, N.; Fisher-Pearson, N.; Forrest, K.; Garcia, C.; Garrett, D.; Gastmeier, P.; Giref, A. Z.; Greer, R. C.; Gupta, V.; Haller, S.; Haselbeck, A.; Hay, S. I.; Holm, M.; Hopkins, S.; Hsia, Y.; Iregbu, K. C.; Jacobs, J.; Jarovsky, D.; Javanmardi, F.; Jenney, A. W. J.; Khorana, M.; Khusuwan, S.; Kissoon, N.; Kobeissi, E.; Kostyanev, T.; Krapp, F.; Krumkamp, R.; Kumar, A.; Kyu, H. H.; Lim, C.; Lim, K.; Limmathurotsakul, D.; Loftus, M. J.; Lunn, M.; Ma, J.; Manoharan, A.; Marks, F.; May, J.; Mayxay, M.; Mturi, N.; Munera-Huertas, T.; Musicha, P.; Musila, L. A.; Mussi-Pinhata, M. M.; Naidu, R. N.; Nakamura, T.; Nanavati, R.; Nangia, S.; Newton, P.; Ngoun, C.; Novotney, A.; Nwakanma, D.; Obiero, C. W.; Ochoa, T. J.; Olivas-Martinez, A.; Olliaro, P.; Ooko, E.; Ortiz-Brizuela, E.; Ounchanum, P.; Pak, G. D.; Paredes, J. L.; Peleg, A. Y.; Perrone, C.; Phe, T.; Phommasone, K.; Plakkal, N.; Ponce-de-Leon, A.; Raad, M.; Ramdin, T.; Rattanavong, S.; Riddell, A.; Roberts, T.; Robotham, J. V.; Roca, A.; Rosenthal, V. D.; Rudd, K. E.; Russell, N.; Sader, H. S.; Saengchan, W.; Schnall, J.; Scott, J. A. G.; Seekaew, S.; Sharland, M.; Shivamallappa, M.; Sifuentes-Osornio, J.; Simpson, A. J.; Steenkeste, N.; Stewardson, A. J.; Stoeva, T.; Tasak, N.; Thaiprakong, A.; Thwaites, G.; Tigoi, C.; Turner, C.; Turner, P.; van Doorn, H. R.; Velaphi, S.; Vongpradith, A.; Vongsouvath, M.; Vu, H.; Walsh, T.; Walson, J. L.; Waner, S.; Wangrangsimakul, T.; Wannapinij, P.; Wozniak, T.; Young Sharma, T. E. M. W.; Yu, K. C.; Zheng, P.; Sartorius, B.; Lopez, A. D.; Stergachis, A.; Moore, C.; Dolecek, C.; Naghavi, M. Global Burden of Bacterial Antimicrobial Resistance in 2019: A Systematic Analysis. *The Lancet* **2022**, *399*(10325), 629–655. https://doi.org/10.1016/S0140-6736(21)02724-0.

(93) *Global Tuberculosis ReporT 2022*; 2022. http://apps.who.int/bookorders.

(94) Martins-Santana, L.; Rezende, C. P.; Rossi, A.; Martinez-Rossi, N. M.; Almeida, F. Addressing Microbial Resistance Worldwide: Challenges over Controlling Life-Threatening Fungal Infections. *Pathogens* **2023**, *12*(2), 293. https://doi.org/10.3390/pathogens12020293.

(95) Kainz, K.; Bauer, M. A.; Madeo, F.; Carmona-Gutierrez, D. Fungal Infections in Humans: The Silent Crisis. *Microbial Cell* **2020**, 7(6), 143–145. https://doi.org/10.15698/mic2020.06.718.

(96) Qiu, H.; Si, Z.; Luo, Y.; Feng, P.; Wu, X.; Hou, W.; Zhu, Y.; Chan-Park, M. B.; Xu, L.; Huang, D. The Mechanisms and the Applications of Antibacterial Polymers in Surface Modification on Medical Devices. *Front Bioeng and Biotechnol* **2020**, *8*, 1-16. https://doi.org/10.3389/fbioe.2020.00910.

(97) Li, J.; Koh, J. J.; Liu, S.; Lakshminarayanan, R.; Verma, C. S.; Beuerman, R. W. Membrane Active Antimicrobial Peptides: Translating Mechanistic Insights to Design. *Front Neurosci* **2017**, *11*, 1-18. https://doi.org/10.3389/fnins.2017.00073.

(98) Malanovic, N.; Lohner, K. Gram-Positive Bacterial Cell Envelopes: The Impact on the Activity of Antimicrobial Peptides. *Biochim Biophys Acta Biomembr* **2016**, *1858*(5), 936–946. https://doi.org/10.1016/j.bbamem.2015.11.004.

(99) Vincent, A. T.; Nyongesa, S.; Morneau, I.; Reed, M. B.; Tocheva, E. I.; Veyrier, F. J. The Mycobacterial Cell Envelope: A Relict from the Past or the Result of Recent Evolution? *Front Microbiol* **2018**, *9*, 1-9. https://doi.org/10.3389/fmicb.2018.02341.

(100) Pham, P.; Oliver, S.; Boyer, C. Design of Antimicrobial Polymers. *Macromol Chem Phys*. **2023**, *224*, 1-28. https://doi.org/10.1002/macp.202200226.

(101) Sant, D. G.; Tupe, S. G.; Ramana, C. V; Deshpande, M. V. Fungal Cell Membrane—Promising Drug Target for Antifungal Therapy. *J Appl Microbiol* **2016**, *121*(6), 1498–1510. https://doi.org/10.1111/jam.13301.

(102) Bowman, S. M.; Free, S. J. The Structure and Synthesis of the Fungal Cell Wall. *BioEssays* **2006**, *28*, 799–808. https://doi.org/10.1002/bies.20441.

(103) Garcia-Rubio, R.; de Oliveira, H. C.; Rivera, J.; Trevijano-Contador, N. The Fungal Cell Wall: Candida, Cryptococcus, and Aspergillus Species. *Front Microbiol* **2020,** *10*, 1-13. https://doi.org/10.3389/fmicb.2019.02993.

(104) Huan, Y.; Kong, Q.; Mou, H.; Yi, H. Antimicrobial Peptides: Classification, Design, Application and Research Progress in Multiple Fields. *Front Microbiol* **2020**, *16*(11), 1-16. https://doi.org/10.3389/fmicb.2020.582779.

(105) Brown, L.; Wolf, J. M.; Prados-Rosales, R.; Casadevall, A. Through the Wall: Extracellular Vesicles in Gram-Positive Bacteria, Mycobacteria and Fungi. *Nat Rev Microbiol* **2015**, *13*, 620–630. https://doi.org/10.1038/nrmicro3480.

(106) Jiang, X.; Yang, K.; Yuan, B.; Han, M.; Zhu, Y.; Roberts, K. D.; Patil, N. A.; Li, J.; Gong, B.; Hancock, R. E. W.; Velkov, T.; Schreiber, F.; Wang, L.; Li, J. Molecular Dynamics Simulations Informed by Membrane Lipidomics Reveal the Structure-Interaction Relationship of Polymyxins with the Lipid A-Based Outer Membrane of Acinetobacter Baumannii. *J Antimicrob Chemother* **2020**, *75* (12), 3534–3543. https://doi.org/10.1093/jac/dkaa376.

(107) Khondker, A.; Rheinstädter, M. C. How Do Bacterial Membranes Resist Polymyxin Antibiotics? *Commun Biol* **2020**, *3*, 1-4. https://doi.org/10.1038/s42003-020-0803-x.

(108) Yang, X.; Huang, E.; Yousef, A. E. Brevibacillin, a Cationic Lipopeptide That Binds to Lipoteichoic Acid and Subsequently Disrupts Cytoplasmic Membrane of Staphylococcus Aureus *Microbiol Res* **2017**, *195*, 18–23. https://doi.org/https://doi.org/10.1016/j.micres.2016.11.002.

(109) Heesterbeek, D. A. C.; Martin, N. I.; Velthuizen, A.; Duijst, M.; Ruyken, M.; Wubbolts, R.; Rooijakkers, S. H. M.; Bardoel, B. W. Complement-Dependent Outer Membrane Perturbation Sensitizes Gram-Negative Bacteria to Gram-Positive Specific Antibiotics. *Sci Rep* **2019**, *9* (1), 3074. https://doi.org/10.1038/s41598-019-38577-9.

(110) Jain, A.; Duvvuri, L. S.; Farah, S.; Beyth, N.; Domb, A. J.; Khan, W. Antimicrobial Polymers. *Adv Healthc Mater* **2014**, *3*(12), 1969–1985. https://doi.org/10.1002/adhm.201400418.

(111) Timofeeva, L.; Kleshcheva, N. Antimicrobial Polymers: Mechanism of Action, Factors of Activity, and Applications. *App. Microbiol Biotechnol* **2011**, *89*, 475–492. https://doi.org/10.1007/s00253-010-2920-9.

(112) Huang, K. C.; Mukhopadhyay, R.; Wen, B.; Gitai, Z.; Wingreen, N. S. Cell Shape and Cell-Wall Organization in Gram-Negative Bacteria. *PNAS* **2008**, *105*(49), 19282–19287. https://doi.org/10.1073/pnas.0805309105.

(113) Brown, S.; Santa Maria, J. P.; Walker, S. Wall Teichoic Acids of Gram-Positive Bacteria. *Annu Rev Microbiol* **2013**, *67* (1), 313–336. https://doi.org/10.1146/annurev-micro-092412-155620.

(114) Schneewind, O.; Missiakas, D. Lipoteichoic Acids, Phosphate-Containing Polymers in the Envelope of Gram-Positive Bacteria. *J Bacteriol* **2014**, *196*(6), 1133–1142. https://doi.org/10.1128/JB.01155-13.

(115) Velazco-Medel, M. A.; Camacho-Cruz, L. A.; Lugo-González, J. C.; Bucio, E. Antifungal Polymers for Medical Applications. *Med Devices Sens* **2021**, *4*(1), 1-23. https://doi.org/10.1002/mds3.10134.

(116) Kwaśniewska, D.; Chen, Y.-L.; Wieczorek, D. Biological Activity of Quaternary Ammonium Salts and Their Derivatives. *Pathogens* **2020**, *9* (6), 459. https://doi.org/10.3390/pathogens9060459.

(117) Ikeda, T.; Hirayama Hiroki, '; Yamaguchi, H.; Tazuke, S.; Watanabe2, M. *Polycationic Biocides with Pendant Active Groups: Molecular Weight Dependence of Antibacterial Activity*; 1986. https://journals.asm.org/journal/aac.

(118) Sahariah, P.; Cibor, D.; Zielińska, D.; Hjálmarsdóttir, M.; Stawski, D.; Másson, M. The Effect of Molecular Weight on the Antibacterial Activity of N,N,N-Trimethyl Chitosan (TMC). *Int J Mol Sci* **2019**, *20*(7), 1743. https://doi.org/10.3390/ijms20071743.

(119) Guo, J.; Qin, J.; Ren, Y.; Wang, B.; Cui, H.; Ding, Y.; Mao, H.; Yan, F. Antibacterial Activity of Cationic Polymers: Side-Chain or Main-Chain Type? *Polym Chem* **2018**, *9*(37), 4611–4616. https://doi.org/10.1039/C8PY00665B.

(120) Santos, M. R. E.; Mendonça, P. V.; Almeida, M. C.; Branco, R.; Serra, A. C.; Morais, P. V.; Coelho, J. F. J. Increasing the Antimicrobial Activity of Amphiphilic Cationic Copolymers by the Facile Synthesis of High Molecular Weight Stars by Supplemental Activator and Reducing Agent Atom Transfer Radical Polymerization. *Biomacromolecules* **2019**, *20*(3), 1146–1156. https://doi.org/10.1021/acs.biomac.8b00685.

(121) Pham, P.; Oliver, S.; Wong, E. H. H.; Boyer, C. Effect of Hydrophilic Groups on the Bioactivity of Antimicrobial Polymers. *Polym Chem* **2021**, *12*(39), 5689–5703. https://doi.org/10.1039/d1py01075a.

(122) Phuong, P. T.; Oliver, S.; He, J.; Wong, E. H. H.; Mathers, R. T.; Boyer, C. Effect of Hydrophobic Groups on Antimicrobial and Hemolytic Activity: Developing a Predictive Tool for Ternary Antimicrobial Polymers. *Biomacromolecules* **2020**, *21*(12), 5241–5255. https://doi.org/10.1021/acs.biomac.0c01320.

(123) Xue, Y.; Xiao, H. Antibacterial/Antiviral Property and Mechanism of Dual-Functional Quaternized Pyridinium-Type Copolymer. *Polymers* **2015**, *7*(11), 2290–2303. https://doi.org/10.3390/polym7111514.

(124) Ikeda, T.; Yamaguchi, H.; Tazuke, S. *New Polymeric Biocides: Synthesis and Antibacterial Activities of Polycations with Pendant Biguanide Groups*; 1984; Vol. 26.

(125) Lienkamp, K.; Madkour, A. E.; Kumar, K.; Nüsslein, K.; Tew, G. N. Antimicrobial Polymers Prepared by Ring-Opening Metathesis Polymerization: Manipulating Antimicrobial Properties by Organic Counterion and Charge Density Variation. *Chem Eur J* **2009**, *15*(43), 11715–11722. https://doi.org/10.1002/chem.200900606.

(126) Hoque, J.; Adhikary, U.; Yadav, V.; Samaddar, S.; Konai, M. M.; Prakash, R. G.; Paramanandham, K.; Shome, B. R.; Sanyal, K.; Haldar, J. Chitosan Derivatives Active against Multidrug-Resistant Bacteria and Pathogenic Fungi: In Vivo Evaluation as Topical Antimicrobials. *Mol Pharm* **2016**, *13*(10), 3578–3589. https://doi.org/10.1021/acs.molpharmaceut.6b00764.

(127) Qin, Y.; Li, P.; Guo, Z. Cationic Chitosan Derivatives as Potential Antifungals: A Review of Structural Optimization and Applications. *Carbohydr Polym* **2020**, 15, 11602. https://doi.org/10.1016/j.carbpol.2020.116002.

(128) Zhang, A.; Liu, Q.; Lei, Y.; Hong, S.; Lin, Y. Synthesis and Antimicrobial Activities of Acrylamide Polymers Containing Quaternary Ammonium Salts on Bacteria and

Phytopathogenic Fungi. *React Funct Polym* **2015**, *88*, 39–46. https://doi.org/10.1016/j.reactfunctpolym.2015.02.005.

(129) Lin, Y.; Liu, Q.; Cheng, L.; Lei, Y.; Zhang, A. Synthesis and Antimicrobial Activities of Polysiloxane-Containing Quaternary Ammonium Salts on Bacteria and Phytopathogenic Fungi. *React Funct Polym* **2014**, *85*, 36–44. https://doi.org/10.1016/j.reactfunctpolym.2014.10.002.

(130) Huang, Z.; Liuyang, R.; Dong, C.; Lei, Y.; Zhang, A.; Lin, Y. Polymeric Quaternary Ammonium Salt Activity against Fusarium Oxysporum f. Sp. Cubense Race 4: Synthesis, Structure-Activity Relationship and Mode of Action. *React Funct Polym* **2017**, *114*, 13–22. https://doi.org/10.1016/j.reactfunctpolym.2017.02.013.

(131) Dong, C.; You, W.; Liuyang, R.; Lei, Y.; Zhang, A.; Lin, Y. Anti-Rhizoctonia Solani Activity by Polymeric Quaternary Ammonium Salt and Its Mechanism of Action. *React Funct Polym* **2018**, *125*, 1–10. https://doi.org/10.1016/j.reactfunctpolym.2018.01.020.

(132) Zhong, W.; Chang, Y.; Lin, Y.; Zhang, A. Synthesis and Antifungal Activities of Hydrophilic Cationic Polymers against Rhizoctonia Solani. *Fungal Biol* **2020**, *124*(8), 735–741. https://doi.org/10.1016/j.funbio.2020.04.007.

(133) Lv, H.; Zhang, S.; Wang, B.; Cui, S.; Yan, J. Toxicity of Cationic Lipids and Cationic Polymers in Gene Delivery. *J Control Release* **2006**, *114*(1), 100–109. https://doi.org/10.1016/j.jconrel.2006.04.014.

(134) Cai, J.; Yue, Y.; Rui, D.; Zhang, Y.; Liu, S.; Wu, C. Effect of Chain Length on Cytotoxicity and Endocytosis of Cationic Polymers. *Macromolecules* **2011**, *44*(7), 2050–2057. https://doi.org/10.1021/ma102498g.

(135) Correia, J. S.; Mirón-Barroso, S.; Hutchings, C.; Ottaviani, S.; Somuncuoğlu, B.; Castellano, L.; Porter, A. E.; Krell, J.; Georgiou, T. K. How Does the Polymer Architecture and Position of Cationic Charges Affect Cell Viability? *Polym Chem* **2022**, *14*(3), 303–317. https://doi.org/10.1039/d2py01012g.

(136) Zhao, Y.; Lord, M. S.; Stenzel, M. H. A Polyion Complex Micelle with Heparin for Growth Factor Delivery and Uptake into Cells. *J Mater Chem B* **2013**, *1*(11), 1635. https://doi.org/10.1039/c3tb00360d.

(137) Monnery, B. D.; Wright, M.; Cavill, R.; Hoogenboom, R.; Shaunak, S.; Steinke, J. H. G.; Thanou, M. Cytotoxicity of Polycations: Relationship of Molecular Weight and the Hydrolytic Theory of the Mechanism of Toxicity. *Int J Pharm* **2017**, *521*(1–2), 249–258. https://doi.org/10.1016/j.ijpharm.2017.02.048.

(138) Balouiri, M.; Sadiki, M.; Ibnsouda, S. K. Methods for in Vitro Evaluating Antimicrobial Activity: A Review. *J Pharm Anal*. **2016**, 2(6), 71–79. https://doi.org/10.1016/j.jpha.2015.11.005.

(139) Judzewitsch, P. R.; Zhao, L.; Wong, E. H. H.; Boyer, C. High-Throughput Synthesis of Antimicrobial Copolymers and Rapid Evaluation of Their Bioactivity. *Macromolecules* **2019**, *52*(11), 3975–3986. https://doi.org/10.1021/acs.macromol.9b00290.

(140) Peng, C.; Vishwakarma, A.; Mankoci, S.; Barton, H. A.; Joy, A. Structure-Activity Study of Antibacterial Poly(Ester Urethane)s with Uniform Distribution of Hydrophobic and Cationic Groups. *Biomacromolecules* **2019**, *20*(4), 1675–1682. https://doi.org/10.1021/acs.biomac.9b00029.

(141) Wu, C. L.; Peng, K. L.; Yip, B. S.; Chih, Y. H.; Cheng, J. W. Boosting Synergistic Effects of Short Antimicrobial Peptides with Conventional Antibiotics Against Resistant Bacteria. *Front Microbiol* **2021**, *12*, 1-10. https://doi.org/10.3389/fmicb.2021.747760.

(142) Viejo-Dĭaz, M.; Andrés, M. T.; Fierro, J. F. Effects of Human Lactoferrin on the Cytoplasmic Membrane of Candida Albicans Cells Related with Its Candidacidal Activity. *FEMS Immunol Med Microbiol* **2004**, *42*(2), 181–185. https://doi.org/10.1016/j.femsim.2004.04.005.

(143) Ghasemi, M.; Turnbull, T.; Sebastian, S.; Kempson, I. The MTT Assay: Utility, Limitations, Pitfalls, and Interpretation in Bulk and Single-Cell Analysis. *Int J Mol Sci* **2021**, *22*(23), 12827. https://doi.org/10.3390/ijms222312827.

(144) Paslay, L. C.; Abel, B. A.; Brown, T. D.; Koul, V.; Choudhary, V.; McCormick, C. L.; Morgan, S. E. Antimicrobial Poly(Methacrylamide) Derivatives Prepared via Aqueous RAFT Polymerization Exhibit Biocidal Efficiency Dependent upon Cation Structure. *Biomacromolecules* **2012**, *13* (8), 2472–2482. https://doi.org/10.1021/bm3007083.

(145) Cantón, E.; Martín, E., *M27 Reference Method for Broth Dilution Antifungal Susceptibility Testing of Yeasts; Approved Standard,* 4th ed.; Polgar Patrice E., Ed.; 2008; Vol. 22.

(146) Cakmak, I.; Ulukanli, Z.; Tuzcu, M.; Karabuga, S.; Genctav, K. Synthesis and Characterization of Novel Antimicrobial Cationic Polyelectrolytes. *Eur Polym J* **2004**, *40*(10), 2373–2379. https://doi.org/10.1016/j.eurpolymj.2004.06.004.

(147) Liu, L.; Huang, Y.; Riduan, S. N.; Gao, S.; Yang, Y.; Fan, W.; Zhang, Y. Main-Chain Imidazolium Oligomer Material as a Selective Biomimetic Antimicrobial Agent.

Biomaterials **2012**, *33*(33), 8625–8631. https://doi.org/10.1016/j.biomaterials.2012.08.006.

(148) Pierce, C. G.; Uppuluri, P.; Tristan, A. R.; Wormley, F. L.; Mowat, E.; Ramage, G.; Lopez-Ribot, J. L. A Simple and Reproducible 96-Well Plate-Based Method for the Formation of Fungal Biofilms and Its Application to Antifungal Susceptibility Testing. *Nat Protoc* **2008**, *3* (9), 1494–1500. https://doi.org/10.1038/nprot.2008.141.

(149) Moss, B. J.; Kim, Y.; Nandakumar, M. P.; Marten, M. R. Quantifying Metabolic Activity of Filamentous Fungi Using a Colorimetric XTT Assay. *Biotechnol Prog* **2008**, *24*, 780–783. https://doi.org/10.1021/bp070334t.

(150) Kean, R.; Delaney, C.; Rajendran, R.; Sherry, L.; Metcalfe, R.; Thomas, R.; McLean, W.; Williams, C.; Ramage, G. Gaining Insights from Candida Biofilm Heterogeneity: One Size Does Not Fit All. *Journal of Fungi* **2018**, *15*, 1-12. https://doi.org/10.3390/jof4010012.

(151) Staudinger, H. "Uber Polymerisation." *Berichte der Deutschen Chemischen Gesellschaft* **1920**, *53* (6), 1073-1085. https://doi.org/10.1002/cber.19200530627.

(152) Braun, D. Origins and Development of Initiation of Free Radical Polymerization Processes. *Int J Polym Sci* **2009**, 1–10. https://doi.org/10.1155/2009/893234.

(153) Mishra, V.; Kumar, R. Living Radical Polymerization: A Review. *J Sci Res* **2012**, *56*, 141–176.

(154) Rizzardo, E.; Chiefari, J.; Chong, B. Y. K.; Ercole, F.; Krstina, J.; Jeffrey, J.; Le, T. P. T.; Mayadunne, R. T. A.; Meijs, G. F.; Moad, C. L.; Moad, G.; Thang, S. H. Tailored Polymers by Free Radical Processes. *Macromol Symp* **1999**, *143*, 291–307. https://doi.org/10.1002/masy.19991430122.

(155) Lin, Y.; Zhang, C.; Hou, M.; Li, R.; Zhang, A. Polymeric diallyl quaternary ammonium salts for inhibiting banana Fusarium wilt. *React Funct Polym* **2022**, 172, 105174. https://doi.org/10.1016/j.reactfunctpolym.2022.105174.

(156) Timofeeva, L. M.; Kleshcheva, N. A.; Moroz, A. F.; Didenko, L. V. Secondary and Tertiary Polydiallylammonium Salts: Novel Polymers with High Antimicrobial Activity. *Biomacromolecules* **2009**, *10*(11), 2976–2986. https://doi.org/10.1021/bm900435v.

(157) Timofeeva, L. M.; Kleshcheva, N. A.; Shleeva, M. O.; Filatova, M. P.; Simonova, Y. A.; Ermakov, Y. A.; Kaprelyants, A. S. Nonquaternary Poly(Diallylammonium) Polymers with Different Amine Structure and Their Biocidal Effect on Mycobacterium Tuberculosis and Mycobacterium Smegmatis. *Appl Microbiol Biotechnol* **2015**, *99*(6), 2557–2571. https://doi.org/10.1007/s00253-014-6331-1.

(158) Konai, M. M.; Bhattacharjee, B.; Ghosh, S.; Haldar, J. Recent Progress in Polymer Research to Tackle Infections and Antimicrobial Resistance. *Biomacromolecules* **2018**, *19*(6), 1888–1917. https://doi.org/10.1021/acs.biomac.8b00458.

(159) Klibanov, A. M. Permanently Microbicidal Materials Coatings. *J Mater Chem* **2007**, *17*(24), 2479–2482. https://doi.org/10.1039/b702079a.

(160) Fu, Y.; Yang, Y.; Xiao, S.; Zhang, L.; Huang, L.; Chen, F.; Fan, P.; Zhong, M.; Tan, J.; Yang, J. Mixed Polymer Brushes with Integrated Antibacterial and Antifouling Properties. *Prog Org Coat* **2019**, *130*, 75–82. https://doi.org/10.1016/j.porgcoat.2019.01.038.

(161) Krishnan, S.; Weinman, C. J.; Ober, C. K. Advances in Polymers for Anti-Biofouling Surfaces. *J Mater Chem* **2008**, *18*(29), 3405–3413. https://doi.org/10.1039/b801491d.

(162) Leckband, D.; Sheth, S.; Halperin, A. Grafted Poly(Ethylene Oxide) Brushes as Nonfouling Surface Coatings. *J Biomater Sci Polym Ed* **1999**, *10*(10), 1125–1147. https://doi.org/10.1163/156856299X00720.

(163) Chen, S.; Li, L.; Zhao, C.; Zheng, J. Surface Hydration: Principles and Applications toward Low-Fouling/Nonfouling Biomaterials. *Polymer* **2010**, *51*(23), 5283–5293. https://doi.org/10.1016/j.polymer.2010.08.022.

(164) Chen, W. L.; Cordero, R.; Tran, H.; Ober, C. K. 50th Anniversary Perspective: Polymer Brushes: Novel Surfaces for Future Materials. *Macromolecules* **2017**, *50*, 4089–4113. https://doi.org/10.1021/acs.macromol.7b00450.

(165) Tang, J.; Han, Y.; Chen, H.; Lin, Q. Bottom-Up Fabrication of PEG Brush on Poly(Dimethylsiloxane) for Antifouling Surface Construction. *Int J Polym Sci* **2016**, *2016*, 1-5. https://doi.org/10.1155/2016/8458752.

(166) Liu, Q.; Singh, A.; Lalani, R.; Liu, L. Ultralow Fouling Polyacrylamide on Gold Surfaces via Surface-Initiated Atom Transfer Radical Polymerization. *Biomacromolecules* **2012**, *13*(4), 1086–1092. https://doi.org/10.1021/bm201814p.

(167) Zhao, W.; Ye, Q.; Hu, H.; Wang, X.; Zhou, F. Grafting Zwitterionic Polymer Brushes via Electrochemical Surface-Initiated Atomic-Transfer Radical Polymerization for Anti-Fouling Applications. *J Mater Chem B* **2014**, *2*(33), 5352–5357. https://doi.org/10.1039/c4tb00816b.

(168) Fu, Y.; Yang, Y.; Xiao, S.; Zhang, L.; Huang, L.; Chen, F.; Fan, P.; Zhong, M.; Tan, J.; Yang, J. Mixed Polymer Brushes with Integrated Antibacterial and Antifouling Properties. *Prog Org Coat* **2019**, *130*, 75–82. https://doi.org/10.1016/j.porgcoat.2019.01.038.

(169) Riga, E. K.; Vöhringer, M.; Widyaya, V. T.; Lienkamp, K. Polymer-Based Surfaces Designed to Reduce Biofilm Formation: From Antimicrobial Polymers to Strategies for Long-Term Applications. *Macromol Rapid Commun* **2017**, *38*(20), 1–18. https://doi.org/10.1002/marc.201700216.

(170) Isquith, A. J.; Abbott, E. A.; Walters, P. A. Surface-Bonded Antimicrobial Activity of an Organosilicon Quaternary Ammonium Chloride. *Appl Microbiol* **1972**, *24*(6), 859–863. https://doi.org/10.1128/am.24.6.859-863.1972.

(171) Kanazawa, A.; Ikeda, T.; Endo, T. Polymeric Phosphonium Salts as a Novel Class of Cationic Biocides. III. Immobilization of Phosphonium Salts by Surface Photografting and Antibacterial Activity of the Surface-treated Polymer Films. *J Polym Sci A Polym Chem* **1993**, *31*(6), 1467–1472. https://doi.org/10.1002/pola.1993.080310615.

(172) Tiller, J. C.; Liao, C. J.; Lewis, K.; Klibanov, A. M. Designing Surfaces That Kill Bacteria on Contact. *Proc Natl Acad Sci* **2001**, *98*(11), 5981–5985. https://doi.org/10.1073/pnas.111143098.

(173) Kyzioł, A.; Khan, W.; Sebastian, V.; Kyzioł, K. Tackling Microbial Infections and Increasing Resistance Involving Formulations Based on Antimicrobial Polymers. *J Chem Eng* **2020**, *385*, 123888. https://doi.org/10.1016/j.cej.2019.123888.

(174) Tröger, J. Ueber Einige Mittelst Nascirenden Formaldehydes Entstehende Basen. *Journal für Praktische Chemie* **1887**, *36*(1), 225–245. https://doi.org/10.1002/prac.18870360123.

(175) Spielman, M. A. The Structure of Troeger's Base. *J. Am. Chem. Soc.* **1935**, *57*, 583–585.

(176) Agentits, A. N. A. Structura of 5,11-Methano-2,8-Dimethyl-5,6,11,12-Tetrahydrodibenzo[b,f] [1,5]Diazocine (Triiger's Base) at 163 K. *Acta Crystallogr.* **1986**, *42*, 224–227.

(177) Rúnarsson, Ö. V.; Artacho, J.; Wärnmark, K. The 125th Anniversary of the Tröger's Base Molecule: Synthesis and Applications of Tröger's Base Analogues. *European J Org Chem* **2012**, *36*, 7015–7041. https://doi.org/10.1002/ejoc.201201249.

(178) Jeon, Y. M.; Armatas, G. S.; Kim, D.; Kanatzidis, M. G.; Mirkin, C. A. Tröger's-Base-Derived Infinite Co-Ordination Polymer Microparticles. *Small* **2009**, *5*(1), 46–50. https://doi.org/10.1002/smll.200801160.

(179) Du, X.; Sun, Y.; Tan, B.; Teng, Q.; Yao, X.; Su, C.; Wang, W. Tröger's Base-Functionalised Organic Nanoporous Polymer for Heterogeneous Catalysis. *ChemComm* **2010**, *46*(6), 970–972. https://doi.org/10.1039/b920113k.

(180) Carta, M.; Malpass-Evans, R.; Croad, M.; Rogan, Y.; Lee, M.; Rose, I.; McKeown, N. B. The Synthesis of Microporous Polymers Using Tröger's Base Formation. *Polym Chem* **2014**, *5*(18), 5267–5272. https://doi.org/10.1039/c4py00609g.

(181) Hu, X.; Lee, W. H.; Bae, J. Y.; Zhao, J.; Kim, J. S.; Wang, Z.; Yan, J.; Lee, Y. M. Highly Permeable Polyimides Incorporating Tröger's Base (TB) Units for Gas Separation Membranes. *J Memb Sci* **2020**, *615*, 118533. https://doi.org/10.1016/j.memsci.2020.118533.

(182) Yang, Z.; Guo, R.; Malpass-Evans, R.; Carta, M.; McKeown, N. B.; Guiver, M. D.; Wu, L.; Xu, T. Highly Conductive Anion-Exchange Membranes from Microporous Tröger's Base Polymers. *Angew Chem* **2016**, *55*(38), 11499–11502. https://doi.org/10.1002/anie.201605916.

(183) Jeon, J. W.; Shin, J.; Lee, J.; Baik, J. H.; Malpass-Evans, R.; McKeown, N. B.; Kim, T. H.; Lee, J. C.; Kim, S. K.; Kim, B. G. Hierarchically Structured Carbon Electrodes Derived from Intrinsically Microporous Tröger's Base Polymers for High-Performance Supercapacitors. *Appl Surf Sci* **2020**, *530*, 147146. https://doi.org/10.1016/j.apsusc.2020.147146.

(184) Antonangelo, A. R.; Hawkins, N.; Tocci, E.; Muzzi, C.; Fuoco, A.; Carta, M. Tröger's Base Network Polymers of Intrinsic Microporosity (TB-PIMs) with Tunable Pore Size for Heterogeneous Catalysis. *J Am Chem Soc* **2022**, *144*(34), 15581–15594. https://doi.org/10.1021/jacs.2c04739.

(185) Shanmughan, A.; Nithasha, M. A.; Mohan, B.; Umadevi, D.; Shanmugaraju, S. Tröger's Base-Containing Fluorenone Organic Polymer for Discriminative Fluorescence Sensing of Sulfamethazine Antibiotic at Ppb Level in the Water Medium. *Polym Chem* **2023**, *14* (36), 4153–4159. https://doi.org/10.1039/d3py00857f.

(186) Xu, Z.; Liao, J.; Tang, H.; Efome, J. E.; Li, N. Preparation and Antifouling Property Improvement of Tröger's Base Polymer Ultrafiltration Membrane. *J Memb Sci* **2018**, *561*, 59–68. https://doi.org/10.1016/j.memsci.2018.05.042.

(187) Zhang, C.; Huang, R.; Tang, H.; Zhang, Z.; Xu, Z.; Li, N. Enhanced Antifouling and Separation Properties of Tröger's Base Polymer Ultrafiltration Membrane via Ring-Opening Modification. *J Memb Sci* **2020**, *597*(117763), 1–9. https://doi.org/10.1016/j.memsci.2019.117763.

(188) Huang, T.; Yin, J.; Tang, H.; Zhang, Z.; Liu, D.; Liu, S.; Xu, Z.; Li, N. Improved Permeability and Antifouling Performance of Tröger's Base Polymer-Based Ultrafiltration Membrane

via Zwitterionization. *J Memb Sci* **2022**, *646*(120251), 1–9. https://doi.org/10.1016/j.memsci.2022.120251.

(189) Scheuerman, T. R.; Camper, A. K.; Hamilton, M. A. Effects of Substratum Topography on Bacterial Adhesion. *J Colloid Interface Sci* **1998**, *208*(1), 23–33. https://doi.org/10.1006/jcis.1998.5717.

(190) Erkoc, P.; Ulucan-Karnak, F. Nanotechnology-Based Antimicrobial and Antiviral Surface Coating Strategies. *Prosthesis* **2021**, *3*(1), 25–52. https://doi.org/10.3390/prosthesis3010005.

(191) Cunliffe, A. J.; Askew, P. D.; Stephan, I.; Iredale, G.; Cosemans, P.; Simmons, L. M.; Verran, J.; Redfern, J. How Do We Determine the Efficacy of an Antibacterial Surface? A Review of Standardised Antibacterial Material Testing Methods. *Antibiotics* **2021**, *10*(9), 1069. https://doi.org/10.3390/antibiotics10091069.

(192) Stenzel, M. H.; Davis, T. P. Star Polymer Synthesis Using Trithiocarbonate Functional B-cyclodextrin Cores (Reversible Addition–Fragmentation Chain-transfer Polymerization). *J Polym Sci A Polym Chem* **2002**, *40*(24), 4498–4512. https://doi.org/10.1002/pola.10532.

(193) Teh, C. H.; Nazni, W. A.; Nurulhusna, A. H.; Norazah, A.; Lee, H. L. Determination of Antibacterial Activity and Minimum Inhibitory Concentration of Larval Extract of Fly via Resazurin-Based Turbidometric Assay. *BMC Microbiol* **2017**, *17*(1), 1–8. https://doi.org/10.1186/s12866-017-0936-3.

(194) Mukherjee, A.; Barman, R.; Das, B.; Ghosh, S. Highly Efficient Biofilm Eradication by Antibacterial Two-Dimensional Supramolecular Polymers. *Chem Mater* **2021**, *33*(22), 8656–8665. https://doi.org/10.1021/acs.chemmater.1c02392.

(195) Wu, C. L.; Peng, K. L.; Yip, B. S.; Chih, Y. H.; Cheng, J. W. Boosting Synergistic Effects of Short Antimicrobial Peptides with Conventional Antibiotics Against Resistant Bacteria. *Front Microbiol* **2021**, *12*, 1–10. https://doi.org/10.3389/fmicb.2021.747760.

(196) Chamsaz, E. A.; Mankoci, S.; Barton, H. A.; Joy, A. Nontoxic Cationic Coumarin Polyester Coatings Prevent Pseudomonas Aeruginosa Biofilm Formation. *ACS Appl Mater Interfaces* **2017**, (8), 6704–6711. https://doi.org/10.1021/acsami.6b12610.

(197) Singhsa, P.; Diaz-Dussan, D.; Manuspiya, H.; Narain, R. Well-Defined Cationic N-[3-(Dimethylamino)Propyl]Methacrylamide Hydrochloride-Based (Co)Polymers for SiRNA Delivery. *Biomacromolecules* **2018**, *19*(1), 209–221. https://doi.org/10.1021/acs.biomac.7b01475.

(198) Azuma, R.; Nakamichi, S.; Kimura, J.; Yano, H.; Kawasaki, H.; Suzuki, T.; Kondo, R.; Kanda, Y.; Shimizu, K. I.; Kato, K.; Obora, Y. Solution Synthesis of N,N-Dimethylformamide-Stabilized Iron-Oxide Nanoparticles as an Efficient and Recyclable Catalyst for Alkene Hydrosilylation. *ChemCatChem* **2018**, *10*(11), 2378–2382. https://doi.org/10.1002/cctc.201800161.

(199) Ramage, G.; Wickes, B. L. Standardized Method for In Vitro Antifungal Susceptibility Testing. *Antimicrob Agents Chemother* 2**001**, *45*(9), 2475–2479. https://doi.org/10.1128/AAC.45.9.2475.

(200) O'Donnell, L. E.; Smith, K.; Williams, C.; Nile, C. J.; Lappin, D. F.; Bradshaw, D.; Lambert, M.; Robertson, D. P.; Bagg, J.; Hannah, V.; Ramage, G. Dentures Are a Reservoir for Respiratory Pathogens. *J Prosthodont* **2016**, *25*(2), 99–104. https://doi.org/10.1111/jopr.12342.

(201) Bai, S.; Li, X.; Zhao, Y.; Ren, L.; Yuan, X. Antifogging/Antibacterial Coatings Constructed by N-Hydroxyethylacrylamide and Quaternary Ammonium-Containing Copolymers. *ACS Appl Mater Interfaces* **2020**, *12*(10), 12305–12316. https://doi.org/10.1021/acsami.9b21871.